Développement d'aptamères pour la détection de biomarqueurs de cancers ovariens dans les urines

Antonija Hanzek

THÈSE

Pour obtenir le grade de

Docteur

Délivrée par **L'UNIVERSITÉ DE NÎMES**

Préparée au sein de
l'École Doctorale 583 - Risques et Sociétés
et de l'unité de recherche UPR CHROME - Risques CHROniques et éMErgents

Spécialité :
BIOCHIMIE – BIOLOGIE MOLÉCULAIRE

Présentée par **Antonija HANŽEK**

DÉVELOPPEMENT D'APTAMÈRES POUR LA DÉTECTION DE BIOMARQUEURS DE CANCERS OVARIENS DANS LES URINES

Soutenue le 23 juin 2023 devant le jury composé de

M. **Philippe BERTA**, Pr, Université de Nîmes	Président du jury
Mme. **Catherine ALIX-PANABIÈRES**, MCU-PH, Université de Montpellier, LCCRH-IURC	Rapporteure
M. **Éric PEYRIN**, Pr, Université Grenoble-Alpes, UMR 5063-CNRS	Rapporteur
M. **Jean-Charles BRES**, Directeur de recherche, EFS Occitanie	Examinateur
M. **Frédéric DUCONGÉ**, Directeur de recherche, Institut de biologie François Jacob, CEA	Examinateur
M. **Christophe HIRTZ**, Pr, Université de Montpellier, IRMB	Invité
M. **Christian SIATKA**, Pr, UPR CHROME, Université de Nîmes	Directeur de thèse
Mme. **Anne-Cécile DUC**, MCF, UPR CHROME, Université de Nîmes	Co-directrice de thèse

RESUME

Le cancer ovarien est le huitième cancer le plus répandu et le cancer gynécologique le plus meurtrier. Avec des symptômes non spécifiques de la maladie et le manque de méthodes de diagnostic efficaces, les mauvais pronostics sont souvent le résultat d'un diagnostic tardif. Par conséquent, le développement de nouvelles approches diagnostiques est nécessaire. Les biomarqueurs de ce cancer ont été l'axe principal de l'amélioration des méthodes diagnostiques. La protéine 4 de l'épididyme humain (HE4) est une protéine surexprimée chez les patientes atteintes de cancer de l'ovaire, et ne l'est pas dans des conditions saines ou bénignes. Le marqueur HE4 urinaire apparaît comme un biomarqueur de diagnostic non invasif intéressant du fait de sa grande stabilité. Dans cette étude, nous avons cherché à évaluer le potentiel des aptamères comme outils de diagnostic pour la détection de biomarqueurs du cancer de l'ovaire dans l'urine. Les aptamères sont de courts oligonucléotides simple brin qui peuvent se lier sélectivement à des molécules cibles spécifiques avec une haute affinité. Les aptamères d'ADN anti-HE4 de haute affinité ont été sélectionnés par 10 cycles d'évolution systématique haute-fidélité des ligands par enrichissement EXponentiel (Hi-Fi SELEX) dans l'urine, cette méthode de sélection des aptamères est basée sur la PCR digitale en gouttelettes (ddPCR). Le séquençage ADN et l'analyse bioinformatique ont révélé un panel d'aptamères enrichis pour cibler la protéine HE4. Les 10 séquences candidates les plus enrichies ont été criblées par résonance des plasmons de surface (SPR), tandis que les 3 séquences les plus enrichies et les plus prometteuses ont été caractérisées par analyse thermofluorimétrique (TFA). La TFA a révélé la liaison de deux aptamères anti-HE4, appelés AHE1 et AHE3, au biomarqueur HE4 du cancer de l'ovaire dans l'urine. Les aptamères se lient à HE4 dans l'urine dans la gamme nanomolaire, avec respectivement des constantes de dissociation K_d (AHE1) = 87 ± 9 nM et K_d (AHE3) = 127 ± 28 nM. De plus, un autre aptamère anti-HE4 A3 trouvé dans la littérature présentait une liaison à HE4 dans l'urine, avec un K_d (A3) = 338 ± 35 nM. Dans l'ensemble, ces résultats suggèrent que les aptamères décrits pourraient être des outils prometteurs pour une application par tests urinaires ou par biocapteurs dans le diagnostic du cancer de l'ovaire.

Mots clés : aptamères, cancer, cancer ovarien, biomarqueurs, SELEX, urine

ABSTRACT

Ovarian cancer is the 8th most common malignancy in women and the deadliest gynecological cancer. Due to the non-specific symptoms and the lack of effective diagnostic methods, late diagnosis remains the main barrier for improval of the poor prognosis. Therefore, development of novel diagnostic approaches are needed. Recently, urine has emerged as simple source of cancer biomarkers. Human epididymis protein 4 (HE4) is a protein found overexpressed in ovarian cancer, but not in healthy or benign conditions. With high stability and diagnostic value for detection of ovarian cancer, urine HE4 appears as an attractive non-invasive biomarker. In this thesis work, the aim was to evaluate the potential of aptamers as diagnostic tools for detection of ovarian cancer biomarkers in urine. Aptamers are short, single-stranded oligonucleotides that can selectively bind to specific target molecules with high-affinity. To select anti-HE4 DNA aptamers, 10 cycles of High-Fidelity Systematic Evolution of Ligands by EXponential enrichment (Hi-Fi SELEX) were carried out in urine to target HE4 protein. This particular SELEX method was optimized and is based on the digital droplet PCR (ddPCR) amplification of aptamers. High-throughput sequencing and bioinformatics analysis identified a panel of aptamers enriched to target HE4 protein. The 10 most-enriched sequences were screened using surface plasmon resonance (SPR), while the three most enriched and promising sequences were characterized by thermofluorimetic analysis (TFA). The TFA analysis revealed binding of two anti-HE4 aptamers, called AHE1 and AHE3, to ovarian cancer biomarker HE4 in urine. The aptamers were binding to HE4 in urine in the high nanomolar range, with K_d (AHE1) = 87 ± 9 nM and K_d (AHE3) = 127 ± 28 nM. Additionally, another anti-HE4 aptamer A3 found in literature exhibited binding to HE4 in urine, with a K_d (A3) = 338 ± 35 nM. Overall, the data suggest that these aptamers could be promising tools for application in urine tests or biosensors for ovarian cancer in future.

Keywords : aptamers, cancer, ovarian cancer, biomarkers, SELEX, urine

ACKNOWLEDGEMENTS

I would like to thank University of Nîmes and UPR CHROME for providing the resources and opportunities necessary to complete my doctoral degree. Also, I thank La Region Occitanie for financial support of the project *CARIBOU (CAncer ovaRIan BiosensOr in Urine)*, in which this doctoral thesis belong. I would like to thank all the members of the jury, for accepting being the part of my thesis jury and for the evaluation of this research.

Most deeply, I would like to thank my supervisors Dr A.C. Duc and Pr C. Siatka. I express my gratitude for Dr. Duc for giving me the freedom to pursue all my research interests. Her guidance, encouragements and support have helped me to become the scientist I am today. I thank her for all the moments we shared, all the advices, and help she generously offered, both professionally and personally, in what were one of the most challenging years of my life. She has inspired me to persevere and strive for excellence. I thank Pr Siatka for always having great organizational skills, fast feedbacks and very kind words. I could not imagine having better mentors and this experience would not have been the same if it was not with you.

I would like to thank the members of the comité de suivi de thèse for following and evaluating my work for 3 years, with a special acknowledgements to Dr F. Ducongé, providing the expertise in the aptamers field; and Dr. C. Fournier-Wirth, for providing expertise in the field of diagnostics. Your critics and thoughtful feedbacks were crucial for development and course of the project and have greatly improved its quality.

I would like to thank and acknowledge Dr Ducongé (CEA) for the DNA sequencing and bioinformatics analysis on MIRCen platform; Pr Hirtz (Université de Montpellier and Plateforme de Proteomique Clinique) for the kind donation of the Vivacon® tubes; Dr Pugnière and Dr Ngo (PP2I Plateforme Protéomique et Interactions Moléculaires, IRCM) for SPR analysis, Ecole l'ADN Nîmes for conceptualization of the figures using BioRender.com; and A. Gotte for the thermofluorimetric analysis.

I would also like to thank the members of the laboratory Dr P. Gianonni and Dr Z. Benfodda, the two incredible women scientists, for the support and life advices through years. I am

grateful for the conversations we shared, even if they seemed insignificant to you in the moment, they gave me hope in the moments I needed it.

I would like to express my appreciation to my colleagues and friends I have met during these years. Firstly, I would like to thank my dear friend Julie. We have arrived at the same day, laughed and cried together, grew together, shared many moments and drinks, and ultimately we did it. She is a badass person and incredible scientist. I would like to thank my friend Jeanne, who is a little ray of sunshine. Also, Anastasia, Chaimae and Alex for all the great moments we shared together. Thank you all for the memories, you made it easier. Also, I would like to thank Damien and Estelle for sharing the office moments. I am proud of all of you and excited to see what the future brings. I would also like to share my appreciations to other colleagues I encountered, my students and my interns I have supervised. I am especially grateful for M2 student Alicia, who really helped advance the project.

I am deeply thankful for all my family and friends in Croatia, for always being there for me. I am especially grateful and lucky for my friend Nataša. Her belief in my abilities and support during times of stress and uncertainty have been invaluable.

Finally, I would like to express my deepest gratitude to my love and life partner Valentin, who has been my unwavering source of unconditional support throughout my academic journey. His constant encouragement, patience, and understanding helped me overcome the challenges that I faced during the course of this thesis. I thank him for celebrating all my successes, but also standing by me during my failures. His strength and the faith in me has been a constant source of inspiration and motivation. Without him, this thesis would not have been possible.

Thank you all, for everything.

Antonija

TABLE OF CONTENTS

ABBREVIATIONS

ALFA : Aptamer Lateral Flow Assay
ANSES : Agence nationale de sécurité sanitaire de l'alimentation, de l'environnement et du travail (The french national agency for food, environmental and occupational health safety)
APCE : Affinity Probe Capillary Electrophoresis
BRCA 1/2 : BReast CAncer gene 1 and 2
BSA : Bovine Serum Albumin
CA-15 : Cancer Antigen 15
CA125 : Cancer Antigen 125
CE : Capillary Electrophoresis
CEA : CarcinoEmbryonic Antigen
CMIA : Chemiluminescence Microparticle ImmunoAssay
CRE : Creatinine
CXCL-12 : Chemokine ligand 12
ddPCR : Digital Droplet Polymerase Chain Reaction
DNA : DeoxyriboNucleic Acid
dNTP : Deoxynucleotide TriPhosphate
ECLIA : ElectroChemiLuminescence ImmunoAssay
EDN : Eosin-Derived Neurotoxin
EDTA : EthyleneDiamineTetraacetic Acid
EGFR : Epidermal Growth Factor Receptor
EIA : Enzyme ImmunoAssay
ELISA : Enzyme Linked ImmunoSorbent Assay
ELONA : Enzyme Linked OligoNucleotide Assay
EOC : Epithelial Ovarian Cancer
FA : Fluorescence Anisotropy
FANA : FluoroArabino Nucleic Acid
FDA : Food and Drug Agency
FIGO : International Federation of Gynecology and Obstetrics
GST : Glutathione-S-Transferase
HE4 : Human Epididymis protein 4
HER2 : Human Epidermal Growth Factor Receptor-2
Hi-Fi SELEX : High-Fidelity Systematic Evolution of Ligands by EXponential enrichment
HNA : 1,5-anhydro Hexitol Nucleic Acids
HRP : HorseRadish Peroxidase
IPTG : IsoPropyl ß-D-1-ThioGalactopyranoside
ITC : Isothermal Titration Calorimetry
K_d : Constant of Dissociation
LFA : Lateral Flow Assay
LNA : Locked Nucleic Acid
LOD : Limit Of Detection
LRG1 : Leucine-Rich alpha-2-Glycoprotein

MMP : Matrix MetaloProteinase
MSLN : Mesothelin
NGS : Next Generation Sequencing
Ni-NTA : Nickel-NitriloTriacetic Acid
NTC : Non Template Control
OC : Ovarian Cancer
OPN : Osteopontin
P-LAP : Placental Leucine Aminopeptidase
PARP : Poly ADP Ribose Polymerase
PBS : Phosphate Buffered Saline
PCR : Polymerase Chain Reaction
PD-L1 : Programmed death-ligand 1
POC : Point Of Care
RFU : Relative Fluorescence Units
RLS : Resonance Light Scattering
RNA : RiboNucleic Acid
ROC : Receiver Operating Characteristic
ROMA : Risk of Ovarian Malignancy Algorithm
RT : Room Temperature
RT-PCR : Reverse Transcription Polymerase Chain Reaction
SELEX : Systematic Evolution of Ligands by EXponential enrichment
SPR : Surface Plasmon Resonance
STIP1 : Stress-induced phosphoprotein 1
TAE : Tris Acetate EDTA
TFA : ThermoFluorimetric Analysis
TRA : Threose Nucleic Acid
TVUS : Transvaginal ultrasound
VEGF-A : Vascular Endothelial Growth Factor A
VOC : Volatile Organic Compounds
WAP : Whey Acidic Protein
WHO : World Health Organization

LIST OF FIGURES AND TABLES

Figures

Tables

I. GENERAL INTRODUCTION

1. OVARIAN CANCER

1.1. Epidemiology of ovarian cancer

According to the World Health Organization (WHO), deaths from cancer are one of the leading causes of mortality, accounting for approximately 10 million deaths per year [1,2]. Currently, it is projected that the number of new cases of cancer will increase by 70 % until 2034, rising to over 22 million new cases per year [2,3]. **Ovarian cancer (OC)** is a major contributor to cancer-related deaths. Ovarian cancer is the 8th most common malignancy and 8th most frequent cause of cancer death in women in the world [4]. The number of new cases diagnosed in France is estimated at 4395, while the deaths recorded for the year 2020 are 2998 (**Figure 1**). That means that 68 % of women could die, making OC the 5th cause of cancer mortality [5]. Moreover, the GLOBOCAN study predicts that by the year 2035 there will be a worldwide increase of 55 % in the incidence, and an 67 % increase in deaths, making OC a global public health problem [4]. Unfortunately, most patients are diagnosed in advanced stages, with a 5-year survival rate of 15 – 40 % [6,7]. However, when diagnosed in early stages, the 5-year survival rate is 90 % [6]. As the diagnosis is often late, the prognosis is highly unfavorable.

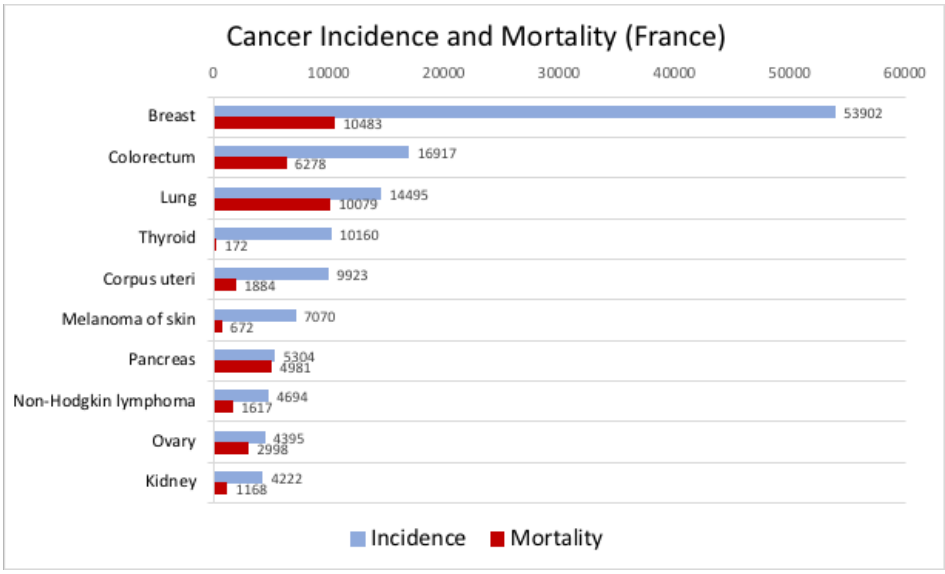

Figure 1. Estimated global incidence and mortality for 2020 in France.

(female, all age groups) (From https://gco.iarc.fr[5], *accessed on 25 of March 2023*)

1.2. Symptoms and risk factors for ovarian cancer

The most significant contribution to the high mortality from OC is late diagnosis [7]. Due to the asymptomatic or non-specific nature of the disease, and the lack of accurate diagnostic methods, most patients are diagnosed in advanced stages [6,8].

Patients with localized OC have few or no symptoms, making clinical diagnosis of early disease very difficult. Recognized **symptoms** include abdominal or pelvic pain, constipation, diarrhea, frequent need to urinate, vaginal bleeding, and fatigue [8]. In advanced OC, ascites and abdominal masses can lead to increased abdominal volume, causing bloating, nausea or early satiety. Patients may become aware of an abdominal or nodal mass [8]. Women seek medical attention once they start to feel the symptoms, which is when the disease already progressed [8].

The exact cause of OC is not known, but several associated **risk factors** have been identified. It is predominantly a disease of older, postmenopausal woman with the majority (> 80 %) of cases being diagnosed in women over 50 years [8]. Lifestyle factors (such as obesity, smoking, sedentary lifestyle) are associated with an increased risk [9]. A woman's reproductive history appears to contribute to lifetime risk of OC [8]. Not having children, early menarche and late natural menopause increase the risk. On the other hand, having children at early age, multiple pregnancies, late menarche, early menopause, and use of oral contraceptives are protective factors that reduce the risk of OC [8]. All of those risk factors point to a number of ovulation as a factor for development of OC [10–12]. Over many repeated cycles of ovulation, the epithelial cells go repeated disruption and repairs. They are stimulated to proliferate, increasing the probability of spontaneous mutations [8,13]. Hereditary and genetic predispositions are related to dysfunctional BRCA1 and BRCA2 genes and are implicated in 20 % of cases [14,15]. Women who carry germline mutations in BRCA1 and BRCA2 have a substantially increased risk of ovarian, tubal, and peritoneal cancer. BRCA1 mutation carriers were found to have a 40 to 50 % cumulative lifetime risk and BRCA2 mutation carriers to have a 20 to 30 % cumulative lifetime risk of OC [15,16]. Another genetic are inherited mutations in the mismatch repair genes associated with Lynch syndrome type II. Women carrying these mutations have an increased risk of a number of cancers including colon, endometrial, and ovarian cancer [17]. Moreover, certain environmental factors could cause increased risk of OC. In 2022, *The French national agency for food, environmental and occupational health safety ANSES* reported a proven causal relationship between the risk of occurrence of OC and occupational exposure to asbestos [18].

1.3. Biology and characteristics of ovarian cancer

OC includes different histological and molecular types of ovarian malignancies [11,15]. OC is a group of diseases that originates in the ovaries, or in the related areas of the fallopian tubes and the peritoneum [15]. The majority of primary tumors arise from ovarian surface epithelium (90 %), called the epithelial ovarian cancer (EOC) [13,15]. More rare types include sex-cord stromal tumors, and germ cell tumors [15]. EOC is further divided into hystotypes by *WHO classification* into serous, mucinous, endometrioid, clear cell, Brenner tumors, undifferentiated and mixed tumors [15]. Each of the subtype vary in the pattern of gene expression, differences in clinical behavior, prognosis and response to therapy [6]. Based on prevalence and mortality, serous ovarian carcinoma represents the majority of all carcinomas and is further divided into high-grade and low-grade carcinomas [6].

Staging of OC (stage I, II, III and IV) by the *International Federation of Gynecology and Obstetrics (FIGO)* defines how far the tumor has spread and is currently the most powerful indicator of prognosis [8,15] (**Figure 2**). Unfortunately, most patients are diagnosed in advanced stages, when disease have spread. Therefore, early diagnosis is essential for the good prognosis and outcome of OC [8]

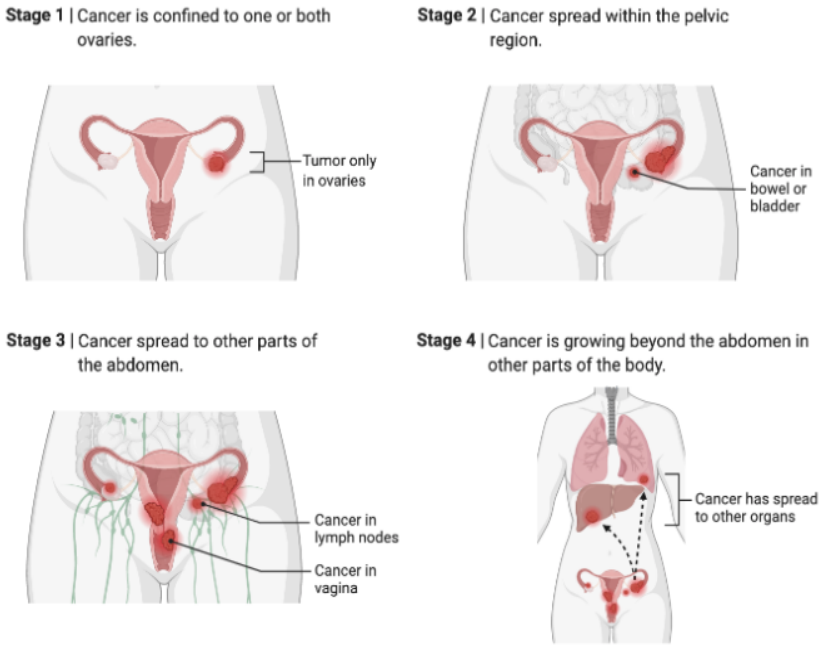

Figure 2. Staging classification of ovarian cancer.

Ovarian cancer is divided into 4 stages based on the cancer localization and spread: stage 1 cancer is present only on ovaries, stage 2 is spread in local pelvic region, stage 3 cancer is spread throughout abdomen, and stage 4 is spread to distant organs through metastasis (*Created with Biorender.com*).

The clinical management and the treatment will depend on how advanced the disease is. It includes the surgery followed by the chemotherapy [8,19]. The aim of surgery is to remove the tumor and to undertake staging [8]. It can involve removal of all the affected organs or parts in the abdominal cavity [8]. All women with EOC in stages II/III/IV receive the chemotherapy, which include the combination of drugs, paclitaxel and carboplatin, every three weeks (cycles of chemotherapy). The treatment can involve targeted therapy with Bevacizumab, an antibody that blocks tumor angiogenesis by inhibiting vascular endothelial growth factor A (VEGF-A); or Olaparib, an inhibitor of the poly ADP ribose polymerase (PARP), an enzyme needed for DNA repair and growth of tumor cells. Olaparib is registered for women who have been shown positive for BRCA1/BRCA2 mutation [8,19].

2. DIAGNOSTICS AND CLINICAL BIOMARKERS FOR OVARIAN CANCER

2.1. Current diagnostic methods for ovarian cancer

Current diagnostic approaches for OC include a combination of pelvic examination, transvaginal ultrasound (TVUS) and increased blood concentration of Cancer Antigen 125 (CA125), which are not sensitive enough to detect the OC in the early course of disease [6,8].

A transvaginal ultrasonography (TVUS) is a type of pelvic ultrasound used by doctors to examine female reproductive organs. Ultrasonography of the abdomen and pelvis is usually the first imaging investigation recommended for women in whom OC is suspected. It presents good diagnostic accuracy[1], with a sensitivity of ~ 86 % and specificity ~ 94 % to differentiate benign from malignant adnexal masses [20].

A pelvic examination is performed by a gynecologist and includes evaluation of the genitalia and the pelvic organs. Along with external visual inspection, a speculum exam is performed to

[1] Diagnostic tests and cancer biomarkers are described by the **diagnostic accuracy** with a *sensitivity*, the ability of a test to detect the cancer when it is truly present; and *specificity*, the probability of a test to exclude cancer in patients who do not have the disease [205]. The formulas are : $Sensitivity = \frac{\text{True Positives}}{\text{True Positives+False Negatives}}$ $Specificity = \frac{\text{True Negatives}}{\text{True Negatives+False Positives}}$

evaluate the internal genitalia. This allows evaluation of the masses [20,21]. In the context of OC, the procedure presents limited accuracy. It is non-specific, since pelvic masses can be caused by other health conditions [20]. Indeed, it is reported that abnormal pelvic examination failed to identify OC in 96,7 to 100 % of cases [21]. This weak accuracy can either lead to false reassurance and false negative results. On the contrary, it can cause over diagnosis, leading to unnecessary procedures, treatments, and psychological harm. It was reported that misdiagnosis of OC using pelvic examination resulted in unnecessary surgery in 1,5 % of screened women [21].

Tissue biopsy and histopathological examination is required for definitive diagnosis [20]. The biopsy is most commonly done by removing the tumor during surgery. Doctors do not typically recommend stand-alone ovarian biopsies due to the risks of cancer spreading [22]. In rare cases, a suspected OC may be biopsied during a laparoscopy or with a needle placed directly into the tumor through the skin of the abdomen, guided by ultrasound or scan. This is done if woman cannot have surgery due to the advanced cancer or serious medical condition [22].

2.2. Ovarian cancer biomarkers in clinical practice

The *cancer biomarkers* are substances that indicate the presence of tumor in a body and can be detected in plasma or other body fluids [23]. They include proteins, nucleic acids, antigens, genes, hormones, oncofetal antigens, or receptors. Cancer biomarkers have an important role in all aspects of cancer care. Therefore, biomarkers can be *prognostic* (the possibility to develop cancer, or have a progression of the disease), *diagnostic* (confirm the presence of cancer and which type), *monitoring* (to evaluate the response to therapy or course of the disease), *predictive* (probability to develop a clinical event after exposure to treatment), *pharmacodynamic* (finding the optimal dose of the drug), *recurrence* (return of the cancer) or *safety biomarkers* (to predict toxicity of the treatment) [23]. In the last decade, multiple biomarkers have been studied in the management of OC [24–26]. However, most valuable and clinically relevant are Cancer Antigen 125 (CA125*)* and Human Epididymis protein 4 (HE4) (**Figure 3**).

CA125 is the golden standard biomarker for OC [27–29]. Assessing the serum levels of CA125 is routinely used to aid differential diagnosis in women presented with pelvic masses [28,30] or to monitor the therapy [8,28]. However, it has low specificity and sensitivity. Elevated serum CA 125 can be found in women during menstruation and pregnancy, in the benign gynecological

conditions (ovarian cysts, myomas and endometriosis), in malignancies (endometrial, breast, colorectal or lung cancer) and in liver and renal failure [28,31]. Utility of CA 125 in early disease detection is questionable as it is elevated only in about 50 % of patients with the stage I disease [29]. In more advanced disease (stage III/IV), CA 125 is elevated in about 85-90 % of patients [29]. The sensitivity of serum CA125 is 74 %, while specificity is 83 % for detection of OC [32].

Human Epididymis protein 4 **(HE4)** as a single biomarker has a highest sensitivity and specificity for detection of OC [33]. HE4 has an important role in differential diagnosis, in prognosis, monitoring the therapy or detection of recurrence [33]. A more recent test, a Risk of Malignancy Algorithm (ROMA) combines the serum CA125 and HE4 with the menopausal status into a score that predicts the risk for cancer [34]. The FDA has approved HE4 in 2007 for detection of recurrence and ROMA in 2011 for distinguishing malignant from benign masses [34]. Measuring HE4/ROMA is more sensitive and reliable than CA125 and it is implemented as a test in conjunction with gynecological examinations in routine clinical practice in certain centers.

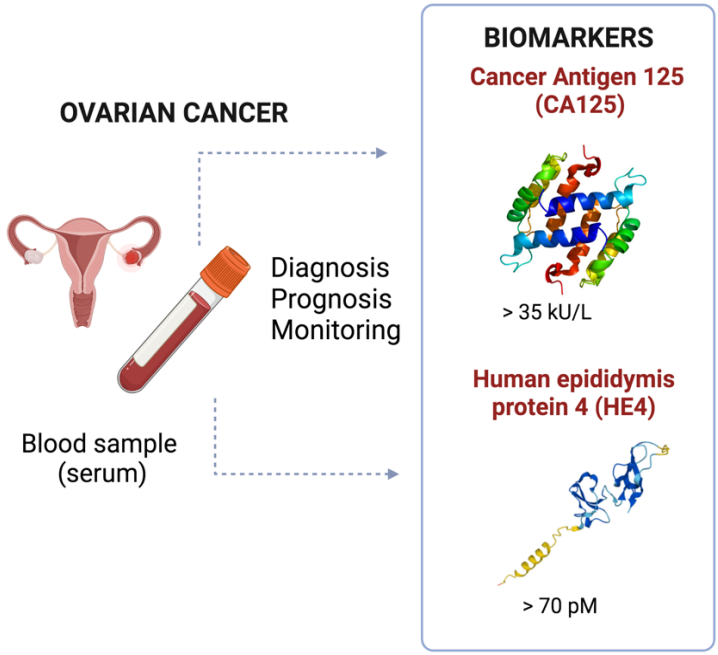

Figure 3. Clinical biomarkers of ovarian cancer. (*Created with Biorender.com)*

2.3. Problematic of current diagnostic approaches

The late diagnosis remains the crucial factor for poor prognosis and high mortality of OC. The lack of awareness of the symptoms is a potential barrier for early visit to the doctors. However, there is little evidence that patient education about OC symptoms can result in detecting early-stage disease [35]. All the diagnostic methods available lack sensitivity and specificity, especially in detecting cancer early. Indeed, pelvic examination has been found to have extremely poor sensitivity (around 5% only) [35]. Adding it to diagnostics procedures either with CA125 or transvaginal ultrasound, does not achieve detection of more cases of OC [36].

Moreover, the screening methods of general or high-risk population do not exist for OC. Despite all the efforts in last decades, neither of the available methods are accurate enough for screening and have failed to reduce the mortality of OC [37].

Potential limitations of currently available diagnostic methods are highlighted in the **Figure 4**:

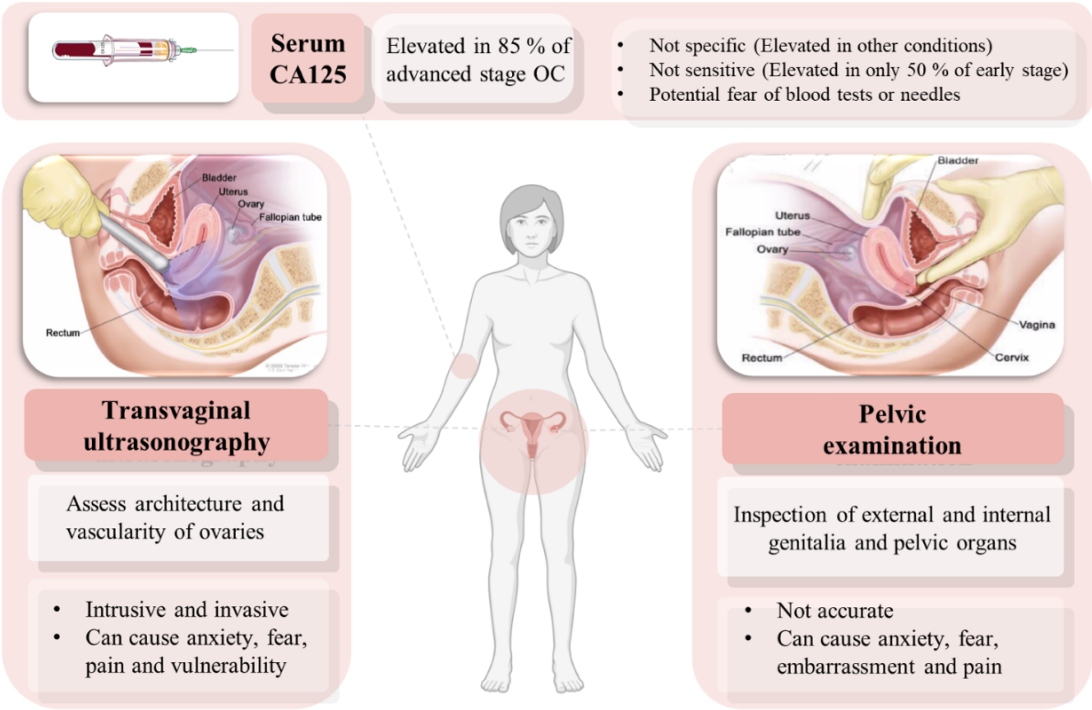

Figure 4. Current ovarian cancer diagnostics with the potential limitations.

Current diagnostic methods include blood test of serum CA125, transvaginal ultrasonography and pelvic examinations, which are not sensitive or specific enough to detect cancer in early stages and can be considered invasive or intrusive for women (*Created with PowerPoint and Biorender.com*).

Moreover, women's concern to attend gynecological exams because of the examination's nature may result in delay or avoidance with a potentially harmful health effects and late diagnosis [21]. For example, ultrasounds have been found to be uncomfortable for some women, who may experience fear and anxiety [38–40].

Recently, the focus has been shifted towards using urine as source of disease information and biomarkers as it is non-invasive and easily available specimen. Indeed, we performed a questionnaire (N=105 participants) about perspective on urine as a sample for OC detection. Interestingly, urine sample was considered most convenient, as half of the participants

expressed their preference for urine (*unpublished data, study in progress*) (**Figure 5**). Moreover, the participants associated current procedures with negative emotions, that would cause the potential delay for seeing a doctor (**Figure 5**). Therefore, using urine as an easy and non-invasive sample could potentially cause increased participation in diagnostics. Therefore, women could get diagnosis and treatment earlier, which could decrease poor prognosis and mortality in future.

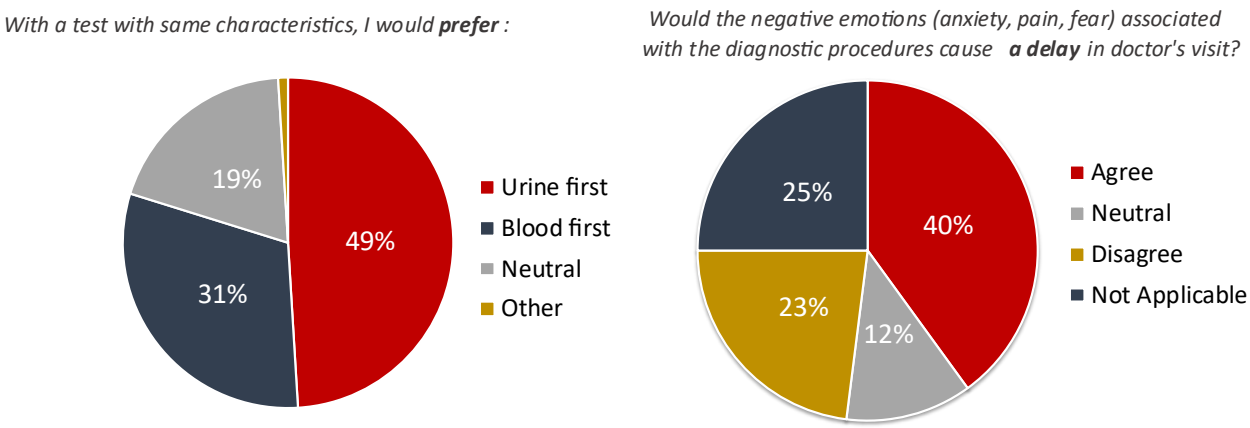

Figure 5. The opinion of sample preference for ovarian cancer detection.

3. URINE AS A SOURCE OF OVARIAN CANCER BIOMARKERS

3.1. Urine as a sample for cancer detection

Urine has emerged as a sample for cancer detection due to the several benefits over tissue or blood. The tissue biopsy is invasive, and bears risks of potential complications and infections. It is a sample taken at specific time point, at specific location, in a case when the location of the primary tumor is known and accessible. On the contrary, urine as a 'liquid biopsy' is non-invasive, always accessible, can be taken multiple times, which enable serial monitoring. The urine has shown potential for easy, quick and affordable cancer detection in numerous cancer types, including bladder, prostate, colorectal, breast and ovarian cancer [41].

Urine has proven beneficial due to ease of access, volume availability, and technical and biological advantages compared to blood. Primary, there is no homeostasis mechanism in urine,

so excreted cancer biomarker levels stay stable, often intact, and therefore reliably reflect the *in vivo* state of the disease [42]. Urine can accommodate more changes in the early-stage of disease, resulting in earlier diagnosis [42]. Urine tests are easy to perform, can used in a self-sampling manner or home setting, without the need for healthcare professionals, opening the door for potential screening strategies. From a technical point of view, urine is cheap and not limited by health status of the individual. It is generally well-accepted samples among patients. The preference for urine tests compared to standard diagnostic methods has been reported in different cancer types, such as bladder and cervical cancer [43,44].

The first step in the any urine test is a collection of a sample that will allow high quality analysis. There are different **urine samples** that can be selected for biomarker detection. *Random urine* is a portion of single voided urine without defining the volume, time of the day, or detail of patient preparation. This is avoidable sample, as urine can be diluted and result in false negative results [45]. *First morning urine* is the specimen voided immediately after an overnight rest before breakfast and other activities. This has been traditionally recommended as the standard specimen for urinalysis, because it is more concentrated and allows time for possible bacterial growth in the bladder [45]. *Time collected urine*, most common 24-hour urine, is a specimen that contains all portions voided over 24 hours [45]. Due to the inconvenience for collection and the intra-individual variations in excretion, an analyte-to-creatinine ratios (for diuresis compensation) have replaced the timed collection [45]. Moreover, urine can differ based on collection time. *Full void* is defined as entire urine flush from start to finish. *First void or first pass urine* is typically first part of urine flush collected at any time of the day. *Midstream clean urine* is collected after discarding the first 10–50 mL of urine, which removes contaminants, so is used as a standard for detection of infections or metabolomics studies [41]. After collection, biomarkers can be detected directly in whole urine without processing, or in the **urine fractions**, such as the supernatant, sediment or exosomal fraction [46]. After centrifugation, the urine sediment at the bottom is removed as it contains cell debris. Typically, cell-free supernatant is used for biomarker detection. Based on the literature review, there is no consensus or guidelines about processing urine [46]. There is either no information reported, or there is high variability in the pre-analytical phase (collection, storage and type of urine sample). Therefore, standardization in the urine fraction choice, processing and method of detection is needed in future [46].

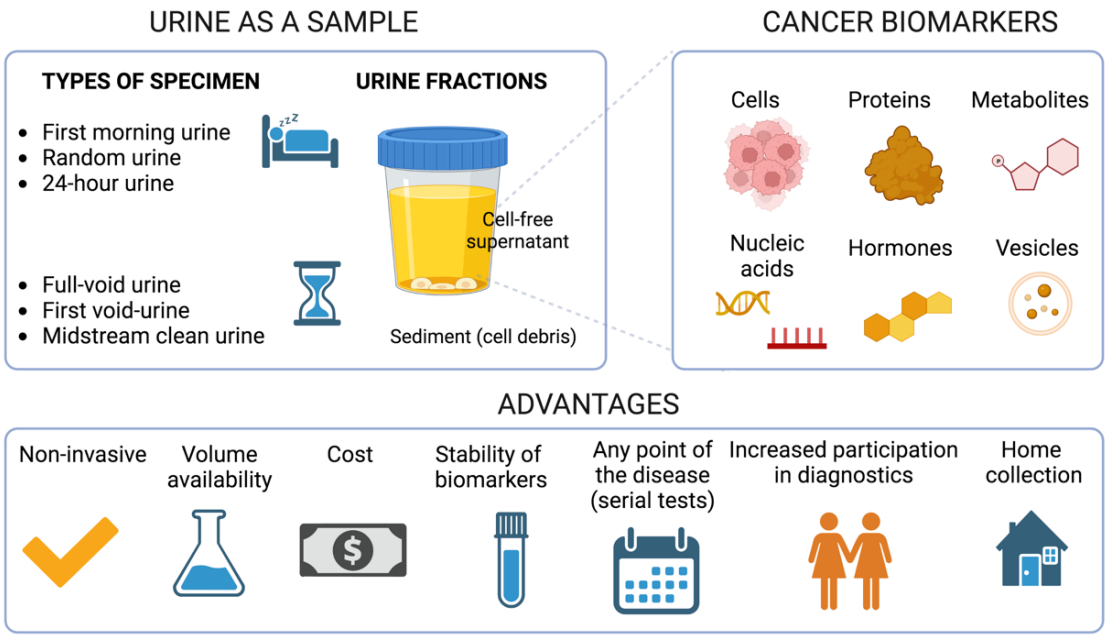

Figure 6. Urine as a sample for cancer detection.

(*Created with BioRender.com*)

3.2. Urinary biomarkers of ovarian cancer: state-of-art

'*Urinomics*' is a growing field in the cancer detection. Indeed, urine contains variety of biomarkers, ranging from proteins, peptides, enzymes, to a small compounds, metabolites or cell-free nucleic acids, such as microRNAs [42,47,48].

Proteins and peptides are most common urinary biomarkers, analyzed by immunoassays or mass spectrometry, either as individual markers or multiple targets combined [47]. Recently, several proteins have been identified in urine of patients and proposed as candidate biomarkers for OC, including WFDC2 (HE4) [49,50], mesothelin (MSLN) [50,51], leucine-rich alpha-2-glycoprotein (LRG1) [52], glycosylated forms of eosin-derived neurotoxin (EDN), COOH-terminal osteopontin fragments [53] or Placental Leucine Aminopeptidase (P-LAP) [54]. Moreover, matrix metalloproteinase (MMP), especially MMP-2 and MMP-9, are investigated as urinary biomarkers for OC [55].

Golden standard CA125 does not seem to be an interesting urine target, which is not surprising due to its huge size. Full-glycoprotein CA125 exhibits a molecular weight of 1–5 MDa and is not expected to pass freely through glomerular membrane [56]. Detected CA125 in urine could be present in fragments, as a result of proteolytic degradation [56]. Although CA125 has been

found in urine of patients, it lacks specificity and sensitivity [47]. Indeed, even by combining urine CA125 with other biomarkers, such as MSLN, the specificity is lower than 40 % for detection of OC [47,57]. The MSLN is a promising urinary biomarker, found to be elevated in OC [51]. Moreover, urine mesothelin provides higher sensitivity than serum mesothelin for early-stage OC, with a specificity of 95 % and sensitivity 68 % [51]. Some of the examples of urinary biomarkers for OC detection are presented in **Figure 7**:

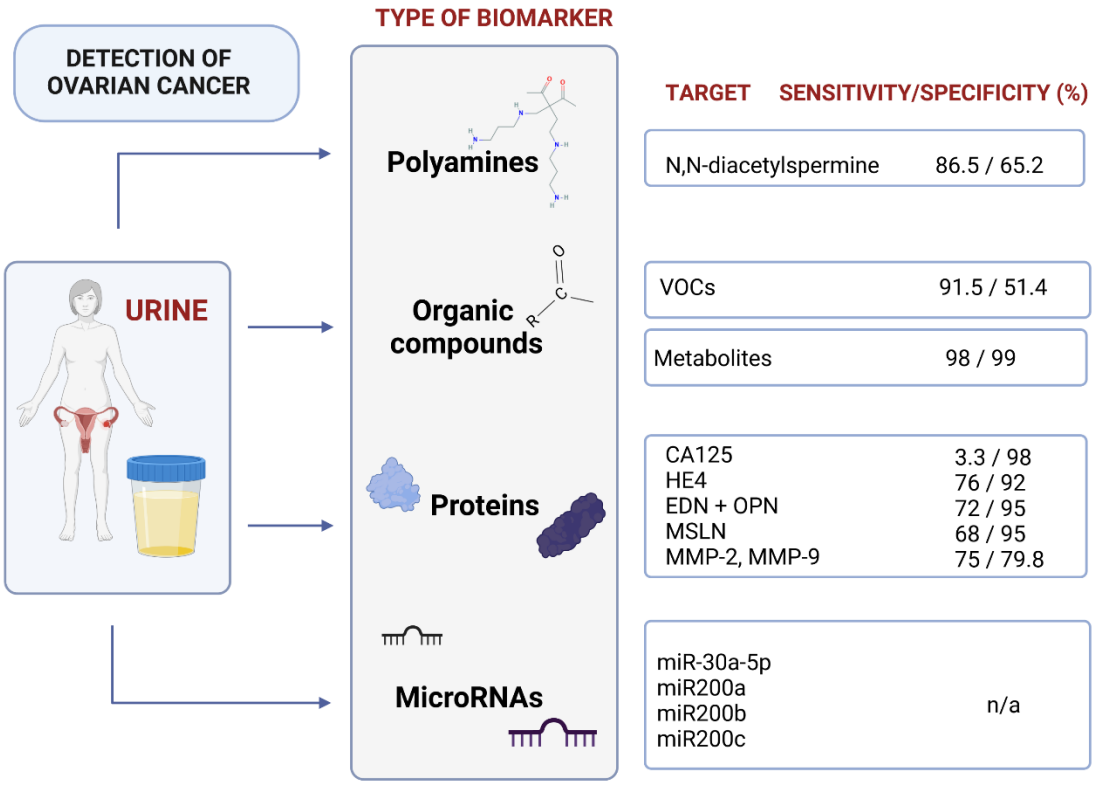

Figure 7. Ovarian cancer biomarkers found in urine.

Urine of ovarian cancer patients contains various classes of markers of disease, including proteins, peptides, microRNA, polyamines or organic compounds. This figure shows the target molecules studied for detection of cancer in urine with corresponding diagnostic sensitivity and specificity. (*Created with BioRender.com*).

Different **metabolites** and organic compounds have been studied. For example, the upregulation of metabolic pathways that support cell proliferation was identified in urine, with an increase concentration of succinic, fumaric, glutamic acid and glutathione [58]. The phenotype of metabolites was found to be different between OC and healthy individuals and could offer early-phase diagnosis [59]. Moreover, urinary polyamines, such as N, N-diacetyl spermine was found to be elevated in malignant, but not in benign disease (Niemi et al. 2017). **Volatile organic compounds** (VOC) were also studied as potential targets in urine, and could

distinguish OC from benign or healthy individuals, as well as differentiate high-grade and low-grade OC [60]. However, more research is needed in this area in order to validate cancer specific biomarkers.

Recently, the **small non-coding RNAs**, called microRNAs emerged as non-invasive urine biomarkers for OC [46]. Indeed, microRNA-30a-5p was proposed as a diagnostic and therapeutic biomarker, upregulated in urine of OC patients [61]. In addition, the upregulation was associated with the clinical stage [61]. Another example of urine microRNA is miR-92a [62] or microRNA-200 family [63], which have been reported in urine of patients. However, all these biomarkers are still in the research phase, detected in a small number of patients, lack specificity and sensitivity, and need to be further investigated.

HE4 is the most sensitive and most extensively researched biomarker found to be elevated in urine of OC patients in multiple independent studies [49,64,65]. It has the highest discriminatory power to distinguish malignant disease from benign or healthy individuals, with a specificity of 98 % and sensitivity of 76 % for OC detection [49]. Therefore, it has been chosen as the most promising urine biomarker and target for this thesis.

4. HUMAN EPIDIDYMIS PROTEIN 4 (HE4)

4.1. Biochemistry and the biological roles of HE4 protein

Human Epididymis protein 4 (HE4) is a secreted glycoprotein known for its overexpression in ovarian cancer. The HE4 protein is encoded in *HE4* or whey-acidic-protein four-disulfide core domain protein 2 (*WFDC2)* gene, located on chromosome 20q12 [66]. The gene encodes a small protein , also known as WAP-four-disulfide core domain protein 2, which belongs to the whey acidic protein (WAP) domain family [66]. The HE4 is disulfide-linked homotrimer post-translationally N-glycosylated on asparagine [67,68]. The WFDC domain, or WAP Signature motif, contains eight cysteines forming disulfide bonds [69]. Depending on the post-translational modifications, the molecular weight of the HE4 ranges from 11–25 kDa [69].

HE4 was first identified in 1991 in the distant epididymis [70], originally predicted to be a protease inhibitor involved in spermatogenesis or sperm maturation [70,71]. HE4 protein can have low expression in a normal tissues, including male reproductive system (epididymis and vas deferens), female reproductive system (fallopian tubes, endometrium, and endocervix), in the

respiratory tract, nasopharynx and salivary glands [72–74], where it has HE4 has a broad range of protease inhibitor activity [68,71]. Therefore, it has a presumptive role in the physiological processes of the antibacterial response and immunity [73]

Since 1999, when HE4 gene overexpression in OC tissue was discovered using cDNA microarrays, HE4 became well known as a biomarker of OC [72,75]. HE4 is overexpressed in OC, but not in healthy ovaries or benign conditions, which was confirmed by numerous independent studies [76,77].

It has been shown that overexpression of HE4 is implicated in several biological roles in the pathogenesis of OC (**Figure 8**). It has been shown that ovarian cells treated with recombinant HE4 exhibit higher growth, greater viability and resistance to chemotherapy [78,79]. Overexpression of HE4 enhances proliferation and metastatic potential [80], resulting in reduced survival [81]. Moreover, expression levels correlate with lower survival and chemoresistance in human patients [81]. HE4 has been connected to oncogenic signaling cascades that play key roles in ovarian cancer progression. (**Figure 8**) [79].

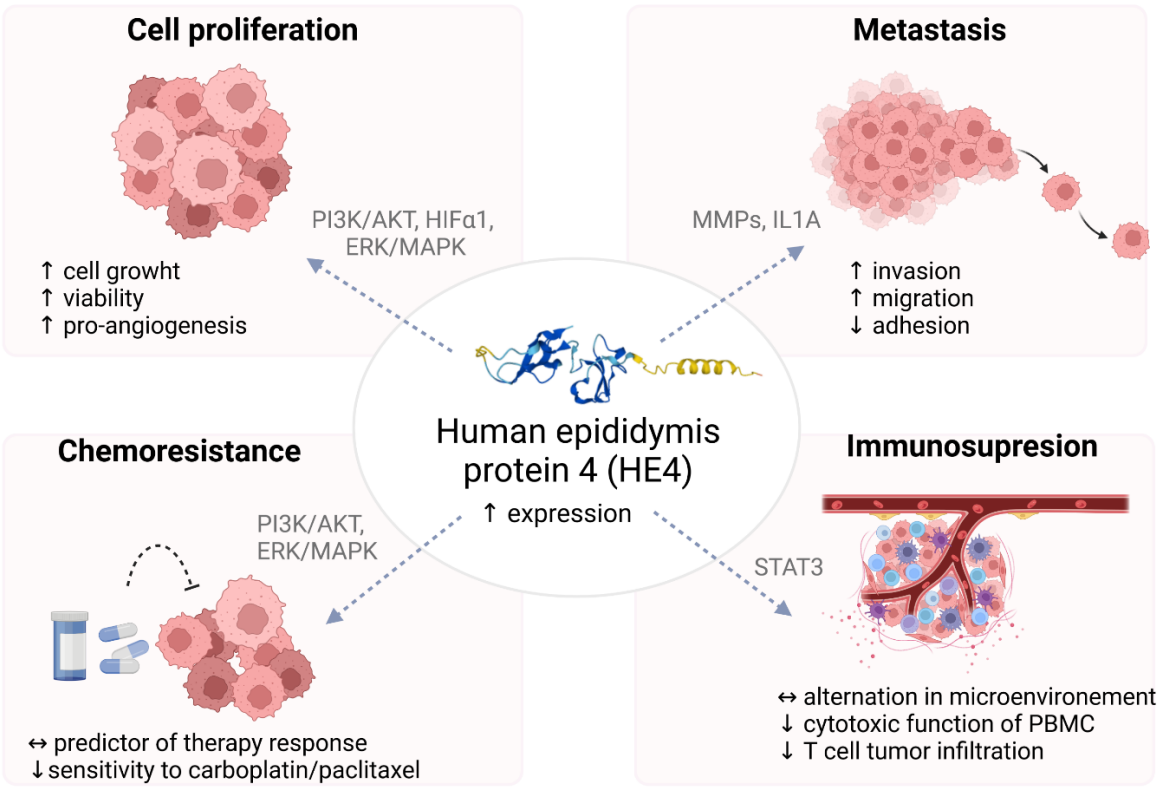

Figure 8. The structure and the role of HE4 in the pathogenesis of ovarian cancer. (*Created with BioRender.com*)

Elevated HE4 suppresses the cytotoxic function of mononuclear cells against the cancer [79]. Therefore, HE4 promotes a pro-angiogenic and immunosuppressive tumor microenvironment [79]. Moreover, high levels of HE4 levels are present in individuals who are resistant to chemotherapy [82,83].

4.2. HE4 as diagnostic biomarker of ovarian cancer

The serum HE4 is a biomarker with roles in differential diagnosis, in prognosis, monitoring the therapy or detection of recurrence [33]. The first double determinant 'sandwich' ELISA was constructed in 2003 by Hellstrom *et al*. for detection of HE4 in human serum. Results indicated that serum from women with OC were likely to have a positive test result compared to healthy or women with benign ovarian diseases [76]. Since then, many independent studies have reported serum HE4 levels in patients with superior sensitivity and specificity than the serum CA125 [84].

The HE4 serum levels in healthy women range from 60 pmol/L to 150 pmol/L with the relationship between HE4 serum levels and increasing age [85]. Therefore, *cut-off* is often clinically considered > 60 pmol/L for premenopausal and > 170 pmol/L for postmenopausal women [85,86]. The HE4 in serum has been identified in mesothelioma, endometrial, pulmonary, and breast cancer, but less frequent [29,87]. The false-positive results is in case of renal failure where HE4 is > 2000 pmol/L. [88,89]. Therefore, HE4 is highly specific for OC. Indeed, it is overexpressed and significantly elevated in serum (≥70.0 pmol/L) in all subtypes [29]. The highest concentration is present in serous, following mixed, endometrioid, clear cell and lowest in mucinous OC [90]. Moreover, serum HE4 is elevated across all stages of OC, with increasing concentration with stage, reflecting a correlation of HE4 expression and tumor burden [90].

According to the guidelines of *European Group on Tumor Markers* [29], HE4 can be used clinically in differential diagnosis and prognosis. As a single marker, HE4 had the highest sensitivity for detecting OC, especially in stage I diseases, the early non-symptomatic stage [57]. HE4 can offer advantages over CA125 in terms of specificity, as there is no variation in serum HE4 concentrations during the menstrual cycle [91]. Therefore, HE4 can be measured at any phase of the cycle and during contraceptive use [91]. Moreover, the level of serum HE4 is decreased during pregnancy, which means HE4 remains as a marker for OC [92]. The serum HE4 has great diagnostic accuracy in differentiation between OC and healthy individuals, with sensitivity of 83 % and specificity of 90 % [93]. Indeed, serum HE4 has been found superior to

CA125 in detection of OC [85,89]. Moreover, elevated HE4 is as strong independent indicator of poor prognosis [94]. Moreover, high levels of HE4 levels are present in individuals who are resistant to chemotherapy, and therefore is predictive indicator of response [33,83]. All considered, HE4 alone or in combination with CA125 in ROMA can be considered for differential diagnosis of pelvic masses, especially in premenopausal patients [29,30]. Detection of HE4/ROMA improved the specificity and sensitivity for detection of OC [30,92]. Recently, urine has become interesting as a source of HE4 and the value of urinary HE4 in the diagnosis of ovarian cancer as a non-invasive alternative is extensively investigated.

4.3. Diagnostic value of urine HE4 in ovarian cancer

As a secreted protein, HE4 can be easily detected in body fluids, including urine. The small molecular weight of 11 kDa, which is below the normal glomerular filtration *cut-off*) allows the HE4 to be excreted and detected in urine. Elevated HE4 levels were previously detected in urine of OC patients, using mass spectrometry [50] or immunoassays [64,65,95]. It is generally thought that urinary HE4 is derived from serum, and as a result, the changes in urine HE4 levels could reflect those in serum HE4 levels [96]. The serum *vs*. urine as a sample have comparable ability to detect OC and discriminate cancer from healthy or benign conditions [65]. However, based on the literature research, there is no correlation between concentration of HE4 in urine compared to serum. It appears than levels of HE4 in urine are 2-3 times higher than in the blood (example in OC HE4 in serum > 60 pmol/L compared to urine > 13 000 pmol/L) **(Table 2 and 3).**

Table 1. Urinary HE4 levels in healthy woman and ovarian cancer patients.

The values are based on the approximate estimation based on the available studies.

Status	Healthy	Cut off value	Stage I/II	Stage III/IV
Urine HE4 (pmol/L)	6 000	13 000	16 000	24 000

Therefore, the hypothesis is that excretion to urine represents the primary mechanism of HE4 elimination from the body, so levels of are higher in the urine. Accumulation in urine can facilitate detection and enable earlier diagnosis as HE4 could be elevated earlier in the course of the disease. Moreover, diagnostic accuracy is similar and urinary HE4 can achieve the same sensitivity and specificity as serum [49]. Therefore, urine can represent an alternative, less invasive source of HE4 compared to serum, with easier detection due to elevated concentration.

Table 2. The summary of all studies of urine HE4 detection in healthy individuals or ovarian cancer patients with corresponding methodology and clinical samples.

Biomarker	Range of HE4 detection (pmol/L)	HE4 detection method	Urine dilution	Subjects	*Cut-off* value	Specificity/Sensitivity	Reference
HE4/CRE ratio	n/a	EIA (Fujirebio Diagnostics Inc., USA)	1:40	92 ovarian cancer; 82 benign conditions; 60 healthy controls	3.5 5.0	Specificity 95 % Specificity 98 %	Liao *et al.* [65]
HE4 **HE4/CRE ratio**	10 - 10 000	EIA (Fujirebio Diagnostics Inc., USA)	1:40	79 ovarian cancer; 20 benign conditions; 36 healthy controls	n/a	Specificity 100 % Sensitivity 73,3 % (OC I/II) Sensitivity 87,5 % (OC III/IV)	Hellstrom *et al.* [64]
HE4	43,8 - 2808,6	microchip ELISA	1:20	19 ovarian cancer, 20 healthy controls	43,81 pmol/L	Specificity 90 % Sensitivity 84,2 %	Wang *et al.* [97]
HE4	8–13 000	CMIA (Abbott Architect, Abbott Laboratories, USA)	1:100	23 ovarian cancer; 37 benign conditions 18 healthy controls	13 000 pmol/L	Specificity 75 % Sensitivity 78,3 %	Macuks *et al.* [98]
HE4	15–1500 (or dilution for high concentration samples)	ECLIA (Roche Cobas 800 e602, Roche Diagnostics, China)	Variable	31 ovarian cancer; 38 chronic kidney disease; 36 healthy controls	14 116 pmol/L	Specificity 100 % Sensitivity 83,9 %	Fan *et al.* [95]
HE4 **HE4/CRE ratio**	n/a	EIA (Fujirebio Diagnostics Inc., USA)	no	72 ovarian cancer or low malignant potential tumors; 160 benign disease controls	HE4: 19 161 pmol/l HE4/CRE: 152,5	HE4 Specificity 89,4 % Sensitivity 65.3 % HE4/CRE Specificity 93.1 % Sensitivity 70.8 %	Zhong-Qian *et al.* [99]
HE4	n/a	Mass spectrometry	n/a	20 ovarian cancer	n/a	n/a	Sandow *et al.* [50]
HE4/CRE	0 — 25 000	EIA (Fujirebio Diagnostics Inc., USA)	no	22 ovarian cancer; 10 borderline ovarian mass; 10 benign conditions; 11 healthy controls	0,89	Specificity 95 % Sensitivity 68 %	Stiekema et al. [100]

** n/a - not applicable (not reported);* ***CRE*** *(creatinine);* ***EIA*** *(Enzyme ImmunoAssay);* ***ELISA*** *(Enzyme Linked ImmunoSorbent Assay);* ***CMIA*** *(Chemiluminescence Microparticle ImmunoAssay)*

Many studies focused on diagnostic value of urine HE4 alone, while some use ratio of HE4 and creatinine (CRE) for normalization of urine volume. Up to date, elevated HE4 levels are found in urine OC patients and are highly specific for OC. It has not been found in other malignancies, except in endometrial cancer [101], but its diagnostic value is still to be evaluated. In 2010, Hellstrom *et al*. first reported that measuring HE4 in urine can identify patients with OC with similar sensitivity as serum measurement [64]. Indeed, urine HE4 alone or ratio HE4/CRE are shown to be useful in discriminating ovarian malignancy from healthy controls. Urinary HE4 is elevated in the urines of women with both early and late serous OC as compared to healthy and benign gynecological diseases. At the specificity of 100 %, 73,3 % of early stage (I//II) patients were positive, and 87,5 % of advanced stages (III/IV) were positive for urine HE4, respectively [64]. In a study by Liao *et al.*, HE4 levels were measured in urine from normal donors, borderline tumors and OC. In addition, HE4 levels were correlated with clinical characteristics. The ratio of urine HE4/CRE could discriminate between cancer and healthy controls. Urine HE4 from women with serous OC were positive more frequently than other subtypes [65]. Archived samples of serum and urine obtained on the same day were tested for HE4 and achieved similar results, suggesting that urine can be used as a non-invasive alternative for HE4 testing [65]. In a recent study by Stiekema *et al.*, HE4 was measured in different body fluids, including serum, urine and ascites of OC patients, benign or borderline conditions and healthy controls. HE4 can be successful detected in all body fluids. HE4 concentration in urine was significantly higher in patients with OC compared to healthy controls, benign or borderline. HE4/CRE ratio could differentiate both healthy or benign controls from EOC with high diagnostic value [100]. Another study demonstrated that HE4 level or HE4/CRE as potential biomarkers for the detection of OC. The HE4/CRE ratio appeared to be better than the HE4 level in correlating with the clinical pathological diagnosis of EOC [99]. In study by Fan *et al.*, diagnostic value was studied for serum HE4, urine HE4 and urine-to-serum HE4 ratio. Urinary HE4 levels could discriminate OC patients from healthy controls and patients with chronic kidney disease, with a specificity 100 % and sensitivity of 83,9 % [95]. In fact, measuring just urine HE4 achieved higher sensitivity and specificity than serum HE4 or urine-to-serum HE4 ratio [95].

Areas in which urine HE4 could offer advantages over serum HE4 are prediction of chemotherapy response, detection of recurrence and detection of low malignant potential (LMP) tumors [65]. The serial measurements of serum CA125, serum HE4 and urine HE4 in patients with OC revealed that blood levels for both CA125 and HE4 decrease in response to

primary surgery and chemotherapy, irrespective of platinum response. However, patients who proved to be platinum resistant, had stable high urine HE4 levels over the longer period of time, while those who proved to be platinum sensitive had decreased urine HE4 levels, indicating that urine HE4 levels could be useful tool for early identification of platinum resistance [65].

In patients who achieved clinical remission after primary treatment, serum CA125 and HE4 and urine HE4 levels were assessed. Patients who had no evidence of disease following cytoreductive surgery and adjuvant chemotherapy but later relapsed, had urine HE4 levels elevated earlier in the course of the disease. In fact, urine that was positive for HE4 before serum became positive for HE4 or CA125 prior to clinical diagnosis of relapse [65]. Therefore, urine HE4 could be useful tool in follow up and detection of recurrence.

Urine HE4 levels have ability to detect a special type of borderline ovarian tumors, called low-malignant-potential (LMP) tumors. The serum and urine HE4 levels were measured on archived samples of healthy individuals, LMP tumors and OC. It was shown that assaying urine and serum has similar sensitivity in healthy individuals and OC patients. However, urine samples from women with LMP are more frequently positive for HE4 than concomitantly obtained serum samples which did not differ from controls [65]. Further studies are needed to learn whether the women who have positive urines are at greater risk to develop cancer.

With a feasibility, stability and high diagnostic accuracy, non-invasive urine HE4-test could be effective in detecting OC early and improving the poor prognosis.

5. APTAMERS

5.1. Introduction to nucleic acid aptamers and their characteristics

The aptamers are small RNA or single stranded DNA oligonucleotides that bind with high-affinity and specificity to a wide range of target ligands, including metal ions, small molecules, proteins, whole cells or microorganisms [102]. Aptamers were first introduced in 1990 as a class of novel affinity ligands when three independent groups presented the *in vitro* method for selection of nucleic acid sequences capable of binding to target with high specificity [103–105]. The proposed method was called SELEX (Systematic Evolution of Ligands by EXponential enrichment) and the oligonucleotides were called aptamers, originating from the Latin for '*aptus*', meaning adapted to [103–105]. The aptamers typically have a size ranging from 6 to 40 kDa, with the typical length ranging from 20 to 60 nucleotides [102].

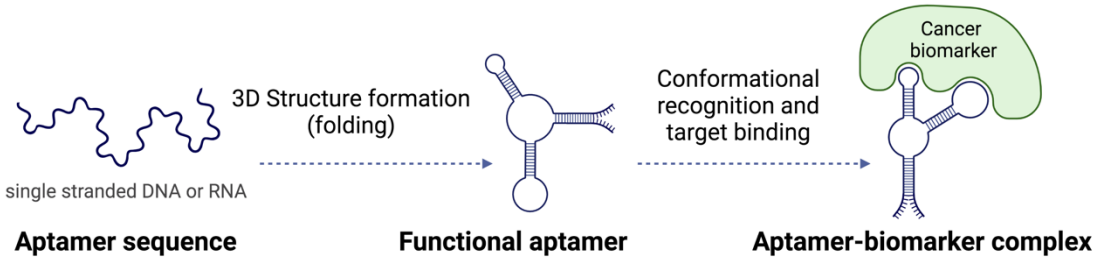

Figure 9. Aptamer structure and the conformational target binding.

Single-stranded DNA or RNA aptamers fold into specific three-dimensional structures responsible for binding to target cancer biomarkers with high-affinity (*Created with BioRender.com*).

The aptamers can include various types of nucleic acids. Most commonly they are non-coding, synthetic RNA or ssDNA sequences. However, the field has drastically expanded by the introduction of the different chemical modifications into the sugar-phosphate backbone modifications during selection, with examples of locked nucleic acids (LNA), threose nucleic acid (TRA), fluoroarabino nucleic acids (FANA) 1,5-anhydro hexitol nucleic acids (HNA) or Slow Off-rate Modified Aptamers (SOMAmers) [106]. Moreover, they can be chemically modified post- selection, with unlimited possibilities of conjugation with various chemical groups or fluorophores [107].

The first decade of aptamer research and development was marked by the dominance of the RNA aptamers [106,107]. It was believed that only RNA molecules can have motifs and secondary structures responsible for recognition of the target. Since demonstrating the ability of single-stranded DNA to fold into functional spatial structures, including G-quadruplex, loops and hairpins, distribution became opposite [103,108]. In the last decade, majority of the aptamers are DNA, probably due to their superior stability and resistance to nucleases.

The aptamers as a class of molecules for target recognition in a wide range of applications are studied as a substitute for antibodies, because they have several advantageous features [109]:

(1) *Production of aptamers:* The identification and production of monoclonal antibodies are laborious and expensive processes that require the use of animals [109]. On the contrary, the aptamer development process is completely *in vitro*. The production of polyclonal antibodies has high variety from batch to batch. Monoclonal antibodies can be more uniform, but they are difficult and expensive to produce. The aptamers are rapidly produced on a large scale ensuring homogenous batches. The aptamers chemical synthesis is easy, low cost and reproducible [102].

(2) *Target choice*: When producing antibodies, protein target needs to be different from any endogenous proteins to induce an immune response in animals. Therefore, the protein target needs to be big enough to be immunogenic and has to be non-toxic to host animals. When selecting aptamers, there are no limitations in target choice either in type of size. Aptamers can be selected to proteins, but also to small molecules, DNA, whole cells or organisms [102].

(3) *High-stability:* Nucleic acid aptamers, especially DNA-based, are extremely stable and resistant molecules. It is well known that proteins are easily denatured and lose their tertiary structure at high temperatures, while oligonucleotides are more thermally stable and can maintain their structures over repeated cycles of denaturation/renaturation [109]. Therefore, they can be reused, while antibodies will undergo irreversible denaturation [109]. Aptamers in the lyophilized or dehydrated form can be stable for years, whereas antibodies are very sensitive to temperature changes, storage conditions and susceptible to degradation [110,111].

(4) *Chemical modifications:* Aptamers can be easily chemically modified to enhance the affinity or binding characteristics [112]. Nucleic acid chemistry is suitable for any type of structure modification, whereas antibody modifications are complex and expensive.

There are limited possibilities of modifying antibodies. Due to their simple structure, aptamers are easily modified, enabling optimization of their clinical properties in therapeutics (ex. resistance to nuclease degradation or increased half-life *in vivo*) or diagnostics (ex. stability and resistance to nucleases in serum and urine) [113]. Aptamers can be linked with drugs, radioisotopes, nanostructures to specifically deliver agents for targeted therapy [114]. In the diagnostic aspect, the same aptamer can be modified for applications in various diagnostic tests, offering multiple detection options. For example, diagnostic aptamer tools can be biotinylated, florescence labeled, coupled with dyes or enzymes, without loss of the binding affinity [115].

Table 3. Comparison of aptamers and antibodies.

Feature	Aptamers	Antibodies
Production	*In vitro*	*In vivo*
Development conditions	Variety of conditions	Limited to physiological conditions
Required animal use	No	Yes
Selection of target protein	No limitations of target protein	Nontoxic and immunogenic protein
Protein target site	Determined by research	Determined by immune system
Protein specificity and stability	High Kd pM-nM range	High Kd pM-nM range
Molecular weight	5–25kDa	125 kDa
Stability	Stable	Sensitive
Usability to temperature variations	Stable	Sensitive
Shelf life	Years (especially dehydrated or lyophilized)	Limited
Chemical modification	Easy	Difficult
Pharmacokinetic modifications	Easy	Difficult
Immunogenicity	Not reported	Yes
Quality control/reproducibility	No variations batch-batch High reproducibility	Variations batch-batch Low reproducibility

The main characteristics of aptamers are defined by their chemical nature. As nucleic acids, they have a significant negative charge and can be susceptible to nuclease degradation and surrounding conditions (pH and the presence of various ions). These conditions can influence the stability of their secondary structure, thus can affect binding to their target [106]. Therefore, it is important to ensure the proper conditions during their development depending on the final application. Moreover, aptamers can be chemically modified to improve their characteristics, such as stability or affinity, making them desired therapeutic and diagnostic tools in various biomedical applications.

5.2. Applications of aptamers in health and cancer

Over the past decades, aptamers have found their way in a variety of applications in human health. They have been used in multiple diagnostic and therapeutic aspects (**Figure 10**), ranging from being therapeutic agents, drug delivery tools, for tissue or *in vivo* imagining, as detection tools for cell capture, biomarker detection or diagnostic tools in biosensors and tests [112,113,115]. In the last decade, aptamers as therapeutics are gaining popularity, with the several candidates that already entered clinical trials. Currently, only one FDA-approved **aptamer therapeutic** is Pegaptanib, used for a treatment of age-related macular degeneration; which targets vascular endothelial growth factor (VEGF)-165, the protein responsible for pathological ocular neovascularization [116]. In the context of tumor treatments, several aptamers have entered clinical trials as well. For example, *AS1411*, aptamer that bind to target protein nucleolin and show the ability to inhibit proliferation and induce cell apoptosis in several cancer types, including lung, breast, kidney and liver cancer [117]. Another example is *NOX-A12*, L-RNA-PEG aptamer in phase II phase for treatment of chronic lymphocytic leukemia. This aptamer is the antagonist of chemokine ligand 12 (CXCL-12) and inhibits tumor cell proliferation and metastasis [118].

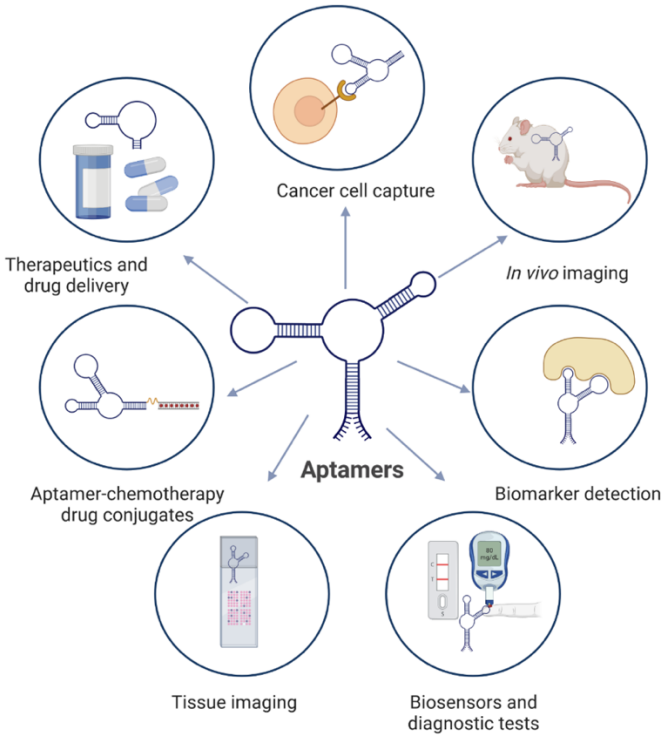

Figure 10. Biological applications of the aptamers.

(Created with BioRender.com)

In the context of cancer diagnostics, numerous **diagnostic aptamers** have been developed for cancer detection, in almost all cancer types, including breast, ovarian, kidney, bladder, prostate, lung, etc. [112,119]. For example, high-affinity aptamers for applications in diagnostic tests have been developed for detection of breast cancer, targeting biomarkers Cancer Antigen 15-3 (CA-15) and Carcinoembryonic antigen (CEA) [120]. The target with the highest number of aptamers developed is Human Epidermal growth factor Receptor 2 (HER2). This is likely since HER2 is only overexpressed in breast cancer and indicates a very specific diagnosis [112] Recently, an observational clinical trial was conducted for bladder cancer detection, aiming to develop molecular sensors specifically for urinary biomarkers of bladder cancer [112].

As illustrated below (**Figure 11**), aptamers can be applied in numerous formats of biosensors or diagnostic tests for cancer detection [121]. For example, surface plasmon resonance (SPR) aptamer biosensor has been developed for detection of lung cancer, by targeting exosomal epidermal growth factor receptor (EGFR) and programmed death ligand 1 (PD-L1) as biomarkers [122]. Another example is SPR sensor for detection of breast cancer, by targeting HER2 protein [123]. Moreover, the aptamer-based fluorescent sensors for the detection of cancer biomarkers have received significant attention because of the high sensitivity, simple operation, quick reaction, and ability to provide in situ and real-time information [124]. This type of sensor has been developed for prostate cancer biomarker PSA; and for a broad-spectrum cancer marker CEA for diagnosing malignancy, including colorectal, pancreatic, ovarian and gastric cancer [125, 126].

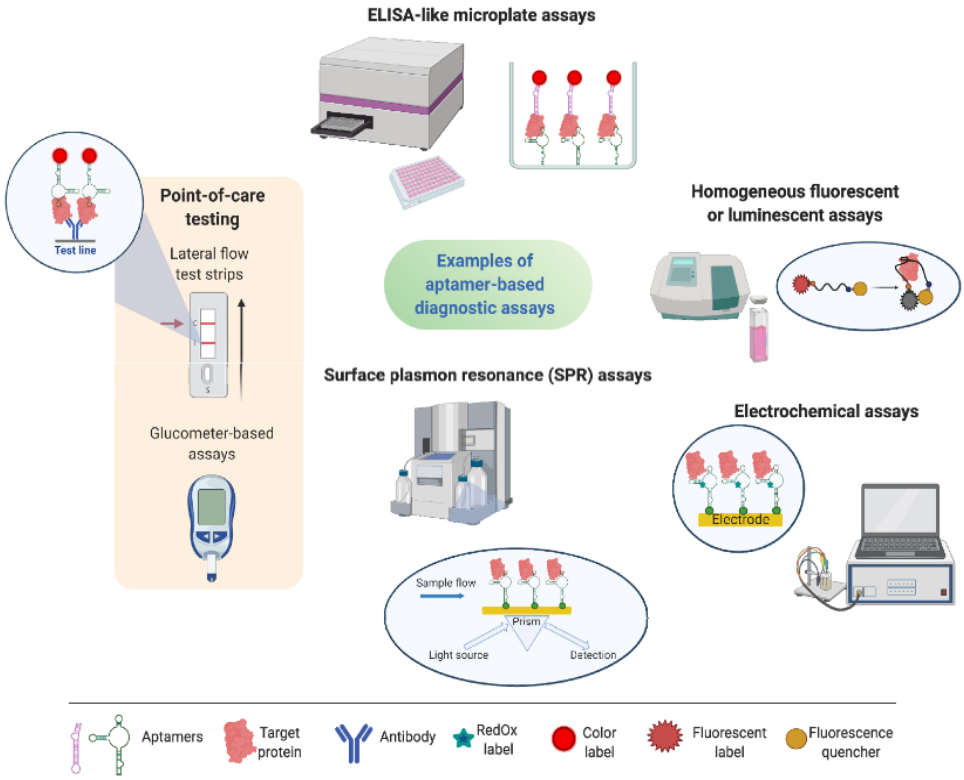

Figure 11. Aptamer-based diagnostics and biosensors for detection of cancer biomarkers.

(From Shatunova et al. 2020)

5.3. Development of the aptamers

The development of the high-affinity aptamers require several steps prior their biological application. Aptamers are obtained by the **selection** of target-binding species from a large library of random oligonucleotides by the method **SELEX** (*Systematic Evolution of Ligands by EXponential enrichment*). After multiple rounds of repeated selection to target molecule, candidate sequences are identified through nucleic acid sequencing and analyzed using bioinformatics. After identification of the several candidate aptamers, those sequences will be subjected to detailed characterization of binding to target molecule. The characterization will obtain affinity, specificity and kinetics of the aptamer-target binding. Once characterized, from all the candidates, one or few aptamers will be chosen for desired application, either as potential therapeutic agent or diagnostic probe. The pipeline of aptamer development from selection to application is illustrated in **Figure 12**.

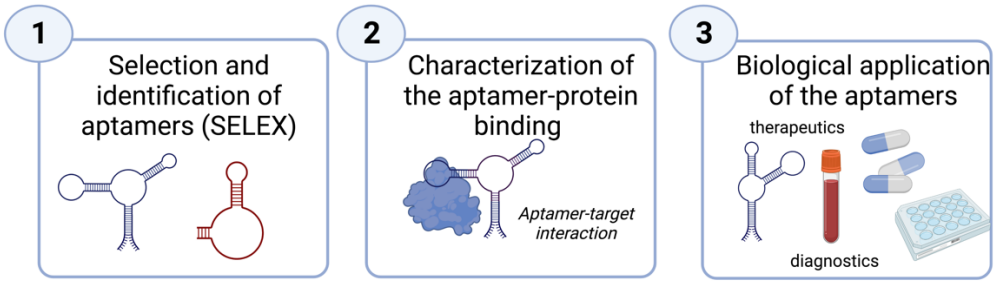

Figure 12. Aptamer development process. (*Created with BioRender.com*)

Throughout the last three decades, variations of SELEX protocol have been applied thousands of times to obtain aptamers for diverse targets and applications. Some of the examples of variations of the methods to different targets include Capture-SELEX (against small molecules) [127]; protein-SELEX (against protein targets) or cell-SELEX (against whole cells)[128]. Depending on the type of immobilization approach, there is magnetic-SELEX (where targets or aptamers are immobilized on magnetic beads) [129], nitrocellulose-SELEX (where targets or aptamers are immobilized on nitrocellulose membrane) [129], or capillary electrophoresis (CE-SELEX) (where selection is performed in tiny capillary) [130].

The classic SELEX procedure starts with a design of a random **ssDNA or RNA library** constituted of millions random sequences [102]. The characteristics and the particular application of the aptamers can influence the choice of the sugar backbone and potential modifications. RNA and ssDNA aptamers can differ from each other in sequence and folding pattern, although they could bind to the same target [131]. The typical aptamer library ranges from 20 to 100 nucleotides (nt) in length, consisted of a random region flanked by two fixed regions. The random region is usually responsible for specific target recognition and binding, while the fixed regions are primer-binding sites required for the amplification [132]. However, influence of the primer regions on the aptamer structure can be aptamer-dependent. The randomization of the sequence provides a diversity of 4^n (n = number of bases in the random region) generating up to ~10^{16} diverse sequences [132]. It is important to ensure optimal size of random region, by maintaining the balance between the diversity of the sequences and the required complexity of the spatial structures they can produce. The most prevalent size is 30–50 nt in length [102,106]. Library can be modified for enhanced stability and resistance, for example by 2′-amino pyrimidines or 2′-fluoro pyrimidines modifications [132].

The overview of the SELEX method is presented in the **Figure 13**. The process consists of a multiple rounds of (1) the incubation of the folded library with the target ligand (small molecules, proteins, whole cells, microorganisms). The intramolecular forces within the aptamer enable formation of a three-dimensional structures responsible for binding to the target. The specific aptamers are bound, while the non-specific sequences are removed by (2) washing steps. Specific bound aptamers are (3) recovered and (4) amplified by polymerase-chain-reaction (PCR) for DNA aptamers or RT-PCR followed by *in vitro* transcriptions for RNA aptamers [132]. After PCR, PCR products (amplified aptamers) are double-stranded DNAs that are (5) recovered back to single-stranded DNAs for the next round of SELEX. Finally, the recovered ssDNA or RNA is used as input for next cycle and the process is repeated [132].

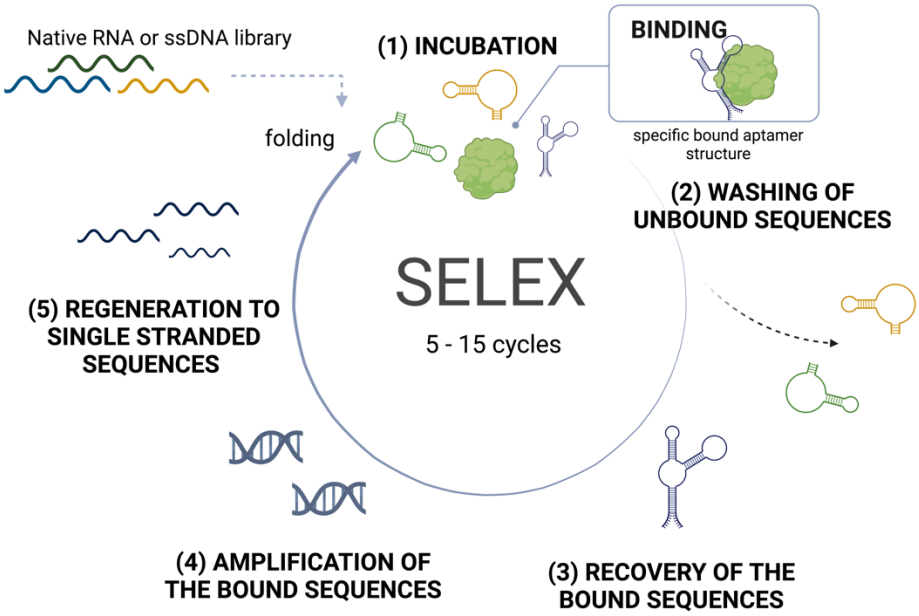

Figure 13. The representation of the SELEX method for selection of aptamers.

Typically, 5–15 cycles of selection are required to obtain high-affinity aptamers enriched to the target [102]. During this iterative process, the aptamer pool can also be *counter-selected* (to a molecule similar or related to target) or *negative-selected* (no target, sample matrix) where the pool is incubated with unwanted targets in order to deplete it of non-specific binders [102].

After multiple rounds of target selection and enrichment, aptamer pools will show increase binding affinity and begin to converge to specific sequences [132]. In the classic method, the resulting enriched nucleic acid pool is cloned into bacterial system and Sanger-sequenced with

the aim of determining a few candidates for the characterization [102]. With the advances in the Next-Generation-Sequencing (NGS) technologies, this approach is considered a time-consuming and obsolete today. NGS offers benefits over Sanger sequencing with earlier identification of more candidates [133,134]. Besides this, it provides maximum information on pool evolution and monitoring the SELEX progress [102]. On the other hand, NGS produces huge amount of data, which requires bioinformatic analysis and specialized softwares [102].

Once the candidates are identified, they are chemically synthesized and characterized. As a prerequisite for application, aptamers must be subjected to **binding characterization**, to determine the affinity, stability and biophysical features [107,135]. Central importance is to determine binding parameters of the aptamer-target interaction, including binding affinity and kinetics. The strength of the affinity of an aptamer for its target is characterized by dissociation constants K_d [136]. The smaller the value of the K_d, the stronger the binding reaction is. Typically, low affinity interactions will have dissociation constants on the order of μmol/L, while high affinity interactions have them on the order of nmol/L [136]. Some of the commonly utilized characterization techniques include fluorescence-based methods, fluorescence anisotropy (FA), Surface Plasmon Resonance (SPR) and Isothermal Titration Calorimetry (ITC) [137]. It should be highlighted that there is no one method that suits every situation. Sensitivity, immobilization, structural changes, expected K_d range, association and dissociation kinetics, and sample environment (buffers), must all be carefully taken into account [137].

Besides determination of target-binding characteristics, an aptamer should be characterized with target specificity. As aptamer structure is susceptible to changes in environment, the aptamer should be tested in conditions (pH, salt concentration, temperature, etc.), which corresponds to its final application. The stability and functionality of aptamer should be ideally tested in target samples, such as blood serum or urine, and in any conditions relevant for intended biomedical application [102].

6. APTAMERS IN DIAGNOSTICS OF OVARIAN CANCER

- *Copyright statement*: This part is partially reproduced with permission from the review article published in 2021 (**publication n°1 related to this thesis work**):
  Hanžek A., Siatka C., Duc ACE. High-specificity nucleic acid aptamers for detection of ovarian cancer protein biomarkers: Application in diagnostics, *Journal Aptamers*, 2021, 5, 7–14

Aptamers have emerged as tools for ovarian cancer diagnosis by recognizing circulating tumor markers in serum or on the surface of tumor cells [138]. The aptamers selected to circulating tumor biomarkers and currently developed diagnostic tests were presented below in **Table 4** and **Table 5** [139]. Most diagnostic aptamers are selected against the gold standard OC biomarker CA125. The first reported were two RNA aptamers CA125.1 and CA125.11 with a binding to recombinant CA125, with CA125.1 appeared a better binder, with a K_d in the nanomolar range (4,13 nM) [140]. In Scoville *et al.,* aptamers were selected using 'One-Pot' SELEX from a 5'FAM-modified ssDNA library (25-nucleotides random region) to human CA125 from ascites. Two aptamers, CA125_1 and displayed concentration-dependent binding with K_d values of 207 ± 109 U/mL by FA and 80 ± 38 U/mL by APCE for aptamer CA125_1; and K_d values of 118 ± 123 U/mL by FA and 131 ± 93 U/mL for aptamer CA125_12, respectively [141]. The aptamer CA125_1 was applied in the aptamer-antigen-antibody sandwich-type assay for electrochemical detection of CA125 [142]. The diagnostic test was evaluated in spiked blood and serum samples. The analytical performance of the biosensor is within the clinically relevant detection range from 2 U/mL to 100 U/mL, with a limit of detection (LOD) of 0.08 U/mL [142].

Another ssDNA aptamer rCAA-8 was selected to recombinant CA125 with a high-affinity to CA125 with a K_d value of 166 nM and it was used in on-chip bioassays based on the anti-CA125 aptamer-antibody pair on a three-dimensional network of carbon nanotubes [143]. This diagnostic platform achieved sensitive detection (as low as 10 pg/mL) and wide detection range (10 pg/mL to 1 μg/mL). Significantly, the sensitivity was superior to ELISA using two antibodies [143]. The simultaneous detection of two markers CA125 and Stress-induced phosphoprotein 1 (STIP1) was achieved using ssDNA aptamers in the resonance light scattering (RLS) biosensor. The RLS biosensor achieved detection in the concentration range from 0.1 to 2 U/mL for CA125 and 1–40 ng/mL for STIP1. The RLS biosensor was tested in

spiked human serum (n=3) and achieved great correlation [144]. However, the clinical concentration for the presence of OC is CA125> 35 U/mL and STIP1> 55 ng/mL, so the concentration range tested in the study appears to be below the *cut-off* value.

A novel DNA aptamer was published by Tripathi and colleagues using a Membrane-SELEX approach. Native CA125 from human ascites was incubated with ssDNA library (30 nt long random region). The aptamer with the best affinity and specificity to CA125, Apt 2.26 was selected for the characterization with membrane-based assessment of bound ssDNA to CA125, with K_d value of 166 x 10^{-9} M. The aptamer was stable in human serum, an important aspect when developing serum-based diagnostics [145]. Using this aptamer, the authors designed Aptamer-nanozyme lateral flow assay (ALFA). The results of the diagnostic test showed specificity (tested with BSA and Ig) and sensitivity (LOD 5,21 U/mL). The assay validation was performed by testing in real human serum (n=35) and yielded high correlation with standard CA125 immunoassays, proving the diagnostic performance [146]. Recently, a biosensor based on ssDNA aptamer and upconversion of luminescence resonance energy transfer was developed for the detection of CA125. Moreover, the test was evaluated using samples from ovarian cancer patients (n=3), with good correlation with clinical values of CA125 [147]

Table 4. Nucleic acid diagnostic aptamers for the detection of ovarian cancer biomarkers CA125 and HE4.

Biomarker	Target protein details	Aptamer type	Aptamer sequence*	Library and length of random region (N)	Number of cycles	Counter-selection	Binding characterization	Dissociation constant	Development of the diagnostic test	References
CA125	Recombinant 6 xHis-tagged CA125	RNA	**CA125.1** 5'GGGAGACAAGAAUAAACGCUCA**AAAAAUGCAUGGAGCGAAGG UGUGGGGGAUACCAACCGCGCCGUG**UUCGACAGGAGGCUCAC AACAGGC-3'	(2'-F-Py) modified ssRNA N = 45	**8** Incubation 30 min at RT	Yes (VEGF)	RT-qPCR SPR	**CA125.1:** 4.13 x 10^{-9} M	No	Lamberti *et al.* [140]
CA125	Purified CA125 from human ascites	DNA	**CA125_1** **ACTAGCTCCGATCTTTCTTATCTAC** **CA125_12** **TGCCTTATTACTCTCTCCTGTTAAC** 5' -FAM-AGC AGC ACA GAG GTC AGA TG (N)25 CCT ATG CGT GCT ACC GTG AA-3'.	5'FAM modified ssDNA N = 25	**4** Incubation 1 hour at RT	No	FA APCE	**CA125_1:** 207 ± 109 U/mL by FA and 80 ± 38 U/mL by APCE **CA125_12:** 118 ± 123 U/mL by FA and 131 ± 93 U/mL	Yes	Scoville *et al.* [141]
CA125	Recombinant human 6xHis-tagged CA125	DNA	**rCAA-8:** 5'-ACCACCACCACGACGCACGAGTACCCCGCG-3' Random region sequence	Unmodified ssDNA N = 30	**10** Incubation 1 hour at 37 °C	Yes (BSA) Negative selection (Ni-NTA sepharose beads)	direct ELISA BLI	166 x 10^{-9} M	Yes	Gedi *et al.* [143]
CA125	Native CA125 from human ascites	DNA	**Apt 2.26** 5'-TAGGGAAGAGAAGGACATATGATTTTA GGGAAGAGAAGGACTTTTATGCCGCCTTGACTAGTA CATGACCACTTGA-3'	Unmodified ssDNA N = 30	**6** Incubation 1 hour at 25 °C	No Negative selection (nitrocellulose membrane)	Membrane-based assessment of bound DNA Dot ELASA NALFA DPV	166 x 10^{-9} M	Yes	Triphati *et al.* [145]
HE4	Human recombinant GST – tagged HE4	DNA	**A1:** 5'-TTATCGTACGACAGTCATCCTACAC-3' **A3:** 5'-CACAGTGCGTCACATTTAGGGCATT-3' **B10:** 5'-CAGTGCGTGCTTATTGGCGTAGCGTC-3'	Unmodified ssDNA N = 25	**5** Incubation 30 min at 25 °C	Yes (GST)	APCE FA	**A1:** 2.2 x 10-6 M with FA and 390 x 10-9 M with APCE **A3:** 9.1 x 10-6 M with FA and 500 x 10-9 M with APCE **B10:** 280 x 10-9 M with FA and 870 x 10-9 M with APCE	Yes	Eaton *et al.* [148]

* Internal aptamer ID provided by authors and corresponding sequence; the sequence in bold indicate random region. Some studies use full sequence (fixed and random region), whereas others use only random region for binding characterization. The aptamer sequence listed above is the sequence synthesized, characterized and assayed post-SELEX ; **CA125 –** Cancer Antigen 125; **HE4 –** Human Epididymis protein 4; **STIP1** – Stress-induced phosphoprotein 1; **VEGF** - Vascular Endothelial Growth Factor; **GST –** glutathione-S-transferase ; **RT** - room temperature; **RT-qPCR** - reverse transcriptase – quantitative polymerase chain reaction ; **BSA** —bovine serum albumin; **SPR** —surface plasmon resonance; **FA** – fluorescence anisotropy; **APCE** - affinity probe capillary electrophoresis; **ELASA –** Enzyme-linked aptamer sorbent assay; **NALFA** – Nucleic acid lateral flow assay; **DPV** – Differential pulse voltammetry; **ELISA –** The enzyme-linked immunosorbent assay; **BLI** – biolayer interferometry; **n/a** – not available (not applicable)

Table 5. Aptamer-based diagnostic tests for the detection of ovarian cancer protein biomarkers and the analytical performances.

Biomarker	Type of test	Description	Aptamer	Aptamer sequence (5' – 3')	Limit of detection	Target protein detection range	Correlation with clinically relevant protein concentration**	Tested in human samples	Type of samples	Tested in patients	Reference
CA125	Biosensor	Field effect transistor type aptasensor based on carboxylated multiwalled carbon nanotubes immobilized onto reduced graphene oxide film	DNA	TTATCGTACGACAGTCATCCTACAC*	5.0 × 10^{-10} U/mL	1 x 10^{-9} U/mL to 1U/mL	No	Yes	Serum	Yes (n=1)	Majd and Salimi [149]
CA125	Fluorescence-based sandwich assay	A chip-based assay using a three-dimensional network of carbon nanotubes surface and anti-CA125 antibody-aptamer pair	DNA	5'— ACC ACC ACC ACG ACG CAC GAG TAC CCC GCG-6-FAM-3	10 pg/mL	1 pg mL/1 to 1 µg/mL	Yes	No	n/a	No	Gedi *et al.* [143]
CA125	Biosensor	Target induced strand displacement on electrospun Ag nanoparticles nanofibers, cyclic voltammetry	DNA	TTATCGTACGACAGTCATCCTACAC*	0,0042 U/mL	0,01 to 350 U/mL	Yes	Yes	Serum	No	Farzin *et al.* [150]
CA125	Lateral flow assay	Aptamer-nanozyme lateral flow assay	DNA	TAGGGAAGAGAAGGACATATGATTTTA GGGAAGAGAAGGACTTTTATGCCGCCTTGACT AGTA CATGACCACTTGA (From Triphati et al., 2020a)	5.21 U/mL	7.5 - 200 U/mL	Yes	Yes	Serum	No	Triphati *et al.* [146]
CA125	Aptamer-antigen-antibody sandwiched assay	Magnetic bead-amplified voltammetric detection with enzyme labels	DNA	SH – 5´ACTAGCTCCGATCTTTCTTATCTAC 3 (CA125_1 from Scoville *et al.*)	0.08 U/mL	2 U/mL - 100 U/mL	Yes	Yes	Whole blood Serum	No	Sadasivam and Sendwitch [142]
CA125	Biosensor	Aptasensor based on upconversion luminescence resonance energy transfer	DNA	5' – AAAAAACTCACTATAGGGAGACAAGAATAAA CGCTC AA-3'	9.0 × 10^{-3} U/mL	0.01 - 100 U/mL	Yes	Yes	Serum	Yes (n=3)	Zhang *et al.* [147]
CA125 + STIP1	Biosensor	Aptasensor based on resonance light scattering intensity	DNA	**CA125 aptamer:** 5′— CGG CAC TCA CTC TTTGTT AAG TGG TCT GCT TCT TAA CCT TCA TAT CAA TTA CTT ACC CTAGTG GTG TGA TGT CGT ATG GAT G-3′ **STIP1 aptamer:** 5′-CAT CCA TAC GAC ATC ACA CCA CTA GGG TAA GTAATT GAT ATG AAG GTT AAG AAG CAG ACC ACT TAA CAA AGA GTGAGT GCC G-3′	n/a	0.1 - 2 U/mL for CA125 1 to 40 ng/mL for STIP1	No	Yes	Serum	No	Chen *et al.* [144,].
HE4	Biosensor	Aptasensor based on upconversion luminescence resonance energy transfer	DNA	5′–NH2-CACCATTATCGTACGACAGTCATC CTACACAATGGT-BHQ-1-3′ (Sequence A1 from Eaton *et al.*)	0.021 ng/mL (buffer) 0.049 ng/mL (serum)	0.4 ng/mL to 7.0 ng/mL	n/a	Yes	Serum	No	Ma *et al* [151].

CA125 – Cancer Antigen 125; **HE4 –** Human Epididymis protein 4; **STIP1** – Stress-induced phosphoprotein 1; n/a – not applicable
* aptamer initially developed against HE4 as a target**;** ** Clinical *cut-off* value for the serum concentration of ovarian cancer biomarkers are CA125> 35 U/mL; STIP1> 55 ng/mL; HE4> 60 p

A single study by Eaton *et al.* reported DNA aptamers targeting HE4. The aptamers were selected using capillary electrophoresis (CE) SELEX. In aptamers A1, A3 and B10 displayed affinity to HE4, with K_d values of $2{,}2 \times 10^{-6}$ M with FA and 390×10^{-9} M with APCE for aptamer A1; $9{,}1 \times 10^{-6}$ M with FA and 500×10^{-9} M with APCE for aptamer A3; and 280×10^{-9} M with FA and 870×10^{-9} M with APCE for aptamer B10, respectively [148]. Recently, the sequence of A1 aptamer was used in the development of the aptasensor for detection of HE4 based on the upconversion luminescence resonance energy transfer. The biosensor achieved HE4 detection in the range of 0.4 ng/ml to 7.0 ng/ml, with a LOD of 0.021 ng/ml in buffer and 0.049 ng/ml in 100-fold diluted serum samples [151]. Aptamers for HE4 detection have potential, but since the clinical concentration of HE4 is in picomolar range, they should be further analyzed in wider concentration range and validated with samples from OC patients for future diagnostic applications.

None of the aptamers for ovarian cancer were previously developed or tested in urine. Moreover, no aptamer so far was tested in clinically relevant concentration range nor tested in human urine from ovarian cancer patients.

II. OBJECTIVES OF THE THESIS

Ovarian cancer is the deadliest gynecological cancer in woman. Due to the lack of effective diagnostic methods, late diagnosis remains a main factor of the poor prognosis. Therefore, development of novel diagnostic approaches are needed. The global aim of the *CARIBOU (CAncer ovaRIan BiosensOr in Urine)* project is the development of aptamer-based biosensor or assay for the detection of ovarian cancer biomarkers in urine. The global objective of this thesis is development of aptamers, the capture part of the future biosensor or test, that target ovarian cancer biomarkers in urine. Aptamers, a single-stranded oligonucleotides that emerged as inexpensive and versatile probes for cancer detection, were chosen as a diagnostic strategy in this project. The first objective of this thesis was to identify the most relevant target biomarkers in urine from literature, and to produce them. The second objective was to select and identify aptamer sequences targeting chosen target biomarkers in urine. After identification of potential high-affinity candidates, the third objective is the characterization of the interaction of the novel aptamers with their target through aptamer-target binding analysis. The potentially developed aptamers will be used as diagnostic probes in the biosensor or urine test for ovarian cancer in future. The specific objectives of the thesis are :

(1) Identify the most promising existing target urine biomarker of ovarian cancer from the literature
(2) Select and identify novel aptamer probes for detection of target biomarker in urine using SELEX method
(3) Evaluate the developed aptamers as diagnostic probes by characterization of aptamer-protein binding and interactions

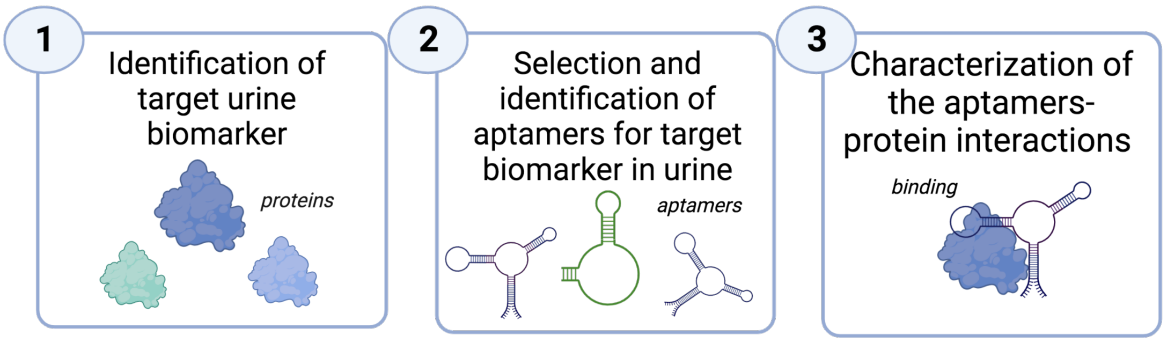

Figure 14. Overview of the thesis project with the specific objectives.

III. MATERIALS AND METHODS

PART 1 : PRODUCTION OF THE TARGET BIOMARKERS: EXPRESSION OF THE HE4 PROTEIN

1.1. Bacterial cultures and plasmids

The human HE4 gene optimized for translation was purchased in a pEX-HE4 plasmid (Eurofins Genomics, Germany) to transfer into a pGEX-2T plasmid (ref. 28-9546-53; GE Healthcare, USA), for N-terminal GST-fusion protein expression. Two different bacterial strain were used: *E.coli DH5α* competent cells (ref. C2987H; New England BioLabs Inc., USA), suitable for high-quality plasmid preparations and *SHuffle® T7 Competent E. coli* (ref. C3026J; New England BioLabs Inc., USA) for expression of proteins with multiple disulfide bonds.

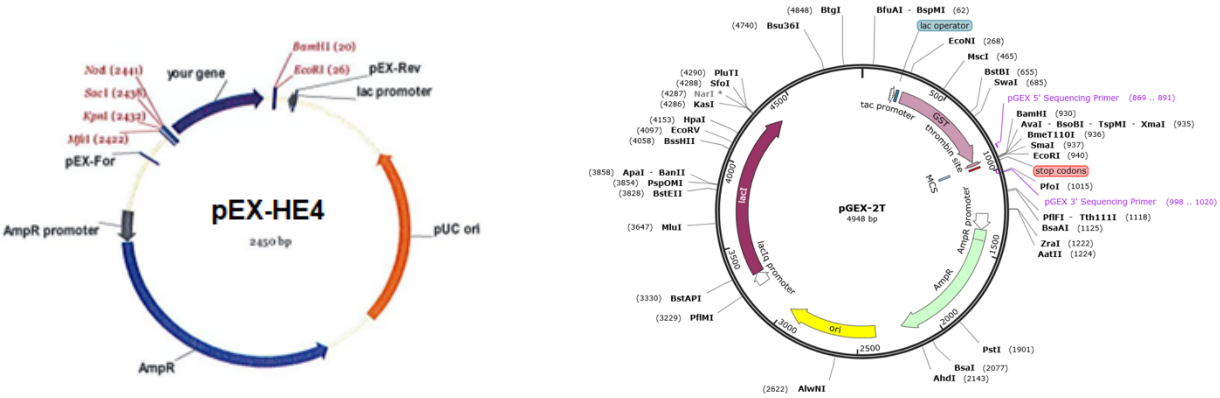

Figure 15. Plasmid maps of the vector pEX-HE4 (carrying the gene coding for protein HE4) and of the pGEX-2T (backbone for constructing the protein expression plasmid).

1.2. Construction of the expression vector pGEX-HE4

The pGEX-HE4 plasmid was constructed from pEX-HE4 (with HE4 gene) and pGEX-2T (backbone) plasmids using restriction digestion. Fast Digest BamHI (ref. FD0054; Thermo Scientific™, USA) and Fast Digest EcoRI (ref. FD0275; Thermo Scientific™, USA) were used according to manufacturer's protocol using 1 µg of plasmid DNA. The products were analyzed on a TAE agarose gels (1 % for the cut plasmid pGEX-2T, and 2 % for the cut insert HE4) in 1X Tris-Acetate-EDTA (TAE) running buffer, with GelRed® nucleic acid staning (ref. SCT123, Biotium, Inc., Canada) at 50 V for 45 minutes. The gels were visualized using BioRad GelDoc™ XR+ (BioRad, USA). Both linearized plasmid (pGEX 2T, expected size: 4938 bp)

and insert (human HE4 gene, expected size: 297 bp) were recovered for ligation using MILLIPORE Ultrafree®-DA (ref. 42600; Merck Milipore, USA). The purified human HE4 gene was ligated into the pGEX-2T plasmid backbone using T4 DNA Ligase (ref. EL0011, Thermo Scientific™, USA) in a 2:1 molar ratio with ligation of 1 hour at 22 °C. A 100 ng of ligated plasmid pGEX-HE4 were transferred by heat shock in competent *E. coli DH5α* bacteria.

1.3. pGEX-HE4 plasmid verification - Colony PCR and DNA sequencing

The colony PCR was performed on a 10 random bacterial colonies using a vector-specific pGEX-primers: 5'pGEX GGGCTGGCAAGCCACGTTTGGTG forward primer and 3' pGEX CCGGGAGCTGCATGTGTCAGAGG reverse primer. The PCR reactions were prepared by mixing 4 µL of Pfu DNA Polymerase 2x PCR Master Mix (ref. P202; GeneBio Systems, Inc., Canada) to a final of 1X, 0.45 µL of stock 10 µM 5' pGEX primer to a final concentration of 0.56 µM; 0.45 µL of stock 10 µM 3' pGEX primer to a final concentration of 0.56 µM, 3.1 µL of water to a final reaction mixture of 8 µL. DNA template is bacteria containing pGEX-HE4 plasmid and is introduced into PCR reaction with touching individual colony with a pipette tip and mixed into PCR reaction. In parallel, negative PCR control, with water as template; and positive PCR control, with pGEX-2T as template were carried out. The PCR products were analyzed on 2 % agarose gel in 1X TAE buffer, with Gel Red nucleic acid staining at 50 V for ~ 45 min. To verify exact DNA sequence of pGEX-HE4 plasmids,the clones were sent to DNA sequencing (Eurofins Genomics, Germany) using standard pGEX primer (Eurofins ID: pGex for_oldprimerEF). DNA sequence of plasmids and expected sequence were aligned in Serial Cloner software. The verified plasmid pGEX-HE4 clone will be used for the production of the GST-HE4 fusion protein.

1.4. HE4 protein overexpression

The plasmid pGEX-HE4 (clone 3) was heat shock transformed into *E. coli T7 shuffle* bacteria following manufacturer protocol. The next morning, individual clone were inoculated into 10 mL LB liquid media, supplemented with ampicilin (100 µg/µL) and incubated at 30 °C overnight with shaking at 230 rpm. The next morning, the bacterial culture was diluted 1:100 into fresh media and grown at 30 °C with shaking at 230 rpm. Bacterial growth was monitored spectrophotometrically by measuring the optical density (OD) at 600 nm by Nanodrop 200c. When an OD_{600} = 0,5 has been reached, a 1 mL of culture is harvested as control prior HE4 expression (before expression, no IPTG), and protein expression was induced by adding 200

µM of IPTG (Isopropyl ß-D-1-thiogalactopyranoside). The temperatures 30 °C and 37 °C were tested to determine the best conditions for N-terminal GST-HE4 protein production. The aliquots of bacterial cultures after induction are taken for analysis after 1, 2, 3 and 4 hours for 37 °C and 3 and 4 hours for 30 °C. The time-point bacterial aliquots were centrifuged at 6000 x g for 20 minutes at 4 °C, and the supernatant was eliminated. The pellets were lysed in buffer (0,5 % Triton X-100 (ref. T8787, Sigma-Aldrich, USA), 1X PBS, pH=7.4 (ref. 10010023, Gibco, USA) and protease inhibitors (ref. 11836153001, Roche, Switzerland), and subjected to sonication (3 cycles of 10 seconds pulsation, 30 seconds period) on ice. Then, the samples were centrifuged at 16 000 x g for 20 minutes at 4° C in order to eliminate cell debris in the form of the pellet, and the supernatant with proteins is recovered. Protein concentration was determined by Nanodrop 200c spectrophotometry. To analyze the proteins by the different growth conditions, 15 % polyacrylamide SDS-PAGE (Sodium dodecyl-sulfate polyacrylamide gel electrophoresis) is carried out, using 20 µg of protein in 1X Laemli buffer (ref. S3401, Sigma-Aldrich, USA) per well, for a final volume of 20 µL/protein sample. The samples are denatured for 5 min at 95 °C. Ten µL of SeeBlue™ Plus2 standard (ref. LC5925, Invitrogen™, USA) was loaded as molecular weight ladder. The gels were run at 150 V and 50 mA for 1 hour. The gels are stained by Coomasie blue, and visualized by Bio-Rad Gel-Doc. The expected size for the GST-HE4 fusion protein is 36,6 kDa (GST 25.5 kDa + HE4 11.1 kDa).

1.5. HE4 protein purification

One hour after IPTG induction, *E.Coli T7 Shuffle* bacterial cultures of 50 mL were harvested (at 6000 g for 20 min at 4°C). The pellets were weighted and lysed (1 g pellet = 5 mL of buffer) in lysis buffer (1X PBS, 0.5% Triton-X and Complete Mini protease inhibitors) and sonicated (3 cycles of 10 seconds pulsation, 30 seconds period). Cell debris is eliminated by centrifugation at 16000 g for 20 min at 4°C, and the supernatants are recovered. Fusion GST-HE4 protein was purified using affinity Pierce™ Glutathione Magnetic Agarose Beads (ref. 78601, Thermo Scientific™, USA). 300 µL of protein lysate was prepared. Then, the sample is diluted with 250 µL Equibrium/Wash (E/W) buffer (125 mM Tris-HCl, 150 mM NaCl, 1 mM DTT, 1 mM EDTA, pH 7.4) to to 500 µL, keeping 10 µL aside as input sample prior purification. The protein sample was added to the beads and mixed for 2 hours on RT. The supernatant (SN) was recovered, and the beads were washed twice with 500 µl of E/W buffer (supernatants were kept only for analysis). The beads (with GST-HE4) were then collected and resuspended in 100 µL of E/W buffer. The samples were analyzed on 15 % SDS-PAGE gel

with Coomasie staining. 10 µL of protein samples are mixed with 10 µL 2X Laemli buffer and denatured for 5 min at 95 °C. The samples are loaded together with SeeBlue™ Plus2 standard and GST tag as a reference on 15 % SDS-PAGE gel and run for 1 hour at 150 V In 1X TG-SDS buffer. The expected size of the GST-HE4 protein is 35.65 kDa (N-terminal GST 25.5 kDa and HE4 protein 10.15 kDA).

PART 2 - SELECTION AND IDENTIFICATION OF APTAMERS TARGETING OVARIAN CANCER BIOMARKER IN URINE

2.1. Aptamers and proteins

The starting aptamers pool was a 70 nucleotide long single-stranded DNA library (Integrated DNA Technologies, Inc., USA) with 30 nucleotide long (30 N) random region flanked by two fixed, 20-nucleotide long (20 nt) constant primer binding sites: TCGCACATTCCGCTTCTACC – N30 – CGTAAGTCCGTGTGTGCGAA, containing ~ 4^{25} = 1^{15} highly diverse random sequences **(Figure 16)**. The library was ordered on a scale of 10 µmol DNA and resuspended in nuclease-free H_2O. To ensure equal nucleotide distribution, the molar ratio of A:C:G:T phosphoramidites was combinatorically synthesized by hand mixing DNA nucleotides and optimized to a ratio 29:29:20:22 %, to achieve equal probability of incorporation of each nucleotide in the core region. The primers (Eurofins Genomics, Germany) for the amplification are previously utilized in SELEX [152,153] and are suitable for qPCR [152] and ddPCR amplification [153,154] : Forward 5'-TCG CAC ATT CCG CTT CTA CC-3' and Reverse 5'-[phos]-TTC GCA CAC ACG GAC TTA CG-3'. The reverse primer is 5'phosphorylated for the ssDNA regeneration by the lambda exonuclease. The primers were validated, and PCR efficacy was tested for designed library prior Hi-Fi SELEX **(Annex 1)**.

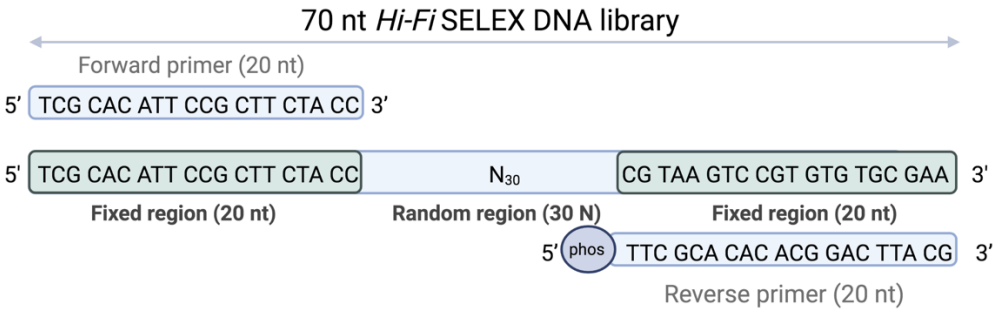

Figure 16. Hi-Fi SELEX library.

The aptamer library used for the selection of aptamers to ovarian cancer biomarker is 70 nucleotide (70 nt) long DNA library with 30 nucleotide (30N) long randomized region flanked with two fixed 20 nucleotides (20nt) long regions used as primer binding sites (*Created with Biorender.com*).

Positive selection was performed to Human Epididymis protein 4. The target is a C-terminal 6xhistidine-tagged human recombinant protein, expressed in HEK293 cells (ref. ab219658, Abcam, United Kingdom), to ensure post-translational modifications present in OC patients. The protein is the full-length protein (amino acids 31-124, without signal peptide) with a molecular weight of 11 kDA including tags. Counter-selection of aptamers potentially binding to tag was performed to 6xhistidine peptide (ref. RP11737, Genscript Biotech Corp, USA).

2.2. Urine preparation

As the goal is the identification of aptamers for application in urine, it is important to ensure conditions corresponding to human urine. Therefore, we needed to ensure a selection of the aptamers that would be functional in urine. The protocol for artificial urine (AU) was taken from Sarigul *et al.* [155]. This specific recipe is designed to mimic the human urine and is based on the empirical analysis of the healthy individuals. One X (1X) urine contains 11,965 mM Na_2SO_4, 1,487 mM $C_5H_4N_4O_3$, 2,450 mM $Na_3C_6H_5O_7$ x $2H_2O$, 7,791 mM $C_4H_7N_3O$, 249,750 mM CH_4N_2O, 30,953 mM KCl, 30,053 mM NaCl, 1,663 mM $CaCl_2$, 23,667 mM NH_4Cl, 0,19 mM $K_2C_2O_4xH_2O$, 4,389 mM $MgSO_4x7H_20$, 18,667 mM $NaH_2PO_4x2H_2O$, 4,667 mM $Na_2HPO_4x2H_2O$. The urine is prepared a day before for pH stabilization (measured pH=6.3). All the reagents were purchased from Sigma-Aldrich (Sigma Aldrich, USA).

2.3. HE4 protein immobilization

The HE4 was immobilized on HisPur™ Ni-NTA beads (ref. 88223, Thermofisher Scientific, USA). The beads were centrifuged at 700 x g at room temperature (RT) for 1 min to remove the storage liquid. Then, the beads were washed with a two-volume of equilibrium buffer (20 mM sodium phosphate, 300 mM sodium chloride with 10 mM imidazole; pH 7.4) and centrifuged again at 700 x g at RT for 1 min. The prepared HE4 protein sample was added and incubated at RT with shaking at 1500 rpm (Eppendorf thermomixer) for 30 min to immobilize the protein. Depending on the cycle of SELEX, a protein sample was prepared to correspond to either 100 pmol or 200 pmol HE4 on beads. After incubation, the beads were centrifuged at 700 x g at RT for 1 min and HE4 immobilized beads were subjected to DNA in SELEX.

2.4. Overview of the *Hi-FI* SELEX method

The high-affinity aptamers for the ovarian cancer protein biomarkers are selected by the *in vitro* method called the *High-Fidelity Systematic Evolution of Ligands by Exponential Enrichment* (*Hi-Fi SELEX*), based on digital droplet polymerase chain reaction (ddPCR). The concept of the *Hi-Fi* SELEX method was previously introduced by Ouellet *et al*. [153] and Ang *et al.* [154], where partitioning capabilities of ddPCR are used for aptamer selection. We have adapted the protocol [154], by integrating the ddPCR into the aptamer selection, but expanded to ddPCR droplet analysis and sequence quantification.

Anti-HE4 aptamers were selected from the highly diverse 70-mer single stranded DNA library after 10 cycles of incubation with immobilized HE4 target in urine. For the last two rounds (after cycle 8) of selection against 6xhistidine-HE4, the recovered DNA aptamers were separated into a two equal branches and subjected to additional 2 rounds of positive selection (6xhistidine-HE4 on beads) and 2 rounds of counter-selection (6xhistidine peptide on beads), to identify potential non-specific binders to the sample matrix (protein tag and charged beads).

The sequences are dissociated from the aptamer-protein complexes, eluted from the beads and purified. The pure ssDNA aptamers are partitioned into droplets, amplified and quantified using ddPCR. The DNA is extracted from the droplets and reamplified to increase the yield of recovered DNA. After purification of the amplicons from the primers, the ssDNA is regenerated by lambda exonuclease. This aptamers are now subjected to the next cycle as new oligonucleotide pool. Specific anti-HE4 sequences are identified by Next-Generation-

Sequencing (NGS) and analyzed by bioinformatics. The schematic overview of ovarian cancer protein HE4 Hi-Fi SELEX is displayed in the **Figure 17** below:

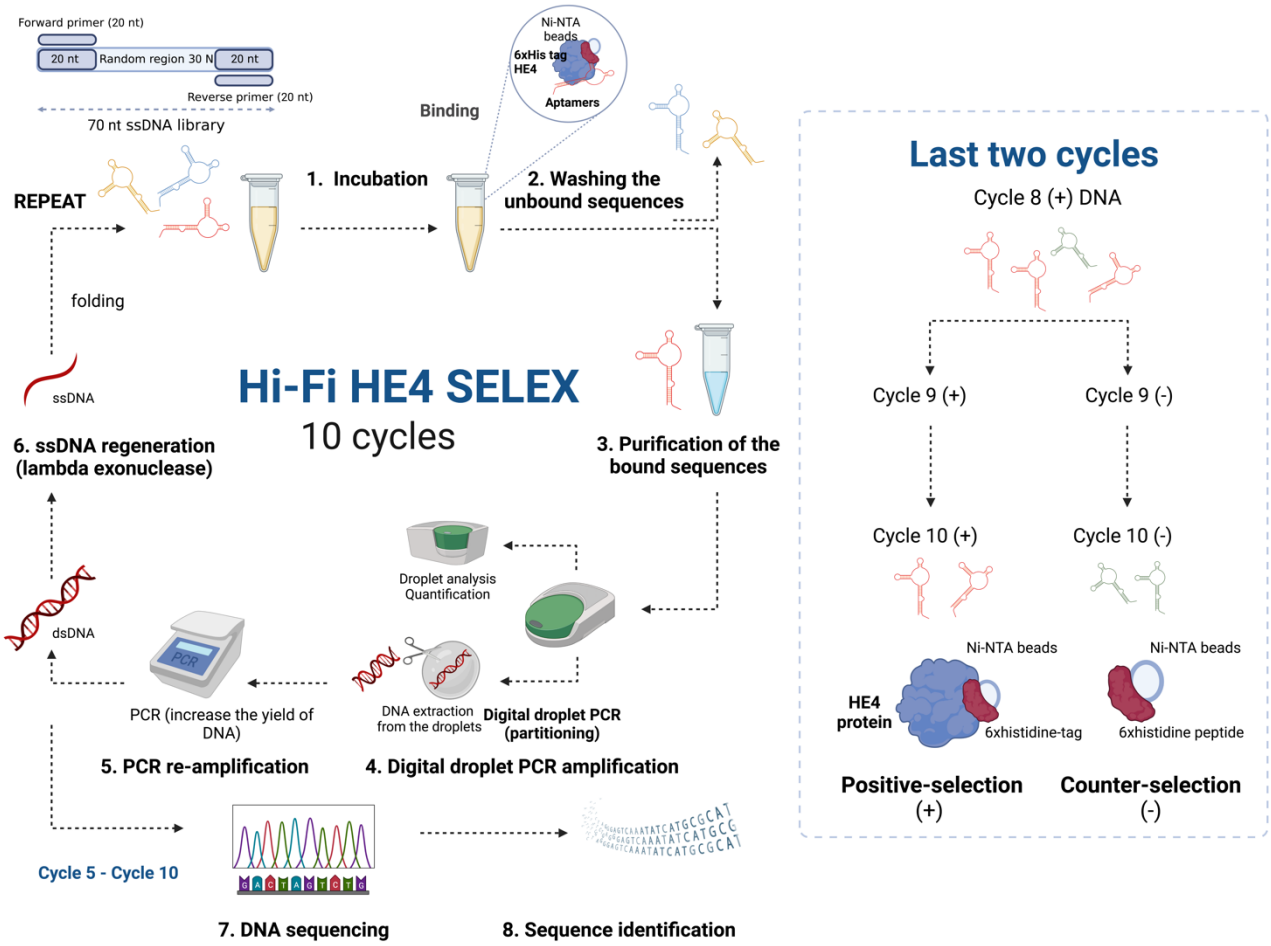

Figure 17. Schematic representation of the digital droplet PCR (ddPCR)-based High Fidelity Systematic Evolution of Ligands by EXponential enrichment (Hi-Fi SELEX) method for the selection of aptamers to ovarian cancer biomarker HE4 in urine.

The high-affinity aptamers are selected from initial 70 nucleotide long (70 nt) single-stranded DNA library consisted of random 30 nucleotide long region (30 N), flanked by 20 nucleotide long (20 nt) constant regions used for PCR amplification. Briefly, the aptamer libraries are incubated with target HE4 protein in urine. Unspecific unbound sequences are washed, while specific bound sequences are recovered and purified. The specific anti-HE4 sequences are partitioned into droplets for sensitive ddPCR amplification. Then, the aptamers are recovered from the droplets and reamplified using regular PCR to increase the yield of DNA. Double stranded PCR products are digested by lambda exonuclease by to single-stranded sequences used as an input for next cycle of selection *(Created with Biorender.com)*.

2.5. DNA preparation

The Initial pool of library consisted of 1,25 nmol ssDNA, which corresponds to ~ 1^{15} random sequences. This initial library was precleared, to eliminate all the sequences that could have bound to bind to Ni-NTA resin. Preclearing was carried out in the first cycle by subjecting the

ssDNA library to NTA-beads without protein. 200 µL of library (corresponding to 1,25 nmol) were added to NTA-beads and incubated at 25 °C for 1 hour at 1500 rpm (same conditions as SELEX). The sample was centrifuged at 700 g at RT for 2 min, the beads were discarded, and the supernatant was recovered. The supernatant should then contain library candidates that do not have affinity for the NTA beads. The initial library and ssDNA in every cycle are denatured at 95 °C for 10 minutes followed by cooling on ice (4°C) before returning to RT. Then, denatured ssDNA is added to 1X urine to ensure the proper folding and structure in selection environment while incubating with target HE4 protein.

2.6. Selection and washing steps

The selection conditions and stringency, such as protein and DNA amount and variations in washing steps were modified from round to round to ensure high stringency of selection. Moreover, input DNA for selection can depend on DNA amount recovered at the end of previous cycle. As shown in the **Table 6** below, the stringency for selection of high-affinity aptamers was increased by increasing the amount of DNA present. The high-affinity anti-HE4 aptamers were selected after 10 cycles of selection. After the 8 cycles of selection to 6xhistidine-HE4, the recovered DNA aptamers were separated into a two equal arms and subjected to additional 2 rounds of positive selection (6xhistidine-HE4 on beads) and 2 rounds of counter-selection (6xhistidine peptide on beads), to identify potential non-specific binders of the sample matrix (protein tag and charged beads).

Before each cycle, DNA was denatured as previously described. Then, 1,25 nmol of the highly diverse DNA aptamer library was incubated with 200 pmol of target human HE4 protein immobilized on Ni-NTA beads for 1 hour at 25 °C with shaking at 1500 rpm in the volume of 200 µL of 1X urine. The specific sequences were obtained through two mechanisms: by the increased washing stringency (using different steps of washing, larger wash volume, wash durations and harsher wash buffer composition) and by increased stringency of the selection (using lower HE4/DNA ratios) **(Table 6)**. The non-specific, unbound sequences are eliminated by three steps of washing with 400 µL of buffers. Two buffers were used: Wash buffer 1 (WB1) which is 1X urine, which represents a more gentle solution; and a more stringent Wash buffer 2 (WB2) which is 1X urine supplemented with detergent 0,01 % Tween-20 **(Table 6)**.

Table 6. Incubation and washing conditions in the HI-FI SELEX selection of aptamers to ovarian cancer protein HE4.

Cycle	DNA (nmol)	HE4 protein (pmol)	Washing steps	Washing duration	Washing buffers (400 µL)
C1 +	1,25	200	1	2 min	W1
C2 +	0,47	200	2	2 min	W1 (2 steps)
C3 +	0,08	100	2	5 min	W1 (2 steps)
C4 +	0,13	100	3	5 min	W1 (1 step) W2 (2 steps)
C5 +	0,15	100	3	5 min	W1 (1 step) W2 (2 steps)
C6 +	0,04	200	3	5 min	W2 (3 steps)
C7 +	0,03	200	3	5 min	W2 (3 steps)
C8 +	0,08	200	3	5 min	W2 (3 steps)
C9 +	0,10	200	3	10 min	W2 (3 steps)
C9 -	0,10	200	3	10 min	W2 (3 steps)
C10 +	0,10	100	3	10 min	W2 (3 steps)
C10 -	0,10	100	3	10 min	W2 (3 steps)

W1 - wash buffer 1 (1X urine) ; W2 - wash buffer 2 (1X urine + 0.01 % Tween-20)

During the selection step, the sequences of interest were bound to the HE4-protein target, yielding a DNA-protein complex. To recover the bound DNA candidates from the complex, 140 µL of AU was added to the tube (required aqueous solution for next step), and the tube was heated-up for 10 min at 95 °C. This step should ensure HE4 protein removal from the beads, and DNA-protein complex dissociation. The beads were discarded and the 140 µL of supernatant with aptamers was subjected to DNA purification.

2.7. Purification of specific DNA sequences

From the eluted ssDNA supernatant, the candidates are extracted and purified using Phenol:Chloroform:Isoamyl alcohol (25:24:1 v/v) extraction and ethanol/GlycoBlue™ (ref. AM9515, Thermofisher-Scientific, USA) co-precipitation. In 140 µL of supernatant containing the ssDNA sequences of interest, 140 µL (one volume) of phenol: chloroform:isoamyl alcohol (25:24:1) were added, and vortexed for approximately 20 seconds. The samples weres centrifuged at RT for 10 minutes at 16 000 × g. The upper aqueous phase was carefully removed and transferred to a fresh tube. In the following order 70 µL of cold ammonium acetate NH_4OA (7.5M) was added to the final concentration of 2,5 M, Glycoblue DNA co-precipitant reagent to the final 50 µg/ml and 420 µL of cold 100 % ethanol (two volumes) were added. The samples were kept overnight at - 20 °C to precipitate the DNAs. The sample were centrifuged at 16 000 x for 30 minutes at 4 °C. The final pellet was air-dried (does not require washing with ethanol, because it can cause loss of sequences) for 15 minutes at room temperature and directly

resuspended in 25 µL of nuclease-free water. This pure ssDNA (aptamer pool after selection to HE4) is stored at - 20 °C until next day, where it will be the used as DNA template for ddPCR amplification.

2.8. Digital droplet polymerase chain reaction (ddPCR) aptamer amplification : principle and advantages

Droplet digital polymerase chain reaction (ddPCR) is an enhanced PCR method that can detect and quantify nucleic acids even when they are present in exceptionally low numbers. The concept of utilizing ddPCR in SELEX was previously introduced into novel selection method, called Hi-Fi SELEX, for development of aptamers, but without droplet reading or quantification [153,154]. In ddPCR-driven type of SELEX, library members are partitioned into water-in-oil emulsion droplets, where each droplet represents an individual PCR reaction. Therefore, sensitive amplification of aptamer sequences is achieved, minimizing PCR bias.

In ddPCR, a single PCR sample is partitioned into 20,000 droplets. Aptamer template sequences are distributed randomly among droplets, such that some droplets have no template molecules and others have one or more (**Figure 18**). Each droplet, or partition, undergoes PCR amplification and analysis separately, and the droplets are then individually counted and scored as positive or negative based on the fluorescence (and selected threshold). The positive droplets are those above the threshold and contain amplified DNA aptamers in double stranded format. The negative droplets, those below threshold, can contain background DNA, such as ssDNA template or primers. The number of positive *versus* negative droplets is used by software to calculate the concentration of the target DNA sequences.

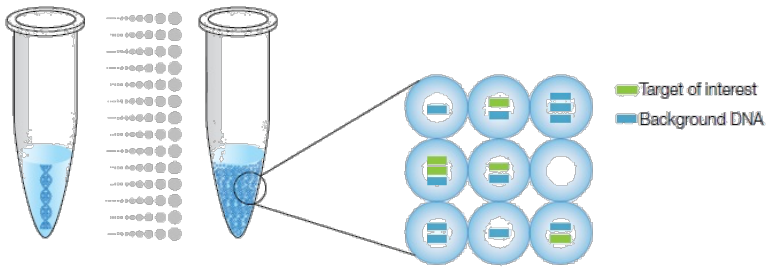

Figure 18. Sample partitioning in ddPCR (*source: Bio-rad.com*).

The ddPCR mixture is prepared in same way as regular qPCR and consist of a aptamer template, primers and a PCR supermix with either probes or intercalating dye (EvaGreen). The methodology is divided in 3 steps: (1) droplet generation and partitioning of PCR reaction into thousands of emulsion droplets, using specific microfluidic chambers and droplet generator machine; (2) qPCR performed in a regular quantitative thermocycler; and finally (3) droplets are read and nucleic acids are quantified using a droplet reader machine. In the context of SELEX, an additional step is required, which is (4) recovery of DNA from the droplets where the amplified DNA is extracted from the droplets, as DNA aptamers are needed for continuation of the SELEX. Therefore, samples must be prepared in the duplicates to allow for droplet reading and quantification on one side, and recovery for further experiments on other side. The experimental flowchart for ddPCR in aptamer discovery is shown in **Figure 19.**

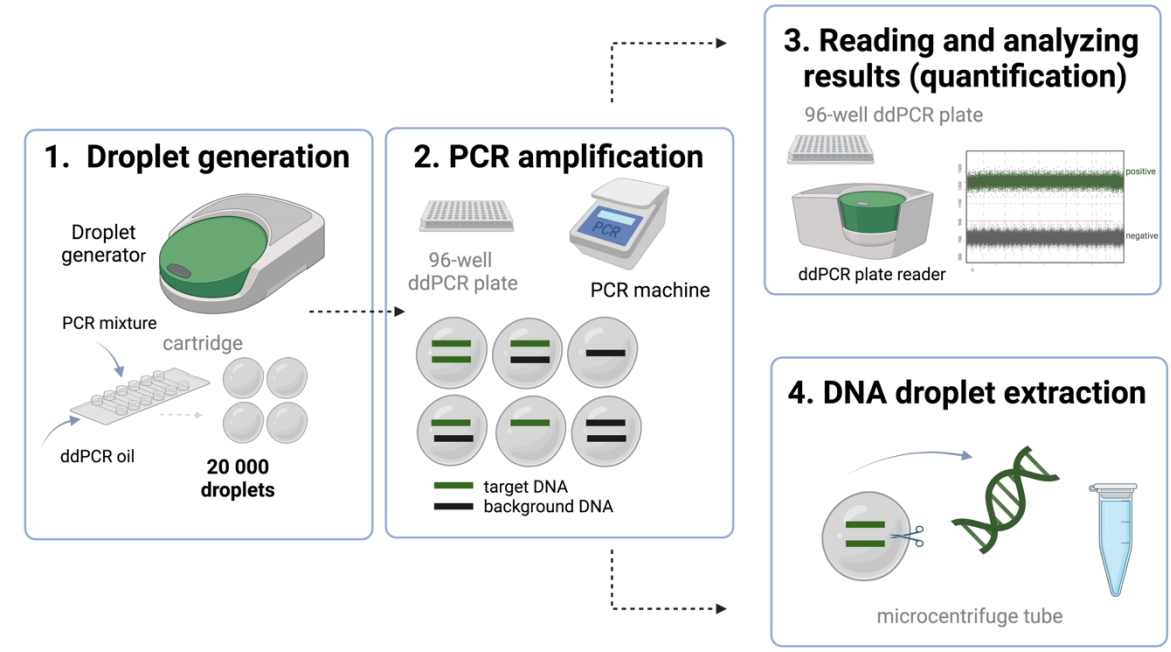

Figure 19. Schematic illustration of ddPCR workflow.

(1) The PCR mix (aptamer template, primers, EvaGreen mix or probes, primers) is prepared and loaded together with oil into ddPCR multi-channel cartridge. The cartridge is placed into the droplet generator machine which partitions the DNA sample into water-in oil droplets. (2) The droplets are transferred into the plate and amplified in thermocycler PCR machine. After amplification, the droplets are divided and subjected to (3) droplet reading by specific ddPCR plate reader machine, which analyses each droplet individually and quantify the aptamer sequences and (4) destruction to extract the DNA from the droplets to be able to proceed with aptamer selection (*Created with Biorender.com*)

In this thesis work, ddPCR analysis has been successfully applied in the selection and amplification of aptamers targeting ovarian cancer biomarker HE4. Prior implementation of

ddPCR in the Hi-Fi SELEX, ddPCR was optimized. Several parameters had to be initially tested, such as annealing temperature, primes and template concentration. Optimal annealing temperature will ensure an easy classification into positive or negative droplets (highest difference in the fluorescence amplitude). The optimal template concentration will enable maximum amplification power, without droplet saturation. The results of the ddPCR optimizations can be found in the **Annex 2**.

2.9. ddPCR amplification of anti-HE4 aptamers during Hi-Fi SELEX

Herein, the optimized ddPCR method was applied and enables both (1) amplification of aptamers and (2) monitoring of the aptamer pool quantity across all cycles *of in vitro* Hi-Fi SELEX for selection of ovarian cancer biomarker HE4. The partitioning of sequences into droplets via ddPCR should help the rare anti-HE4 aptamers to be amplified.

The purified DNA was prepared for droplet digital PCR, in duplicates for (a) the droplet analysis: monitoring and quantification of the anti-HE4 sequences during SELEX and (b) the extraction from droplets after ddPCR to proceed to the next round of SELEX with the amplified DNA.

2.10. ddPCR mixture preparation and droplet generation

A ddPCR reaction includes 2 µL of SELEX selected aptamer template (unknown concentration), 10 µL of 2X QX200™ ddPCR™ EvaGreen Supermix (ref. 1864034, Bio-Rad Laboratories, Inc., USA), 0.2 µL of 10 µM forward primer to a final concentration of 100 nM, 0.2 µL of 10 µM of the phosphorylated reverse primer to a final concentration of 100 nM, and nuclease-free water to final reaction volume of 20 µL. The positive and negative ddPCR controls were systematically added. Positive ddPCR control includes 2 µL of initial library (< 10^{-7} ng DNA) as a template, and a negative non-template control (NTC) using 2 µL of water (no DNA). The experiments were designed to match 8 samples as there are 8 places in the cartridge that must be filled. Experimental layout was also optimized for duplicate samples, to have a samples for ddPCR quantification and the others for droplet extraction post ddPCR.

Table 7. Composition of a ddPCR reaction mixture in Hi-Fi SELEX.

Reagent	Volume (20 µL)	Final concentration
DNA template	2 µL	unknown
2X EvaGreen mix	10 µL	1X
Fw primer (10 mM)	0,2 µL	100 nM
pRev primer (10 mM)	0,2 µL	100 nM
Nuclease-free water	7, 74 µL	n/a

Exactly 20 µL of PCR mixture and 70 µL of QX200™ Droplet Generation Oil for EvaGreen per reaction (ref.1864006, Bio-Rad Laboratories, Inc., USA) were transferred into ddPCR DG8™ Cartridges (ref. 1864008, Bio-Rad Laboratories, Inc., USA) for the droplet generation in a QX200™ Droplet Generator (Bio-Rad Laboratories, Inc., USA). Then, 40 µL of generated droplets (20 µL of ddPCR mix and 20 µL of oil) were transferred into ddPCR plates (ref. 17005224, Bio-Rad Laboratories, Inc., USA) using RAININ p50 pipette with RAININ 200 µL tips strictly dedicated to ddPCR. The plate is heat sealed at 180 °C for 5 seconds using a Bio-Rad PX1 PCR Plate Sealer (Bio-Rad Laboratories, Inc., USA).

2.11. ddPCR amplification and reading

The ddPCR was performed for 40 cycles following optimized EvaGreen program: 5 min at 95 °C (enzyme activation), 30 sec at 95 °C (denaturation), 1 min at 60 °C (annealing/extension), 5 min at 4 °C (signal stabilization) and 5 min at 90 °C (signal stabilization) on a C1000 Touch Thermal Cycler (Bio-Rad Laboratories, Inc., USA). The amplified droplets were analyzed on QX200™ ddPCR System (Bio-Rad Laboratories, Inc., USA) using QuantaSoft™ Software (Bio-Rad Laboratories, Inc., USA).

2.12. DNA extraction from the droplets post ddPCR

After ddPCR, to be able to proceed in SELEX, droplets have to be broken to recover the DNA. Two existing methods to recover DNA from droplets were tested and compared : mechanical extraction using freeze-thaw and chemical extraction using chloroform (**Annex 3**). The chloroform-based method ensured a more homogenous (same volumes obtained) extraction and consistently higher yields of DNA. Therefore, it was used as method of choice for Hi-Fi SELEX. Immediately after ddPCR, the entire volume of wells was pipetted and pooled (if duplicates) into microcentrifuge tube. Then, 20 µL of Tris-HCl buffer (pH 7,4) and 70 µL of

chloroform was added per well, followed by vortexing at maximum speed for 1 min and centrifugation at 15 500 x g for 10 min at RT. The upper aqueous phase, containing the recovered aptamer DNA, is transferred to a fresh tube.

2.13. PCR reamplification

To have enough DNA for the next rounds of SELEX, the droplet-recovered DNA was re-amplified by multiple PCR reactions. Prior amplification, a small-scale pilot PCR is recommended to empirically determine optimal PCR cycle number needed to obtain single amplicon, without by-procuts. After determination of the optimal cycle number, anti-HE4 aptamers from SELEX are re-amplified on big scale using multiple reactions (30 reactions). The PCR reactions using 2 µL DNA template, 4 µL of 10 µM forward primer to a final concentration of 400 nM, 4 µL of 10 µM phosphorylated reverse primer to a final concentration of 400 nM,0.5 µL of 5 U/µL DreamTaq polymerase (ref. EP0705, Thermofisher Scientific, USA), 10 µL of 10X DreamTaq polymerase buffer (ref. EP0705, Thermofisher Scientific, USA) to a final concentration of 1X including 2 mM $MgCl_2$ (Thermofisher Scientific, USA), 2 µL of 10 µM dNTPs (ref. R0191, Thermofisher Scientic, USA) to a final concentration of 0.2 µM each, and nuclease-free H_2O to a final of 100 µL reaction. The DNA is amplified on C1000 Touch Thermal Cycler (Bio-Rad Laboratories, Inc., USA) following PCR program: 95 °C for 5 min (enzyme activation), 95° C for 30 sec (denaturation) and 60 °C for 1 min (annealing/extension) for 10-30 cycles depending on the SELEX cycle **(Table 8).**

Table 8. A. The constitution of the ddPCR mixture in the Hi-Fi SELEX. B. The optimal PCR cycle number (determined empirically) for the re-amplification of anti-HE4 aptamers in the HI-FI SELEX.

A

Reagent	Volume (100 µL)	Final concentration
DNA template	2 µL	unknown
10 X DreamTaq buffer with 50 mM $MgCl_2$	10 µL	1X
DreamTaq polymerase (5 U/ µL)	0.5 µL	1.25 U
dNTPs mix (10 mM)	2 µL	0.2 mM each
Fw primer (10 mM)	4 µL	400 nM
pRev primer (10 mM)	4 µL	400 nM
Nuclease-free water	76.5 µL	n/a

B

HE4 Hi-FI SELEX cycle	n of PCR cycles
C1	n/a
C2	n/a
C3	18
C4	14
C5	14
C6	18
C7	10
C8	10
C9	8
C10	15

2.14. The concentration of the aptamer PCR reactions and the primer removal

The PCR amplification reactions were pooled up to 3 mL and concentrated using Vivacon® MWCO 10 kDa (Sartorius, Germany), after centrifugation in a swinging-bucket rotor, at 4000 x g for 20 min at 4 °C. The retentate containing concentrated PCR reaction was loaded onto MicroSpin Sephadex G-50 (Cytiva, Marlborough, USA) columns to ensure primer removal, following manufacturer recommendation. First the tubes with columns are spun to remove the storage buffer (Tris-acetate-EDTA) and equilibrate the columns 1 min at 2000 x g at RT. In this case, we do buffer exchange to remove EDTA as it is inhibitor of downstream enzymatic reaction of λ exonuclease. Then, 250 µL of 1X λ exonuclease buffer (67 mM glycine-KOH, 2,5 mM $MgCl_2$, pH 9,4) is loaded on the column and spin again at 2000 x g for 1 min at RT. After centrifugation, 25 µL of PCR reaction/column is loaded and eluted by centrifugation again at 2000 x g at RT. Per SELEX cycle, 20 columns were used. The small aliquots of the DNA were kept for sequencing and as a back-up. The rest of the eluted purified DNA is pooled and subjected to ssDNA regeneration.

2.15. ssDNA regeneration by λ exonuclease

For the next round of SELEX, ssDNA need to be regenerated from dsDNA back to ssDNA. The ssDNA was regenerated by λ exonuclease digestion using optimized protocol **(Annex 4**). During Hi-Fi SELEX, the reaction was prepared by adding 20 µL of aptamer dsDNA (concentration unknown), 3 µL 10X buffer (670 mM glycine-KOH (pH 9,4), 25 mM $MgCl_2$, 0,1 % (v/v) Triton X-100), 1 µL of λ exonuclease enzyme (10 U/µL; ref. EN0561, Thermo Fisher Scientific, USA) to a final 10 U/µL, and filled with water to a final volume of 30 µL. The average number of reactions per Hi-Fi SELEX was 10. Then, reactions were incubated for 1 hour at 37 °C, followed by enzyme deactivation for 10 min at 80 °C. After the λ exonuclease reactions, samples were pooled, and the final sample was purified using phenol/chloroform method (same protocol as described previously**)**. The pellet (in duplicate) was resuspended in 25 µL of nuclease-free water. The final volume of aptamers at the end of each cycle was 50 µL. The purified ssDNA was then quantified by spectrophotometry and validated by 4 % agarose gel electrophoresis before starting next round of selection to HE4 target.

2.16. ssDNA quantification

The purified aptamer ssDNA pool was quantified by NanoDrop™ 2000c spectrophotometry (Thermofisher-Scientific, USA) before using it as input for the next round of Hi-Fi SELEX. The concentration was calculated for our library pools by Beer-Lambert Law:

$$A_{260} = \varepsilon \, l \, c$$

Where A is absorbance at 260 nm (no unit), ε is the molar absorptivity (L mol^{-1} cm^{-1}), l is the path length of the sample (cm) and c is the concentration of the sample (mol L^{-1}.)

The ssDNA aptamer concentration (mol/L) was calculated from absorbance at wavelength of 260 nm with 10 mm=1 cm path length, with molar extinction coefficient 654,479 L/(mol x cm). The ssDNA aptamer concentration (ng/µL) are calculated by formula c (ng/µL) = c (mol/L) x MW x 1000 where MW is molecular weight of initial 70 bases aptamer library (21452,5 g/mol). Then, the desired amount of DNA was added to each cycle of selection.

2.17. SELEX gel electrophoresis

Gel electrophoresis was performed at the end of each cycle to validate each selection round. It is important to check for the quality at several steps in SELEX: (1) the ddPCR amplification of the 70 bp aptamer sequence (2) during re-amplification of the 70 bp aptamers (large scale PCR) to ensure the PCR amplicons without by-products formation; (3) successful primer removal after large scale PCR and (4) the efficient conversion to 70 bases ssDNA aptamers using λ exonuclease. The aliquots of the DNAs were loaded on 4 % agarose gel, 1X TAE with GelRed staining next to a DNA ladder (ref. N3233S, New England Biolabs, USA), primers, ssDNA (initial library) and dsDNA (amplified initial library) as a reference. The electrophoresis was run on 50V for 1 h and visualized on Bio-Rad Gel-Doc. This ensures that aptamer library pool used as an input for next cycle is pure ssDNA ready for incubation with HE4 (presence of primers, or mixture of ssDNA and dsDNA could be a problem for selection).

2.18. DNA sequencing and bioinformatics

- **High-throughput sequencing (HTS)**

To study the enrichment to HE4 and to identify the specific anti-HE4 aptamer sequences present in each cycle of selection to ovarian cancer biomarker HE4, the DNA was sequenced

from cycle 5 (including positive selection to HE4 in cycles 5 to 10 (C5+ to C10+) and counter-selection in cycle 9 (C9-) and cycle 10 (C10-). The 1 µL of unpurified PCR product from SELEX was added into 99 µL of nuclease-free water and sent for DNA sequencing at MIRCen facility at CEA, France. The aliquots of the library after several rounds of SELEX were prepared for deep sequencing on Illumina system as previously described [156,157]. Approximately 200,000 sequencing reads were analyzed for the starting library and each cycle of SELEX from cycle 5 using a homemade software PATTERNITYseq (access to this software can be found at MIRCen Platform, CEA at: https://jacob.cea.fr/drf/ifrancoisjacob/english/Pages/Departments/MIRCen/Platforms/Aptamers.aspx, *accessed on 4 January 2023*). The analysis has been previously described [156]. Essentially, the adapter and primer sequences were first removed from each sequence, leaving only the variable regions with a size between 25 and 32 nucleotides. Then, the frequency of each sequence in the different libraries was calculated and any sequences with a frequency < 0,01 % in all libraries were removed to decrease the time of analysis. The remaining sequences (2621 in this case) were then sequentially clustered in families. Finally, the frequency of each family (2189 in this case) was calculated at every cycle.

- **Motifs analysis**

The most enriched anti-HE4 aptamer sequences were aligned and searched for shared or conserved motifs using matrix alignment (random region) and MEME software. A partially conserved motif between the 10 most enriched families was searched using the MEME suite (https://meme-suite.org/meme/; accessed on *3 January 2023*) [158].

- **Phylogenetic tree**

The phylogenetic tree of the top 10 most-enriched sequences (full sequences, with primer regions) was constructed using EMBL-EBI Clustal Omega online platform [159] (https://www.ebi.ac.uk/Tools/msa/clustalo/; accessed on *03 of January 2023*). First, a pairwise distance matrix for all the sequences to be aligned is generated, and a guide tree is created using the neighbor-joining algorithm. Then, each of the most closely related pairs of sequences are aligned to each other.

- **Secondary structure prediction**

The secondary structures of anti-HE4 aptamers are predicted using online DNA folding software Unafold http://www.unafold.org/; accessed on *30 August 2022*) [160]. The software predicts the folding and hybridization of the sequences and gives ensembles of structures based on the average minimum free energy (ΔG) which reflects the stability of each structure. The full-length aptamers (random and fixed regions included) or aptamers with random regions only were folded at urine salt concentration of $[Na^+]$ = 55.4 mM and $[Mg^{2+}]$ = 4.4 mM at temperature 25 °C.

PART 3 : CHARACTERIZATION OF THE CANDIDATE APTAMERS

3.1. The list of characterized anti-HE4 aptamers

The binding of anti-HE4 aptamers to ovarian cancer biomarker HE4 was evaluated using two methods: surface-plasmon-resonance (SPR) and ThermoFluorimetic Analysis (TFA). The characterization included the top 10 most-enriched anti-HE4 sequences AHE1 to AHE10 developed by the Hi-Fi SELEX in Chapter 2 and two anti-HE4 sequences A1 and A3 from the literature [148]. All aptamers were chemically synthesized by Eurofins, Genomics and resuspended at 100 µM nuclease-free H_2O.

Table 9. List of the anti-HE4 aptamers tested for binding to ovarian cancer biomarker HE4.

Aptamer ID	DNA Sequence*	Size (nucleotides)	MW (g/mol)	DNA source	Method
AHE1 (full)	5‘- TCGCACATTCCGCTTCTACC CCC AAC CAA CGT CTA TAC TTC CCC AAC CTC CGTAAGTCCGTGTGTGCGAA-3’	70	21196.6	Hi-Fi SELEX	TFA, ELONA
AHE1 (random)	5‘- CCCAACCAACGTCTATACTTCCCCAACCTC-3’	30	8935.8	Hi-Fi SELEX	SPR
AHE2 (full)	5‘- TCGCACATTCCGCTTCTACC GCCAACATCGTACTCCATCTGCCACCCCCACGTAAGTCCG TGTGTGCGAA-3’	70	21237.6	Hi-Fi SELEX	TFA
AHE2 (random)	5‘-GCCAACATCGTACTCCATCTGCCACCCCCA-3’	30	8976.8	Hi-Fi SELEX	SPR
AHE3 (full)	5‘- TCGCACATTCCGCTTCTACCCATCAATCAGCATACCCACC ATGTACGTCC CGTAAGTCCGTGTGTGCGAA-3’	70	21300.7	Hi-Fi SELEX	TFA
AHE3 (random)	5‘- CATCAATCAGCATACCCACCATGTACGTCC-3’	30	9039.9	Hi-Fi SELEX	SPR
AHE4 (random)	5‘- TAGCACAAGTATGCTCACCATGACCACTAC-3’	30	9000.8	Hi-Fi SELEX	SPR
AHE5 (random)	5‘- T CGCTCTACTCCCGACTAACCCCAAGCTCAA-3’	30	9063.9	Hi-Fi SELEX	SPR
AHE6 (random)	5‘- CAACAGACATCTCCATTGCCATACCACATG-3’	30	9103.9	Hi-Fi SELEX	SPR
AHE7 (random)	5‘- CCAATGCACAAGTGGCAGTCCCATATTCAC-3’	30	9119.9	Hi-Fi SELEX	SPR
AHE8 (random)	5‘- CCGATGCCTGCCTCGAATCAACTTCACAAC-3’	30	9055.9	Hi-Fi SELEX	SPR
AHE9 (random)	5‘- CAGATGCCAAAACCTCCACACGTCTGAGAC-3’	30	9022.9	Hi-Fi SELEX	SPR
AHE10 (random)	5‘- ACATCATCCCACCAAGATAAAAGACATCAC-3’	30	9113.9	Hi-Fi SELEX	SPR
A1	5‘- TTA TCG TAC GAC AGT CAT CCT ACA C-3’	25	7560.9	Eaton et al. 2015	SPR, TFA
A3	5‘-CAC AGT GCG TCA CAT TTA GGG CAT T-3’	25	7657	Eaton et al. 2015	SPR, TFA

** The blue color highlights the fixed primer binding regions.*

3.2. Surface Plasmon Resonance (SPR) analysis of the aptamers-protein binding

Surface Plasmon Resonance (SPR) is an optical method to measure the refractive index near a sensor surface, to characterize the interaction between anti-HE4 DNA aptamers and target protein HE4. The analysis was carried out on a Biacore T200 SPR instrument, in collaboration with the Dr Martine Pugniere from PP2I Plateforme Protéomique et Interactions Moléculaires, at the Institut de Recherche en Cancérologie de Montpellier (IRCM).

The screening was performed to twelve different sequences, including 30-mer (random region) anti-HE4 aptamers AHE1 to AHE10 developed by Hi-Fi SELEX and two 25-mer sequences A1 and A3 from Eaton *et al* [148]. Only aptamers without the primer-binding regions were used. The stock aptamers were resuspended in nuclease-free H_2O to a final concentration of 100 µM and the stock HE4 (ref. ab219658, Abcam, USA) was resuspended in nuclease-free H_2O to a final concentration of 400 µg/ml (36.36 µM). To perform a screening of the different aptamers with their target, the 6xhstidine-tagged HE4 was immobilized on the sensor chip using Anti-His antibody (ref. MAB050, R&D Systems, USA) to an average of 900 Response Unit (RU).

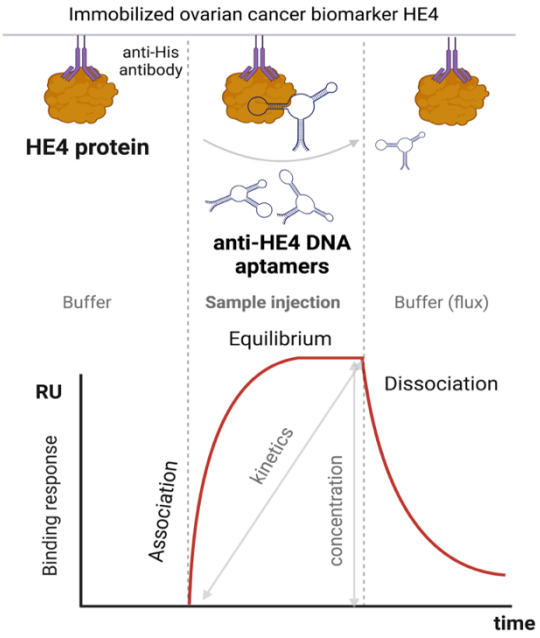

Figure 20. Surface Plasmon Resonance binding of anti-HE4 aptamers and ovarian cancer biomarker HE4.

A SPR sensor chip was chemically modified using EDC-NHS (1-Ethyl-3-[3-dimethylaminopropyl]carbodiimide hydrochloride N-Hydroxysulfosuccinimide sodium salt) chemistry to immobilize the anti-His antibody (average immobilization about 14 000 RU). Then, 500 nM of target 6xHis-HE4 were captured by the anti-His antibody for 120 sec at 10 µl/min. The HE4-aptamer interaction was studied by flowing the different anti-HE4 aptamers, for 2 min at 30 µL/min in a concentration of 2 µM in a buffer PBS-P with added magnesium (137 mM NaCl, 2, 7 mM KCl, 8 mM Na_2HPO_4, and 2 mM KH_2PO4, 0,05 % Polysorbate 20 + 5 mM $MgCl_2$). The change in refractive index due to the formation of aptamer/HE4 interaction is measured in real time and the results are plotted as response units (RU) *versus* time to yield

a sensorgram. Signal from the control flow cell (without HE4) is subtracted from the signal of the flow cell with immobilized HE4.

3.3. Thermofluorimetric analysis (TFA) of the aptamers-protein binding

Thermofluorimetric analysis (TFA) method can be used for the aptamer-protein binding characterization. It is based on the changes in the fluorescence and thermal stability of the aptamers upon interaction with the target [161]. The fluorescence is measured in relative fluorescence units (RFU) in a standard qPCR thermocycler by applying melting profile (0-90°C). The aptamer melting profile is monitored by the fluorescent signal coming from an intercalating dye, such as SYBR green or SYBR gold, which binds to the double-stranded regions within the folded aptamer [162]. This technique exploits the difference in fluorescence of fluorophores whether they are intercalated (high fluorescence) or not (low fluorescence) within double-stranded region of nucleic acids [161]. Therefore, alterations of the melting profile are monitored and changes are observed in presence of the target [162].

The plot of fluorescence decay as a function of temperature is called *melting curve*. To identify the value of *melting temperature* (T_m), a temperature where half of the aptamer is denatured, the negative derivative of fluorescence -d(RFU)/dT is plotted against the temperature. The T_m is the temperature at the maximum of the -d(RFU)/dT peak. Upon introduction of the target protein, recognition and binding occurs and changes in the fluorescence is observed as the aptamer structure changes into a protein-bound state. Protein-bound aptamers are usually more thermodynamically stable, and an increase in the T_m is observed. Generally, the protein-bound melting temperature (T_m, bound) is higher than that of the unbound aptamer (T_m, free). However, not all aptamers will follow the same rule, as the nature and stability of the binding is aptamer or aptamer-target complex dependent [161]. The principle of the TFA is presented below (**Figure 21**).

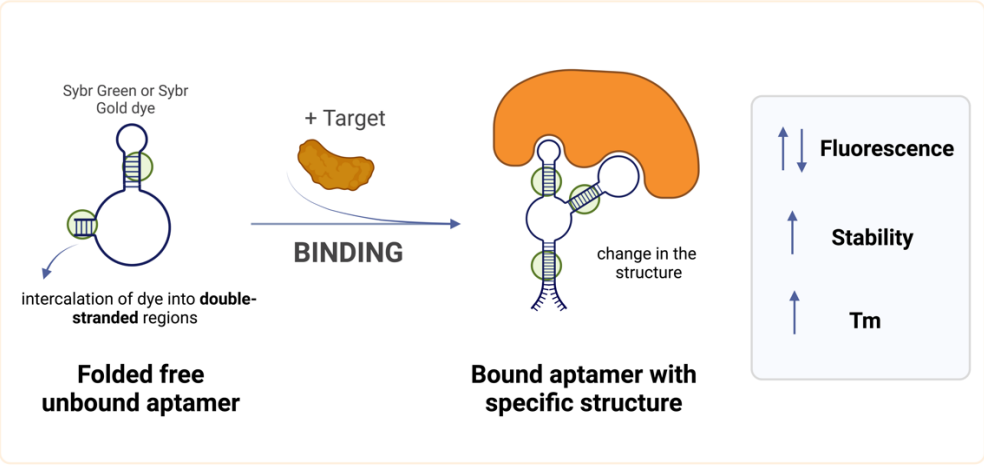

Figure 21. Principle of the thermofluorimetric analysis (TFA) of aptamer-protein binding.

(*Created with BioRender.com*)

Each individual aptamer has its specific T_m depending on its sequence, G/C content, structure stability, length, and the solution environment (buffer composition, pH, salts, Mg). The examination of the melting profile of an aptamer (constant concentration) while titrating the target protein (changing concentration) compared to the melting profile of the aptamer alone, may allow to distinguish peaks corresponding to different DNA structures present in solution. Therefore, it is potentially possible to discriminate between free aptamer and protein-bound aptamer state [162]. After determination of the bound T_m of the aptamer-protein complex, and substraction of the aptamer only signal (blank), the signal of the negative derivative of fluorescence -d(RFU)/dT at the bound T_m is plotted against the protein concentration. This generates a binding curve from which a constant of dissociation K_d can be calculated.

3.3.1. HD22 aptamer and thrombin protein binding

The anti-thrombin aptamer is frequently used as a model aptamer in the development of a novel aptamer assays, due to its well-known characteristics and high-affinity. Therefore, it was used in this thesis to establish TFA method for aptamer-protein binding in urine. Thrombin-aptamer system serves as a *proof-of-concept* for demonstration that aptamer can be functional in urine and bind to its target. The anti-thrombin aptamer HD22 (5′-AGT CCG TGG TAG GGC AGG TTG GGG TGA CT-3′) [163] is a 29-mer single stranded DNA G-quadruplex that specifically recognizes exosite II of human thrombin, with a high-affinity and K_d of 0.5 nM [163].

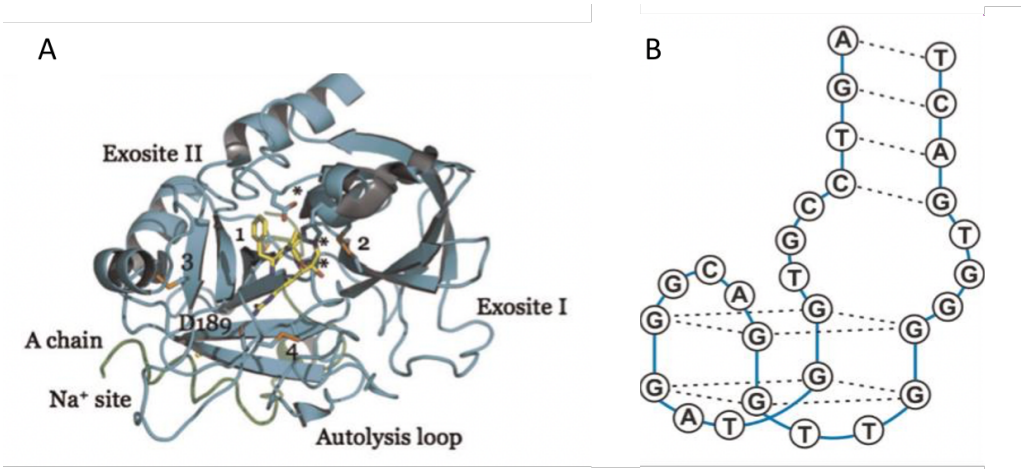

Figure 22. Thrombin protein and HD22 aptamer (from Deng *et al.* 2014)

The characterization of thrombin aptamer was performed during the M2 internship of Alicia GOTTE under my supervision. To validate aptamer signal in TFA settings and urine, and optimize the concentration, HD22 aptamer (Eurofins Genomics, Germany) was tested without protein at concentrations of 0, 50, 100, 200 and 400 nM in 1/125 X diluted urine. To determine whether protein Serum Bovine Thrombin (ref. T4648, Sigma-Aldrich) would give signal in TFA conditions, different concentrations were tested in 1/125 X diluted urine (0, 25, 50, 100, 200, 400, 800, 1000 and 2000 nM. Finally, the aptamer HD22: protein thrombin interaction was tested by subjecting 200 nM constant HD22 aptamer to increasing concentration of thrombin ranging from 0 to 2000 nM in presence (1/125X) and absence (protein buffer) of urine, to evaluate the impact of urine on binding.

3.3.2. Anti-HE4 aptamers and HE4 protein binding

Five different candidate anti-HE4 DNA aptamers were tested for binding characterization to ovarian cancer biomarker HE4: A1 and A3 from the literature [164], and AHE1, AHE2 and AHE3 developed by Hi Fi-SELEX in this thesis work. AHE2 did not exhibit binding to HE4 and is therefore not shown. Aptamers were tested in diluted urine environment (1/125X) and in protein buffer (10,1 mM Na_2HPO_4, 137 mM NaCl, 2,7 mM KCl, 1,8 mM KH_2PO_4, 1 mM $MgCl_2$). First, optimized aptamer concentration was determined by testing a range of concentrations: 0, 50, 100, 200 and 400 nM, to confirm signal contribution to aptamer and to determine optimal probe concentration. Then, human recombinant HE4 protein (ref. ab219658, Abcam, USA) in 0-2000 nM was tested in 1/125X urine or buffer to establish whether the protein alone yielded signal in presence of the intercalating dye. Finally, to characterize the

anti-HE4 aptamers binding to ovarian cancer biomarker HE4, increasing concentration of HE4 was added to a constant concentration of aptamers (200 nM for A1/A3 and 100 nM for AHE1/AHE3) to a HE4 conentrations ranging from 0 (aptamer only, blanc), 5, 15, 25, 50, 100, 200, 300, 400, 600 to 800 nM either in presence (1/125X) or absence (protein buffer) of urine.

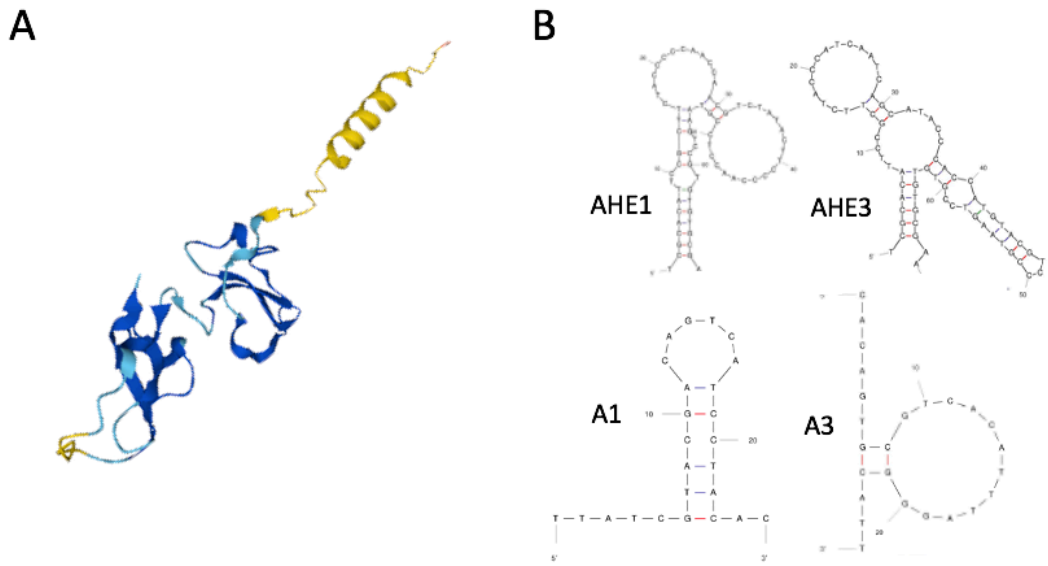

Figure 23. HE4 protein and characterized anti-HE4 aptamers.

A. Structure of human HE4 protein (*created with Alphafold*) **B.** Secondary structures of tested anti-HE4 aptamers A1, A3, AHE1 and AHE3 in urine (*created with Unafold*).

3.3.3. Effect of urine on the TFA measurements

To test the effect of the urine on the aptamer fluorescent signal, different urine dilutions were tested. Aptamers were denatured in an aptamer buffer (10 mM Tris–HCl, 50 mM KCl, 3.3 mM $MgCl_2$; pH = 8.0) for 5 min at 95 °C, placed 10 min on ice before cooling down to RT. The samples were prepared by mixing denatured aptamers to a final of 200 nM for anti-thrombin aptamers and 100 nM for anti-HE4 aptamers, artificial urine to final concentration of 1X (just urine), 1/125X (diluted urine) and 0X (just protein buffer). The dilution of urine is prepared in protein buffer (10,1 mM Na_2HPO_4, 137 mM NaCl, 2,7 mM KCl, 1,8 mM KH_2PO_4, 1 mM $MgCl_2$), to final reaction of 20 µL.

3.3.4. Sample preparation for aptamer-protein binding

All experiments were performed using same protocol : denaturation of the aptamer in aptamer buffer as stated in 0 before being diluted in 1/125X urine or protein buffer and incubated with

different concentrations of protein for 1 h at 25 °C. The constant aptamer concentration (100 nM for AHE1/AHE3 or 200 nM for HD22/A1/A3) was subjected to the target protein in concentrations ranging from 0 to 800 nM. The TFA reaction mixture (**Figure 24)** of total 20 µL consisted of 5 µL of denatured aptamer DNA to a final concentration of 100 or 200 nM (in aptamer buffer), 5 µL of urine to a final dilution of 1/125 X urine (diluted in protein buffer), 5 µL of Sybr-Gold dye (ref. S11494, Invitrogen, USA), to a final concentration of 1 X, and 5 µL of protein in the protein buffer (10,1 mM Na_2HPO_4, 137 mM NaCl, 2,7 mM KCl, 1,8 mM KH_2PO_4, 1 mM $MgCl_2$) to a final concentration ranging from 0 to 800 nM. In a samples without aptamer, 5 µL of aptamer buffer was added in place of aptamer. For the "blank" sample needed for subtraction (aptamer only), 5 µL of protein buffer was added in place of protein. For the sample without urine, 5 µL of protein buffer was added in place of urine.

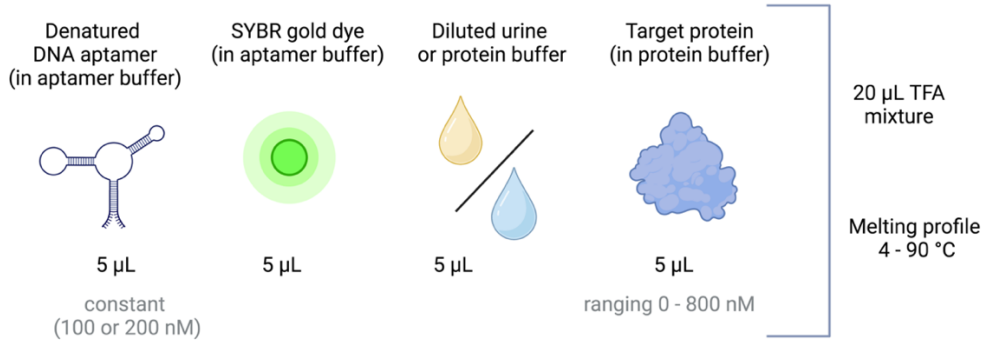

Figure 24. Sample composition for aptamer-protein binding characterization by TFA.

(Created with BioRender.com)

The melting profile of aptamer-protein binding was analyzed on a C1000 Touch/CFX96 Deep Well real-time instrument (Bio-Rad Laboratories, USA) with a temperature gradient from 4 °C to 90 °C at 0.5 °C/min. Fluorescence excitation was set at 450/490 nm and fluorescence emission was measured at 515/530 nm.

The *melting curve* was constructed by plotting the negative derivative fluorescence signal −d(RFU)/dT against temperature. The new T_m, corresponding to the melting of the aptamer-protein complex was observed after blank subtraction (signal from free aptamer only, without protein). Finally, the *binding curve* was constructed with plotting the negative derivative fluorescence signal −d(RFU)/dT at the T_m of the bound aptamer and concentration of the target protein. The estimation of the constant of dissociation (K_d) was performed using the online platform **https://mycurvefit.com** on the nonlinear sigmoidal regression model. The data presents results from a minimum of three independent experiments. Different steps in the

thermofluorimetric analysis of the aptamer-protein binding characterization is presented below (**Figure 25**).

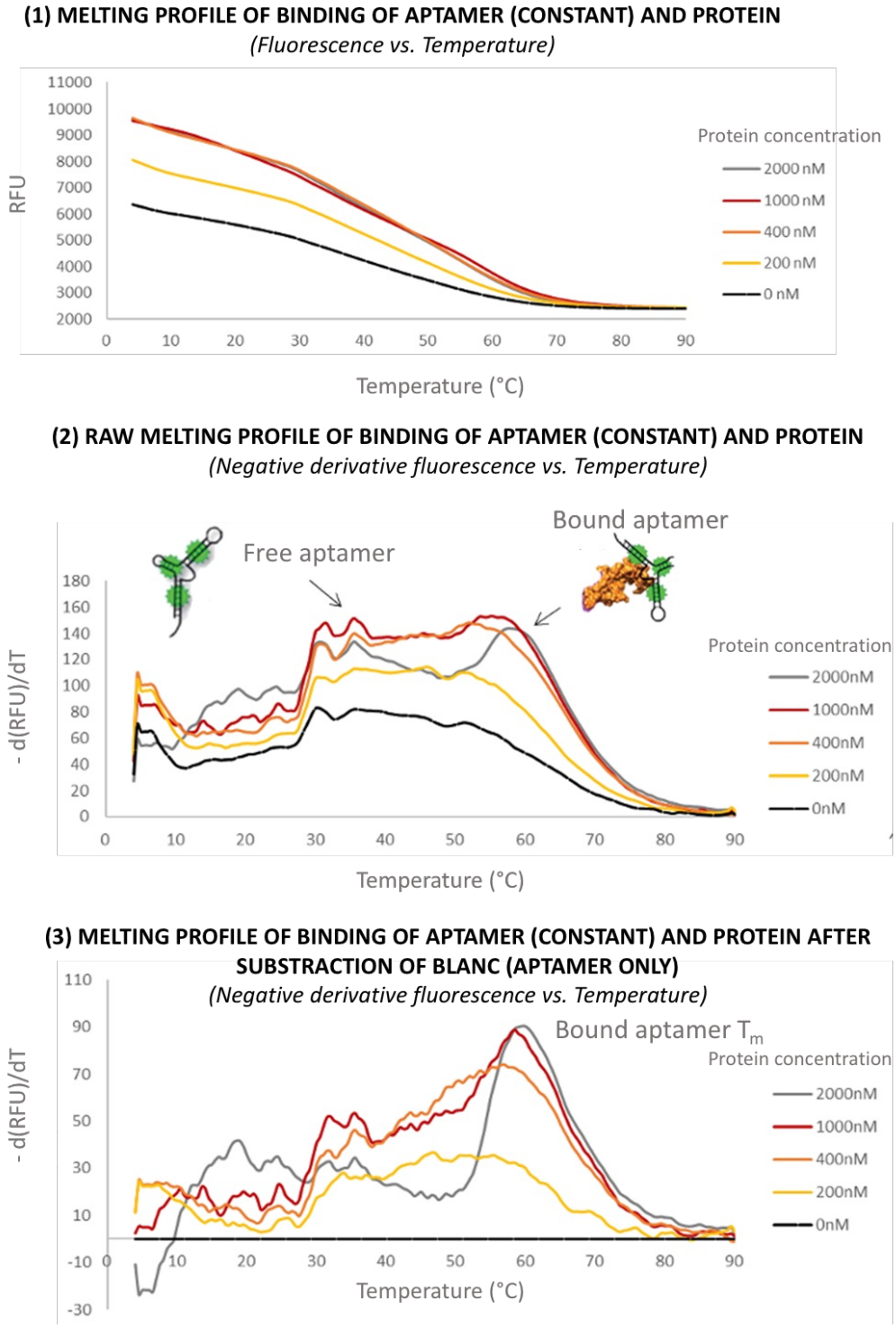

Figure 25. Different steps in characterization of aptamer-protein binding by TFA.

3.4. HE4 Enzyme-Linked-OligoNucleotide Assay (ELONA)

The aptamer-based ELONA (Enzyme-Linked OligoNucleotide Assay) was designed for detection of HE4 protein and studying the aptamer-protein binding. We applied anti-HE4 aptamer in direct colorimetric ELONA to evaluate its ability to recognize and bind to its target HE4 protein. The schematic representation of the assay is shown in below (**Figure 26**). The ELONA was performed by immobilization of recombinant C-terminal 6xHistidine-tagged human HE4 on Ni-NTA beads followed by addition of biotinylated aptamers. Streptavidin-horseradish peroxidase (HRP) system was used for signal revelation. Streptavidin-HRP can recognize and bind to the biotin tag on the aptamer. After adding the TMB (3,3',5,5'-Tetramethylbenzidine) substrate for HRP, the reaction results in a blue product. The reaction can be stopped by adding H_2SO_4, and the blue is converted into the yellow product. The color can be read using a plate reader at the wavelength of 450 nm.

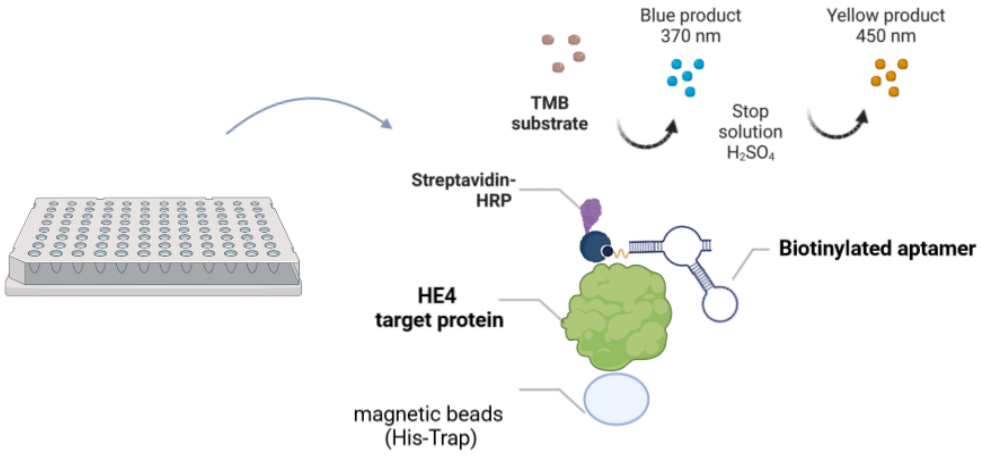

Figure 26. Enzyme-Linked-OligoNucleotide Assay (ELONA) for detection of HE4.

First, to evaluate the potential of anti-HE4 aptamers as diagnostic probes, anti-HE4 aptamers with the best binding properties exhibited by previous TFA method were tested: AHE1 (70 nt), AHE3 (70 nt) and A3 (25 nt). To evaluate the impact of the biotinylation depending on the position of the biotin tag, both 5' or 3' biotin-DNA aptamers were tested for binding to HE4 protein in a pilot study (**Annex 7**). From all the aptamers, only aptamer 5'biotin AHE1 displayed signal coming from potential aptamer-HE4 binding and is shown in this thesis. More research is needed and binding of aptamers and HE4 by ELONA is undergoing.

First, HE4 protein was immobilized on the Ni-NTA beads. The slurry was equilibrated with equilibrium buffer (20 mM sodium phosphate, 300 mM sodium chloride with 10 mM imidazole; pH 7,4). The beads were centrifuged at 700 x g for 2 min at RT and supernatant was discarded to remove the storage liquid. Then, 100 µl/well of HE4 protein solution was added to correspond to 0,5, 5,10, 50 and 100 pmol of immobilized HE4 and incubated for 30 minutes at RT with mild shaking at 1300 rpm. For blank reactions, empty beads were added without HE4 to the control wells (0 pmol HE4),. The working solution of 5'-AHE1 (70 nt, full size with primer regions) was prepared in binding buffer (100 mM NaCl, 20 mM Tris-HCl pH 7,6, 10 mM $MgCl_2$, 5 mM KCl, 1 mM $CaCl_2$, 0,005 % Tween-20) to a final concentration of DNA of 100 nM. The DNA aptamers were denatured for 5 min at 95 °C, cooled for 10 min on ice, and kept at RT before exposure to HE4 protein. Then, 100 µL/per sample of denatured aptamer solution (100 nM in binding buffer) were added to the immobilized HE4. The aptamers and HE4 protein were incubated at 25 °C for 1 hour to allow for binding of aptamers to target protein. After binding, the beads were washed three times with 200 µL of binding buffer to remove unbound oligonucleotides. Then, 100 µL of ExtrAvidin®-Peroxidase (ref. E2886, Sigma-Aldrich, USA; prepared as 0.25 g/mL in binding buffer) was added and incubated at 21 °C for 1 hour with mild shaking. Then, the samples were washed five times with 200 µL of binding buffer. Then, 100 µL of TMB (3,3',5,5'-Tetramethylbenzidine) substrate solution was added and incubated 15 min in a dark room at RT. The reaction was stopped by addition of 50 µL of 0,5 M H_2SO_4 in each sample and the optical density was measured at 450 nm using the plate reader (ref. Tecan Infinite® 200 Pro, Männedorf, Switzerland).

IV. RESULTS

PART 1 – IDENTIFICATION AND PRODUCTION OF THE TARGET URINE BIOMARKERS

1.1. Selection of the target urine biomarkers

The global aim of the *CARIBOU (CAncer ovaRIan BiosensOr in Urine)* project, which this thesis takes part in, is the development an aptamer-based biocaptor for the detection of ovarian cancer biomarkers in urine. The initial idea was to perform multiplex detection of several urine biomarkers using aptamers. Therefore, at the beginning of the first year, extensive bibliography research was performed to identify existing and reliable biomarkers found in urine. Different biomarker types were studied, with a focus on proteins, peptides and microRNAs. Initially, the target biomarkers of interest included *Human Epididymis Protein 4 (HE4), Osteopontin (OPN)* and microRNAs. *Osteopontin (OPN)* is a phosphoprotein upregulated in cancer. Serum OPN protein is a known cancer biomarker, implicated in progression of solid tumors [165,166]. It has been studied as a biomarker for detection of OC [167,168]. It is detected in blood of OC patients, but has not yet been detected in urine. Single study by Ye *et al.* in 2006 reported presence of ostepontin in urine of OC patients, in a form of digested COOH-terminal fragments [53]. The available data in the literature could not enable to find the exact fragment structures and sequences of urine OPN to use as a target in this study for selection of aptamers. Moreover, it was found to be non-specific biomarker, elevated in numerous diseases and cancer types. Indeed, dysregulated OPN levels in urine are associated with individuals with kidney disease, urolithiasis and lupus nephritis [169–171]. Therefore, it was not ideal candidate for this project at this moment. A splicing isoform of the OPN protein, a shorter version *Osteopontin-c (OPNc)*, was found to be more specific to OC, and connected to OC proliferation, metastasis and chemoresistance [172–174]. However, it was not yet found detected in urine. Therefore, it was out of the scope of this thesis, but it would be interesting target to study in the future of this project.

Furthermore, microRNAs were studied as potential targets. *MicroRNAs* are a small non-coding RNA molecules dysregulated in OC. Based on the insight of the literature, several species have been found as potential OC targets, including miR-200a, miR-200c and miR-30a-5p [46,61,63]. Indeed, miR-30a-5p was found upregulated in urine of patients, associated with early stage of OC and metastasis [61]. The idea of the microRNAs was dismissed, due to potentially not being

able to detect it directly in urine using aptamers, without prior pre-amplification. In addition, validations of the specific miRNA signatures in urine of patients are still undergoing. Moreover, the inability to work in a complete *RNAse-free* environment would additionally complicate the research. This bibliographical research was performed during pandemic lockdown and resulted in a review paper published in the peer-reviewed journal (IF = 4,56):

- Hanžek A, Siatka C, Duc A-C E. Extracellular urinary microRNAs as non-invasive biomarkers of endometrial and ovarian cancer. *J Cancer Res Clin Oncol.,* 2023, https://doi.org/10.1007/s00432-023-04675-5

Finally, as the thesis focuses on the urine as a sample, it was decided that the main target of this thesis is *Human Epididymis protein 4* (HE4). From all the available biomarkers for OC, HE4 appeared as currently only reliable urine biomarker, due to the several reasons. As a secreted small protein, it is excreted and easily detected in urine. HE4 is a protein overexpressed in urine of OC [49,64,95]. Serum HE4 is FDA-approved biomarker clinically used in the management of OC [30,33]. Moreover, it is elevated early in the course of disease and validated through numerous independent studies. It has been found elevated in serum and urine of OC patients in multiple studies and its diagnostic value in urine has been investigated [49,65,98].

According to the **Table 10** which summarizes the characteristics of an ideal tumor biomarker [175], urine HE4 possesses several advantageous traits.

Table 10. The characteristics of HE4, the main target of this thesis work.

Characteristics	Description
Highly specific	Elevated only in ovarian cancer
Highly sensitive	Elevated in physiological or benign disease states
Levels correlate with tumor burden	Prognostic and predictive utility of HE4
Short half-life	HE4 with $T_{1/2} < 4$ h [176] enable frequent serial monitoring of patients (efficiency of surgery or therapy)
Simple and cheap test	Enables applicability as a potential screening test
Easily obtainable specimens	Urine is acceptable by target population

Indeed, urine HE4 is highly specific (elevated in urine of ovarian cancer patients), highly sensitive (not elevated in urine of benign conditions or healthy individuals), urine HE4 correlates with tumor burden and has prognostic or predictive potential [65]. Urine HE4 has been shown stable and non-invasive, while having same diagnostic accuracy compared to serum

[49,65,95]. Moreover, detecting HE4 in urine using aptamers presents simple and cheap test that could be applicable in healthcare setting or as screening test in the high-risk population. Additionally, urine is an easily obtainable sample, generally well-accepted by patients.

Therefore, urine HE4 presents ideal target biomarker for this thesis and is chosen as main target for the development of high-affinity aptamers for detection in urine.

1.2. Construction of the expression plasmid pGEX-HE4

The initial idea was to produce Human Epididymis protein 4 (HE4) by overexpression in bacterial system. The protein expression plasmid pGEX-HE4 was constructed by cloning the target *WFDC2* (*HE4*) *gene*, a gene amplified in ovarian cancer, from a plasmid pEX-HE4 into pGEX-2T backbone by double digestion with BamHI/EcoRi endonucleases. (**Figure 27A**). The samples include just plasmid (no restriction enzymes), individual restrictions with BamHI and EcoRI and double digestion BamHI/EcoRI (**Figure 27B**). The last sample, double digested BamHI/EcoRI, is the sample of interest, while the others serve as controls for plasmid integrity. The pGEX-2T (on the left) is digested successfully and observed as expected single band of 4938 bp linear backbone pGEX-. The pEX-HE4 plasmid (on the right) is digested successfully and observed as two individual bands, containing linear 2450 bp PEX- backbone and linear 291 bp HE4 gene of interest (**Figure 27B**).

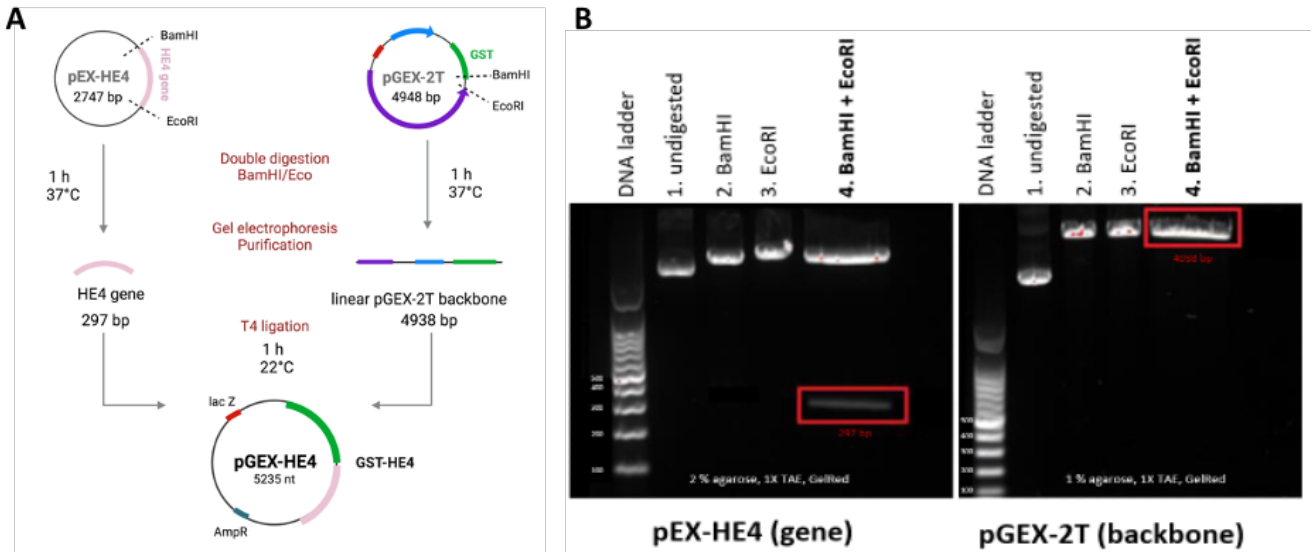

Figure 27. The cloning and construction of HE4 expression plasmid pGEX-HE4.

A. The pEX-HE4 (with HE4 gene) and pGEX-2T (backbone with GST tag) plasmids are double digested with EcoRI and BamHI and ligated to create pGEX-HE4, which contains genes for protein expression of recombinant GST-HE4 protein **B**. Gel electrophoresis of restriction endonuclease digestion of plasmids pGEX-2T (on left) and pEX-HE4 (on right). DNA ladder 100 bp (ref. N3231S, New England BioLabs Inc., USA); 1 - undigested circular plasmid, 2 - linear plasmid digested by BamHI; 3 - linear plasmid digested by EcoRi; 4 - double digsestion by BamHI/EcoRI. The restriction was successful and HE gene with the size of 297 bp and pGEX-2T backbone with the size of 4938 bp were extracted from the gel and ligated.

Then, purified HE4 gene was cloned into purified pGEX-2T backbone using T4 ligase to create protein expression vector pGEX-HE4. The 10 individual clones owere subjected to colony PCR to confirm the insert of a HE4 gene. As seen in **Figure 28A**, the results of the colony PCR show the amplicon of around 141 bp visible in positive PCR control (but negative cloning control), while no band is observed in negative non template (NTC) control. It is observed that 9 out of 10 bacterial clones have visible amplicon around the expected size of 438 bp (HE4 gene 297 bp + plasmid DNA 141 bp). Only one clone (clone 8) have an amplicon around 141 bp (empty plasmid DNA) and it was discarded. The amplification of the 438 bp PCR product confirms the successful construction of pGEX-HE4.

To verify the exact DNA sequence and orientation of the HE4 gene, several clones were sent to DNA sequencing. The sequences of plasmid DNA and expected HE4 gene were aligned as seen on **Figure 28B**. The clones 3, 6, 7 and 10 have 100 % correct sequence of desired human *HE4* gene.

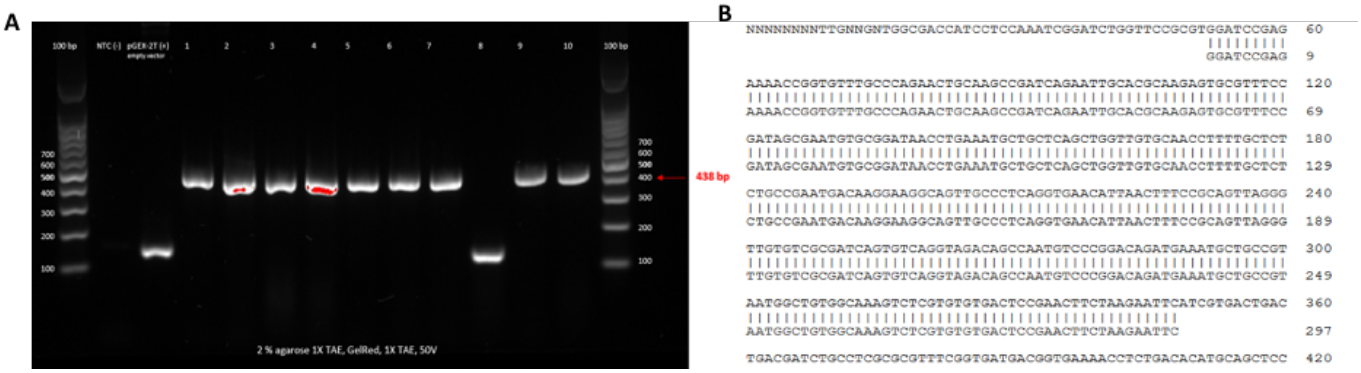

Figure 28. Verification of the pGEX-HE4 expression plasmid.

A. Colony PCR screening of pGEX-HE4 plasmids ligation in *E.Coli DH5α*. The HE4 gene is ligated into pGEX-2T plasmid. The bacterial clones were screened for successful transformants using pGEX-2T primers. Lanes: (100 bp) DNA ladder (ref. N3231S, New England BioLabs Inc., USA), NTC (non-template control) – negative PCR control; pGEX-2T (+) – positive PCR control, but negative ligation control, pGEX-2T plasmid as template; with expected amplicon of 141 bp; (1-10) bacterial clones of pGEX-HE4 transformants in *E.Coli DH5α* with HE4 gene of interest, with expected amplicon of 438 bp (HE4 gene 297 bp + plasmid DNA 141 bp) **B. Alignment analysis of pGEX-HE4 plasmid DNA and expected sequence of the HE4 gene.** The sequence show 100 % correct alignment of sequence of expected HE4 gene and backbone of pGEX-HE4 plasmid. Therefore, the plasmid pGEX-HE4 is verified and ready for HE4 protein expression (*Created with Serial Cloner software*).

The verified pGEX-HE4 protein expression plasmid is ready to use and carries genes required for protein expression, ampicillin resistance and the gene for ovarian cancer biomarker, the recombinant GST-HE4 protein.

1.3. HE4 protein expression and purification

The objective was to produce the ovarian cancer biomarker HE4. The pGEX-HE4 plasmid was transformed into *E.Coli T7 Shuffle strain* (NEB C3026J), bacteria suitable for disulfide bonds formation. The HE4 protein expression was induced by IPTG at 30 °C and 37 °C. The samples were taken prior induction, 1, 2, 3 and for 4 h for expression at 37 °C and after 3 and 4 h for 30 °C, respectively. The bacterial protein profile was studied by the SDS-PAGE and is shown at **Figure 29**. The results show expression of target GST-HE4 protein after induction with IPTG at 37 °C, but not on 30 °C, with a band at 37°C appearing around expected size of 35,65 kDa.

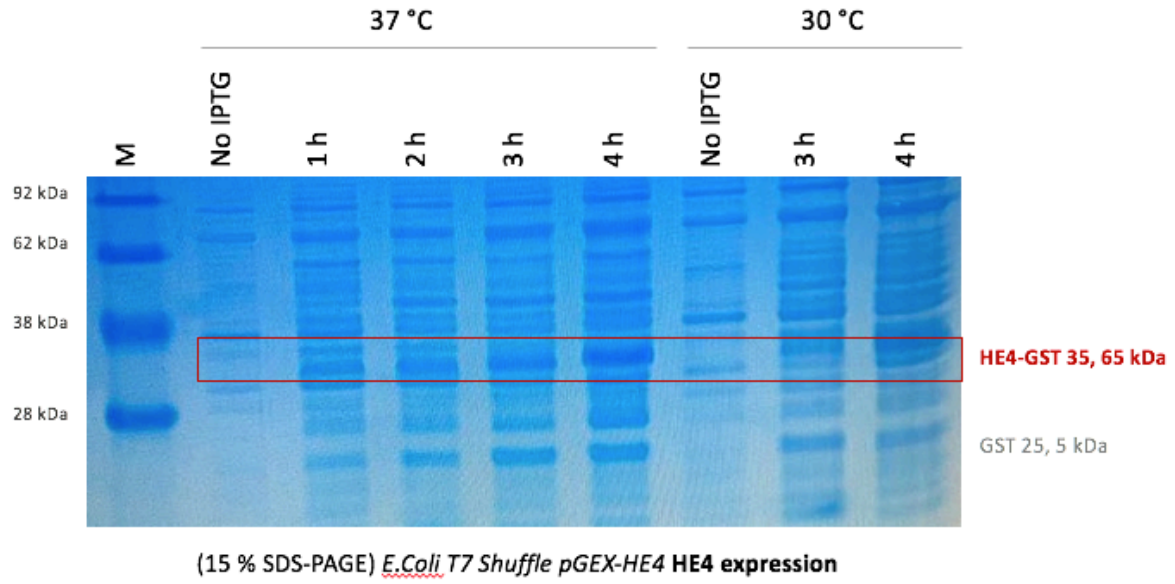

Figure 29. GST-HE4 protein overexpression in E.Coli T7 Shuffle.

M - SeeBlue™ Plus2 protein standard (ref. LC5925, Invitrogen™); **no IPTG** - sample prior IPTG induction of protein expression; **1 h** - 1 hour post induction; **2 h** - 2 hours post induction; **3 h** - 3 hours post induction; **4 h** - 4 hours post induction. Expected size of the target protein GST-HE4 is 35,65 kDa, with a band visible after 1, 2, 3 and 4 h of protein expression at 37 °C, but not at 30°C.

Both fusion protein (35.65 kDa) and protein tag GST (25.5 kDA) are visible at 37 °C after 1, 2, 3 and 4 hours of induction, without increased amount of HE4 protein with time. Therefore, HE4 expression at 37 °C and 1 hour could be sufficient condition for further experiments. Moreover, at this conditions, the GST tag band is lower intensity than after 2, 3 and 4 hours (**Figure 29**). The potential co-expression of both GST-HE4 fusion protein and GST-protein tag could be problematic and result in a mixture of proteins, which cannot be used in further experiments where only GST-HE4 is required for selection of high-affinity aptamers. The presence of both HE4-GST and GST could indicate the potential instability of the GST-HE4 construct or preference for GST expression. For example, after induction at 30°C, only GST protein tag is present, without target fusion protein of interest. Therefore, the process should be further optimized to obtain individual GST-HE4 protein, or potentially switch to different protein tag, for example 6xHistidine, which is smaller in size compared to the target protein. However, as GST-HE4 target protein is present, it was subjected to further purification.

From the protein lysate after IPTG protein induction (37 °C, 1 h), GST-HE4 protein was purified using Pierce™ Glutathione magnetic beads. The results in the **Figure 30** show the purification process. The samples loaded include: the input prior protein purification consisted of *E.coli T7 Shuffle (pGEX-HE4)* total proteins; flow through (FT) consisted of all bacterial

proteins except GST-HE4 immobilized on beads; supernatant after first wash step (SN1-W1) and supernatant after second wash step (SN2-W2), which should not contain proteins if washing was successful; the purified GST-HE4 protein of interest, with expected size of 35.65 kDa (N-terminal GST 25.5 kDa and HE4 protein 10.15 kDA); and GST tag loaded as a reference, with expected size of 25.5 kDa (**Figure 30**).

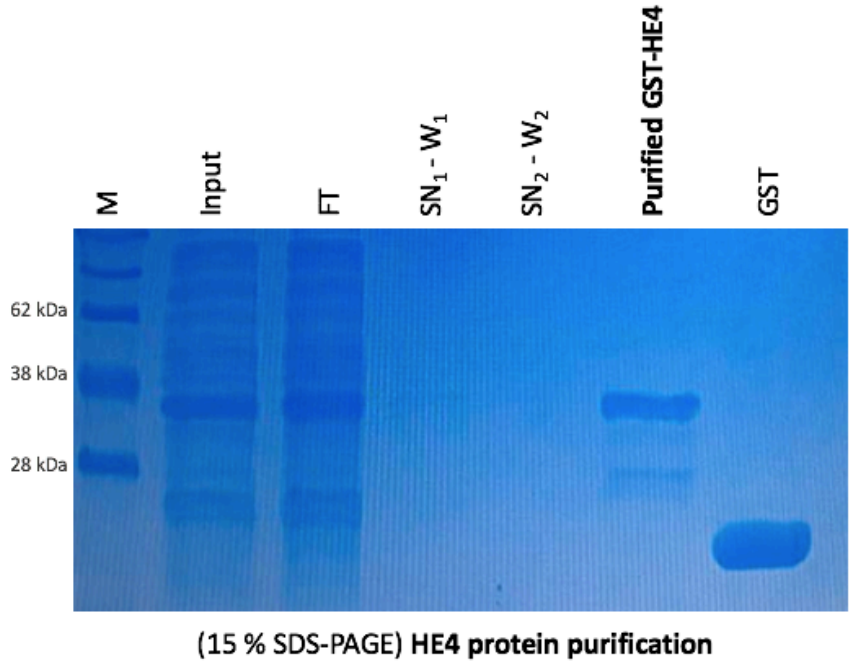

Figure 30. HE4 protein purification from E.coli T7 Shuffle (pGEX-HE4).

M - SeeBlue™ Plus2 protein standard (ref. LC5925, Invitrogen™); **input** - sample prior protein purification; **FT** - flow through; **SN_1-W_1** - supernatant after first wash step; **SN_2-W_2** - supernatant after second wash; the purified **GST-HE4** protein of interest, with expected size of 35.65 kDa (N-terminal GST 25.5 kDa and HE4 protein 10.15 kDA); **GST tag** as a reference (expected size of 25.5 kDa).

The results in **Figure 30** indicate that GST-HE4 was overexpressed and was bound to the magnetic beads. However, a second band at around 28 kDa size is visible in the purified sample. This could be result of potential degradation of target protein, or some unwanted byproduct present either from expression or purification process. Preliminary optimizations were attempted, but with analysis of all results, did not yield HE4 with high purity. With the recommendations from experts in the field at the end of the first year of thesis, this part of the project was stopped. Instead, it was recommended to use a commercially available human HE4, to ensure high quality and purity of the biomarker used as a target in SELEX. In addition, as HE4 contains disulfide bridges and is subjected to significant post-translational modifications, the use of a bacterial strain could neither ensure proper folding of disulfide bridges, nor provide

the required glycosylation (one N-glycosylation on asparagine). Therefore, the protein target used in the selection of the high-affinity aptamers is 6xHis-tagged HE4 (ref. ab219658, Abcam) expressed from human cells, which ensures that protein target used is as similar as possible as in ovarian cancer patients.

1.4. Part 1 - Conclusions

- The extensive bibliography research has been performed to identify the candidate urine biomarkers of ovarian cancer. This part of the thesis is going to be valorized with a two review articles:

  Publication n °2 related to this thesis: Hanžek A, Siatka C, Duc A-C E. Extracellular urinary microRNAs as non-invasive biomarkers of endometrial and ovarian cancer. *J Cancer Res Clin Oncol.,* 2023, https://doi.org/10.1007/s00432-023-04675-5

  Publication n °3 related to this thesis: Hanžek A, Siatka C, Duc A-C E. Diagnostic role of urine Human Epididymis 4 (HE4) in the clinical management of ovarian cancer. *In preparation*

- From all the available urine ovarian cancer biomarkers, the best candidate and the main target of the thesis was decided to be Human Epididymis protein 4 (HE4).
- The initial idea was to produce the HE4 protein in the lab. The plasmid pGEX-HE4 was successfully cloned and constructed for the bacterial expression of ovarian cancer biomarker HE4.
- The target GST-HE4 protein was observed after expression in the *E.coli T7 Shuffle*, but with lower yield than expected.
- The target GST-HE4 protein was purified from the total bacterial proteins, but the purity must be improved.
- Target GST-HE4 protein does not exhibit desired yield and purity and experiments would require further optimizations.
- The part 1 of the project was stopped and human recombinant 6xhistidine HE4 expressed from human cells was purchased instead. This can ensure that target protein has high purity, protein features and post-translational modifications as similar as found in the ovarian cancer patients' prior selection of aptamers.

PART 2 - SELECTION AND IDENTIFICATION OF APTAMERS TARGETING OVARIAN CANCER BIOMARKER HE4 IN URINE

2.1. Selection of the anti-HE4 diagnostic aptamers

A modified variant of High-Fidelity (Hi-Fi) SELEX method was used to select DNA aptamers specifically binding to the ovarian cancer biomarker HE4, from a highly diverse, 70 nucleotide long ssDNA library. The library consist of 30 nucleotide (30 N) long random region flanked by two constant, 20 nucleotide (20 nt) long regions used for PCR amplification. In the first cycle 1,25 nmol of the DNA aptamer library was incubated with 200 pmol of target human HE4 protein immobilized on Ni-NTA beads for 1 h at 25 °C in 1 X urine.

The Hi-Fi SELEX method for aptamer selection to HE4 protein is based on digital droplet PCR amplification to reduce amplification bias. This approach partition the DNA into emulsion droplets for a more homogenous and sensitive amplification. This can enable potential amplification or rare sequences or sequences hard to amplify, that could be specific to ovarian cancer target HE4. Moreover, it can simultaneously perform absolute quantification and monitoring of the sequence pools.

As described, 10 cycles of positive selection steps were performed to target human 6xhistidine-HE4 in urine (C1+ to C10+). After 8 cycles of selection to 6xhistidine-HE4, the recovered DNA aptamers were separated into two equal branches and subjected to an additional 2 rounds of positive selection to 6xhistidine-HE4 on beads (C9+ and C9-) and 2 rounds of counter-selection to 6xhistidine peptide on beads. (C9- and C10-), to identify potential non-specific binders to the sample matrix (protein tag and charged beads). To obtain specific sequences, the selection stringency is increased by increasing the amount of DNA and decreasing the amount of protein. The conditions obtained at each SELEX round are reported in **Table 11** below:

Table 11. Overview of the Hi-Fi SELEX conditions for selection of aptamers to ovarian cancer protein biomarker HE4 in urine.

Cycle	DNA source	DNA (nmol)	HE4 protein (pmol)	Ratio
C1 +	Library	1,25	200	6,25 : 1
C2 +	C1+	0,47	200	2,35 : 1
C3 +	C2+	0,08	100	0,80 : 1
C4 +	C3+	0,13	100	1,30 : 1
C5 +	C4+	0,15	100	1,50 : 1
C6 +	C5+	0,04	200	0,20 : 1
C7 +	C6+	0,03	200	0,15 : 1
C8 +	C7+	0,08	200	0,40 : 1
C9 +	C8+	0,10	200	0,50 : 1
C9 -	C8+	0,10	200	0,50 : 1
C10 +	C9+	0,10	100	1 : 1
C10 -	C9-	0,10	100	1:1

At the end of each cycle, the quality of the aptamer DNA was checked prior starting the next cycle. Gel electrophoresis was carried out (4 % agarose,1X TAE) at each round of selection to ovarian cancer biomarker HE4 at following points of Hi-Fi SELEX: amplification of the 70 bp anti-HE4 aptamers by ddPCR; re-amplification of the 70 bp anti-HE4 aptamers after large scale PCR to confirm presence of the desired amplicon and without by-products; successful removal of the primers after Sephadex purification; and confirmation of the presence of the 70 bases anti-HE4 aptamers with complete conversion to ssDNA at the end of the cycle (**Figure 31**). As seen below, the anti-HE4 aptamers (here, cycle 8 is shown as an example) were successfully amplified by ddPCR and PCR, primers were efficiently removed, and full ssDNA was regenerated by the λ exonuclease (**Figure 31**). Therefore, the cycle of selection is validated, and ssDNA yielded can be used as an input aptamer pool for the next cycle of selection.

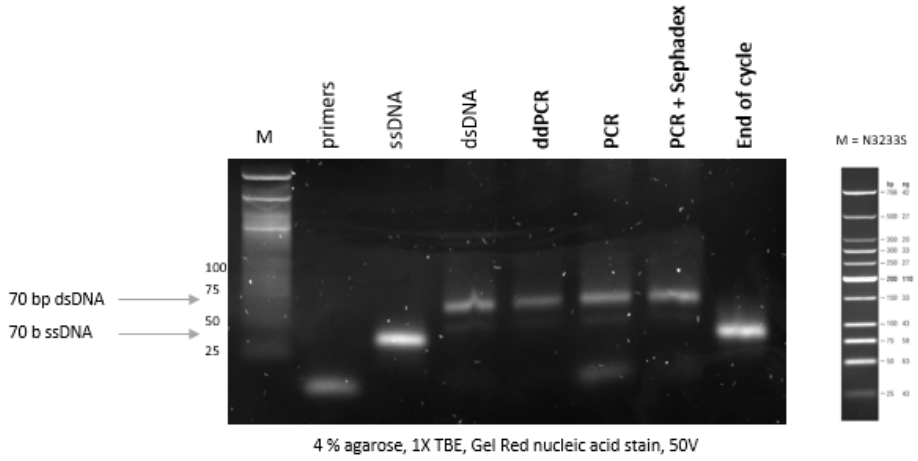

Figure 31. Gel electrophoresis of a typical cycle of Hi-Fi SELEX to ovarian cancer biomarker HE4.

The figure represents electrophoresis gel of each validation step during one Hi-Fi SELEX cycle to protein HE4 (herein, cycle 8 as example). It is important to confirm proper amplification after ddPCR/PCR and obtain specific anti-HE4 aptamer amplicon of expected size (70 bp) ideally without by-products, as well as ensure primer removal by Sephadex G-50. At the end of cycle, it is important to confirm ssDNA generation by λ exonuclease with complete conversion of 70 bp dsDNA to 70 bases ssDNA before next cycle. **M** - low molecular weight DNA ladder (ref. N3233S, New England Biolabs, USA); **primers** - reference 20 bases primers DNA; **ssDNA** - reference 70 bases ss DNA (original library); **dsDNA** - reference 70 bp ds DNA (amplified original library); **ddPCR** - dsDNA aptamers after ddPCR amplification and chloroform extraction; **PCR** - dsDNA aptamers after PCR re-amplification; **PCR + Sephadex** - dsDNA aptamers after purification and primer removal with Sephadex G-50 columns; **End of cycle** - ssDNA, regenerated aptamer ssDNA after λ exonuclease digestion and input DNA used for the next cycle.

The same procedure was carried out in each round of selection. The amplicon of the 70 bp anti-HE4 DNA aptamers is detected in all cycles of selection, as seen in **Figure 31.**

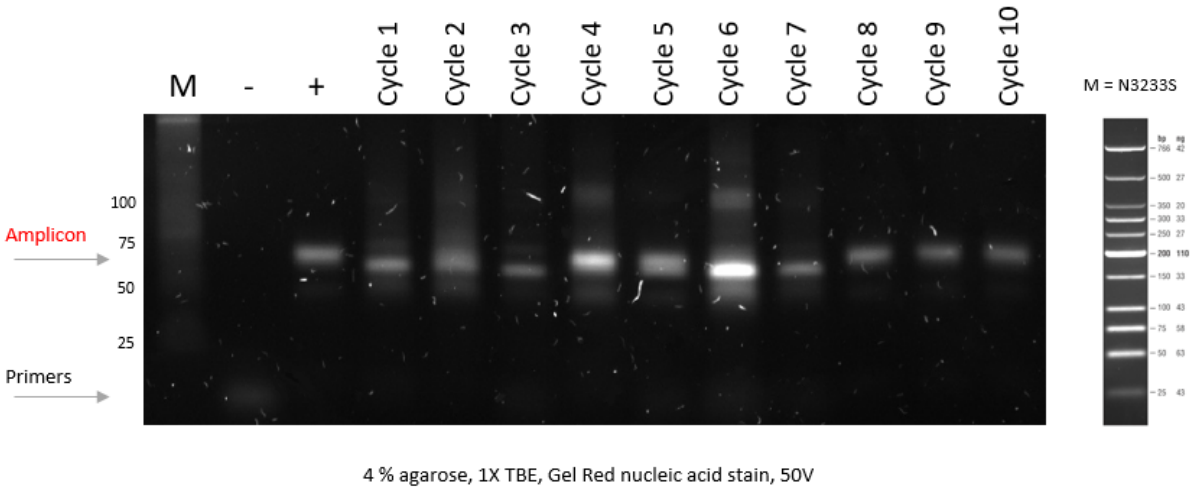

Figure 32. Gel electrophoresis of anti-HE4 aptamers during all 10 cycles of Hi-Fi SELEX to ovarian cancer biomarker HE4.

The results show electrophoresis gel of all cycles of Hi-Fi SELEX of all aptamer DNA obtained during selection to protein HE4. The expected amplicon size is 70 bp double-stranded DNA. **M** - molecular weight DNA ladder (ref. N3233S, New England Biolabs, USA); **-** = negative PCR control (non template control); **+** - positive PCR control (70mer ssDNA library as template) and aptamer samples from cycle 1 to cycle 10 (70mer ssDNA selected aptamers as template) after ddPCR amplification and PCR re-amplification and prior purification from the primers.

The intensity of the amplicon varies depending on the cycle as expected, and presence of the potential by-products were detected in the cycle 4 and cycle 6. Therefore, optimization of the number of cycles and the concentration of template was carried out on the small scale before upscaling for aptamer DNA production. Although, it appears that small number of by-products present in those cycles did not limit the selection, as single pure 70 bp amplicon is detected again from cycle 7 to the end of selection to cycle 10 to ovarian cancer biomarker HE4.

2.2. ddPCR amplification of the anti-HE4 diagnostic aptamers

The central point of the Hi-Fi SELEX is ddPCR amplification of the aptamer sequences. The aptamers after incubation and selection to HE4 are partitioned into up to 20 000 individual emulsion ddPCR droplets, where each individual droplet is subjected to end-point sensitive amplification. The data can be viewed as a 1-D plot with each droplet from a sample plotted on the graph of fluorescence intensity *vs*. droplet number. The threshold establishes the distinction between positive (anti-HE4 target DNA aptamers present) and negative droplets (background DNA), based on their fluorescent signal reading (**Figure 33**). The droplet is considered positive if there is at least 1 copy of the anti-HE4 aptamer sequence present. Many aptamer sequences were detected and amplified in all 10 cycles of SELEX (**Figure 33**). The early rounds were performed using soft washing conditions, and as expected, high amounts of DNA were found in the early rounds, such that we observed saturation of droplets due to the excess of 70-mer ssDNA template (fluorescence ~ 5000-6000 RFU). Therefore, the amplification at those stages may not have been optimal, and the amplification bias may not have been avoided. Indeed a very high number of sequences present (maximum sequences detected >$1x10^6$) can be observed at the very beginning of selection (C1+ to C4+). From cycle 5 (C5+), the amount of DNA was reduced, sequence diversity is reduced, while it is expected that specificity for HE4 increase. Then optimal classification into positive and negative clusters with 70 bp dsDNA amplicons are observed (fluorescence ~ 10 000-12 000 RFU), presumably due to enrichment to target HE4. The last two positive selection steps (C9+ and C10+) to HE4 and two rounds of counter selection (C9- and C10-) to 6xhistidine peptide immobilized on Ni-

NTA beads (no HE4) were performed, after equally distributing previously recovered DNA (C8+) to each branch of selection. This step is essential to identify the high-affinity sequences to ovarian cancer HE4 target, and to eliminate non-specific binders with affinity to sample matrix (no target). As the DNA is negatively charged and Ni-NTA beads are positively charged, it is expected that some aptamers could exhibit binding properties due to electrostatic interactions. Inded, DNA is amplified and detected, but in smaller amount in counter-selection (**Figure 33**). DNA sequencing can further elucidate the sequences that could be potential binders to 6xhistidine tag, and if found, those can be eliminated. Positive ddPCR control (library) is important to ensure the amplification is working and to use it as a reference to track expected height of the specific amplicon fluorescence. Negative PCR control (water) should not have any amplification and all droplets should be classified as negative (**Figure 33**).

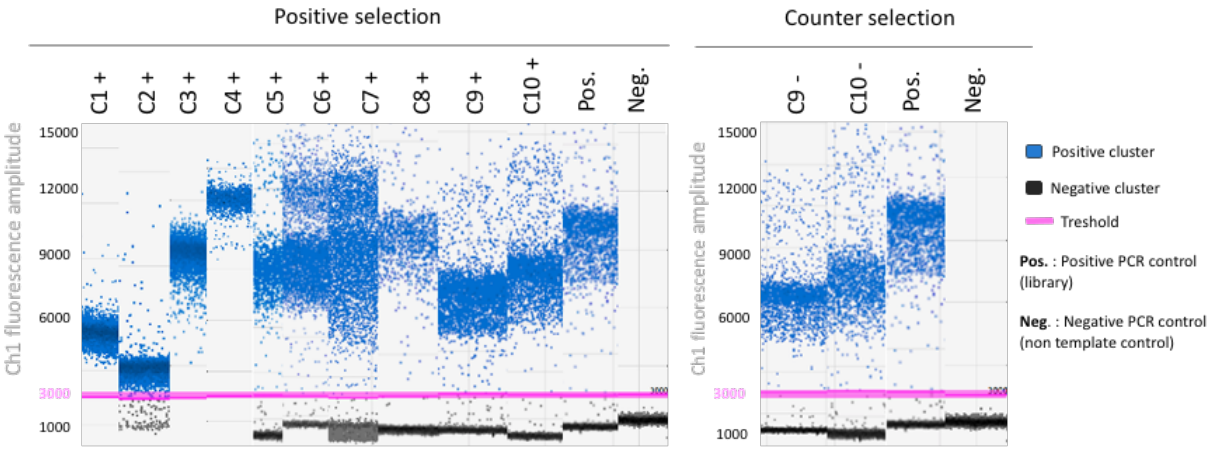

Many sequences are detected in all cycles of selection. In the plot, each droplet from a sample in each

Figure 33. ddPCR analysis of anti-HE4 aptamers: 1-D plot of Hi-Fi SELEX positive selection to target HE4 protein and counter selection to 6xhistidine peptide.

SELEX cycle is plotted on the graph of the fluorescence intensity *vs*. droplet number. All positive droplets with anti-HE4 aptamer present (in blue), are those above the pink threshold line and are scored as positive. All negative droplets below the pink threshold line, are those without target aptamers present (in dark gray) and are scored as negative.

Another way to look at the ddPCR data can be through 1-D fluorescence amplitude histograms, which display frequency of droplets at specific fluorescence amplitudes (**Figure 34**). In the selection of anti-HE4 aptamers to ovarian cancer biomarker HE4 in the Hi-Fi SELEX, 3 populations with different fluorescence can be observed, and correspond to primers DNA (with fluorescence ~ 2000 RFU), ssDNA aptamer template (fluorescence ~ 5000-6000 RFU) and ds amplified aptamers (fluorescence ~ 10 000-12 000 RFU). Therefore, histograms can be helpful to monitor what is exactly happening in selection to HE4 and if amplification of aptamers is successful. As seen in the results, the amount of template at the beginning of the selection in

cycle 1 (starting from 1,25 nmol DNA), even after washing, was too high for sensitive ddPCR setup. Therefore, droplets are saturated and only population of ssDNA and primers can be observed (**Figure 34**). Therefore, the amplification to double stranded aptamers is inhibited by excess of template and was not optimal. As the selection progresses, the sequence number and diversity is reduced, while specificity for target HE4 increases. Therefore, the amplification starts to be more successful, as seen in cycle 3, with all 3 populations observed. At the cycle 5, all the aptamers are amplified into double stranded DNA and ddPCR capacities are maximal, as only population of dsDNA can be observed. Therefore, we can assume that number of sequences is reduced and the enrichment to HE4 proteins started to occur. The same was observed from cycle 5 to the end of selection at cycle 10, with number of sequences amplified varying on each cycle (**Figure 34**).

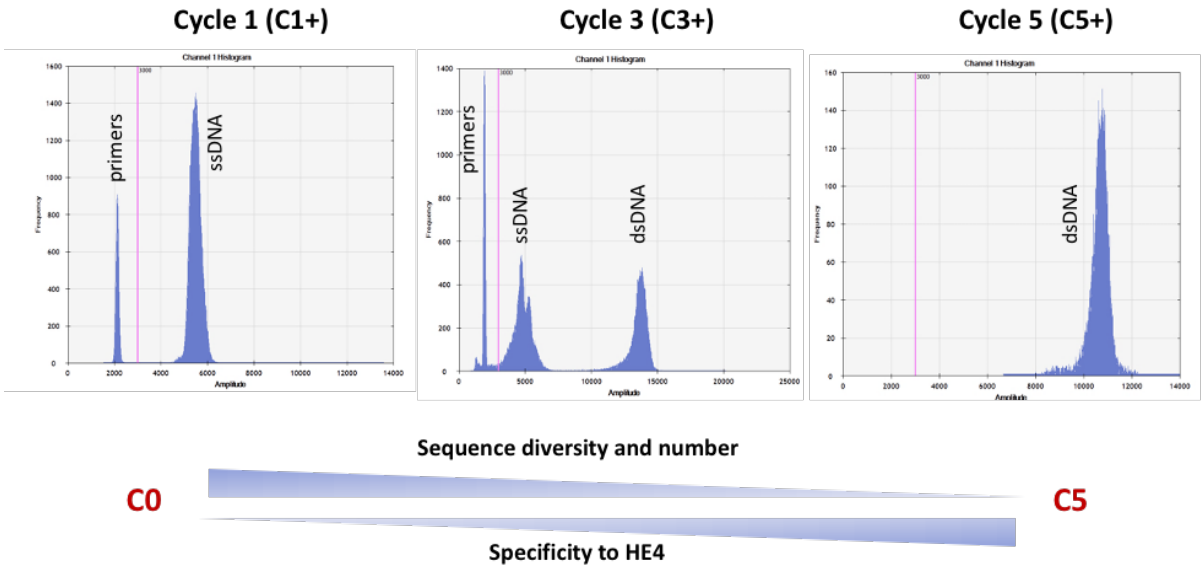

Figure 34. ddPCR fluorescence amplitude histograms of the first 5 cycles of Hi-Fi SELEX to ovarian cancer biomarker HE4.

The droplets can be qualified as total, positive and negative and then counted (**Figure 35**). The accurate absolute quantification of the aptamer sequences is achieved if the total number of droplets is >10 000, so total droplet count is used as a quality assurance tool. As the selection of aptamer against HE4 moves forward, a clearer repartition into positive and negative droplets is observed after cycle 5 (C5+). As selection progresses on, the positive droplets number decreases, while negative droplet number increases, probably due to lower amount of DNA template, and with potentially more specific sequences present are amplified (**Figure 35**).

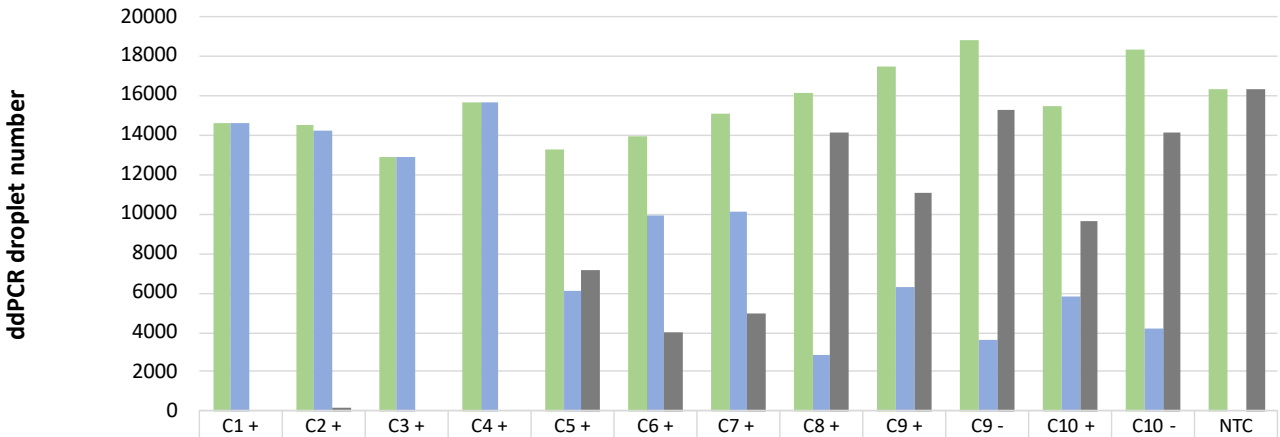

	C1 +	C2 +	C3 +	C4 +	C5 +	C6 +	C7 +	C8 +	C9 +	C9 -	C10 +	C10 -	NTC
Total droplet count	14661	14476	12921	15633	13276	13915	15074	16139	17440	18863	15483	18341	16364
Positive droplets	14661	14248	12921	15633	6111	9909	10118	2832	6340	3617	5857	4243	0
Negative droplets	0	228	0	0	7165	4006	4956	14119	11100	15246	9626	14098	16364

Figure 35. ddPCR droplet enumeration in Hi-Fi SELEX positive and negative selection.

The droplets are classified and quantified as positive (target anti-HE4 aptamers present), negative (no target aptamers) and total (positive + negative droplets). In the first few selection cycles, all droplets are positive (saturation) due to the excess of aptamer sequences present. After cycle 5, repartition is optimal, with positive and negative droplets present, due to the decrease of aptamers present. Decrease of aptamer sequences present equals increase of sequence specificity to HE4 protein. As SELEX evolves, many specific sequences are being enriched to target HE4 protein.

After cycle 5 (C5+), it seems many sequences are successfully amplified and detected as bound to HE4, although the number varies in each cycle throughout the selection process (**Figure 36**). The DNA is found to be amplified in both positive and counter selection. However, above all, a significantly higher number of aptamer sequences were present in positive selection to HE4 protein, compared to that in counter selection, suggesting high-affinity and potential enrichment to target HE4 protein (**Figure 36**). These conclusions were validated by deep sequencing, with specific sequences only being enriched to target HE4, and not to peptide tag or beads.

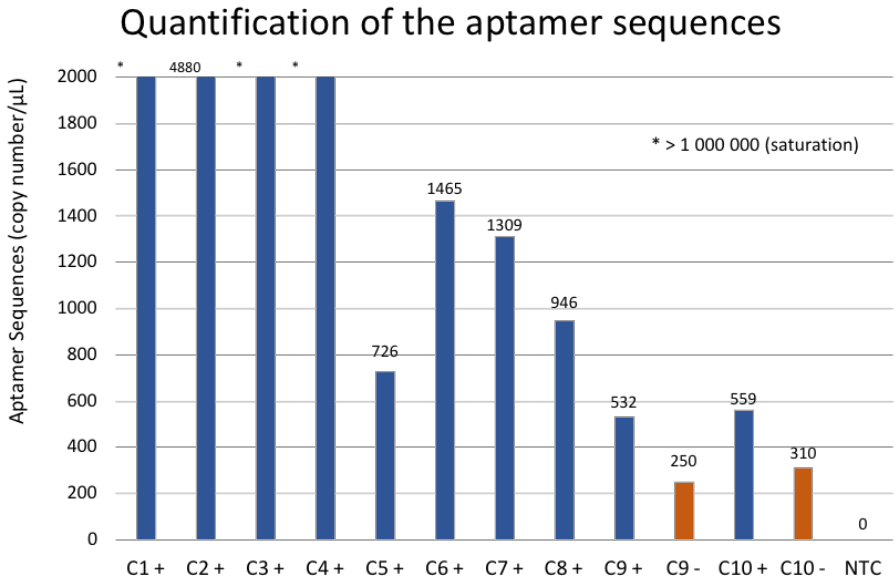

Figure 36. Quantification of the anti-HE4 aptamers throughout Hi-Fi SELEX positive and negative selection.

Numerous sequences are detected and quantified in each cycle. At the beginning of selection, maximum number of sequences are observed (saturation). After cycle 5, sequence number and diversity decreased. Most importantly, higher number of sequences are observed as enriched in positive selection to target 6xhistidine-HE4 protein compared to the counter-selection to 6xhistidine peptide (sample matrix), in both cycle 9 and 10, suggesting enrichment of specific sequences to HE4 occurred.

2.3. DNA sequencing and identification of the enriched aptamers to HE4

To study the enrichment through the Hi-Fi selection procedure, Illumina deep sequencing was performed to analyze the starting library and the aptamers libraries after cycle 5, in both positive selection to target 6xhistidine-HE4 (C5+ to cycle C10+), and negative selection to 6xhis peptide (C9- and C10-). Several anti-HE4 aptamers have been identified as enriched to target ovarian cancer biomarker human HE4. The sequences of the identified top 10 most-enriched anti-HE4 aptamer sequences are presented below in the **Table 12**.

Table 12. The identified DNA sequences of the top 10 most enriched anti-HE4 aptamers.

ID	Lenght	DNA sequence (random region)
AHE1	30	CCCAACCAACGTCTATACTTCCCCAACCTC
AHE2	30	GCCAACATCGTACTCCATCTGCCACCCCCA
AHE3	30	CATCAATCAGCATACCCACCATGTACGTCC
AHE4	30	TAGCACAAGTATGCTCACCATGACCACTAC
AHE5	30	CGCTCTACTCCCGACTAACCCCAAGCTCAA
AHE6	30	CAACAGACATCTCCATTGCCATACCACATG
AHE7	30	CCAATGCACAAGTGGCAGTCCCATATTCAC
AHE8	30	CCGATGCCTGCCTCGAATCAACTTCACAAC
AHE9	30	CAGATGCCAAAACCTCCACACGTCTGAGAC
AHE10	30	ACATCATCCCACCAAGATAAAAGACATCAC

The DNA sequencing and analysis is presented in **Figure 37**. In order to focus our analysis on the most enriched sequences, we have retained for analysis only 2.621 sequences whose frequency is greater than 0.01 % in at least one cycle. As expected, the starting, naive, library contains a large diversity of sequences where each sequence is at a very low frequency. In contrast, the library contains sequences whose frequency has strongly increased from the fifth cycle (**Figure 37A and 37B**). Among these sequences, some have been regrouped in common family when they were separated by an edit distance lower than 6. This clustering created 2.189 families, the most abundant of which contains 29 sequences. It is interesting to note that the number of sequences and families increases between cycle 5 and 6 and then decreases during the following cycles (**Figure 37B and 37C**) but their percentage in the bank remains constant despite the increase of the selection pressure except for the last cycle (**Figure 37A**). This suggests an evolutionary pattern where some sequences and families increase in the library while others less suitable decrease. In addition, the number of sequences and families decreases significantly more in the last two cycles in the absence of protein and especially their percentage in the library is about 50 % less (**Figure 37A and 37E**), suggesting that many sequences should bind to the HE4 protein. This is the case for the 10 most enriched families whose frequency increases to represent more than 1 % of the library for some of them in the two last cycles with the protein, while it is about 5 to 10 times less without it (**Figure 37D**).

Sequences whose frequency is higher than 0.01 % at least in one cycle have been recovered and their

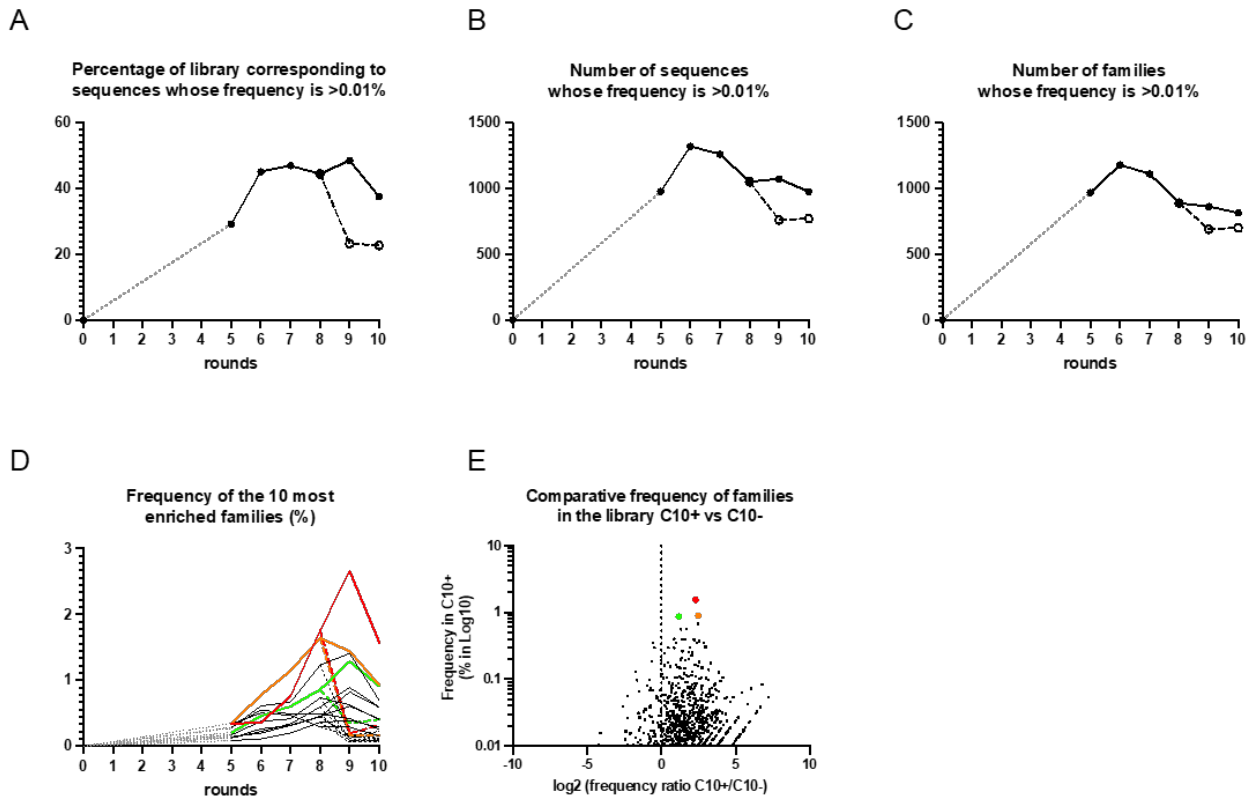

Figure 37. Deep sequencing analysis of the Hi-Fi SELEX (the analysis of the starting library and the aptamer pools after cycle 5).

percentage in the library as well as their number have been measured for several cycles (**A** and **B**, respectively). Those sequences have been clustered in families based on an edit distance of 6. The evolution of the number of families is presented in **C**. The frequency of the 10 most enriched families is presented in **D**. The frequency of each family in the last C10+ cycle relative to its enrichment in the presence or absence of the HE4 protein (C10+/C10- ratio) is presented in E. The evolution in solid lines and black dots correspond to libraries from positive selection in the presence of HE4 protein, while the evolution of dashed lines and light dots correspond to the two cycles without protein. The gray dotted lines correspond to cycles that have not been sequenced. The colored curves and dots correspond to the evolution of the 3 families which have been selected for binding evaluation (red, orange and green for AHE1, AHE2 and AHE3, respectively)

The bioinformatics analysis revealed that many aptamers were enriched to ovarian cancer protein HE4 with clear enrichment in positive selection to target HE4 compared to counter selection to sample matrix. As seen below in **Table 13**, most enriched cluster families were enriched from 0,1 – 2 %. Moreover, three sequences, internally named AHE1, AHE2 and AHE3 have clear systematic enrichment to target HE4 (**Table 13**) starting from C5 + to last cycle of selection (with frequency 2,7 % for AHE1, 1,4 % for AHE2, and 1,2 % for AHE3 in C9 + and 1,5 % for AHE1, 0,7 % for AHE2 and 0,9 % for AHE3 in C10 +, respectively). In addition, the same aptamers are not enriched in the counter selection (with frequency < 0,4 % in C9- and C10- for all three aptamers), indicating them as the most promising binders to HE4.

Table 13. Evolution and of the top 10 most enriched DNA aptamer families targeting ovarian cancer biomarker HE4 obtained with DNA sequencing.

ID	C0	C5 +	C6 +	C7 +	C8 +	C9 +	C10 +	C9 -	C10 -
AHE1	0.0000	0.625	0.3566	0.7481	1.7293	2.6197	1.5402	0.1897	0.3091
AHE2	0.0000	0.2729	0.6067	0.6643	1.2172	1.3891	0.6761	0.1726	0.1208
AHE3	0.0000	0.2017	0.4420	0.5841	0.8261	1.2394	0.8692	0.3337	0.3852
AHE4	0.0000	0.1222	0.2538	0.3005	0.4324	0.7971	0.5621	0.1612	0.2223
AHE5	0.0000	0.1716	0.3650	0.4017	0.7080	0.6048	0.3844	0.1093	0.0805
AHE6	0.0000	0.1233	0.2139	0.3313	0.5730	0.8625	0.5695	0.1246	0.1747
AHE7	0.0000	0.1385	0.1914	0.3059	0.4361	0.5806	0.3983	0.0918	0.0868
AHE8	0.0000	0.2862	0.5495	0.4806	0.4885	0.4124	0.2543	0.0803	0.0602
AHE9	0.0000	0.3417	0.5039	0.4699	0.2933	0.2884	0.1546	0.1540	0.1038
AHE10	0.0000	0.0986	0.1662	0.2738	0.2944	0.3647	0.3536	0.4397	0.5163

Green color = no enrichment to HE4, yellow = intermediate enrichment, orange = mild enrichment, red = intense enrichment to HE4 protein.

The anti-HE4 aptamers were selected from a highly diverse DNA library, which was optimized to have the molar ratios of nucleotides 29:29:20:22 %, for an equal probability of incorporation of each nucleotide in the core region. High throughput sequencing combined with bioinformatics analysis was used to determine the nucleotide composition of the random region core (positions 21-52) of the sequence pools from the initial library and the various aptamer selections. The results revealed inherent bias in the initial library coming from the chemical synthesis, with a very high content of the adenine-rich sequences present in the naive library (**Figure 38**). However, it was been reported that bias in the initial library does not limit the selection of high-affinity aptamers to target protein [177–179].

At the end of selection at cycle 10 in the selected anti-HE4 aptamers, loss of guanines, while preference for incorporation of cytosines is observed compared to the unselected library (cycle 0) (**Figure 38**). Both adenine and thymine composition stay almost constant, with a high prevalence of adenine (**Figure 38**). Indeed, the top 10 most-enriched anti-HE4 aptamers targeting ovarian cancer biomarker human HE4 have a high prevalence of cytosine content, covering 30-50 % of all bases in all sequences (**Table 14).** It has been reported in the literature that a bias toward pyrimidine (C/T)-rich sequences can exists during SELEX [177].

Cycle 0 (unselected initial DNA library)

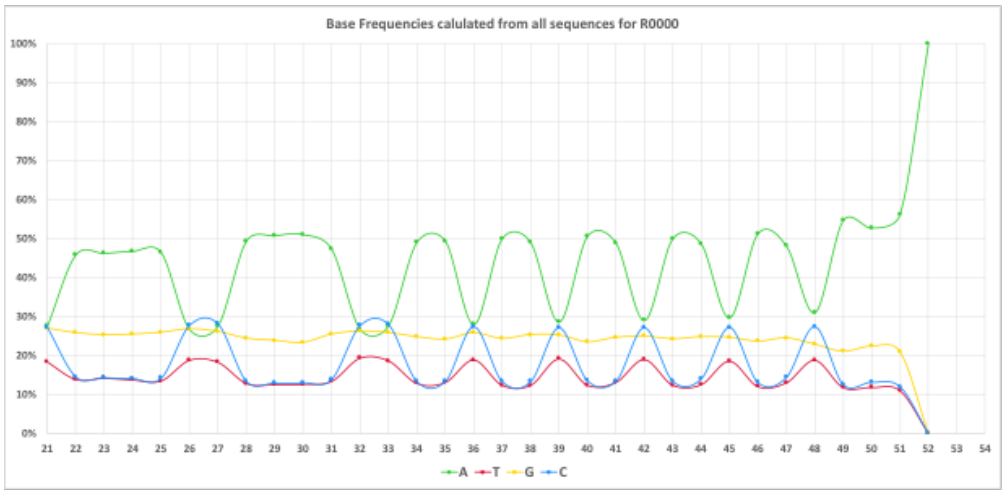

Position	A	T	G	C
21	28%	18%	27%	27%
22	46%	14%	26%	15%
23	46%	14%	25%	14%
24	47%	14%	25%	14%
25	46%	13%	26%	14%
26	27%	19%	27%	28%
27	28%	18%	26%	28%
28	49%	13%	24%	13%
29	51%	12%	24%	13%
30	51%	13%	23%	13%
31	47%	13%	25%	14%
32	27%	19%	26%	28%
33	28%	19%	26%	28%
34	49%	13%	25%	13%
35	49%	13%	24%	13%
36	28%	19%	26%	27%
37	50%	12%	24%	13%
38	49%	12%	25%	13%
39	29%	19%	25%	27%
40	51%	12%	23%	14%
41	49%	13%	25%	13%
42	29%	19%	25%	27%
43	50%	12%	24%	13%
44	49%	13%	25%	14%
45	30%	19%	25%	27%
46	51%	12%	24%	13%
47	48%	13%	24%	14%
48	31%	19%	23%	27%
49	55%	12%	21%	13%
50	53%	12%	22%	13%
51	56%	11%	21%	12%
52	100%	0%	0%	0%

Cycle 10 (selected anti-HE4 aptamer library)

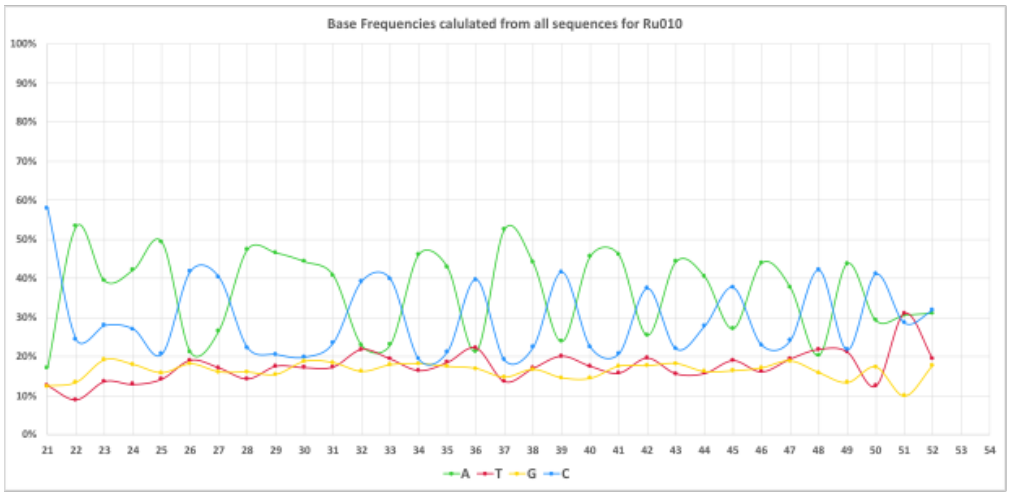

Position	A	T	G	C
21	17%	13%	12%	58%
22	53%	9%	13%	24%
23	39%	14%	19%	28%
24	42%	13%	18%	27%
25	49%	14%	16%	21%
26	21%	19%	18%	42%
27	27%	17%	16%	40%
28	47%	14%	16%	22%
29	47%	18%	15%	21%
30	44%	17%	19%	20%
31	41%	17%	18%	23%
32	23%	22%	16%	39%
33	23%	19%	18%	40%
34	46%	16%	18%	19%
35	43%	19%	17%	21%
36	21%	22%	17%	40%
37	53%	14%	15%	19%
38	44%	17%	17%	22%
39	24%	20%	15%	42%
40	46%	18%	14%	23%
41	46%	16%	17%	21%
42	25%	20%	18%	37%
43	44%	16%	18%	22%
44	41%	16%	16%	28%
45	27%	19%	16%	38%
46	44%	16%	17%	23%
47	38%	19%	19%	24%
48	20%	22%	16%	42%
49	44%	21%	13%	22%
50	29%	12%	17%	41%
51	31%	31%	10%	29%
52	31%	19%	18%	32%

Figure 38. DNA sequencing analysis of the nucleotide distribution in the random regions of aptamer libraries.

The functional aptamers depend on the defined secondary structure for function. Therefore, the increase in cytosine in the selected anti library could result in the higher prevalence of the more stable aptamer species that bind to target HE4 protein in urine.

Table 14. The base distribution in the Top 10 most enriched anti-HE4 aptamer sequences (in the random core region, position 21-52).

Aptamer ID	A %	T %	G %	C %
AHE1	26,6	20	0,3	50
AHE2	23,3	16,6	10	50
AHE3	30	20	20	40
AHE4	33,3	20	13,3	33,3
AHE5	26,6	16,6	10	46,6
AHE6	33,3	20	10	36,6
AHE7	30	20	16,6	33,3
AHE8	26,6	20	13,3	40
AHE9	33,3	13,3	16,6	36,6
AHE10	46,6	13,3	6,6	33,3

Furthermore, bioinformatic analysis was performed to search for potential shared motifs between the anti-HE4 aptamers. As seen below (**Figure 39**), multiple matrix alignment of the random region of the 10 most enriched sequences did not reveal the presence of a conserved motif.

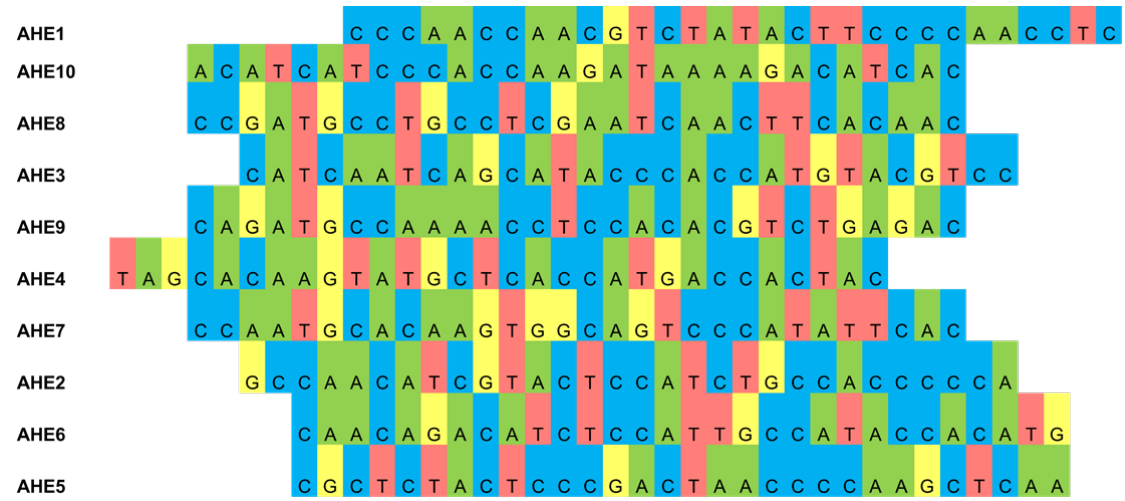

Figure 39. Matrix alignment of the top 10 most enriched anti-HE4 aptamer sequences.

The figure presents the matrix alignment of 10 most enriched sequences (random regions) to ovarian cancer biomarker HE4. The matrix alignment did not reveal specific shared motifs between aptamers.

However, further analysis using the MEME suite identified a partially conserved motif of 7 nucleotides in the 10 most enriched anti-HE4 aptamer families (**Figure 40**). DNA structural motifs can be important for their biological function. Therefore, this conserved DNA sequence could be important for binding to target HE4 protein.

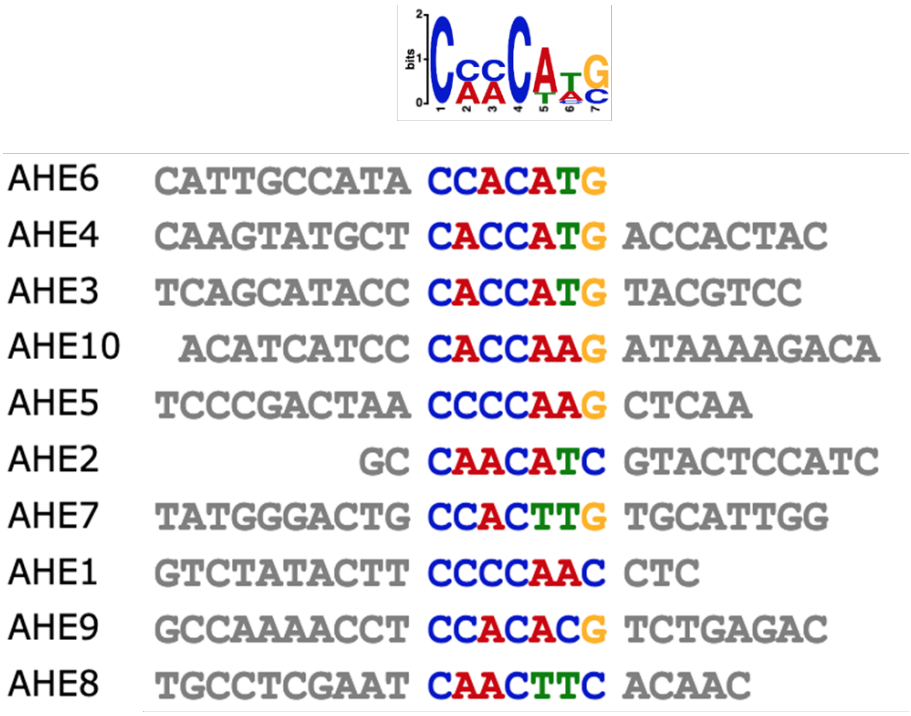

Figure 40. Conserved motif between the 10 most enriched anti-HE4 aptamer families was identified using the MEME suite.

Furthermore, an evolutionary diagram constructed using Clustal Omega online software shows the phylogenetic tree of top 10 most-enriched anti-HE4 sequences (**Figure 41**). It represents the evolutionary relationships among aptamers, which can be an important aspect to consider when choosing aptamers for further characterization. For example, it would be interesting to characterize distinct DNA aptamer sequences, for example AHE1 and AHE3. Those sequences, while also being most enriched, appear evolutionary distinct and could have different structural features responsible for binding to HE4 protein (**Figure 41**).

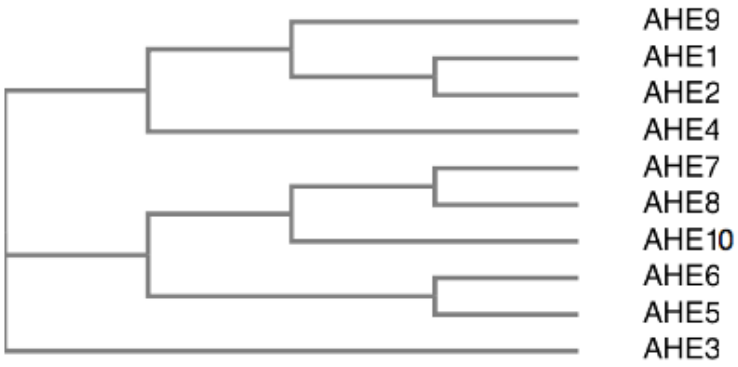

Figure 41. The phylogenetic tree of the 10 most enriched anti-HE4 aptamer sequences created using Clustal Omega software.

Finally, the secondary structure of the most enriched anti-HE4 aptamers were constructed by Unafold software in the conditions of the aptamer selection and potential diagnostic application. Therefore, urine salt concentrations and temperature of 25 °C were chosen as folding conditions. As seen in **Figure 42**, the top 3 most enriched aptamers AHE1, AHE2 and AHE3 possess several interesting secondary structures, which could be involved in their potential high-affinity binding to ovarian cancer biomarker HE4.

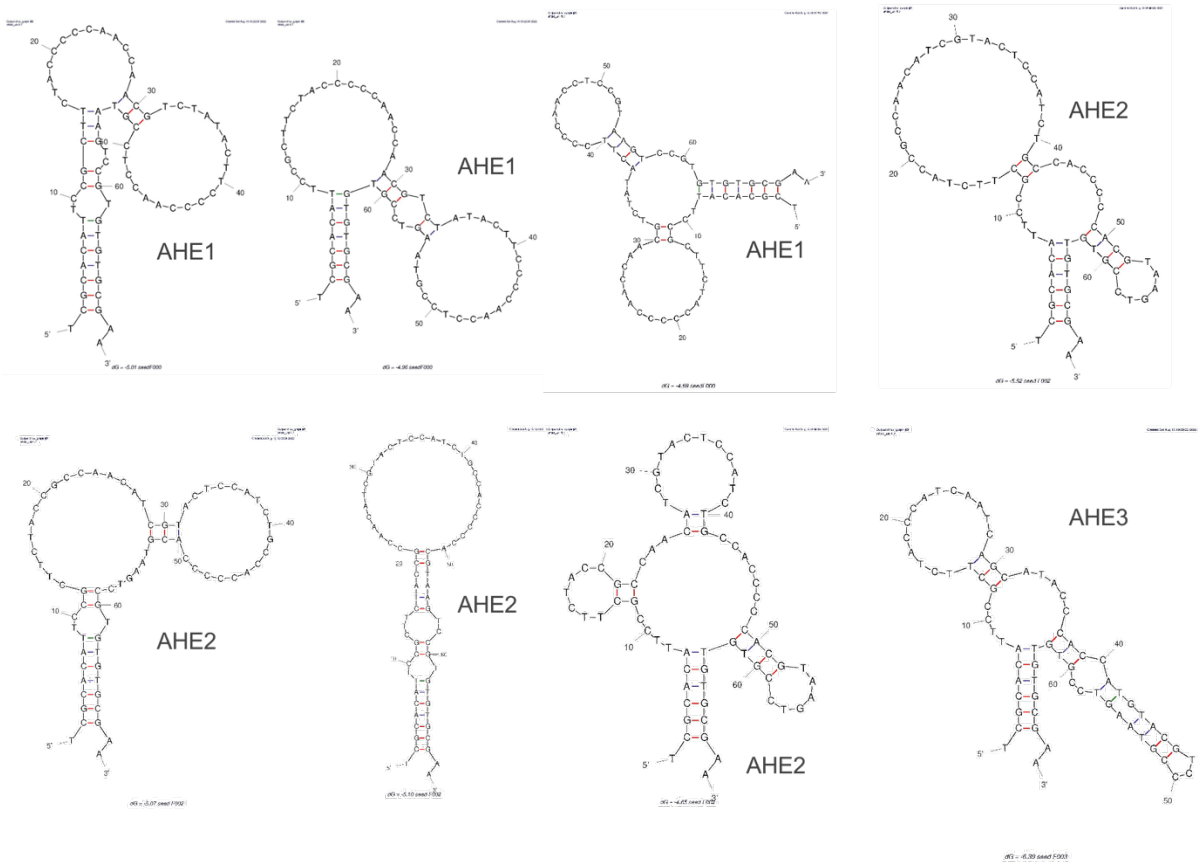

Figure 42. Predicted secondary structures of anti-HE4 aptamers.

The secondary structures of full length 70-mer DNA aptamers (random and fixed regions included) were created using online DNA folding software Unafold (http://www.unafold.org) at temperature 25 °C and urine concentration of $[Na^+]$ = 55.4 mM and $[Mg^{2+}]$ = 4.4 mM. Anti-HE4 aptamer sequences AHE1 and AHE2 could have 3 or more interesting structures, while AHE3 has one potential structure predicted.

Therefore, based on the enrichment to target ovarian cancer biomarker HE4 (**Figures 37 and Table 13**); the differences between positive and negative selection - with enrichment to HE4 protein, but not to protein tag/sample matrix (**Table 13**); the distinct structures in the evolutionary pattern (**Figure 41);** and predicted secondary structures (**Figure 42)**, aptamers named **AHE1, AHE2 and AHE3** were chosen as candidate anti-HE4 aptamers for further characterization of binding to HE4 in urine.

2.4. Part 2 - Conclusions

- Digital droplet PCR (ddPCR) method for the partitioning and amplification for the designed 70-mer ssDNA aptamer library was optimized.
- ddPCR-based Hi-Fi SELEX for selection of aptamers was optimized and set up in the lab *(aptamer method applicable to any diagnostic and therapeutic targets).*
- The Hi-Fi SELEX method has been successfully applied to select and identify aptamers to ovarian cancer biomarker HE4 in urine.
- DNA sequencing and bioinformatics data analysis identified many anti-HE4 sequences enriched to target ovarian cancer biomarker HE4 in urine (2189 families, the most abundant of which contains 29 sequence).
- The analysis of the 10 most-enriched anti-HE4 sequences in urine revealed a preference to a selection of cytosine-rich sequences, a partially conserved motif of 7 nucleotides and secondary structures that could be important for their biological function.
- The candidate aptamers were chosen based on the following criteria: the enrichment (most enriched to ovarian cancer biomarker HE4); the differences in enrichment between positive (enriched to target HE4) and negative (not enriched to protein tag and sample matrix); and the differences in structures (distinct sequences in evolutionary patterns and secondary structures).
- Candidate anti-HE4 aptamers targeting ovarian cancer biomarker HE4, called **AHE1, AHE2 and AHE3**, were chosen for further characterization and potential diagnostic application in urine.

PART 3 - CHARACTERIZATION OF THE CANDIDATE APTAMERS

3.1. Anti-HE4 aptamers binding to ovarian cancer biomarker HE4 by Surface plasmon resonance (SPR)

3.1.1. Immobilization of the target HE4 protein

First, after functionalization of the sensor chip using EDC-NHS, anti-His antibody was immobilized on the surface of the SPR chip (**Figure 43A**), with a signal obtained 14530 RU (signal at channel Fc=2). Then, 6xHis-HE4 was captured using the anti-His antibody using a concentration of 500 nM 6xHis-HE4 protein flown at 10µl/min for 120 sec (**Figure 43B**). The obtained signal (signal at channel Fc=2) was 889 RU. After successful immobilization of the HE4 protein, general screening of the DNA aptamers binding to HE4 protein were performed.

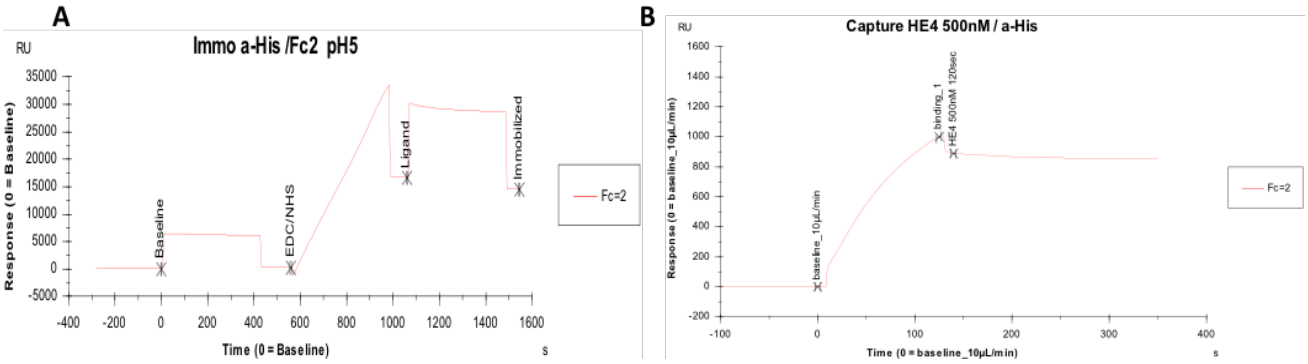

Figure 43. Immobilization of the target ovarian cancer biomarker HE4.

A. Immobilization of the anti-His-tag antibody on the surface of the Xantec SPR Chip **B**. Capture of the target protein 6xHis-HE4 by the anti-His antibody on the surface of the SPR Chip (Fc = flow cell).

3.1.2. Screening of the anti-HE4 DNA aptamers - HE4 protein binding

12 different DNA sequences were tested: the top 10 most-enriched 30-mer aptamers (core random regions) AHE1 to AHE10 selected with Hi-Fi SELEX to biomarker HE4 in urine and the 25-mer aptamers A1 and A3 from Eaton et al. [148]. The 2 μM of denatured aptamers (90 °C for 3 min) were injected over immobilized HE4 protein on the surface of the chip. The results below (**Figure 44**) show a typical sensorgram of the anti-HE4 aptamers-HE4 protein binding (on the left). The table (on the right) represents reached RU levels with and without aptamers.

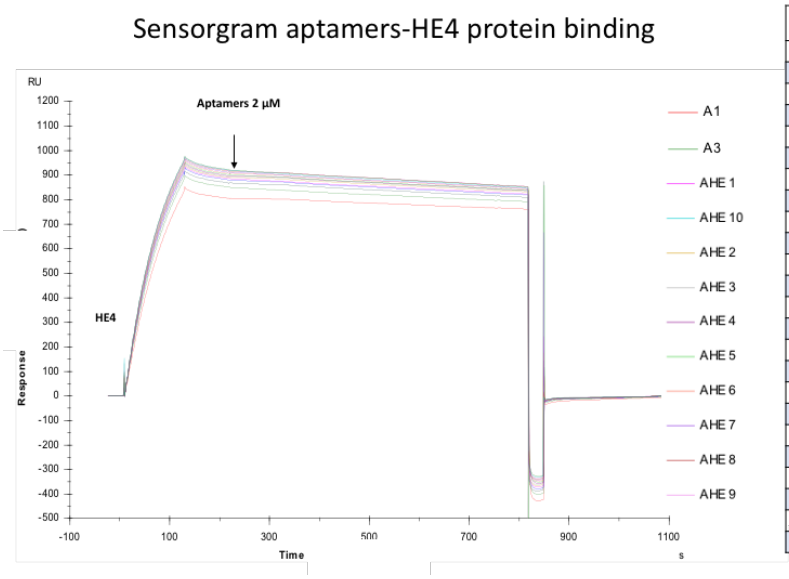

Aptamer	Response (RU)	Conc (µM)	MW (Da)	Capture level
A1	0	0	7561	721,7
A1	2,6	2	7561	835,9
A3	0	0	7657	860,1
A3	-1,7	2	7657	884,6
AHE 1	0	0	8936	919,6
AHE 1	-1,3	2	8936	921,8
AHE 2	0	0	8977	925,2
AHE 2	3,1	2	8977	927
AHE 3	0	0	9040	928,9
AHE 3	6,3	2	9040	930,4
AHE 4	0	0	9001	932,5
AHE 4	6,9	2	9001	934,6
AHE 5	0	0	9064	937,4
AHE 5	2,5	2	9064	939,3
AHE 6	0	0	9104	941,6
AHE 6	4,5	2	9104	944,5
AHE 7	0	0	9120	946,3
AHE 7	2,2	2	9120	949,6
AHE 8	0	0	9056	952,8
AHE 8	2,8	2	9056	954,5
AHE 9	0	0	9023	955,7
AHE 9	0,2	2	9023	957,5
AHE 10	0	0	9114	958,1
AHE 10	-4,3	2	9114	958,8

Figure 44. SPR sensorgram of the binding analysis of the anti-HE4 aptamers to the ovarian cancer biomarker HE4.

Whenn subtracting the signal from the aptamer only, remaining signal is extremely low, ranging from 0-10 RU for all sequences (expected theoretical signal based on the molecular weights of the aptamers is ~ 700 RU). There could be several potential reasons for this low signal: either the aptamers are not binding as expected, the interaction and binding could be very slow (need longer time than 2 min of injection time to achieve binding) or the method is not appropriate for this aptamer-protein binding and could be further optimized. Knowing the fact that aptamers are very small DNA molecules, with a size of 25 and 30 nucleotides only, subtraction of the signal can result in high background and low signal as seen. Based on the results in the table (**Figure 44**), which present negative values after subtraction of the aptamer signal, and the individual sensorgrams in the figure below (**Figure 45**), we can observe no binding to HE4 protein for the sequences A3, AHE2, AHE9 and AHE10. Therefore, these sequences were excluded from further analysis. On the contrary, low interaction is observed for several aptamers, with a binding potential to ovarian cancer biomarker HE4 of the sequences A1, AHE1, AHE3, AHE6 and AHE8, respectively (**Figure 45**).

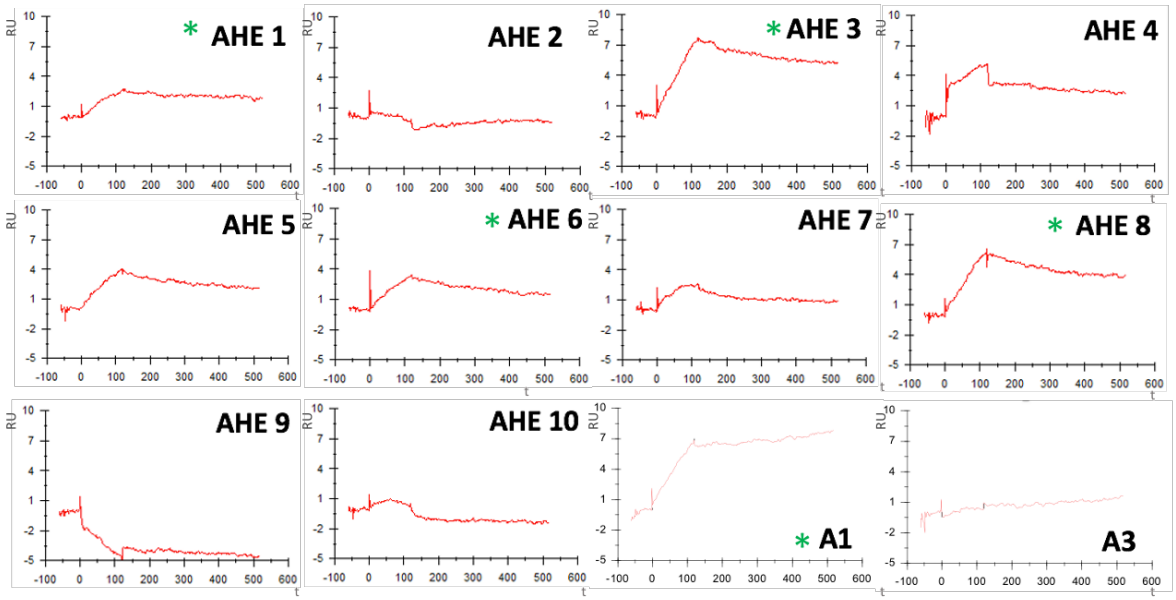

Figure 45. Individual SPR sensorgrams of the binding analysis of the 12 DNA sequences of the anti-HE4 aptamers to the ovarian cancer biomarker HE4.

The fact that aptamers were injected at high concentration of 2 μM and the signal obtained was low (in units of RU instead of expected hundreds RU) could be due to several reasons: the aptamers do not recognize the protein immobilized of a flat surface (*versus* beads on SELEX), the buffer conditions were not optimal (1X-PBS, 5 mM $MgCl_2$ and not urine), the protein is degraded or unfolded, or the binding is not significant in this conditions. Also, this experiment was done with the inner core of the aptamer (30 nt), without including the primer binding regions. Further characterization should be performed, including the binding of the full size 70 nt aptamers with primer binding regions. The limitation of this method was the inability to use urine, and AHE1 to AHE10 were developed in urine. Therefore, aptamers selected in urine should be functional in urine, and appear not functional in the buffers, as they may adopt different secondary structures.

However, based on the low interaction and the shape of the curves, which show a fast on-rate and a pretty slow off-rate, the most promising aptamers could be AHE1, AHE3, AHE6, AHE8 and A1. Interestingly, sequences AHE1 and AHE3, which are the most enriched aptamers in the Hi-FI SELEX, are confirmed as potential candidate aptamers as previously described and will be subjected to further analysis.

3.2. Aptamers-protein binding characterization by thermofluorimetic analysis (TFA)

The aptamer-protein binding was characterized in urine by thermofluorimetic analysis (TFA). The advantage of the method is that it does not require immobilization of target or the ligand, thus aptamer-protein binding is tested in solution. Moreover, it has been shown that is applicable for the aptamer characterization in body fluids [162]. Prior characterization of the anti-HE4 aptamers, the method was established in the laboratory for the first time. As urine has never been used in aptamer binding experiments, it was required to test the functionality of aptamer binding to their target in urine (high salt, pH, presence of denaturing agent urea). For this purpose, the well-known aptamer model system of the HD22 aptamer and thrombin protein target were used. After validation of the method, the TFA was applied to evaluate the binding affinity of different anti-HE4 aptamers with their target ovarian cancer biomarker human HE4 in urine. Different anti-HE4 aptamers were tested in urine: 25-mer A1 and A3 found in literature [164] and the three most-enriched 70-mer aptamers selected by the Hi-Fi SELEX performed in the laboratory AHE1, AHE2 and AHE3. The aptamer AHE2 did not exhibit binding, so it is not shown here, while other four sequences exhibited binding to target HE4.

3.2.1. Determination of the length of the aptamers AHE1 and AHE3 for TFA analysis

To determine the length of the aptamers for TFA and the effect of the primer binding regions on the secondary structure, both aptamers with core random sequence without primer regions (30 nucleotides) and full sequence with primer regions (70 nucleotides) were folded in urine environment using Unafold. The results (**Figure 46**) showed significant impact of the presence of the primer binding regions on the structures and stability of the aptamers. Indeed, the core random region possess 15Cs, while only 1G for AHE1, with structure stability $\Delta G = 0.16$ kcal/mol. For aptamer AHE3, random region contains 12Cs, while only 3Gs, with a stability of $\Delta G = -0.18$ kcal/mol. The full-length aptamer AHE1 possesses 28Cs, 10Gs and increased stability of $\Delta G = -5.20$ kcal/mol, while AHE3 contains 25Cs, 12Gs and stability $\Delta G = -6.39$ kcal/mol. Therefore, utilization of the full sequence with primer regions balances the lack of guanines in the core region and increases the aptamer stability in urine. For this reason, it is

important to use full size 70 mer sequences for further characterizations. Therefore, full 70-mer aptamer sequences were used for TFA tests and further applied in ELONA format.

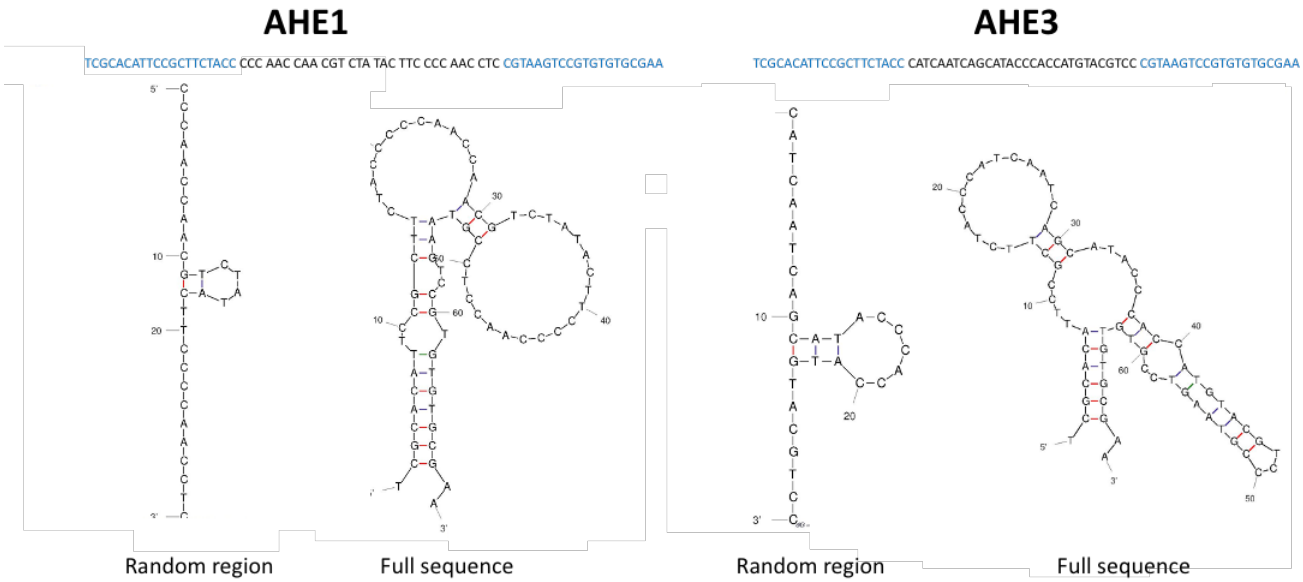

Figure 46. The effect of the primer region sites on the secondary structures of anti-HE4 aptamers AHE1 and AHE3 in urine.

The predicted anti-HE4 structures without the primer regions, only core 30-mer core random region sequence (on left) and with primer regions, full 70-mer aptamer sequence (on right). The structure show that presence of primer binding regions are necessary for aptamer folding. The structures were created using online DNA folding software Unafold (http://www.unafold.org) at temperature 25 °C and urine concentration of [Na+] = 55.4 mM and [Mg2+] = 4.4 mM.

3.2.2. The effect of urine on the thermofluorimetic measurements

To reduce urine interference, while securing the optimal fluorescent signal, urine dilutions were tested. The melting profile of aptamers was measured at constant concentration of 200 nM for the anti-thrombin aptamer and 100 nM for anti-HE4 aptamers at different urine dilutions of 1X (regular concentration of urine), 1/125 X (diluted urine) and 0X (no urine, protein buffer). In the example of the results shown below, all aptamers displayed interference of 1X concentrated urine on the signal intensity (**Figure 47**). Indeed, concentrated urine lowered the fluorescence signal with observed shift to lower T_m of the aptamers (lower DNA stability) and the higher background present. On the contrary, no effect was observed with dilutions of urine or in the absence of urine (just buffer). These conditions show high intensity fluorescence, no background and T_m around the expected values. The results were consistent for all other aptamers. Therefore, the characterization was performed in presence of 1/125X diluted urine.

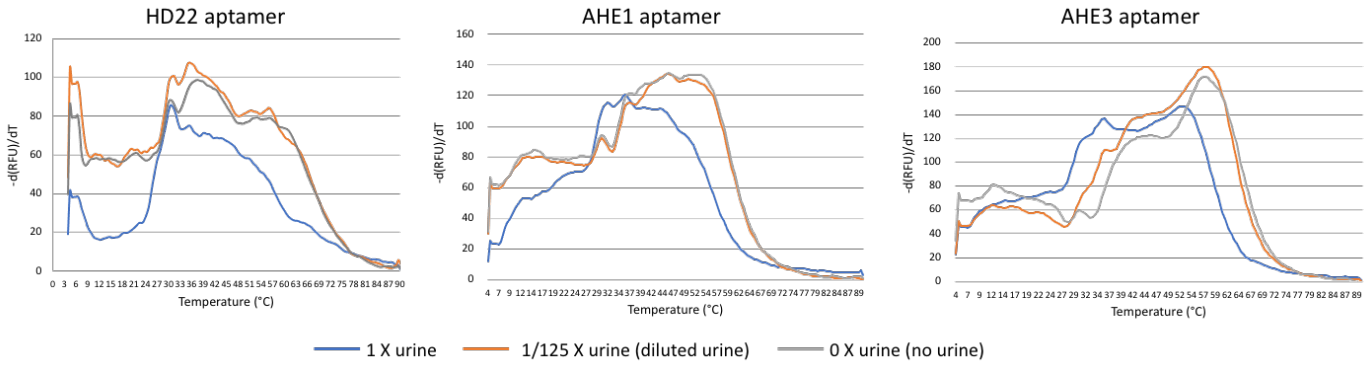

Figure 47. Effect of the urine on the thermofluorimetric signal of aptamers.

The anti-thrombin aptamer HD22 (200 nM) and anti-HE4 aptamers AHE1 and AHE3 (100 nM) are measured in 3 different conditions: undiluted urine 1X, diluted urine 1/125X and no urine (only protein buffer present). It has been shown that undiluted 1X urine decrease the −d(RFU)/dT signal in all three sequences, shifting the aptamers to lower values of T_m (potential lower stability state), suggesting interferences of concentrated urine to the analysis. Between diluted urine of 1/125 and no urine, no difference is observed. The data presented is average from three independent replicates. Therefore, all the experiments of aptamer-protein binding are performed in the presence of urine, in diluted form 1/125X.

3.2.3. The *proof-of-concept* for aptamers binding to target protein in urine (HD22-Thrombin)

To determine if aptamer can bind to its target in urine, the model aptamer HD22 [163] was tested for interaction with its target protein thrombin in presence and absence of urine (in protein buffer). First, only aptamer HD22 was tested in concentrations 0-400 nM of to verify the signal attribution to aptamer due to SYBR-Gold binding to DNA. The 200 nM of aptamer appears to be optimal for obtaining high fluorescence signal without background noise. Moreover, the signal is linearly proportional to the concentration of aptamer with a same results with and without urine (1/125X), with a measured melting temperature T_m of free aptamer of 46 °C (**Figure 48A**). Then, only protein thrombin was measured in concentration 0-2000 nM, and no signal was observed coming from protein (**Figure 48B**). Finally, the aptamer in constant concentration of 200 nM was subjected to thrombin protein ranging from 0-2000 nM concentration, in 1/125X urine and in protein buffer (no urine). The negative derivative data -d(RFU)/dT showed that a more thermally stable species were formed in both urine and buffer upon binding to target thrombin, with a two peaks detected, corresponding to the free aptamer state and the protein-bound state. After subtraction of the blank (aptamer only) the appearance of peak corresponding to the aptamer-protein complex was visible at higher T_m of bound aptamer of 58 °C in 1/125X and 61 °C in protein buffer (*data not shown*). The results below

display the binding melting profile of HD22-thrombin protein in 1/125 X urine, with a detection of more stable aptamer species with T_m bound of aptamer at 58 °C, compared to free aptamer of 46 °C, respectively (**Figure 48C**). The fluorescence signal of the negative derivative data −d(RFU)/dT at new bound Tm of aptamer (58 °C for 1/125 urine and 61 °C for protein buffer) was plotted against thrombin concentration from 0-2000 nM to yield a binding curve of the aptamer HD22-thrombin protein in urine or buffer environment (**Figure 48D**). Similar results were observed in both 1/125 X urine and buffer, with a high-affinity of HD22 aptamer to its target with the calculated constant of dissociation K_d in the nanomolar range. The obtained K_d corresponds to 227 ± 23 nM in urine, and 220 ±25 nM in buffer, showing that urine does not impair the aptamer binding in this model. Therefore, HD22-thrombin binding serve as a *proof-of-concept* for aptamer functionality for its target binding in diluted urine environment.

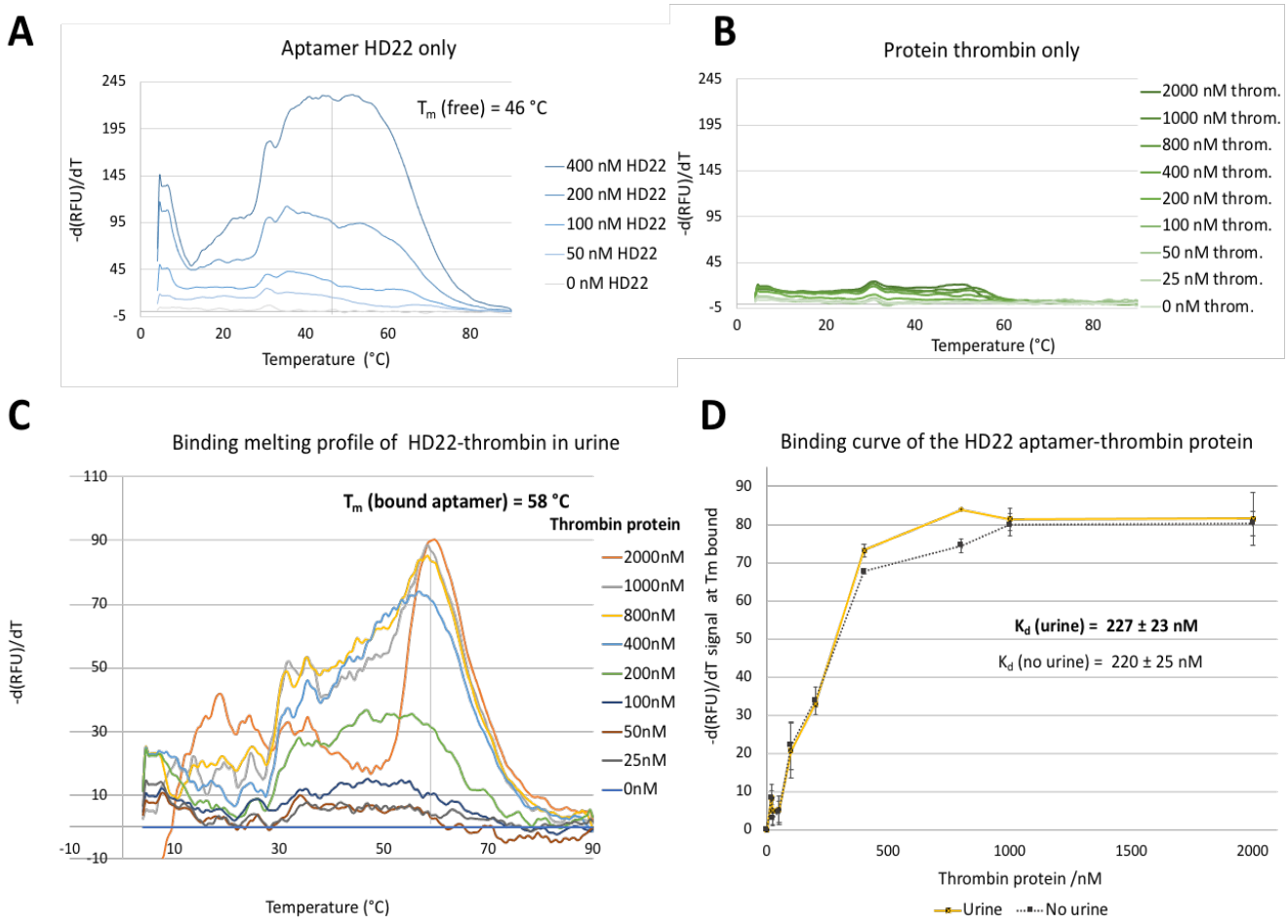

Figure 48. Thermofluorimetric analysis of the HD22 aptamer binding to thrombin in urine

A. HD22 only. The Sybr-Gold is binding proportionally to aptamer quantity. The HD22 at concentration 200 nM exhibits sufficient signal for TFA characterization **B. Thrombin protein only**. Sybr-Gold does not bind to protein. Therefore, the fluorescence signal comes from the aptamer state and TFA can be used for HD22-Thrombin characterization **C.** The melting profile of HD22-Thrombin binding. After subtraction of the blank (aptamer only, no thrombin), peaks of the HD22 bound to

thrombin are visible at with a shift to higher T_m of 58 °C, compared to T_m of free aptamer of 46 °C **D.** Binding curves of aptamers HD22-Thrombin. The HD22 aptamer binds to thrombin with good affinity in nanomolar range in both urine and buffer, with a K_d value in urine of 227 ±23 nM, showing that urine does not impair the binding.

3.2.4. Control experiments of TFA measurements for anti-HE4 aptamers binding to ovarian cancer biomarker HE4 in urine (aptamers and protein only)

The diagnostic potential of anti-HE4 aptamers was evaluated with binding to its target ovarian cancer biomarker HE4 in urine. Prior characterization, control experiments were performed to ensure fluorescent dye Sybr-Gold can intercalate into the aptamer DNA, and that signal contribution originated only from the aptamer. The Sybr-Gold was binding to DNA aptamers with fluorescence signal directly proportional to aptamer quantity (**Figure 49**). Therefore, it was confirmed that aptamers melting profile can be measured using Sybr-Gold in TFA.

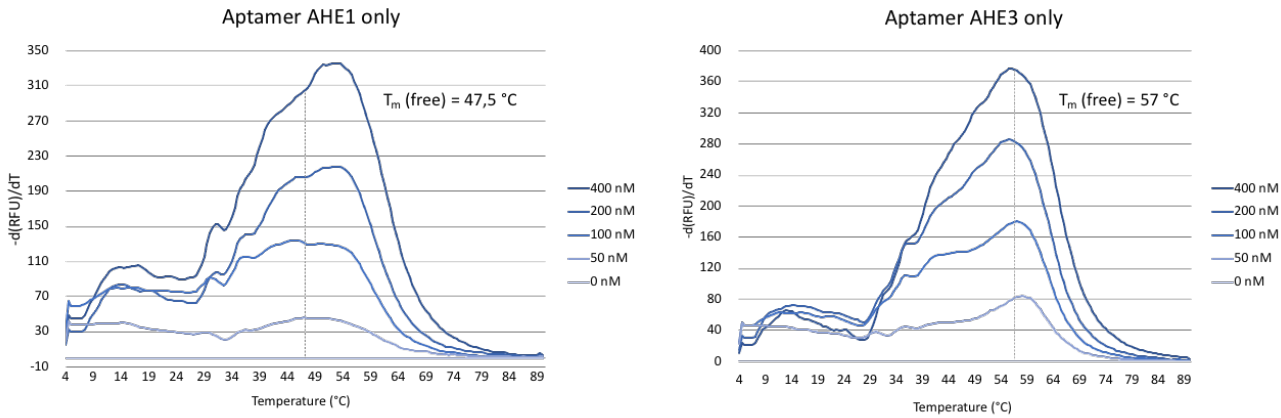

Figure 49. Control measurements of candidate anti-HE4 aptamers in 1/125X urine.

The Sybr Gold is binding to the aptamers with negative derivative fluorescence signal −d(RFU)/dT proportional to the aptamer quantity for all aptamers. The aptamers at 100 nM for AHE1 and AHE3 aptamers exhibit sufficient signal intensity for TFA characterization. The data presented is an average from three independent replicate experiments.

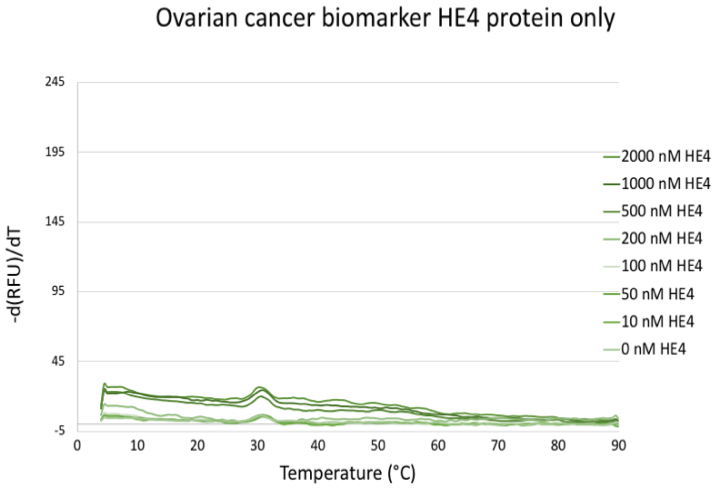

Control experiments confirmed that no fluorescent signal was observe in presence of Sybr-Gold and protein without DNA. Indeed, no signal was originated from HE4 protein only (**Figure 50**). These results confirmed the specificity of the signal corresponding to the aptamers state. TFA can thus possibly be used for characterization of the binding of anti-HE4 aptamers to HE4 in urine.

Figure 50. Control measurements of OC biomarker HE4 protein in 1/125X urine.

The Sybr-Gold is not binding to the HE4 protein, the signal is negligible (just background present). The data presented is average from three independent replicates.

3.2.5. Melting profile of anti-HE4 aptamers and HE4 protein binding in urine

As studies have shown, elevated levels of the protein biomarker HE4 are found in urine of ovarian cancer patients and urine can serve as a non-invasive fluid to detect HE4. Therefore, we wanted to determine the affinity of the aptamers and the binding constant of anti-HE4 aptamers in urine. We performed identical experiments in presence (1/125X) and absence (protein buffer) of urine. For this purpose, artificial human urine or buffer containing a constant 100 nM of AHE1 and AHE3 aptamers was spiked with increasing HE4 protein ranging from 0 to 800 nM. In the same manner, scramble DNA sequence was used as negative binding control. The negative derivative data −d(RFU)/dT showed that a more thermally stable aptamer-HE4 complex was formed for aptamers AHE1 and AHE3 upon binding to target ovarian cancer biomarker HE4 in both urine and buffer (**Figure 51**), as two peaks, corresponding to the free aptamer state and the bound aptamer state, were detected.

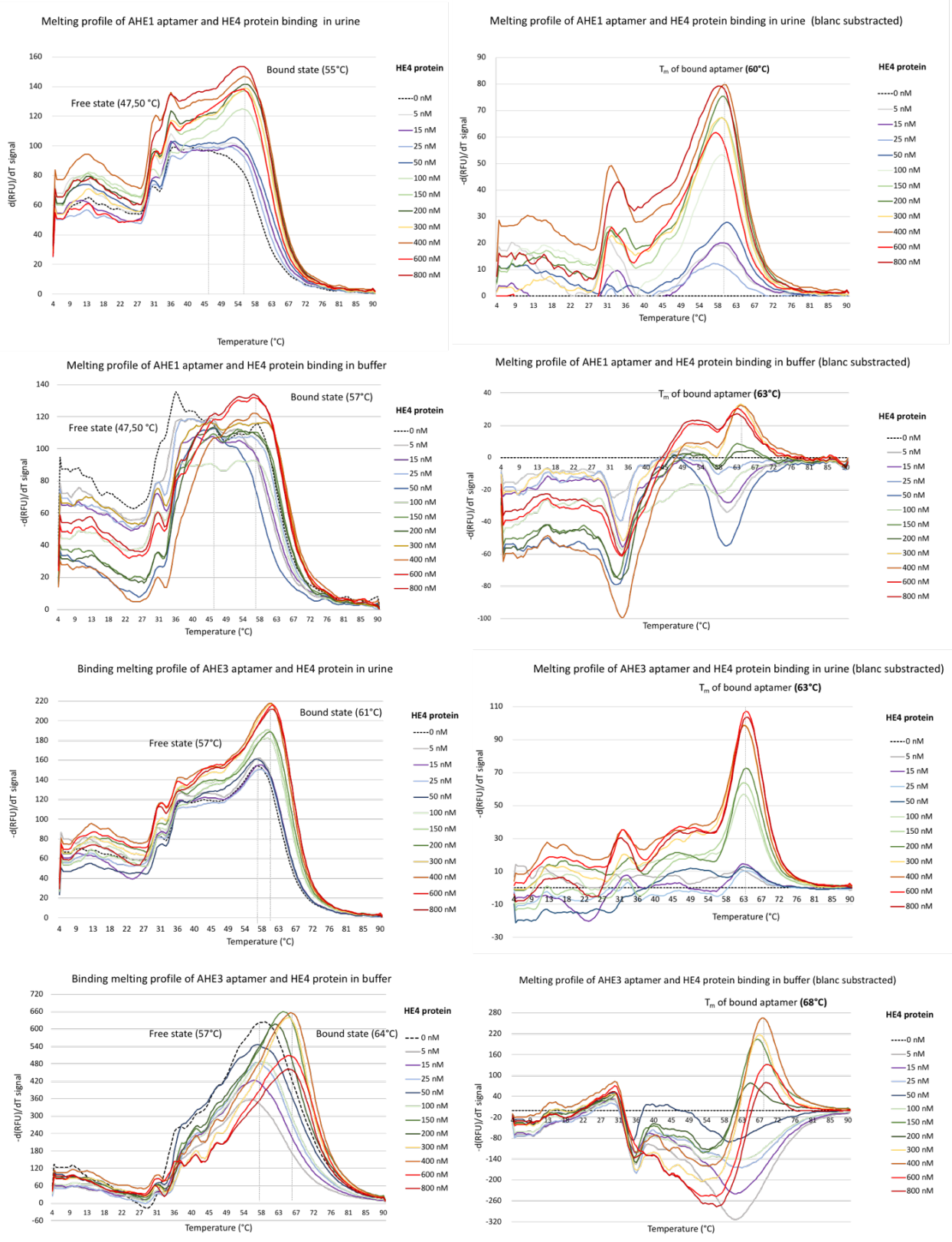

Figure 51. Thermofluorimetic analysis of the anti-HE4 aptamers AHE1 and AHE3 binding to ovarian cancer biomarker HE4.

The constant aptamer concentration of 100 nM was subjected to an increasing concentration of HE4 protein in urine ranging from 0 to 800 nM in presence (1/125X) or absence (protein buffer) of urine. The melting profile was analyzed from 4 °C to 90 °C. The binding thermal curves (melting DNA profile) were constructed by plotting temperature with negative derivative fluorescent signal −d(RFU)/dT. **The raw melting profile (on left)** : The raw melting profile obtained for aptamers showed two distant peaks corresponding to free aptamer (no HE4) state and bound aptamer state (with HE4). Upon binding to HE4 protein, more thermally stable species were present, with a shift to higher T_m. **The melting profile after subtraction of signal from aptamer only (on right).** After subtraction of the blank (aptamer only, no HE4), peaks of the aptamers bound to HE4 were visible, with a shift to higher T_m values, corresponding to 60 °C for AHE1 in urine; 63 °C for AHE1 in buffer; 63 °C for AHE3 in urine and 68 °C for AHE3 in buffer, suggesting binding to target protein HE4.

The free aptamer T_m was reproduced in both environments and corresponds to 47,5 °C for AHE1 and 55 °C for AHE3, respectively. Appearance of the AHE1 aptamer-HE4 complex peak was visible around 55 °C for AHE1 in urine and 57 °C in buffer *versus* the peak of free, unbound aptamers at T_m of 47,5 °C. For aptamer AHE3, the appearance of the aptamer AHE3-HE4 complex peak was visible around 61 °C in urine and 64 °C in buffer, *versus* the peak of free, unbound aptamers at T_m of 57 °C, respectively (**Figure 51**). Therefore, the shift to a more stable thermal species is observable for both aptamers in two different binding environment, with a difference in melting temperature between bound and free aptamers ΔT_m of + 7,5 °C for AHE1 in urine, ΔT_m of + 9,5 °C for AHE1 in buffer, ΔT_m of + 4 °C for AHE3 in urine and ΔT_m of +7 °C for AHE3 in buffer, respectively.

The aptamers AHE1 and AHE3 exhibit different shape of curves in these two different binding environments. Indeed, for both aptamers AHE1 and AHE3 the signal intensity is lower in buffer. Moreover, for aptamer AHE1, the signal does not seem to follow a logical order upon increasing the HE4 concentration. On the contrary, the signal in urine is of higher intensity. Moreover, the shape of the curves appear as more resolved with a prominent aptamer peak in urine. The difference in fluorescence intensity and signal may be the result of different aptamer behaviors, folding pattern and secondary structures in two different environments varying in salts and pH.

Both AHE1 and AHE3 exhibited binding to HE4 in urine. In urine, AHE1 exhibited binding to HE4 protein at a concentration as low as 50 nM of HE4, which corresponded to aptamer-protein ratio 1 : 0,5. For the AHE3 sequence, the shift of the ΔT_m of +4 °C was observed and binding appeared to be significant at higher concentration of HE4, with the AHE3-HE4 complex T_m peak identified at a concentration of 100 nM HE4, which corresponded to a aptamer-protein ratio of 1:1. The binding of the aptamers at crucial points (ratios of aptamer:protein) can be

found in supporting information (**Annex 5**). Subtraction of blank (aptamer only) on the melting curve on the right (**Figure 47**) eased the observation of a clear shift upon introducing HE4 protein in urine with the new melting temperature of bound aptamer T_m (bound AHE1) = of 60 °C and T_m (bound AHE3) = of 63 °C. The increase in the thermal stability indicate significant changes in tertiary structure of the aptamers upon binding. These results indicate potential binding for both aptamers, with AHE1 being superior to AHE3 sequence in binding to HE4 protein. Therefore, thermofluorimetric results display useful potential of aptamers AHE1 and AHE3 with binding to ovarian cancer biomarker HE4 in urine.

3.2.7. Binding curves of the anti-HE4 aptamers-HE4 protein

The binding curve was constructed by plotting the concentration of HE4 protein *versus* the negative derivative fluorescence −d(RFU)/dT signal at the aptamer-protein complex, at the new melting temperature T_m of the bound aptamer. The non-linear regression model was used to calculate K_d value for two binding environments: urine (**Figure 52A**) and protein buffer (**Figure 52B**). Aptamers AHE1 and AHE3 selected in urine display high-affinity binding to target HE4 in urine (**Figure 52A**). Both aptamers AHE1 and AHE yielded determined K_ds in the nanomolar range in diluted urine, showing they could be potential candidates for urine diagnostic tests. For AHE1, the determined K_d (AHE1) was 87 ± 9 nM, with the saturation clearly visible at a concentration of HE4 of 200 nM; while for AHE3, the K_d (AHE3) was 127 ± 28 nM, and with the saturation of HE4 binding to AHE3 was observed starting from 300 nM. The negative control, scrambled aptamer DNA, did not exhibit significant changes in T_m upon introducing HE4 protein, suggesting no affinity to HE4 and confirms a sequence-specific interaction of HE4 with AHE1 and AHE3. Plotting of the scrambled aptamer signal against HE4 concentration showed no significant binding, therefore suggesting specificity of binding of AHE1 and AHE3 aptamers to their target HE4 (**Figure 52A**). When applied in buffer environment, aptamers AHE1 and AHE3 behaved differently than what was observed in urine (**Figure 52B**). The signal intensity and binding affinity was different for both aptamers.

A

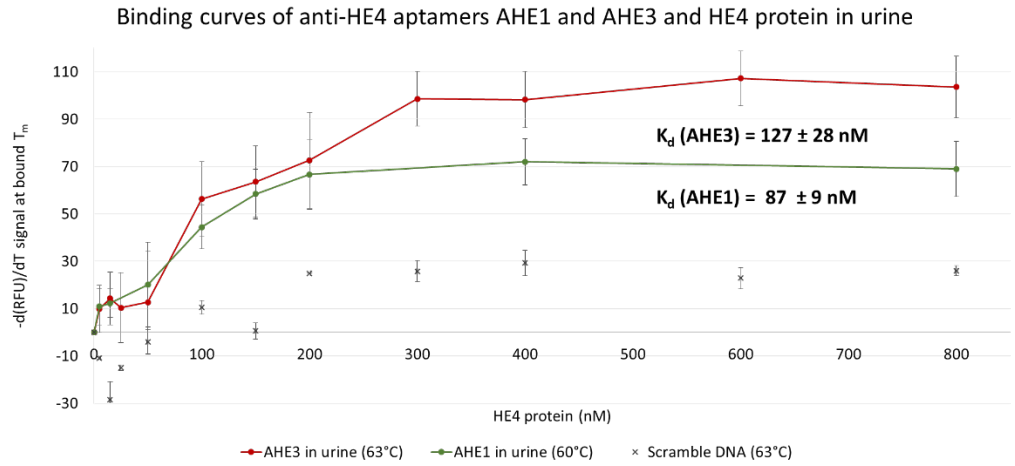

B

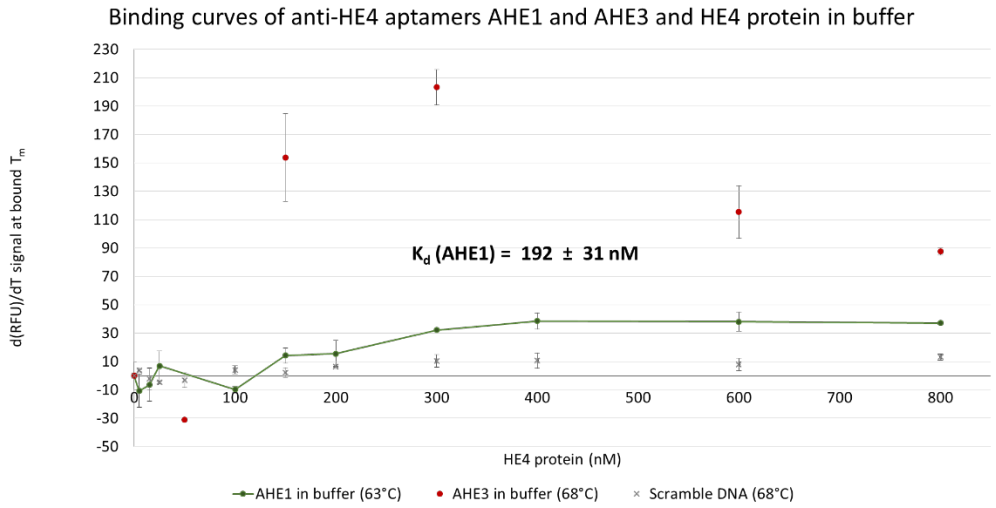

Figure 52. Binding curves of anti-HE4 aptamers to ovarian cancer biomarker HE4.

The binding curve was constructed by plotting HE4 protein concentration with negative derivative fluorescence signal −d(RFU)/dT at the Tm corresponding to bound aptamer state **A. Binding curves of aptamers AHE1 and AHE3 to HE4 protein in 1/125 X urine.** The aptamers show good affinity in nanomolar range of anti-HE4 aptamers for HE4 in urine, with high affinity and calculated K_d (AHE1) = 87 ± 9 nM and Kd (AHE3) aptamer of 127 ± 28 nM. **B. Binding curves of aptamers AHE1 and AHE3 to HE4 protein in protein buffer.** The aptamer AHE1 exhibited binding to HE4 protein in buffer with the affinity the nanomolar range, and calculated Kd of 192 ± 31 nM, while aptamer AHE3 does not seem to bind in the buffer. Overall, these results suggest that the described aptamers could have diagnostic potential as detection probes for HE4 in urine tests for ovarian cancer.

Indeed, the aptamer AHE1 displayed a lower signal intensity than in urine, but did exhibited binding to HE4 in buffer environment, with a calculated K_d value of 192 ± 31 nM in buffer (slightly lower affinity to HE4 in buffer than in urine). The signal was visible from 100 nM of HE4, which correspond to aptamer:protein ratio 1:1. For the aptamer AHE1, even though the shift to higher T_m values was observed, when plotting the data at aptamer-HE4 complex T_m, and substracting the signal from aptamer only, AHE1 does not appear to bind to HE4 in buffer (**Figure 52B**). The points until 150 nM HE4 are negative, while when increasing the concentration of HE4 protein > 150 nM, the signal is increasing and then decreasing again. Therefore, the K_d value could not be calculated, and AHE1 does not seem to exhibit binding to HE4 in buffer. Plotting of the scrambled aptamer signal against HE4 concentration showed no significant binding again, therefore suggesting specificity of binding for AHE3 aptamer to target HE4 in buffer, although in lower intensity (**Figure 52B**).

3.2.7. Comparison of the anti-HE4 aptamers

An TFA analysis was applied to 25-mer DNA aptamers A1 and A3 from the literature to compare with the novel anti-HE4 aptamers and find the best candidates for application in diagnostic test. As they were developed by Capillary-SELEX in buffer, their diagnostic potential for application in urine test was still to be evaluated. As previously described, the binding to ovarian cancer biomarker HE4 was characterized in presence (1/125X) and absence (protein buffer) of urine. The aptamer A3 exhibited a shift in thermal stability and binding to HE4 in both urine and buffer, with no significant differences between two environments, achieving similar binding affinity to HE4. The melting profiles of aptamers A1 and A3 in urine can be found in supplementary data (**Annex 6**). The A3 exhibited binding in urine from a concentration of HE4 at 300 nM, which corresponds to the aptamer:protein ratio 1:1.5. The plotting of signal at the T_m of formed A3 aptamer-HE4 protein of 51 °C with HE4 protein concentration in urine, revealed binding affinity of aptamer A3 in a nanomolar range, with an obtained K_d value of 338 ± 35 nM (**Figure 53**). The affinity of A3 aptamer was higher in buffer than it was in urine, with a K_d value of 291 ± 27 nM in buffer. On the contrary, the aptamer A1 did not exhibit increase in thermal stability upon introducing HE4 protein or binding to HE4 protein in urine, while it did in buffer, with a high-affinity to HE4 and yielded a K_d value of 274 ± 29 nM in buffer (**Figure 53**). Therefore, A1 does not bind in urine, unlike A3 that does bind to HE4 in urine. Therefore, aptamer A3 could serve as positive binding

control in future experiments or additional diagnostic probe for development of aptamer-based urine test for ovarian cancer.

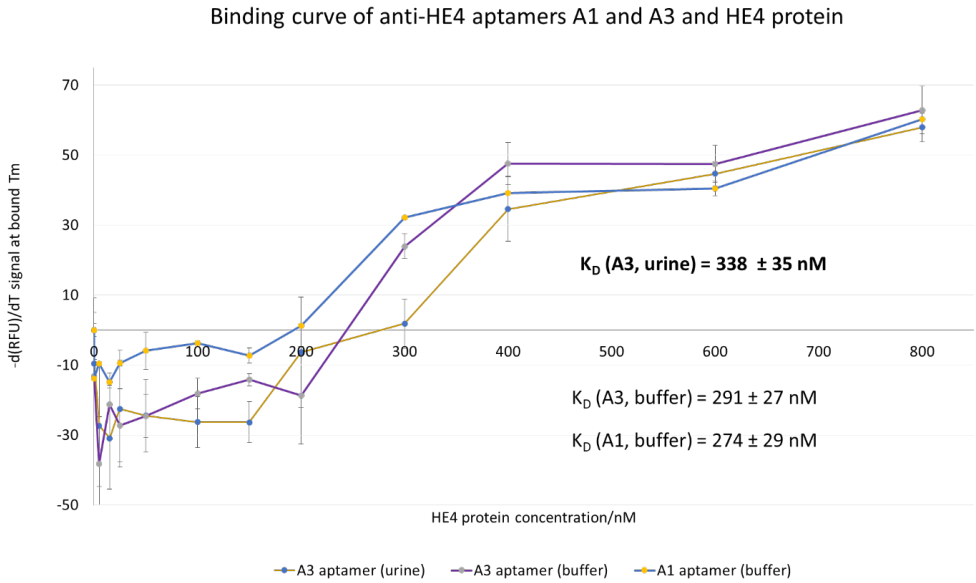

Figure 53. Binding curves of aptamers A1 and A3 in buffer and urine.

The aptamers show good affinity in nanomolar range of anti-HE4 aptamers for HE4 in buffer, with high affinity and calculated K_d (A1) of 274 ± 29 nM and K_d (A3) of 291 ± 27 nM. A1 did not exhibit binding to HE4 in urine and A3 show binding to HE4 with a calculated K_d value of 338 ± 35 nM in urine. These results suggest that the aptamer A3 could be used as positive binding control for future experiments or have diagnostic potential as additional detection probe for HE4 in urine tests for ovarian cancer.

The comparison and the summary of all obtained data in this thesis work and binding characterization are presented in the table below (**Table 15**).

Table 15. Comparison of the TFA analysis of the different anti-HE4 aptamers binding to ovarian cancer biomarker HE4.

	URINE					BUFFER			
Aptamer	**T_m alone (°C)**	**T_m bound (°C)**	**Shift to more stable thermal state**	**Seems to bind**	**K_d (nM)**	**T_m bound (°C)**	**Shift to more stable thermal state**	**Seems to bind**	**K_d (nM)**
AHE1	47,50	60	Yes	**Yes**	87 ± 9	63	Yes	Yes	192 ± 31
AHE3	55	63	Yes	**Yes**	127 ± 28	68	Yes	Yes	n/a
A1	34/35	34	No	No	n/a	47	Yes	Yes	274 ± 29
A3	40	50	Yes	**Yes**	338 ± 35	51	Yes	Yes	291 ± 27

Aptamers A1 and A3 that were selected by SELEX in buffer displayed better functionality and binding to HE4 in buffer than in urine. On the contrary, aptamers AHE1 and AHE3 selected in urine display high-affinity binding to target HE4 in urine. These results can explain the importance of using correct solution in SELEX depending on the final application of aptamer (ex. buffer, serum, urine), which will influence functionality of aptamer.

All things considered, aptamers AHE1, AHE3 and A3 exhibited high-affinity binding to ovarian cancer biomarker HE4 in urine, with a K_d in the nanomolar range. The potentially most potent sequence and best candidate for application in urine could be AHE1, followed by AHE3, followed by A3. Therefore, they could serve as diagnostic probes for the application in urine, in the development of the future urine tests or biosensors for ovarian cancer.

3.3. Enzyme-Linked-Oligonucleotide-Assay (ELONA) for detection of HE4

The enzyme-linked immunosorbent assay (ELISA) is a fundamental tool of biomedical research and method for detection of cancer biomarkers [180], including CA125 and HE4 [27,77]. With the emergence of aptamers as diagnostic probes, their potential to replace or complement antibodies resulted in the developments of ELONA (Enzyme-Linked OligoNucleotide Assay) [180]. Herein, we applied anti-HE4 aptamers in direct colorimetric ELONA to evaluate their ability to recognize and bind to its target HE4 protein. The system involves immobilization of HE4 protein and biotin-conjugated aptamers as detection probes. The signal is revealed by the streptavidin-HRP system, as in standard ELISA. The diagnostic potential and aptamer-protein binding was tested for aptamers that previously exhibited biding to HE4 in urine: AHE1 (70 nt, full size), AHE3 (70 nt, full size) and A3 (25 nt). The biotinylated aptamers at a constant concentration of 100 nM were added to ovarian cancer biomarker HE4 ranging from 0-100 pmol on immobilized beads. First, the effect of the biotinylation on the aptamers signal for ELONA was tested by conjugation of biotin on either 3' or 5' prime of the DNA and can be found in supporting information (**Annex 7**). From all the aptamers, only aptamer 5'-biotin AHE1 displayed potential signal coming from aptamer-protein binding in ELONA format. As seen on results below (**Figure 54A**), the choice of the DNA extremity for conjugation could have the impact on aptamer functionality in ELONA format. It is observed that no signal by ELONA was obtained when biotin is conjugated on the 3' prime of the aptamer AHE1. The subtraction of the blank (no HE4 protein), results in a negative values. Oppositely, when biotin

was conjugated on the 5'prime of the DNA, signals of absorbance at 450 nm were obtained by ELONA assay (**Figure 54A**)

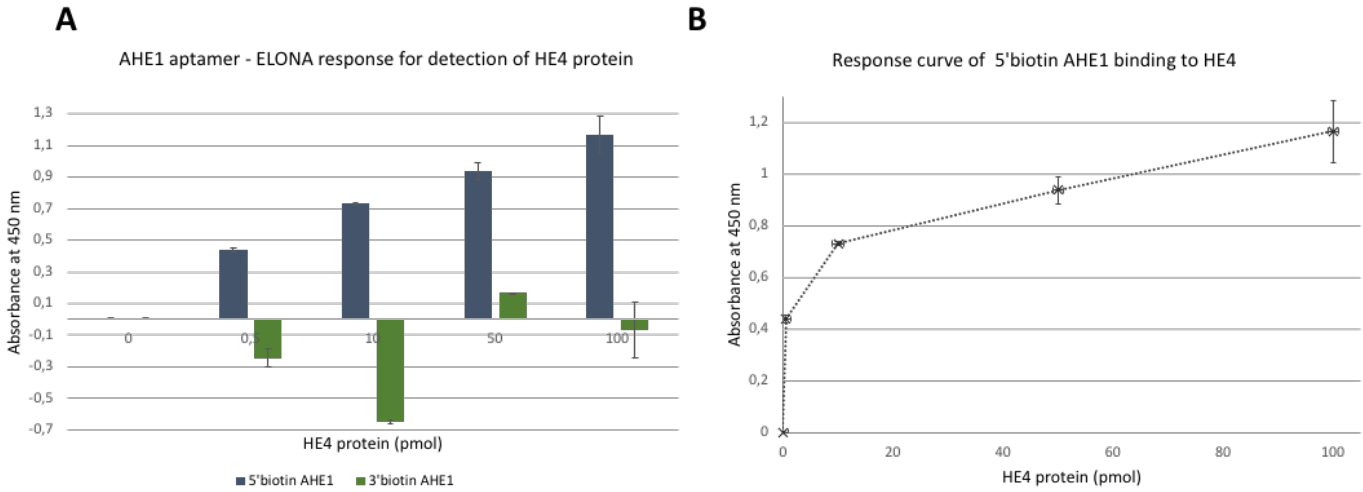

Figure 54. Enzyme-Linked-OligoNucleotide Assay (ELONA) for detection of HE4.

The anti-HE4 aptamer AHE1 was added as a diagnostic probe reagent to immobilized HE4 protein ranging from 0-100 pmol (0-1000 pM) to monitor absorbance signal that comes from potential aptamer-HE4 binding. **A.** The effect of the biotinylating on 3' or 5'-end of DNA aptamer AHE1 (70mer, full size with primer binding regions)**. B.** ELONA response curve for the aptamer 5'biotin AHE1.

Moreover, 5'biotin-AHE1 displayed potential binding to HE4 protein, with an increasing signal as HE4 protein is increased, indicating potential interaction between aptamer and protein in a dose-dependent manner as seen on the response curve (**Figure 54B**).

These results confirm the potential of developed anti-HE4 aptamer AHE1 to be used as a probe in future urine test. The purpose of this experiment was to only to assess the potential of aptamers to binding to its target by ELONA assay. However, it is important to highlight the significant limitation of this assay : HE4 protein is in extremely low quantity, ranging from 0-100 pmol (0-1000 pM), which can be too low to obtain any relevant signal. The concentrations of HE4 found in urine of ovarian cancer patients can range from 13-24 000 pM of HE4. Herein, those quantity of protein could not be immobilized on beads due to the capacity of beads. Therefore, higher concentration of HE4 protein should be tested in future in similar format. In the development of diagnostic assay in future, different formats should be considered, taking into account the immobilization of the aptamer instead of the protein, as HE4 without a tag is present in urine of ovarian cancer patients. However, the results obtained for AHE1 aptamer

are promising and more characterizations by ELONA are undergoing. Interestingly, In both TFA and ELONA methods, the same trend is observed for full size 70mer AHE1 aptamer sequence as the most potent binder to HE4. Therefore, this results further indicate that aptamer AHE1 could be the best anti-HE4 binder for diagnostic application.

3.2.8. Part 3 - Conclusions

- The binding between several anti-HE4 potential diagnostic DNA aptamers and ovarian cancer biomarker HE4 was characterized.
- The screening was performed on the top 10 most enriched sequences with random regions developed by the Hi-Fi SELEX in Part 2 of thesis (AHE1 to AHE10) and two sequences from literature (A1 and A3). The analysis revealed very low potential interaction of AHE1, AHE3, AHE6, AHE8 and A1 and target human HE4 protein.
- The thermofluorimetric analysis (TFA) for aptamer-protein binding characterization in urine was established in the laboratory.
- The anti-thrombin HD22 aptamer was used for development of the TFA and as a *proof-of-concept* for aptamer functionality in urine with a successful binding to target protein in nanomolar range, with a K_d value of 227 ± 23 nM in urine.
- Anti-HE4 aptamer sequences AHE1, AHE2, AHE3, A1 and A3 were characterized and compared for their binding affinity to ovarian cancer biomarker HE4 in urine and buffer
- The sequence AHE2 did not exhibit significant binding to HE4 protein (with SPR and TFA methods).
- The sequence A1 exhibited binding in buffer (with SPR and TFA methods), with a K_d value of 274 ± 29 nM, but did not bind in urine (with TFA method).
- Anti-HE4 aptamers AHE1 (70mer), AHE3 (70mer) and A3 (25mer) displayed significant binding to ovarian cancer biomarker HE4 in urine.
- The anti-HE4 aptamers AHE1, AHE3 and A3 displayed high-affinity to target HE4 protein in urine, with constants of dissociation K_d in nanomolar range, with a K_d (AHE1) of 87 ± 9 nM, K_d (AHE3) of 127 ± 28 nM and K_d (A3) of 338 ± 35 nM, respectively.
- The preliminary data of the aptamer-HE4 binding provided by The Enzyme-linked-OligoNucleotide (ELONA) for HE4 detection displayed aptamer AHE1 (70 mer) as

most potential diagnostic probe, with the dose-dependent response. However, more research is needed to validate those results.

- Therefore, characterized anti- HE4 **aptamers AHE1, AHE3 and A3** could serve as potential diagnostic probes in development of a future urine test or biosensor for ovarian cancer.

- The partial results from PART 2 and PART 3 of the thesis were published [181] in the peer-review Journal Cancers (IF = 6.575):

  Publication n °4 related to this thesis: Hanžek, A.; Ducongé, F.; Siatka, C.; Duc, A.-C.E. Identification and Characterization of Aptamers Targeting Ovarian Cancer Biomarker Human Epididymis Protein 4 for the Application in Urine. *Cancers*, **2023**, *15*, 452. https://doi.org/10.3390/cancers15020452

V. DISCUSSION

Urine as a sample for the detection of ovarian cancer

Cancer ranks as a leading cause of death and is an important barrier to increasing life expectancy in every country of the world [1], accounting for approximately 10 million deaths in 2020 [1,4]. Overall, the burden of cancer incidence is rapidly growing worldwide, which reflects both aging and growth of the population, as well as changes in the prevalence and distribution of the main risk factors for cancer [2]. Currently, it is projected that the number of new cases of cancer will increase by 70 % until 2034, rising to over 22 million new cases per year [2,3].
Ovarian cancer (OC) is accounting for a high number of cancer-related deaths worldwide [1]. Currently available diagnostic methods lack the specificity and sensitivity for detection of OC [8]. The main problematic of the high mortality is the lack of accurate diagnostic methods that can detect the malignancy in early-phase. Indeed, if OC can be detected earlier in the course of the disease, the prognosis drastically improves, with a 5-year survival of 90 % [6]. Unfortunately, 90 % of the women are diagnosed in advances, metastatic stages, with a 5-year survival rate of 15–40 % .[6,7].

There is growing evidence that screening can have impact on the improving the cancer mortality. Many countries have national screening programs for breast, bowel and cervical cancers, which have been associated in 50–90 % reduction in mortality [35]. However, screening for OC, a fairly rare cancer, does not exist, as none of the current diagnostic methods are accurate enough for screening and have failed to improve the mortality of OC [182]. The future of ovarian cancer diagnostics does look promising, as researchers and clinicians are constantly exploring new approaches and technologies to improve early detection and diagnosis of this disease. Mainly, the focus on finding an accurate test for detection of OC has been on biomarkers (initially in blood and increasingly in other bodily fluids) [35]. There is a growing need for a novel and more sensitive methods for detection of biomarkers. Biomarkers are measurable substances in the body that can indicate the presence or progression of a disease [175]. Currently, there are several biomarkers used in ovarian cancer diagnosis, including CA-125 [29,30]. Currently used routine biomarker CA125 has important limitations in specificity and sensitivity, as it is not elevated early in the disease and is found in many other diseases. It is

not always reliable, as it can lead to false-positives and false-negative results [26,29,30]. Therefore, novel biomarkers and diagnostic approaches are urgently needed.

Urine has emerged as interesting sample for detection of many diseases and types of cancer [183]. Urine tests could present easy, cheap and non-invasive alternatives in OC diagnostics. Cancer biomarkers remain stable and intact in urine in the pathophysiologic condition [42]. Urinary analysis may enhance patient care and lower the mortality toll because urine can tolerate more alterations in the early stages of disease [42]. Some advantages of the urine test for cancer are:

(1) Non-invasive: Urine tests are non-invasive, meaning that they do not require any invasive procedures, such as biopsies or surgeries, to collect a sample. This can make them less stressful, less painful and more acceptable for patients [43,44].
(2) Easy to collect: Urine tests are easy to collect and do not require any special preparation. Patients can collect urine samples in the privacy of their own homes. Performing urine tests in self-sampling manner could allow for the possibility of screening women [41].
(3) Cost-effective: Urine tests can be less expensive than other types of cancer tests, such as imaging tests or biopsies [42].
(4) Early detection: Some urine tests can detect cancer at an early stage, which can increase the chances of successful treatment [48].

Currently, urine tests for cancer are not widely used for cancer screening or in the routine healthcare system. However, researchers are studying the potential of urine tests for detecting various types of cancer, including bladder, prostate, lung, kidney, and colorectal cancer. For example, a urine test called the UroSEEK has been developed to detect genetic mutations associated with bladder cancer in urine samples [184,185]. Another test, called the PCA3 test, can detect prostate cancer in urine samples by measuring levels of a specific gene [186]. Overall, urine tests have the potential to be useful tools for detecting cancer, but more research is needed to determine their effectiveness and reliability. Urine test for OC could represent a promising diagnostic option in future, as many different biomarkers of OC has been found elevated and extremely stable in urine environment [42,47–49]. An especially sensitive and specific biomarker found in urine of OC patients is Human epididymis protein 4 (HE4) [64,99]. HE4 is an important clinical biomarker of ovarian cancer. Serum HE4 is routinely employed in differential diagnoses of women with pelvic masses and its clinical utility has been validated [28,30,33]. In the

last decade, the diagnostic power of HE4 has been investigated in urine, as urine is a non-invasive and easy to collect sample [49,65,96].

Potential of aptamers as diagnostic probes

The current methods for HE4 are antibody-based immunoassays. Moreover, one of limitation of current urine tests, including in detection of HE4, is the standardization of the urine volume. The concentration of HE4 protein measured will depend on urine volume, which is highly heterogeneous between patients. This is observed using currently available immunoassays for HE4. These conventional tests sometimes require application of creatinine as an internal standard for volume normalization [64]. Depending on a format of a test, the aptamers could be potentially be used as a probes in a biosensor directly in urine, without a need for normalization of urine volume. The aptamers combine many advantages, they are low-molecular-weight substances, with high affinity, specificity and production at low cost. For all these reasons, it seems important to explore the use of aptamers for disease diagnosis as a tool that could be potentially validated and standardized in clinical use in future [112]. Aptamers have several advantages in diagnostic tests:

(1) High specificity and affinity: Aptamers can be designed to bind to specific targets with high specificity and affinity, which allows for accurate and efficient detection of target molecules in complex biological samples, such as urine [112].

(2) Stability: Aptamers are stable at a wide range of temperatures and pH levels, and are resistant to degradation by nucleases and proteases, which makes them suitable for use in various diagnostic urine assays. The nucleic acid structure possesses high stability at the different temperatures in transport and storage, which is convenient for diagnostic tests [111].

(3) Ease of synthesis and modification: Aptamers can be synthesized in large quantities using automated methods, and can be easily modified with fluorescent, biotinylated, or other tags to enable detection in different types of urine assays [111].

(4) Low cost: Aptamers can be synthesized at a relatively low cost compared to antibodies, which makes them an attractive alternative for diagnostic urine assays that require high specificity and sensitivity.

(5) Versatility: Aptamers possess adaptability and unlimited options of chemical modifications, paving the way to various detection systems in the development of future urine tests and biosensors [187].

Development of the novel aptamers in urine

Urine is a complex biological fluid that contains various components, such as salts, metabolites, proteins, and other molecules that may interfere with the selection and binding of aptamers. However, several studies have successfully developed and identified aptamers that can specifically bind to various targets in urine samples, including proteins, organic compounds or cells. Overall, the use of SELEX to identify aptamers from urine samples has the potential to for the development of novel diagnostic tools for various diseases and conditions. Some examples of the aptamers that have been developed to detect or target molecules in urine:

(1) Pharmaceutical compounds-binding aptamers: DNA aptamer has been develop to detect several opioids in urine samples to diagnose opioid intoxication[188]. Another DNA aptamer have been developed to detect ampiciline in urine samples, to determine the optimal antibiotic dosage and monitoring compliance with treatment, in order to reduce the multi-drug resistant infections [189].

(2) Toxins-binding aptamers: The area with most advances in aptamer development has been detection of various toxins in food or environmental samples. Recently, the same has been applied to urine, with a aptamers for detection of α-amanitin, a lethal toxin found in mushrooms [190].

(3) Cancer-related targets-binding aptamers: A sensitive DNA aptamer for detection of oncomarker in urine was recently developed for colorectal cancer [191]. Moreover, DNA-aptamer was developed for detection of biomarker EN2 for prostate and bladder cancer from urine [192].

The aptamer development for application in urine is a promising field, but still remain very small, with only few aptamers available for detection of targets from urine. Small number of studies used human urine to perform SELEX in order to extract and discover new biomarkers. However, using urine environment in SELEX to an existing target biomarker is not common, as selections are performed in buffers. Up to this date, no aptamers have been developed or applied in urine in the context of ovarian cancer detection.

Herein, described aptamers are shown to be functional and stable in the urine environment and exhibit binding to a urinary cancer biomarker target. The novel aptamer diagnostic probe has demonstrated that it can function in artificial urine, with high-affinity binding to ovarian cancer biomarker HE4 in the nanomolar range, holding the potential to application in future diagnostic tests.

When developing an aptamer with diagnostic application, it is important to select and identify aptamers that are functional and stable in desired environment. Therefore, several aspects are important to consider when performing selection of high-affinity aptamers, especially the choice of the selection environment. This is especially true for diagnostic aptamers intended for diagnostic assays and final use in patients' sample, which involves complex matrixes of body fluids, such as blood or urine. This thesis work produced novel anti-HE4 aptamer probes for the application in urine. As the final goal is to apply these aptamers to function as diagnostic probes in human urine, it was important to ensure a selection environment of high salts and slightly acidic pH equivalent to urine, which will provide the formation of the relevant three-dimensional structures responsible for binding to HE4. The aptamers were developed after 10 rounds of selection to HE4 in 1X urine. After characterization of these aptamers, it was visible that the choice of urine as a selection milieu was advantageous. The anti-HE4 aptamers developed from urine AHE1 and AHE3 exhibited high-affinity to ovarian cancer biomarker human HE4 in urine. However, the same aptamer AHE1 did not exhibit binding in buffer, while AHE3 did. On contrary, the anti-HE4 aptamers from literature [148] A1 and A3 developed in buffer were either not functional (A1) or less potent (A3) in urine. As they were selected in buffer, they both exhibited binding to HE4 in buffer. Although aptamer binding and behavior is aptamer-dependent, it appears that the environment of selection can influence final aptamer functionality and binding abilities, as aptamers selected in urine had better performances in urine, while aptamers selected in buffer had better performances in buffer. It appears that choice of the solution for the incubation of aptamers and target molecules in SELEX does influence the characteristics of developed aptamers, as well as their binding abilities in final application.

Development of novel aptamers for cancer-related targets

Another important aspect to consider is choice of a target protein in SELEX, which needs to be relevant to proteins found in patients suffering from cancer. The optimal type and quality is

a crucial step in ensuring successes towards selecting aptamers with high-affinity and high specificity. Initially, the expression of recombinant proteins from bacteria was considered, as it can provide large quantity of target, with a low cost. As human HE4 target protein contains eight cysteines forming disulfide bonds at the core of the protein in the WFDC domain [67,68], attempts were made to produce HE4 using a special strain of *E.Coli T7 Shuffle* harboring the ability to fold proteins containing disulfide bridges. However, *in house* production did not yield HE4 in sufficient quality or purity to use in SELEX. Use of bacterial recombinant proteins for the human targets in SELEX experiments today appear as obsolete, as they do not ensure all protein features and post-translational modifications present in the patients. Another possibility, not undertaken in this thesis work, is to use the proteins isolated directly from patients with desired disease. For example, aptamers were selected to ovarian cancer biomarker CA125 using protein target isolated from the ascites of OC patients [141]. In the context of HE4, it is important to ensure post-translational modifications found in ovarian cancer patients, to be able to select specific and high-affinity aptamers. Indeed, human HE4 is post-translationally N-glycosylated on asparagine [67–69]. The choice of the correct protein will ensure selection of the high-affinity aptamers whose binding and target recognition are strongly influenced by the charge of the protein and the electrostatic interactions. By the recommendations of the experts, it was decided to choose a human recombinant 6xHis-tagged HE4 protein expressed in HEK 293 cells (ab219658, Abcam) which will hopefully ensure a protein as similar as the one present in ovarian cancer patients.

Common strategy in selection of aptamers in SELEX is immobilization of the protein. In this case, nucleic acid aptamers that interact with the target can be physically separated from non-interacting oligonucleotides, which stay in the solution above and are washed away [102]. For this purpose, target protein is tagged, for example with GST or 6xHistidine, used for immobilization. In this thesis work, aptamers were selected to a 6xhistidine-HE4 protein immobilized on beads. Taking into the account the small size of HE4 protein, with molecular weight of approximately 11 kDa, choice of the 6xhistidine seemed more reasonable. Using GST as a tag could lead to increase selection of aptamers specific to the GST tag rather than target protein despite counter selection. This could have decreased the chances of selecting aptamers sequences that can identify HE4 when applied in ovarian cancer patients' samples. Indeed, GST as a protein is double the size of HE4, with a molecular weight of 25.5 kDa. Moreover, presence of GST in characterization of aptamer-protein binding experiments can result in false-positive results, which come from self-assembly of the proteins, and not from

aptamer-protein binding. Therefore, the protein tag in both selection and characterization of aptamers is an important aspect to consider when interpreting results. Using a small tag such as 6xHistidine tag in this thesis work, could potentially lead in selection of the more specific anti-HE4 aptamers that will be better suitable for the detection of actual non-tagged human HE4 present in patients urine samples.

Utilization of digital droplet PCR in context of aptamer selection

While it has been proven to be valuable in numerous applications, digital droplet PCR has failed to be widely adopted in aptamer studies, regardless of the PCR being a central point in the aptamer selection process. The concept of utilizing ddPCR in SELEX was introduced by Ouellet *et al*. and Ang *et al*. who have used a novel selection method, called Hi-Fi SELEX, for development of DNA aptamers targeting α-thrombin and human coagulation factors IXa, X [153,154]. The authors used the partitioning capabilities of ddPCR to select high-affinity aptamers, but without the droplet reading or aptamer quantification. This thesis work adapted the protocol for the sensitive amplification and expanded it to the quantification of the aptamer sequences recovered at each cycle against target protein. The modified Hi-Fi SELEX method has been successfully applied to select DNA aptamers to ovarian cancer biomarker HE4.

Indeed, a choice of a PCR drastically influence the aptamer diversity and SELEX efficacity [179]. One of the main problems in aptamer selection is the formation of PCR by-products during SELEX experiments. Indeed, accumulation of amplification artifacts can seriously hamper the enrichment of high-affinity aptamers, and can even cause the failure of the whole selection [179,193]. As initial libraries are highly diverse, solution PCR amplification have limitations, such as low efficiency or formation of non-specific products [179,193]. Moreover, previous studies have demonstrated that aptamer amplification by standard PCR in SELEX is susceptible to non-specific primer hybridization [102,106,179]. Very recently, ddPCR has been introduced into the SELEX experiments, to reduce the propagation of non-specific by-products and PCR bias [153,154]. In ddPCR, aptamer template is partitioned into water-in-oil emulsions, where each droplet represents an individual PCR reaction. Therefore, each droplet contains a smaller number of templates, keeping the sequence heterogeneity per droplet very low [179]. Therefore, it ensure sensitive amplification of potentially rare aptamer sequences or those sequences hard to amplify, while reducing the risk of by-product formation. Also, it offers absolute quantification of aptamers during selection, without the need for standard calibration curves.

One advantage for using ddPCR-driven SELEX is the amplification of a selected library members in a manner that ensures each amplicon exist in a fully complementary duplex [153]. This outcome is not achieved using conventional solution bulk PCR, which can result in an incomplete conversion of double-stranded aptamers into the desired single-stranded library using λ exonuclease [153,154]. Indeed, conversion using solution PCR and λ exonuclease is commonly up to 60 % of ssDNA regeneration only [102,194]. Herein, using ddPCR-driven SELEX achieved complete conversion of ssDNA at the end of each cycle to biomarker HE4.

Recently, Takahashi *et al*. used a high-throughput analysis to compare standard solution PCR and digital droplet PCR on aptamer library diversity and the SELEX efficacy [179]. The authors showed that ddPCR-driven SELEX preserve a higher sequence diversity throughout the selection process, with molecular evolution progressing more slowly [179]. The ddPCR is a better way to preserve molecular diversity and allows more chances of obtaining highly structural sequences. However, ddPCR is costly and time-consuming compared to solution PCR. For example, ddPCR requires extra steps, including droplet generation and amplicon extraction by organic solvent from the droplets [179]. Indeed, the main limitations observed in this project were the high cost and low recovery of DNA. As ddPCR was not originally intended for downstream analysis (once droplets are analyzed, they are discarded), re-amplification is needed to increase the yield of DNA to be able to proceed in the next cycle of SELEX. Moreover, aptamer samples are complex, constituted of diverse DNA sequences, which can make interpretation of the results difficult. In this case, ddPCR ensured sensitive and non-biased pre-amplification before classical PCR.

Since ddPCR is an extremely sensitive method enabled to amplify only a few aptamer sequences present in sample (i.e., 3 present bound sequences in 20 µL = 0.15 copy/µL will result in 3 positive droplets), it is important to achieve optimal template concentration to maximize the effect of partitioning capabilities and recovering of all relevant specific aptamer library members. Thus, I would highly recommend the dilution of bound aptamer fractions and separation in multiple ddPCR reactions rather than adding the total quantity of a bound DNA template. The presence of a high amount of template will inhibit the ddPCR efficiency and saturate the droplets, as what was observed in the first few cycles of selection. Therefore, the capacity to fully amplify rare sequences is reduced. Also, ddPCR can quantify the anti-HE4 sequences, but it does not provide information in which sequences are present. For that reason, DNA sequencing is always crucial to be able to identify specific enrichment to target cancer

biomarkers. Hi-Fi SELEX was successful in selecting and identifying high-affinity aptamers to ovarian cancer biomarker human HE4. These findings provide *proof-of-concept* for using ddPCR in aptamer selection and can be applied for future development of any diagnostic or therapeutic aptamers.

Development of a novel anti-HE4 aptamers for the application in urine: characterization and comparison

Using described Hi-Fi SELEX, a panel of enriched anti-HE4 aptamers has been selected to ovarian cancer biomarker HE4 in 1X urine. The deep DNA sequencing and bioinformatics analysis identified 2189 families, the most abundant of which contained 29 sequences. From all the sequences, the top 10 most-enriched aptamers called AHE1 to AHE10 were screened with SPR, while the top 3 most-enriched aptamers AHE1, AHE2 and AHE3 were characterized with TFA in diluted urine. The aptamer AHE2 did not exhibit binding to target protein, which was consistent in both methods. The two promising candidates AHE1 and AHE3 displayed binding to HE4 protein in both methods.

As elevated concentrations of HE4 are present in patients, it is important to validate binding of anti-HE4 aptamer probes in urine. Aptamers AHE1, AHE3, A1 and A3 were tested and compared in presence of diluted urine (1/125X) and in absence of urine. Artificial human urine or protein buffer were spiked with HE4 protein ranging to 0-800 nM, and the aptamers AHE1, AHE3 and A3 showed high affinity to target HE4 in urine, with K_d in the nanomolar range.

Table 16. Comparison of the anti-HE4 aptamers as diagnostic probes targeting ovarian cancer biomarker HE4 in urine.

Aptamers			URINE		BUFFER	
ID	**Size (nt)**	**Origin**	**Binding (TFA)**	**K_d (nM)**	**K_d (nM)**	**Binding (TFA)**
AHE1	70	Hi-Fi SELEX	**Yes**	87 ± 9	192 ± 31	Yes
AHE3	70	Hi-Fi SELEX	**Yes**	127 ± 28	n/a	Yes
A1	25	Eaton *et al*. 2015	No	n/a	274 ± 29	Yes
A3	25	Eaton *et al*. 2015	**Yes**	338 ± 35	291 ± 27	Yes

For the aptamer AHE1, the binding was observed is observed in both environments, with a K_d of 87 ± 9 nM in urine and K_d of 192 ± 31 nM in buffer. Therefore, aptamer AHE1 exhibited high-affinity to ovarian cancer biomarker HE4, but with higher affinity in urine environment. The aptamer AHE3 exhibited high-affinity to ovarian cancer biomarker HE4 in urine, with a K_d of 127 ± 28 nM. However, it did not exhibit binding to HE4 in buffer. When comparing those two probes, both aptamers have a similar range of affinity in urine (AHE1 = AHE3 in urine), while AHE1 was better in buffer (AHE1>AHE3 in buffer). Therefore, aptamers developed in urine exhibited functionality and higher performance in urine. On the contrary, aptamers A1 and A3 exhibited better functionality and performance in buffer compared to urine. The aptamer A1 binds to HE4 in buffer with a K_d of 274 ± 29 nM. However, it does not bind to HE4 in urine. Aptamer A3 exhibited binding in both environments, with a determined K_d value of 338 ± 35 nM in urine and K_d of 291 ± 27 nM in buffer. Therefore, it shows a higher affinity in buffer compared than in urine. The aptamers A1 and A3 were developed in buffer (25 mM Tris, 192 mM glycine, 5 mM KH_2PO_4, pH 8,3) and were characterized in the same buffer by capillary electrophoresis (CE) and additionally fluorescence anisotropy (FA). The obtained K_d values were 2200 nM with FA and 390 nM with CE for aptamer A1; 9100 nM with FA and 500 nM with CE for aptamer A3. Therefore, aptamer A1 was a better probe than aptamer A3 in literature (A1>A3 in buffer). In this study, the aptamers A1 and A3 exhibited similar behavior with a same scale of affinity in buffer (A1=A3 in buffer), but aptamer A3 was superior in urine, as A1 did not bind (A3>A1 in urine). Therefore, aptamer A3 available from literature could serve in future as positive binding control or another probe for development of urine test for ovarian cancer. It is important to note that different aptamer-protein binding characterization methods possess different features and limitations, so aptamer K_d values obtained with different methods may not be directly compared.

In all cases, all four aptamers behaved differently when placed into different binding environments tested by thermofluorimetry. Depending if they are in urine or buffer, they could have different secondary structures that influence either TFA assay (pattern of binding of SYBR Gold within aptamer structure) or the binding to ovarian cancer biomarker human HE4. Indeed, urine is complex matrix with various compounds present. It contains several salts, urea, uric acid, citrate, oxalate, creatinine, *etc.* One of the factors that could be influencing the binding and cause the differences in binding properties of same aptamer in two different solutions could be concentration of magnesium ions (Mg^{2+}). Magnesium ions play an important role in the structure and function of aptamers [195,196]. One of the main functions of magnesium

ions in aptamers is to stabilize the folded structure of the molecule. In 1X artificial urine used in this work, the concentration of $MgCl_2$ is 4,4 mM, so 1/125X urine contains 0,0352 mM, while protein buffer contains 1 mM $MgCl_2$. Depending on the variations of Mg^{2+}, anti-HE4 aptamers could have different structural features. Indeed, aptamers can adopt a variety of complex secondary and tertiary structures, including hairpins, loops, bulges, and stem-loops. Magnesium ions can stabilize these structures by neutralizing negative charges on the phosphate backbone and promoting the formation of electrostatic interactions between nucleotides. In addition to stabilizing aptamer structure, magnesium ions can also play a direct role in aptamer-target binding [195]. Some aptamers require magnesium ions to form specific interactions with their target molecules, such as coordinating metal ions or interacting with specific amino acid residues in a protein target. Overall, the presence of magnesium ions is critical for the proper folding and function of aptamers, so understanding the role of magnesium in anti-HE4 aptamers could be interesting to study in future.

Another factor influencing the difference in aptamer binding could be the pH, which could impact DNA aptamer structure or ovarian cancer HE4 protein structure. Indeed, the artificial urine used for TFA has a pH of 6,3, while protein buffer has pH of 7,4. The different pH can change the structure of aptamers and consequently influence the binding to HE4 (pI = 4,5). Therefore, at lower pH (in urine), amino acids could be protonated and have a positive charge, while at higher pH (buffer), they could be deprotonated and have a negative charge. As DNA is negatively charged, this could potentially be one of the factors for higher-affinity of aptamers AHE1 and AHE3 in urine, compared to buffer.

All things considered, it appears that urine environment stabilize the structure of aptamers AHE1 and AHE3, resulting in a clear peak coming from aptamer-HE4 complex in TFA. The results further proved the concept of utilization of aptamers as diagnostic probes in urine for the development of future OC urine tests. The mean urine levels of urine HE4 present in patients with ovarian cancer described in literature are 28.56 nM [95] and 29.83 nM [99]. The *cut-off* value which is able to distinguish healthy individuals from cancer patients is approximately 13 nM [98], so binding of aptamers in urine should ideally be observed at concentrations >13 nM urinary HE4, which correspond to cancer patients. Indeed, the K_d value of aptamers AHE1 of 87 ± 9 nM, K_d of aptamer AHE3 of 127 ± 3 nM and K_d of aptamer A3 of 338 ± 35 nM in urine show binding in nanomolar range.

- **Aptamers validation and future perspectives**

The top 10 aptamer families called AHE1 to AHE10 enriched to ovarian cancer biomarker HE4 has been presented and analyzed. Those sequences have been subjected to screening for binding to HE4 protein by SPR. The SPR data revealed potential interaction of aptamers AHE1, AHE3, AHE6 and AHE8 to target HE4 protein. Indeed, aptamers AHE1 and AHE3 were previously identified as candidates, so SPR only confirmed those sequences as good choice for further characterization. Those sequences were characterized in detail by TFA as previously described and showed binding to HE4 in urine. Therefore, AHE1 and AHE3 are potential diagnostic probes for application in future urine test or biosensor for OC. However, SPR data indicated low potential interaction of aptamers AHE6 and AHE8 with HE4 protein. These sequences have not yet been analyzed. Therefore, one of the future objective is to analyze aptamers AHE6 and AHE8 for binding to ovarian cancer HE4 in urine.

Following identification of putative sequences using Hi-Fi SELEX and bioinformatics, described aptamers could be modified to potentially enhance the specificity and affinity to HE4. Another future objective could be the creation of an expanded panel of aptamers from top 10 anti-HE4 sequences AHE1 to AHE10 for further characterization and diagnostic application. Several strategies can be employed:

(1) Modification of the aptamer sequence: Aptamer sequences can be modified through various methods, such as nucleotide substitution or modification to improve their binding affinity, specificity, or stability. This can be achieved through steps such as random mutagenesis, directed evolution, or bioinformatics-guided design.

(2) Length optimization: The length of an aptamer can also affect its binding affinity and specificity. Shorter aptamers tend to be more flexible while longer aptamers can adopt a more stable structures. Aptamers can be shortened by truncation or lengthened by elongation to optimize properties of binding to HE4.

(3) Structural optimization: Aptamer structure is also critical for its binding properties. Structural optimization can involve modifying the secondary or tertiary structure of an aptamer through the introduction of bulges, loops, or stem regions.

(4) Conjugation or chemical modification: Chemical modifications can be introduced to anti-HE4 aptamers to improve their specificity or stability in urine. Modifications can include the introduction of chemical groups, such as biotin or fluorescein, or the use of modified nucleotides, such as locked nucleic acids (LNAs) or 2'-O-methyl nucleotides.

(5) Multimerization of aptamers: Aptamers can be multimerized to form larger structures, such as dimers or tetramers, to increase their binding affinity and specificity. Multimerization can also improve the stability of the aptamer complex and reduce the likelihood of dissociation.

According to the International Society of Aptamers (INSOAP) guidelines for *de novo* aptamer development [197], it is recommended to validate the binding of aptamers in conditions that correspond to the final application. It is important to characterize aptamers under conditions of pH, temperature, and ion composition, that are similar to the ones used during their selection and that resemble the physiological milieu that will be found in future biomedical applications, such as blood, serum, urine, or saliva [197]. Therefore, as the final desired diagnostic application of aptamers are detection of HE4 in urine, aptamers in this study have been characterized in urine, in pH and ionic composition that match the human urine. The aptamers AHE1 and AHE3 were characterized in detail and exhibit binding to ovarian cancer biomarker HE4 in urine, with a high-affinity in the nanomolar range, with a K_d value of aptamers AHE1 of 87 ± 9 nM, K_d of aptamer AHE3 of 127 ± 3 nM and K_d of aptamer A3 of 338 ± 35 nM in urine. Although presented data suggested the potential of described aptamers, more studies are needed to validate the specificity of described aptamers. Further characterizations and optimizations of the sequences will be performed in future. One important experiment is to evaluate the specificity of aptamers by testing their binding to different cancer biomarkers, such as CA125 or CEA; or to proteins potentially present in human urine, such as albumin or uromodulin, which can be found in low quantity in physiological or pathophysiological urine [198–200].

Future experiments can include testing aptamers with ELONA in spiked urine samples in a wide range of HE4 corresponding to the human samples on the picomolar scale. This can include urine HE4 concentration that corresponds to the healthy individuals (0 - 13 000 pmol/L), early ovarian cancer (stage I/II) (>16 000 pmol/L) and advanced ovarian cancer (stage III/IV) (>24 000 pmol/L). Furthermore, the aptamers should be tested in clinical samples, in urine of ovarian cancer patients. The performance of the aptamer should be assessed in clinical

samples with a sufficient number of cases and controls to support statistical significance. The collaboration with hospital has been established and urine samples are currently in the collection phase.

The overview of the potential further development of the aptamers for detection of HE4 protein in urine and future implications is presented below (**Figure 55).**

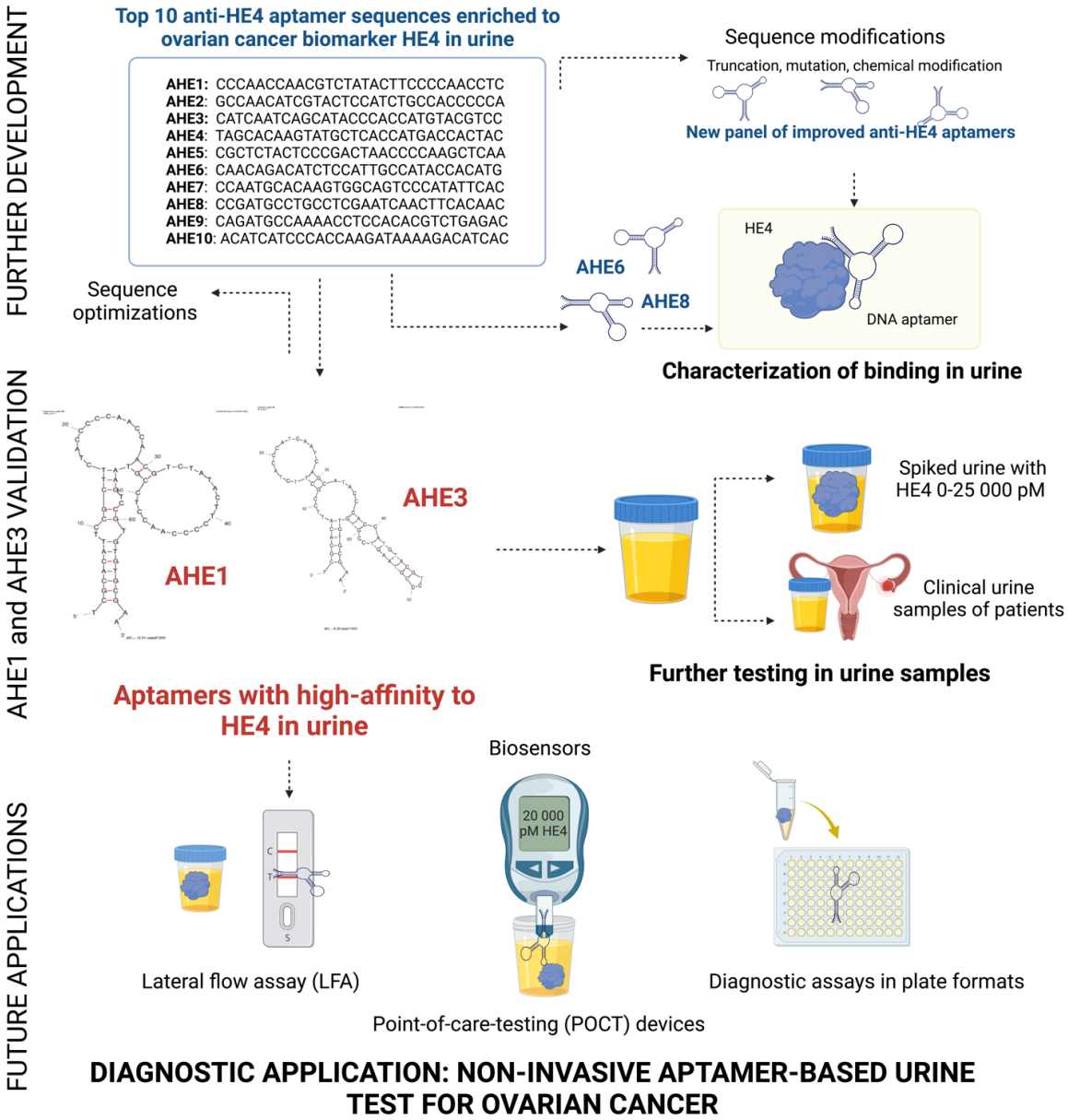

Figure 55. Potential future perspectives and further characterization of aptamers for detection of the ovarian cancer biomarker HE4 in urine.

The described DNA aptamers with high binding affinity to urine HE4, reflected by nanomolar K_d values, can be potentially used as molecular probes in aptamer-based urine bioassays or biosensors. There are many aptamer-based diagnostics that are currently being developed and evaluated for their potential future clinical applications [112]. An aptamer biosensor is a type of biosensor that uses aptamers as the recognition element to detect and measure the presence of a cancer-related molecule in a sample [201]. The aptamer biosensor typically consists of a transducer and a bioreceptor. The transducer converts the binding event between the aptamer and the target molecule into a measurable signal. According to the signal conversion elements of different types of aptasensors, biological information is usually converted to fluorescent signals, electrochemical signals or color changes, which can be divided into fluorescence, electrochemistry, and colorimetric aptasensors [201]. The bioreceptor, which hypothetically could be the aptamer AHE1 or AHE3 or both, could be immobilized on the surface of the transducer, allowing for selective and sensitive detection of target HE4 in urine sample.

Another option for application of aptamers AHE1 or AHE3 could be in a format of lateral flow assays (LFAs). Indeed, with the ease of operation, low cost, test rapidity, disposable format, small sample volume and fast turnaround time, they are used as point-of-care (POC) diagnostic tests [202]. The most famous LFA example for detection of analyte from urine is a pregnancy test. LFAs are gaining popularity in recent years and the technology is one of the fastest growing industry in the *In Vitro* Diagnostics (IVD) sector [202, 203]. Recently, lateral LFA for the identification of theranostic exosomes isolated from human lung carcinoma cells was developed [204]. However, in the context of cancer detection , there is a potential in the development of novel aptamer-based LFAs as they are currently not existing.

Indeed, there are numerous possibilities to develop an aptamer-based assay for detection of HE4 in urine. In all cases, the diagnostic sensitivity and specificity of the aptamer-based assay should be determined using a Receiver Operating Characteristic (ROC) curve to benchmark the performance of the aptamer with the existing gold standard test. For detection of HE4 in body fluids, this is currently ELISA [49]. Therefore, the performance of the aptamer AHE1 or AHE3 should be compared with an antibody-based detection of urine HE4 by ELISA in future. Antibodies are typically used as recognition elements in diagnostic assays. However, with a low cost, high reproducibility and uniformity, aptamers are increasingly being investigated to replace or complement antibodies. For example, the average price of a commercial detection anti-HE4 antibody used in our laboratory is 505 euros, with a quantity sufficient for 20 ELISA

tests. On contrary, chemical synthesis of 70-mer 5'biotin AHE1 detection aptamer costs 70 euros for a quantity that is sufficient for 6000 ELONA tests. Therefore, just by replacing detection antibody with a detection aptamer in a same diagnostic format, 2525 x more tests can be achieved. Therefore, 2525 x more women could have access to HE4 urine test for the same price. This could allow more women to get tested, leading to more ovarian cancers getting detected early. Therefore, using aptamers for detection of ovarian cancer could be beneficial.

All things considered, novel aptamer probes AHE1 and AHE3 could be promising molecular probes for the detection of ovarian cancer biomarker HE4 in urine. Indeed, they showed high-affinity binding to ovarian cancer biomarker HE4 protein in urine. Additionally, aptamer A3 was found to bind to urine HE4. Therefore, those anti-HE4 sequences could be used in future to develop an aptamer-based non-invasive urine test or biosensor for ovarian cancer.

VII. CONCLUSIONS

Ovarian cancer is the deadliest gynecological cancer. With the lack of effective diagnostic methods, late diagnosis remains the crucial hurdle of the poor prognosis. Therefore, development of novel diagnostic approaches are needed. Recently, urine has become an interesting non-invasive source of cancer biomarkers. In this thesis work, the aim was to evaluate the potential of aptamers as diagnostic tools for detection of ovarian cancer protein biomarkers in urine. Aptamers are short, single-stranded oligonucleotides that can selectively bind to specific target molecules with high-affinity. Human epididymis protein 4 (HE4) is a protein elevated in urine of patients with ovarian cancer, but not in healthy or benign conditions. With high stability and diagnostic value for detection of ovarian cancer, urine HE4 was chosen as a target of this study.

The high-affinity anti-HE4 DNA aptamers were selected through 10 cycles of the *High-Fidelity Systematic Evolution of Ligands by EXponential enrichment* (Hi-Fi SELEX) in urine, a method for aptamer selection based on digital droplet PCR (ddPCR). The sequencing and bioinformatics analysis revealed a panel of novel anti-HE4 aptamers enriched to target HE4 protein. Candidate aptamers were screened by surface plasmon resonance (SPR) and characterized for binding to HE4 protein by thermofluorimetic analysis (TFA). As HE4 levels are elevated in the urine of patients, the anti-HE4 aptamers were characterized in urine and exhibited binding and a high-affinity to target human HE4 in urine, with dissociation constants in the nanomolar range.

The results of the binding characterization by TFA revealed high-affinity binding of two novel anti-HE4 DNA aptamers, called AHE1 and AHE3, to ovarian cancer biomarker HE4 in urine. The aptamers were binding to HE4 in urine in the nanomolar range, with K_d (AHE1) = 87 ± 9 nM and K_d (AHE3) aptamer of 127 ± 28 nM. Additionally, DNA aptamer A3 found in literature exhibited binding to HE4 in urine, with a K_d (A3) aptamer of 338 ± 35 nM. Overall, these results suggest that described aptamers could be promising tools for application in urine tests or biosensors for ovarian cancer in future. More research and further characterizations of anti-HE4 aptamers are needed to validate those findings.

- Urine is a feasible, easy, cheap and non-invasive source of ovarian cancer biomarkers.

- Human epididymis protein 4 is a valuable urine biomarker, with the high specificity and sensitivity for detection of ovarian cancer and high stability in urine.
- Aptamers, a small synthetic oligonucleotides, are versatile and cheap diagnostic tools for detection of ovarian cancer biomarkers.
- Hi-Fi SELEX method based on the digital droplet PCR amplification of aptamers has been optimized and applied.
- Anti-HE4 DNA aptamers were selected by Hi-Fi SELEX method in urine.
- The bioinformatic analysis revealed a panel of anti-HE4 sequences enriched to HE4 protein in urine (2189 families, the most abundant of which contains 29 sequences).
- The top 10 most-enriched aptamers called AHE1 to AHE10 were screened by SPR, while top 10 most-enriched aptamers called AHE1, AHE2 and AHE3 were characterized by TFA.
- The binding of four aptamer sequences AHE1, AHE3, A1 and A3 to ovarian cancer biomarker HE4 was characterized in urine and buffer.
- The aptamers AHE2 and A1 did not display binding to HE4 in urine
- Novel anti-HE4 aptamers AHE1 and AHE3 developed in this thesis and anti-HE4 aptamer A3 from literature exhibit binding to ovarian cancer biomarker HE4 in urine.
- The anti-HE4 aptamers AHE1 (70mer), AHE3 (70mer) and A3 (25 mer) displayed high-affinity to target HE4 protein in urine, with constants of dissociation K_d (AHE1) of 87 ± 9 nM, K_d (AHE3) of 127 ± 28 nM and K_d (A3) of 338 ± 35 nM, respectively.
- Preliminary data of ELONA assay exhibited binding of 5'biotin AHE1 (70mer) to HE4 protein in dose-dependent manner
- From all described aptamers, the current data displays trend towards AHE1 as the most potent aptamer probe for detection of HE4 in urine.
- More research is needed to validate those results and the specificity of described aptamers.
- Therefore, aptamers AHE1, AHE3 and A3 could serve as potential diagnostic probes in development of a future urine test or biosensor for ovarian cancer.

LIST OF RELATED PUBLICATIONS AND COMMUNICATIONS

- **Publications related to this thesis**

1. **Hanžek A**, Siatka C, Duc AC (2021) High-specificity nucleic acid aptamers for detection of ovarian cancer protein biomarkers: Application in diagnostics. *Journal Aptamers*, 5, 7-14

2. **Hanžek A**, Duc AC, Siatka C (2023) Extracellular urinary microRNAs as non-invasive biomarkers of ovarian and endometrial cancers. *J Cancer Res Clin Oncol* https://doi.org/10.1007/s00432-023-04675-5

3. **Hanžek A**, Siatka C, Duc AC (2023) Diagnostic role of urine Human Epididymis 4 (HE4) in the clinical management of ovarian cancer*, in preparation*

4. **Hanžek A**, Duconge D, Siatka C, Duc AC (2023) Identification and characterization of aptamers targeting ovarian cancer biomarker Human Epididymis Protein 4 (HE4) for the application in urine. *Cancers*; 15(2): 452, https://doi.org/10.3390/cancers15020452

- **Communications related to this thesis**

Poster presentations at scientific conferences

1. **Hanžek A**, Duconge F, Siatka C, Duc AC (2022) P2-053: Detection of the ovarian cancer biomarker in body fluids using nucleic acid aptamers as diagnostic probes. *The European Association for Cancer Research (EACR) Congress 2022: Innovative Cancer Science: Translating Biology to Medicine*, Sevilla, Spain

2. **Hanžek A**, Siatka C, Duc AC (2021) Aptamers as diagnostic tools for the detection of Human Epididymis protein 4 (HE4), clinical biomarker of ovarian cancer. *17th Annual Meeting of Cancéropôle Grand Sud-Ouest 2021*, Carcassonne, France

https://doi.org/10.13140/RG.2.2.32703.23204

3. **Hanžek A**, Siatka C, Duc AC (2019) Developement of the aptasensor for detection of ovarian cancer biomarkers. *Doctoral Day de l'Universite de Nîmes*, Nîmes, France

Other oral presentations

1. Duc AC, **Hanžek A** (2022) Webinar: "Cancer Biomarker Detection in Urine: Early Detection of Ovarian Cancer using Aptamers"; as recipient of the runner-up grant by Novosanis and The European Association for Cancer Research (EACR) https://novosanis.com/podcasts/webinar-cancer-biomarker-detection-urine-early-detection-ovarian-cancer-using-aptamers
2. **Hanžek A** (2021) Online presentation - doctoral seminar: "Novel approach for the detection of ovarian cancer", on the University's Web TV Twitch https://www.twitch.tv/unimes_webtv
3. **Hanžek A** (2019) Oral seminar presentation: "Detection of the ovarian cancer biomarkes by aptasensor", UPR CHROME seminar, 6th of December 2019, Université de Nîmes, Nîmes, France

SUPPORTING INFORMATION

Annex 1 - PCR validation of primers for Hi-Fi SELEX

Prior ddPCR, it is necessary to validate the primers for designed library in regular qPCR. For this purpose, 70 bases single-stranded model aptamer MA (TCG CAC ATT CCG CTT CTA CCC ATG ATT ACG CCA AGC TTG GTA CCG AGC TCC GTA AGT CCG TGT GTG CGA A) was used a template and diluted ranging from $2x10^{-3}$ ng to $2x10^{-8}$ ng DNA template prior qPCR. The regular qPCR was performed using Hi-Fi SELEX conditions (400 Fw and 400 nM pRev primers, DreamTaq) following PCR program: 95 °C for 5 min, 95° C for 30 sec, and 57, 60 and 63 °C °C for 1 min for 30 cycles. The primers were validated and able to amplify the 70-mer aptamer template at annealing temperature with good efficiency (**Figure 56**). The temperature 60 °C and 63 °C can be used for Hi-Fi SELEX. Based on the results and the PCR efficiency of 99, 67 %, optimal annealing temperature was chosen to be **60°C** for further experiments.

A

Annealing temperature	initial DNA concentration / ng	ΔCp	Slope	PCR efficiency	% PCR efficiency
63 °C	2x10-3		-3,434	1,955	**95,52**
	2x10-4	3,86			
	2x10-5	3,18			
	2x10-6	3,16			
	2x10-7	3,47			
	2x10-8	3,21			
	NTC	n/a			
60 °C	2x10-3		-3,33	1,997	**99,67**
	2x10-4	3,49			
	2x10-5	3,39			
	2x10-6	3,66			
	2x10-7	2,89			
	2x10-8	3,20			
	NTC	n/a			
57 °C	2x10-3		-3,208	2,05	**105**
	2x10-4	3,71			
	2x10-5	2,97			
	2x10-6	3,31			
	2x10-7	3,52			
	2x10-8	2,39			
	NTC	n/a			

B

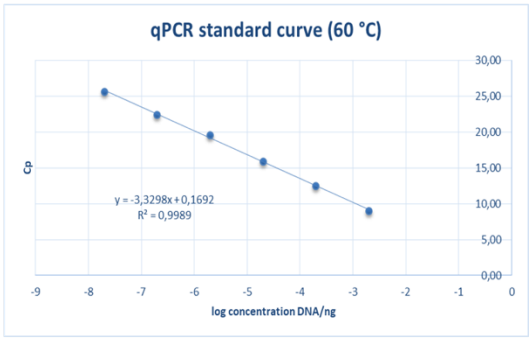

Figure 56. Validation of the Hi-Fi SELEX primers and annealing temperature.

Different primer concentrations were also tested in same conditions with annealing temperature 60 °C for MA and initial Hi-Fi library. Both 100 nM and 400 nM are sufficient to amplify 70-mer aptamer ssDNA (**Figure 57**). Based on the recommendations from the experts in the aptamer field, 100 nM (low concentration of primers) is needed in ddPCR, while 400 nM (high concentration of primers) is needed in reamplification of the aptamers post ddPCR (big scale), to increase the yield of the amplified product in SELEX.

Figure 57. Choice of the primer concentration.

Annex 2 - ddPCR optimization for Hi-FI SELEX

- **Thermal gradient**

Thermal gradient was applied to determine the optimal annealing temperature for ddPCR. Setting the annealing temperature too low may lead to amplification of non-specific PCR products. On the other hand, setting the annealing temperature too high may reduce the yield of a desired target PCR product. Although annealing temperature can be determined in regular qPCR and translated to ddPCR, it is recommended to validate it in ddPCR for optimal classification of droplets into positive and negative populations. The optimal annealing temperature in ddPCR is the temperature that enable highest fluorescence amplitude difference between positive and negative droplets. The initial 70mer ssDNA library was subjected to ddPCR using conditions: $2x10^{-8}$ ng of template DNA (ssDNA library), 100 nM Fw, 100 nM pRev, 1X EvaGreen in a total of 20 µL of reaction. The ddPCR was performed for 40 cycles following optimized EvaGreen program: 5 min at 95 °C (enzyme activation), 30 sec at 95 °C (denaturation), 1 min at **63 – 57 °C thermal gradient** (annealing/extension), 5 min at 4 °C (signal stabilization) and 5 min at 90 °C (signal stabilization) on a C1000 Touch Thermal Cycler (Bio-Rad, USA). The amplified droplets were analyzed on QX200™ ddPCR System (Bio-Rad, USA) using QuantaSoft™ Software (Bio-Rad, USA). As seen on results, the higher temperatures enable better classification into positive and negative droplets. The temperatures 63 – 60 °C seem optimal for best ddPCR results. The temperature < 60°C cause dispersion of droplets and ddPCR "rain", making classification into populations more difficult. (**Figure 58**).

Although 63°C seems like the best temperature for classification into positive and negative droplets, 60°C is suitable as well. Based on the results from qPCR and primers efficiency, ddPCR thermal gradient, recommendation for EvaGreen system from Bio-rad, the annealing of **60 °C** is selected temperature for Hi-Fi SELEX for ovarian cancer biomarkers.

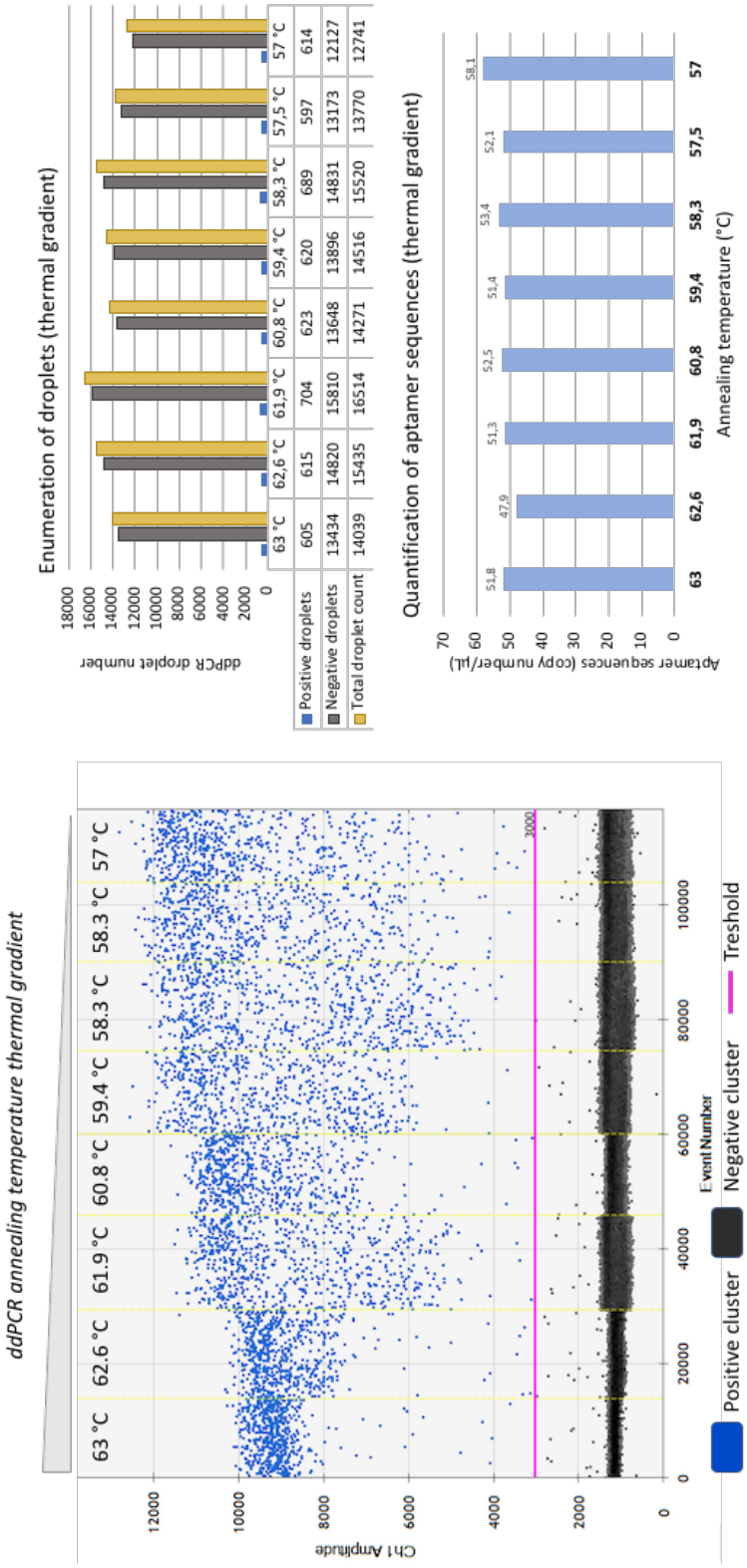

Figure 58. Determination of the ddPCR annealing temperature using thermal gradient on Hi-Fi SELEX library.

- **Template dilution**

To study the effect of template dilution on ddPCR results, the initial 70mer ssDNA library was subjected to ddPCR using conditions: $2x10^{-2}$ – $2x10^{-11}$ ng of template DNA (ssDNA library), 100 nM Fw, 100 nM pRev primer, 1X EvaGreen in a total of 20 µL of reaction. The ddPCR was performed for 40 cycles following optimized EvaGreen program: 5 min at 95 °C (enzyme activation), 30 sec at 95 °C (denaturation), 1 min at 60 °C (annealing/extension), 5 min at 4 °C (signal stabilization) and 5 min at 90 °C (signal stabilization) on a C1000 Touch Thermal Cycler (Bio-Rad, USA). The amplified droplets were analyzed on QX200™ ddPCR System (Bio-Rad, USA) using QuantaSoft™ Software (Bio-Rad, USA). As seen on results (**Figure 59**), the concentration of template is crucial parameter in ddPCR for obtaining quality amplification and results. If the concentration is too high, it will saturate the droplets. The ssDNA in quantity > 2 x 10^{-5} ng is too high for optimal ddPCR amplification. All droplets are positive, with more than 1 000 000 aptamer sequences quantified and saturation. As we can see on diagram, the amplicon appears around fluorescence of 5000-6000 units, which corresponds to ssDNA template. Therefore, there is too much template present and amplification is not optimal. Therefore, ssDNA aptamers will not amplify to dsDNA amplicons and SELEX could be compromised. All the aptamer library from > 2 $x10^{-5}$ ng achieved classification of positive and negative droplets, with expected fluorescence amplitude of 70 bp amplicon around 10 000 - 12 000 units (**Figure 59**). Moreover, the library in middle range quantity of $2x10^{-7}$ ng can achieve classification into both populations. Therefore, it can be used as positive control in Hi-Fi SELEX experiements for ovarian cancer biomarkers.

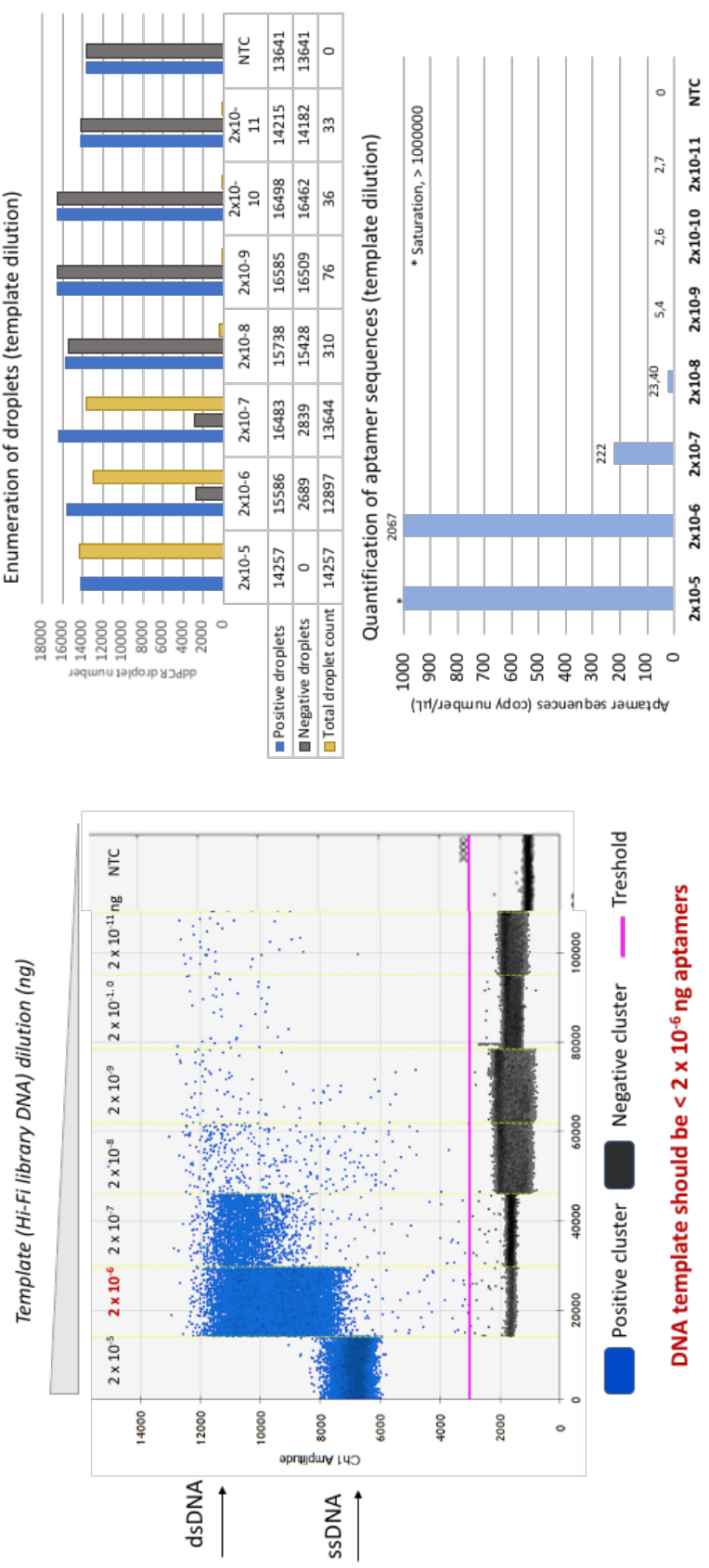

Figure 59. Effect on the Hi-Fi SELEX template dilution in ddPCR.

- **Comparison of qPCR and ddPCR template range for 70mer ssDNA aptamer amplification**

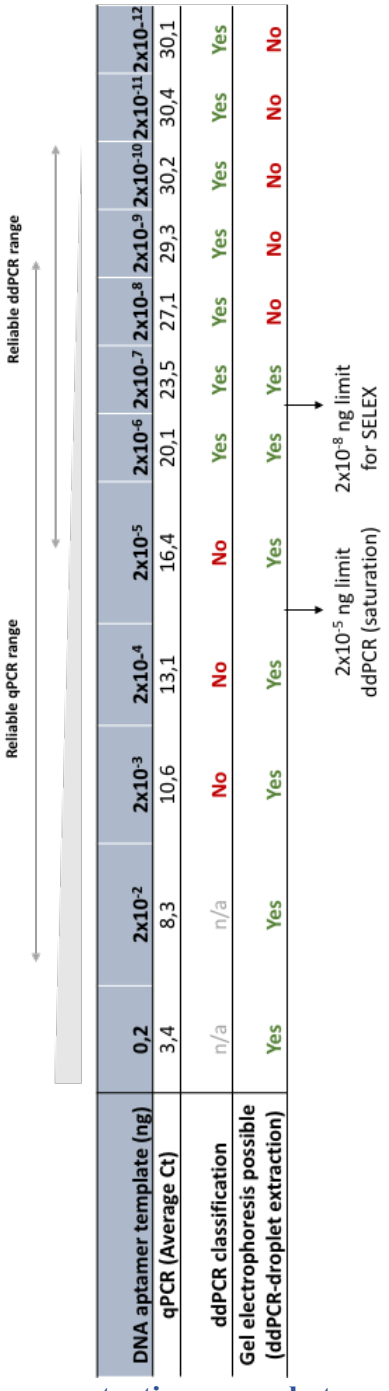

DNA aptamer template (ng)	0,2	2x10⁻²	2x10⁻³	2x10⁻⁴	2x10⁻⁵	2x10⁻⁶	2x10⁻⁷	2x10⁻⁸	2x10⁻⁹	2x10⁻¹⁰	2x10⁻¹¹	2x10⁻¹²
qPCR (Average Ct)	3,4	8,3	10,6	13,1	16,4	20,1	23,5	27,1	29,3	30,2	30,4	30,1
ddPCR classification	n/a	n/a	No	No	No	Yes	Yes	Yes	Yes	Yes	Yes	Yes
Gel electrophoresis possible (ddPCR-droplet extraction)	Yes	Yes	Yes	Yes	Yes	Yes	Yes	No	No	No	No	No

Figure 60. Comparison of the concentration range between ddPCR and qPCR on model aptamer (MA).

Annex 3 - Droplet extraction optimization post ddPCR

Application of ddPCR in SELEX requires extraction of DNA from droplets post ddPCR. 70 bases ssDNA model aptamer MA (TCG CAC ATT CCG CTT CTA CCC ATG ATT ACG CCA AGC TTG GTA CCG AGC TCC GTA AGT CCG TGT GTG CGA A) was used as DNA template in duplicate at 3 different concentration of DNA prior ddPCR: **1** – high aptamer DNA concentration (10^{-4} ng DNA), **2** – medium aptamer DNA concentration (10^{-8} ng DNA), **3** – low aptamer DNA concentration (from 10^{-12} ng DNA). The DNA was amplified by ddPCR using Hi-Fi SELEX conditions (EvaGreen, 100 nM primers, 60 °C annealing). After ddPCR, the aptamer DNA was extracted, and methods were compared. The DNA quantity was measured using Nanodrop spectrophotometry.

(1) FT method: Immediately after amplification, the wells are pooled and centrifuged for 5 min at 5000 x g at RT to separate the reacted aqueous droplets from the oil (bottom) phase. The oil phase is discarded. Then, the DNA is recovered by subjecting the droplet phase to a freeze (-80 °C for 15 min) cycle. The frozen sample is centrifuged at 14 000 x g for 5 min at RT to create sufficient force to burst the droplets. The sample is thawed at RT. The process is repeated 3 times to generate a clear (top) droplet phase with DNA, which is recovered.
(2) CE method: The chloroform extraction was performed by adding 20 µL of Tris-HCl buffer (pH 7.4) and 70 µL of chloroform per well, followed by vortexing and centrifugation at 15,500 × g for 10 min at RT. The upper aqueous phase, containing the recovered DNA, was transferred to a fresh tube.

The obtained results (**Figure 61**) indicated that chloroform extraction was more suitable for aptamer recovery. It yielded higher quantity and quality of recovered DNA. Moreover, the extraction was homogenous (recovered uniform volumes of 35 µL of sample for all three conditions, whereas in freeze-thaw the recovery was 13, 11 and 6 µL for three different conditions). Therefore, chloroform extraction was applied in Hi-Fi SELEX for ovarian cancer biomarker HE4.

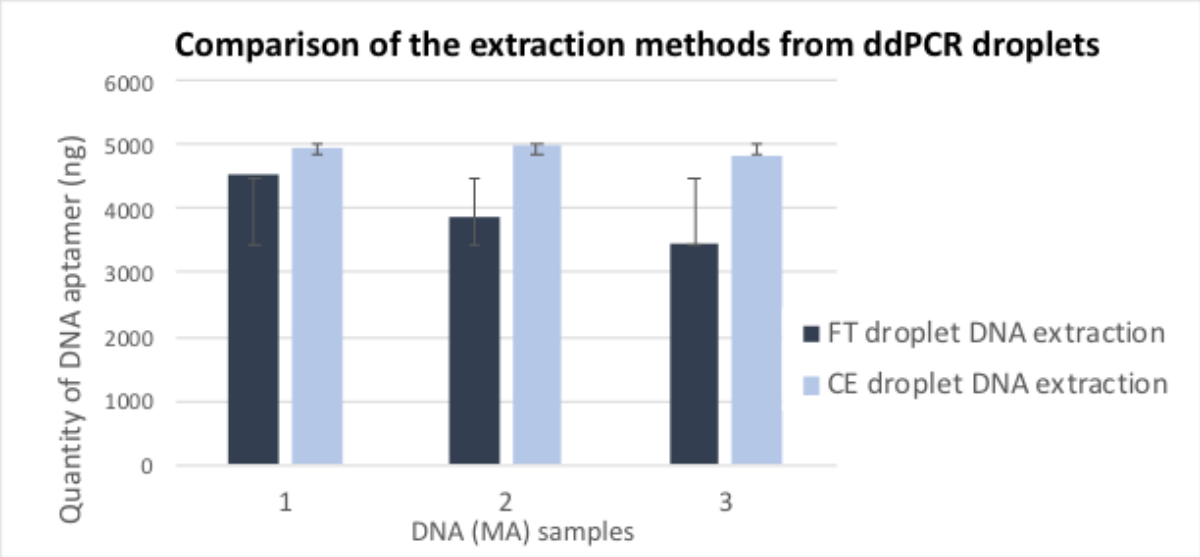

Figure 61. Comparison of the droplet DNA extraction methods post ddPCR.

The model aptamer was amplified by ddPCR and recovered by two different methods: Freeze Thaw (FT) and Chloroform Extraction (CE) at 3 different conditions: 1 – high aptamer DNA concentration (from 10-4 ng DNA prior ddPCR), 2 – medium aptamer DNA concentration (from 10-8 ng DNA prior ddPCR), 3 – low aptamer DNA concentration (from 10-12 ng DNA prior ddPCR). The CE method yielded higher quantity of DNA for all three conditions. Therefore, CE is a method of choice in Hi-Fi SELEX for extraction of aptamer DNA from droplets.

Annex 4 - λ exonuclease optimization

Prior Hi-Fi SELEX, the optimization of λ exonuclease ssDNA regeneration step was performed. For this purpose, 70 bases single-stranded model aptamer MA (TCG CAC ATT CCG CTT CTA CCC ATG ATT ACG CCA AGC TTG GTA CCG AGC TCC GTA AGT CCG TGT GTG CGA A) was used as DNA template. PCR step (SELEX conditions, DreamTaq polymerase, 400 nM primers) was carried out to obtained double-stranded aptamer amplicon. Then, purification from primers was performed with Sephadex G-50 columns with buffer exchange to λ exonuclease buffer (67 mM glycine-KOH, 2.5 mM $MgCl_2$, pH 9.4). The reaction mixtures were prepared wuth 20 µL of aptamer dsDNA (concentration unknown), 3 µL 10 X buffer (670 mM glycine-KOH (pH 9.4), 25 mM $MgCl_2$, 0.1% (v/v) Triton X-100), 1 or 5 µL of λ exonuclease enzyme (10 U/µL; ref. EN0561, Thermo Fisher Scientific, USA) to a final 10 or 50 U/µL and filled with water to a final volume of 30 µL. Then, digestion of DNA was performed on purified double-stranded aptamer amplicon, with incubation at 37 °C for 1 hour and 2 hours, followed by enzyme inactivation at 80 °C. In parallel, one DNA sample without

purification from PCR mix and primers was subjected to ssDNA regeneration with 50 U/ µL of λ exonuclease for 2 hours.

The results (**Figure 62**) indicate that 1 hour and 2 hours incubation with 10 U/µL of λ exonuclease are sufficient for complete conversion from double-stranded aptamer amplicon to single-stranded aptamer DNA. Moreover, 1 hour appears to be optimal, as 70 bases ssDNA band of highest intensity is observed, without double-stranded 70 bp aptamer DNA. Increasing the quantity of enzyme to 50 U/µL with incubation at either 1 hour or 2 hours results in incomplete conversion to ssDNA, as both bands of 70 bp and 70 bases are present. Moreover, the digestion on unpurified aptamer template (with presence of PCR mixture and primers) results in lower yield of conversion with double-stranded 70 bp amplicon is higher intensity compared to other conditions. Therefore, condition of **10 U/µL** of lambda exonuclease with incubation at **1 hour** is applied to Hi-Fi SELEX to ovarian cancer biomarker HE4.

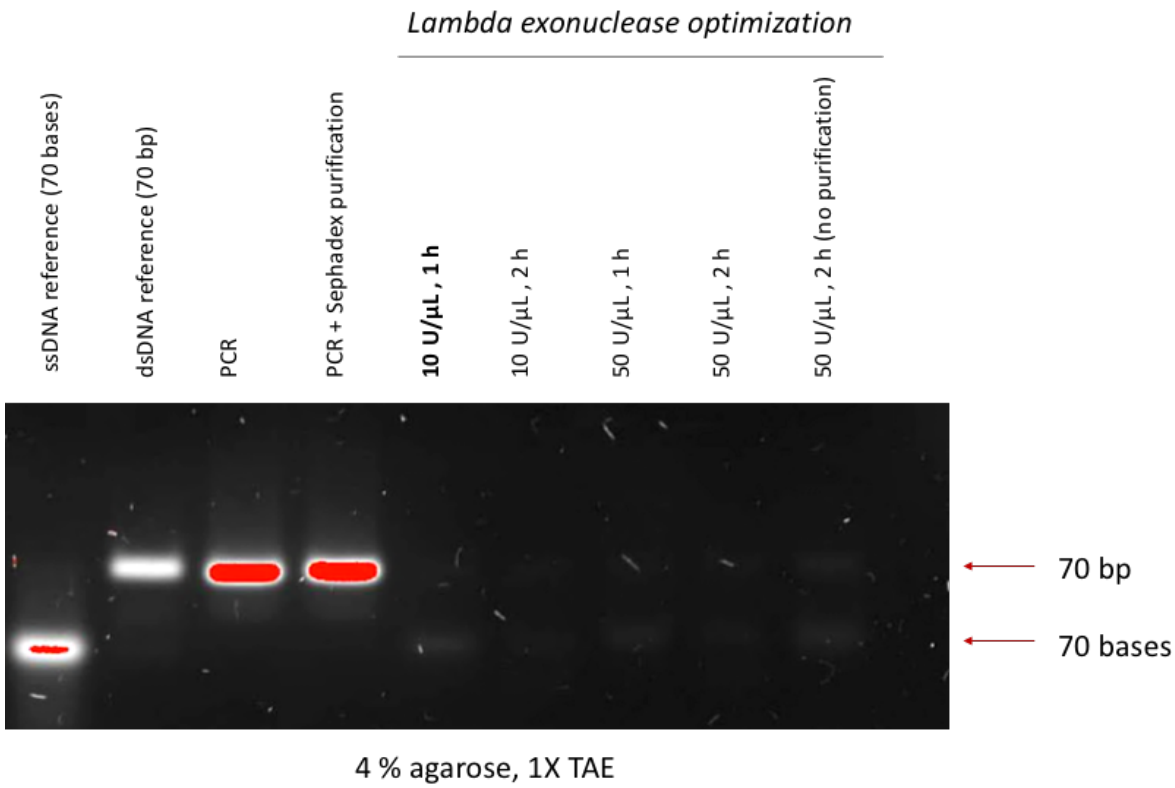

Figure 62. Optimization of the ssDNA regeneration using lambda exonuclease.

Annex 5 - TFA binding analysis of aptamers AHE1 and AHE3 with HE4 protein at crucial aptamer:HE4 ratios

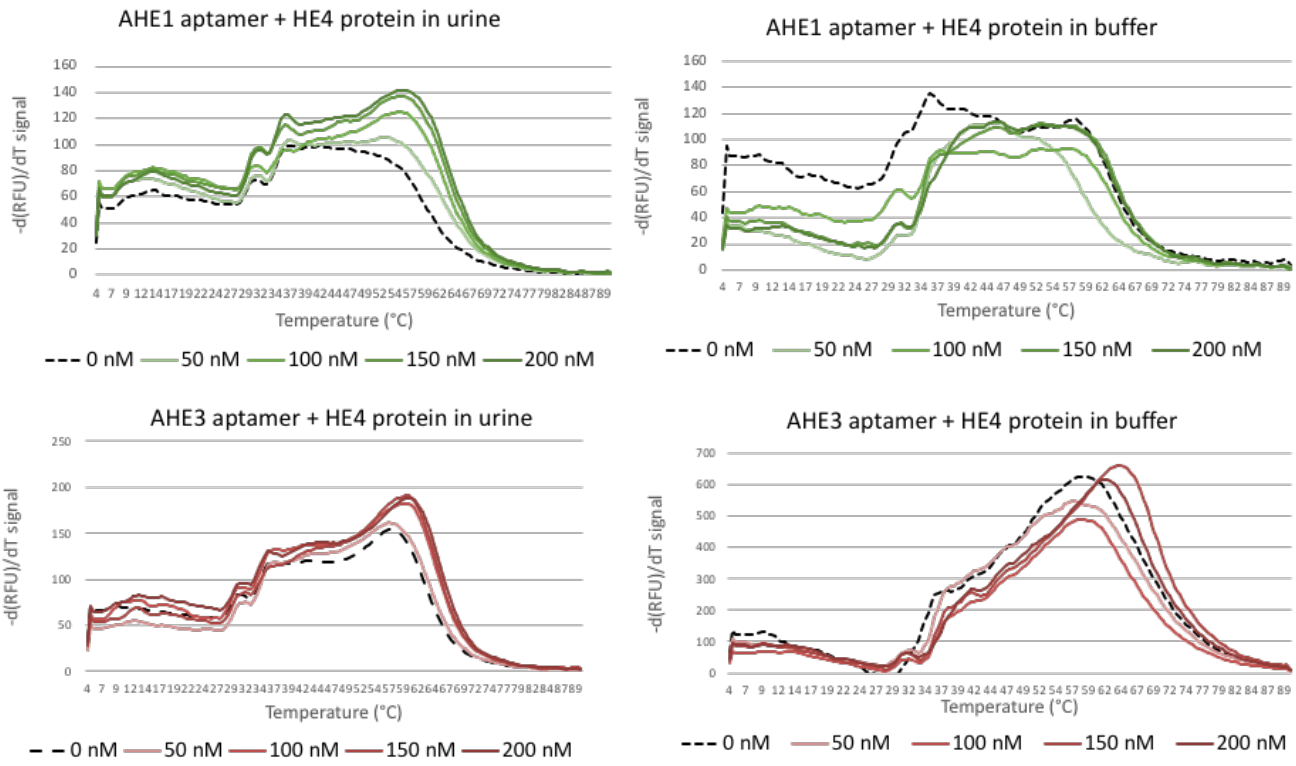

Figure 63. TFA melting profile (raw) for aptamers AHE1 and AHE3 at important concentrations of HE4 protein (ratio aptamer:protein 0,5 : 1, 1 : 1, 1 : 1,5, 1 : 2).

Annex 6 - Melting profile of aptamers A1 and A3 in urine

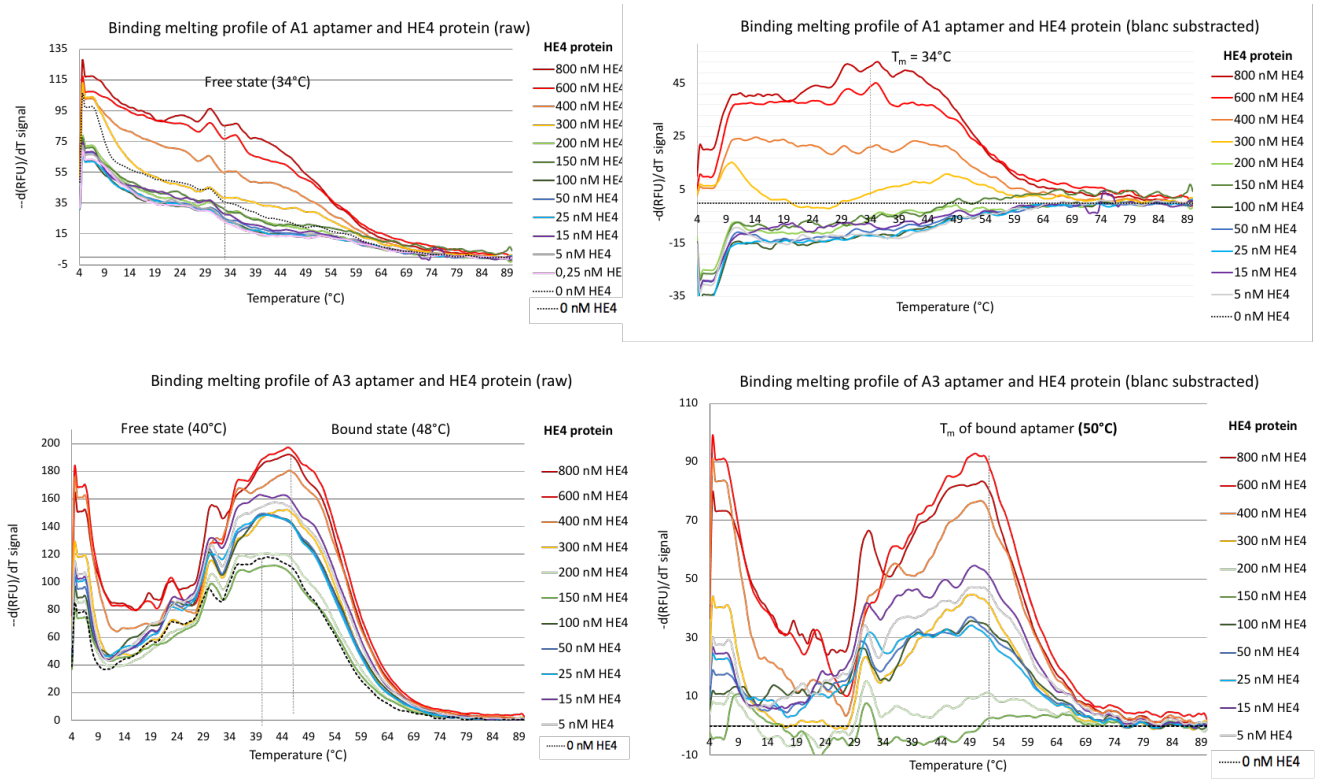

Figure 64. Thermofluorimetic analysis of the anti-HE4 aptamers A1 and A3 binding to ovarian cancer biomarker HE4 in urine.

The constant aptamer concentration of 200 nM was subjected to an increasing concentration of HE4 protein in urine ranging from 0 to 800 nM in presence (1/125X) of urine. The melting profile was analyzed from 4 °C to 90 °C. The binding thermal curves (melting DNA profile) were constructed by plotting temperature with negative derivative fluorescent signal −d(RFU)/dT. **The raw melting profile (on the left)** The raw melting profile obtained for aptamer A3 showed two distant peaks corresponding to free aptamer (no HE4) state and bound aptamer state (with HE4). Upon binding to HE4 protein, more thermally stable species were present, with a shift to higher T_m. For aptamer A1, no binding is observed, with a single peak corresponding to free aptamer state visible. (on right) T**he melting profile after subtraction of signal from aptamer only (on the right)** After subtraction of the blank (aptamer only, no HE4), peaks of the aptamers bound to HE4 were visible only for aptamer A3, with a shift to higher Tm values, corresponding to 50 °C for A3 aptamer, suggesting binding to target protein HE4.

Annex 7 - Effect of the 3’ or 5’-prime biotinylating on aptamer signal obtained by the HE4 ELONA

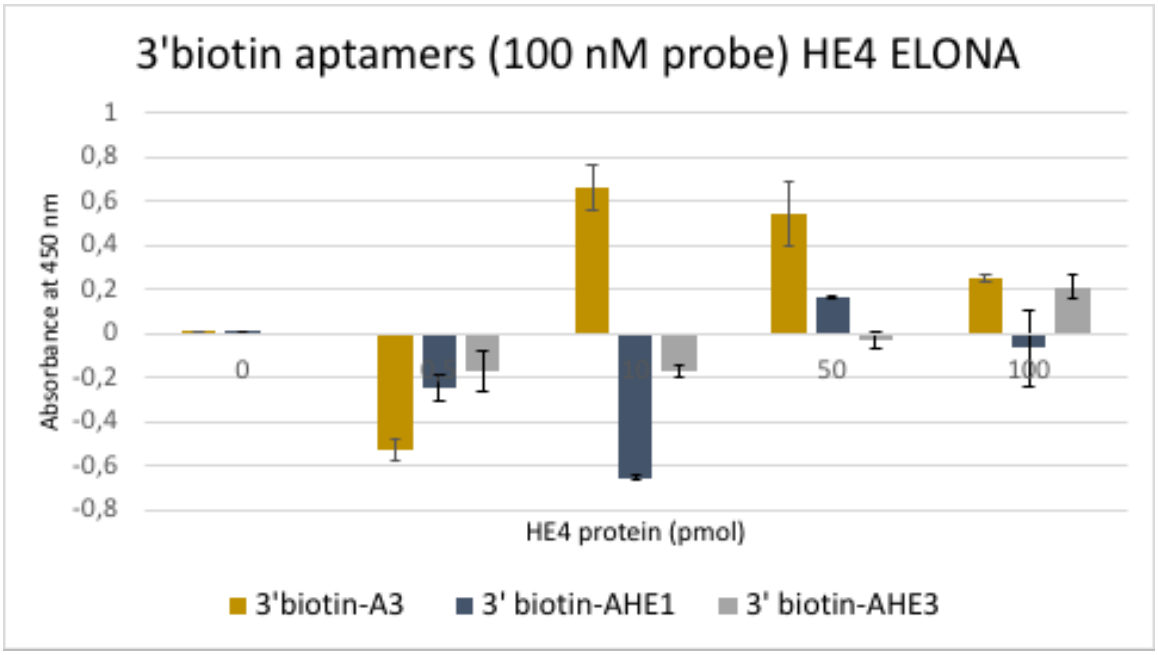

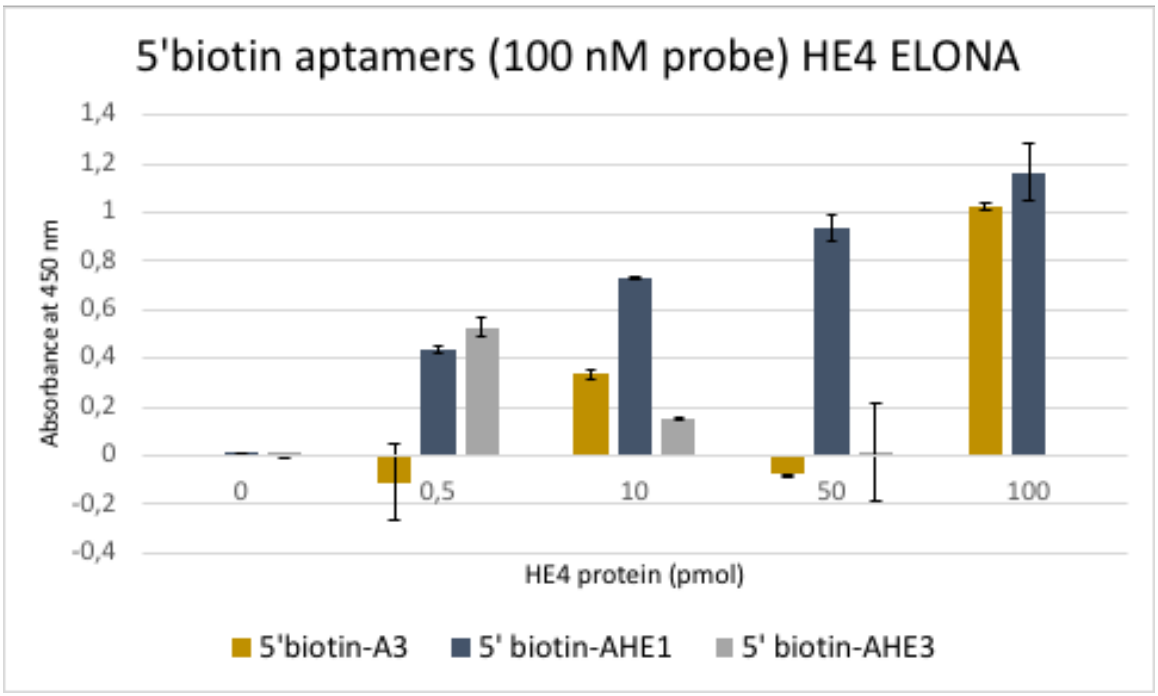

Figure 65. The effect of the 5' or 3'-prime biotinylation on signal of aptamers AHE1 (70mer), AHE3 (70mer) and A3 (25mer) and binding to HE4 protein by ELONA.

REFERENCES

(1) Bray, F.; Laversanne, M.; Weiderpass, E.; Soerjomataram, I. The Ever-Increasing Importance of Cancer as a Leading Cause of Premature Death Worldwide. *Cancer* **2021**, *127* (16), 3029–3030. https://doi.org/10.1002/cncr.33587.

(2) Ferlay, J.; Colombet, M.; Soerjomataram, I.; Parkin, D. M.; Piñeros, M.; Znaor, A.; Bray, F. Cancer Statistics for the Year 2020: An Overview. *Int. J. Cancer* **2021**, *149* (4), 778–789. https://doi.org/10.1002/ijc.33588.

(3) Bray, F.; Ferlay, J.; Soerjomataram, I.; Siegel, R. L.; Torre, L. A.; Jemal, A. Global Cancer Statistics 2018: GLOBOCAN Estimates of Incidence and Mortality Worldwide for 36 Cancers in 185 Countries. *CA. Cancer J. Clin.* **2018**, *68* (6), 394–424. https://doi.org/10.3322/caac.21492.

(4) Sung, H.; Ferlay, J.; Siegel, R. L.; Laversanne, M.; Soerjomataram, I.; Jemal, A.; Bray, F. Global Cancer Statistics 2020: GLOBOCAN Estimates of Incidence and Mortality Worldwide for 36 Cancers in 185 Countries. *CA. Cancer J. Clin.* **2021**, *71* (3), 209–249. https://doi.org/10.3322/caac.21660.

(5) (IARC) *Global Cancer Observatory*. https://gco.iarc.fr (accessed 2023-02-10).

(6) Berek, J. S.; Friedlander, M. L.; Hacker, N. F. Epithelial Ovarian, Fallopian Tube, and Peritoneal Cancer. In *Berek and Hacker's Gynecologic Oncology: Sixth Edition*; Wolters Kluwer Health Adis (ESP), 2014; pp 464–529. https://doi.org/10.1002/9781119000822.hfcm105.

(7) Siegel, R. L.; Miller, K. D.; Fuchs, H. E.; Jemal, A. Cancer Statistics, 2021. *CA. Cancer J. Clin.* **2021**, *71* (1), 7–33. https://doi.org/10.3322/caac.21654.

(8) Ledermann, J. A.; Raja, F. A.; Fotopoulou, C.; Gonzalez-Martin, A.; Colombo, N.; Sessa, C. Newly Diagnosed and Relapsed Epithelial Ovarian Carcinoma: ESMO Clinical Practice Guidelines for Diagnosis, Treatment and Follow-Up. *Ann. Oncol.* **2013**, *24*, vi24-32. https://doi.org/10.1093/annonc/mdt333.

(9) Roett A, M.; Evans, P. Ovarian Cancer: An Overview. *Am. Fam. Physician* **2009**, *80* (6), 609–616.

(10) Grandi, G.; Toss, A.; Cortesi, L.; Botticelli, L.; Volpe, A.; Cagnacci, A. The Association between Endometriomas and Ovarian Cancer: Preventive Effect of Inhibiting Ovulation and Menstruation during Reproductive Life. *Biomed Res. Int.* **2015**, *2015*. https://doi.org/10.1155/2015/751571.

(11) Yang-Hartwich, Y.; Gurrea-Soteras, M.; Sumi, N.; Joo, W. D.; Holmberg, J. C.; Craveiro, V.; Alvero, A. B.; Mor, G. Ovulation and Extra-Ovarian Origin of Ovarian Cancer. *Sci. Rep.* **2014**, *4*, 1–12. https://doi.org/10.1038/srep06116.

(12) Micek, H. M.; Visetsouk, M. R.; Fleszar, A. J.; Kreeger, P. K. The Many Microenvironments of Ovarian Cancer. *Adv. Exp. Med. Biol.* **2020**, *1296*, 199–213. https://doi.org/10.1007/978-3-030-59038-3_12.

(13) Kurman, R. J.; Carcangiu, M. L.; Harrington, C. S.; Young, R. H. *WHO Classification of Tumours of Female Reproductive Organs*; 2014; Vol. 6.

(14) Pal, T.; Permuth-Wey, J.; Betts, J. A.; Krischer, J. P.; Fiorica, J.; Arango, H.; LaPolla, J.; Hoffman, M.; Martino, M. A.; Wakeley, K.; Wilbanks, G.; Nicosia, S.; Cantor, A.; Sutphen, R. BRCA1 and BRCA2 Mutations Account for a Large Proportion of Ovarian Carcinoma Cases. *Cancer* **2005**, *104* (12), 2807–2816. https://doi.org/10.1002/cncr.21536.

(15) Berek, J. S.; Kehoe, S. T.; Kumar, L.; Friedlander, M. FIGO CANCER REPORT 2018: Cancer of the Ovary, Fallopian Tube, and Peritoneum. *Int. J. Gynecol. Obstet.* **2018**, *143* (S2), 59–78.

(16) King, M.-C.; Marks, J. H.; Mandel, J. B. Breast and Ovarian Cancer Risks Due to Inherited Mutations in BRCA1 and BRCA2. *Science (80-.).* **2003**, *302* (5645), 643–646. https://doi.org/10.1126/science.1088759.

(17) Ryan, N. A. J.; Evans, D. G.; Green, K.; Crosbie, E. J. Pathological Features and Clinical Behavior of Lynch Syndrome-Associated Ovarian Cancer. *Gynecol. Oncol.* **2017**, *144* (3), 491–495. https://doi.org/10.1016/j.ygyno.2017.01.005.

(18) Agence nationale de sécurité sanitaire de l'alimentation, de l'environnement et du travail (ANSES). *Aiming for better recognition of ovarian and laryngeal cancers related to asbestos exposure*. https://www.anses.fr/en/content/ovarian-laryngeal-cancers-asbestos-exposure (accessed 2023-03-02).

(19) Colombo, N.; Sessa, C.; Du Bois, A.; Ledermann, J.; McCluggage, W. G.; McNeish, I.; Morice, P.; Pignata, S.; Ray-Coquard, I.; Vergote, I.; Baert, T.; Belaroussi, I.; Dashora, A.; Olbrecht, S.; Planchamp, F.; Querleu, D. ESMO-ESGO Consensus Conference Recommendations on Ovarian Cancer: Pathology and Molecular Biology, Early and Advanced Stages, Borderline Tumours and Recurrent Disease. *Ann. Oncol.* **2019**, *30* (5), 672–705. https://doi.org/10.1093/annonc/mdz062.

(20) Doubeni, C. A.; Doubeni, A. R. B.; Myers, A. E. Diagnosis and Management of Ovarian Cancer. *Am. Fam. Physician* **2016**, *93* (11), 937–944.

(21) Qaseem, A.; Humphrey, L. L.; Harris, R.; Starkey, M.; Denberg, T. D. Screening Pelvic Examination in Adult Women: A Clinical Practice Guideline from the American College of Physicians. *Annals of Internal Medicine*. 2014, pp 67–72. https://doi.org/10.7326/M14-0701.

(22) American Cancer Society. *Tests for Ovarian Cancer*. htttps://www.cancer.org/cancer/ovarian-cancer/detection-diagnosis-staging/how-diagnosed.html (accessed 2023-03-15).

(23) Mishra, A.; Verma, M. Cancer Biomarkers: Are We Ready for the Prime Time? *Cancers (Basel).* **2010**, *2* (1), 190–208. https://doi.org/10.3390/cancers2010190.

(24) Bast, R. C.; Lu, Z.; Han, C. Y.; Lu, K. H.; Anderson, K. S.; Drescher, C. W.; Skates, S. J. Biomarkers and Strategies for Early Detection of Ovarian Cancer. *Cancer Epidemiol. Biomarkers Prev.* **2020**, *29* (12), 2504–2512. https://doi.org/10.1158/1055-9965.EPI-20-1057.

(25) Atallah, G. A.; Aziz, N. H. A.; Teik, C. K.; Kampan, N. C.; Shafiee, M. N. New Predictive Biomarkers for Ovarian Cancer. *Diagnostics* **2021**, *11* (3). https://doi.org/10.3390/diagnostics11030465.

(26) Ueland, F. R. A Perspective on Ovarian Cancer Biomarkers: Past, Present and Yet-To-Come. *Diagnostics* **2017**, *7*, 14. https://doi.org/10.3390/diagnostics7010014.

(27) Bast, R. C.; Klug, T. L.; John, E. St.; Jenison, E.; Niloff, J. M.; Lazarus, H.; Berkowitz, R. S.; Leavitt, T.; Griffiths, C. T.; Parker, L.; Zurawski, V. R.; Knapp, R. C. A Radioimmunoassay Using a Monoclonal Antibody to Monitor the Course of Epithelial Ovarian Cancer. *N. Engl. J. Med.* **1983**, *309* (15), 883–887. https://doi.org/10.1056/nejm198310133091503.

(28) Sturgeon, C. M.; Duffy, M. J.; Stenman, U. H.; Lilja, H.; Brünner, N.; Chan, D. W.; Babaian, R.; Bast, R. C.; Dowell, B.; Esteva, F. J.; Haglund, C.; Harbeck, N.; Hayes, D. F.; Holten-Andersen, M.; Klee, G. G.; Lamerz, R.; Looijenga, L. H.; Molina, R.; Nielsen, H. J.; Rittenhouse, H.; Semjonow, A.; Shih, I. M.; Sibley, P.; Sölétormos, G.; Stephan, C.; Sokoll, L.; Hoffman, B. R.; Diamandis, E. P. National Academy of Clinical Biochemistry Laboratory Medicine Practice Guidelines for Use of Tumor Markers in Testicular, Prostate, Colorectal, Breast, and Ovarian Cancers. *Clinical Chemistry*. 2008, pp e11-79. https://doi.org/10.1373/clinchem.2008.105601.

(29) Sölétormos, G.; Duffy, M. J.; Othman Abu Hassan, S.; Verheijen, R. H. M.; Tholander, B.; Bast, R. C.; Gaarenstroom, K. N.; Sturgeon, C. M.; Bonfrer, J. M.; Petersen, P. H.; Troonen, H.; Carlotorre, G.; Kanty Kulpa, J.; Tuxen, M. K.; Molina,

R. Clinical Use of Cancer Biomarkers in Epithelial Ovarian Cancer: Updated Guidelines from the European Group on Tumor Markers. *Int. J. Gynecol. Cancer* **2016**, *26* (1), 43–51. https://doi.org/10.1097/IGC.0000000000000586.

(30) Dochez, V.; Caillon, H.; Vaucel, E.; Dimet, J.; Winer, N.; Ducarme, G. Biomarkers and Algorithms for Diagnosis of Ovarian Cancer: CA125, HE4, RMI and ROMA, a Review. *J. Ovarian Res.* **2019**, *12* (1), 28. https://doi.org/10.1186/s13048-019-0503-7.

(31) Meden, H.; Fattahi-Meibodi, A. CA 125 in Benign Gynecological Conditions. *Int. J. Biol. Markers* **1998**, *13* (4), 231–237. https://doi.org/10.1177/172460089801300411.

(32) Zhen, S.; Bian, L. I. H.; Chang, L. I. L. I.; Gao, X. I. N. Comparison of Serum Human Epididymis Protein 4 and Carbohydrate Antigen 125 as Markers in Ovarian Cancer : A Meta - Analysis. *Mol. Clin. Oncol.* **2014**, *2* (4), 559–566. https://doi.org/10.3892/mco.2014.279.

(33) Scaletta, G.; Plotti, F.; Luvero, D.; Capriglione, S.; Montera, R.; Miranda, A.; Lopez, S.; Terranova, C.; De Cicco Nardone, C.; Angioli, R. The Role of Novel Biomarker HE4 in the Diagnosis, Prognosis and Follow-up of Ovarian Cancer: A Systematic Review. *Expert Rev. Anticancer Ther.* **2017**, *17* (9), 827–839. https://doi.org/10.1080/14737140.2017.1360138.

(34) Moore, R. G.; McMeekin, D. S.; Brown, A. K.; DiSilvestro, P.; Miller, M. C.; Allard, W. J.; Gajewski, W.; Kurman, R.; Bast, R. C.; Skates, S. J. A Novel Multiple Marker Bioassay Utilizing HE4 and CA125 for the Prediction of Ovarian Cancer in Patients with a Pelvic Mass. *Gynecol. Oncol.* **2009**, *112* (1), 40–46. https://doi.org/10.1016/j.ygyno.2008.08.031.

(35) Nash, Z.; Menon, U. Ovarian Cancer Screening: Current Status and Future Directions. *Best Pract. Res. Clin. Obstet. Gynaecol.* **2020**, *65*, 32–45. https://doi.org/10.1016/j.bpobgyn.2020.02.010.

(36) Doroudi, M.; Kramer, B. S.; Pinsky, P. F. The Bimanual Ovarian Palpation Examination in the Prostate, Lung, Colorectal and Ovarian Cancer Screening Trial: Performance and Complications. *J. Med. Screen.* **2017**, *24* (4), 220–222. https://doi.org/10.1177/0969141316680381.

(37) Menon, U.; Gentry-Maharaj, A.; Burnell, M.; Singh, N.; Ryan, A.; Karpinskyj, C.; Carlino, G.; Taylor, J.; Massingham, S. K.; Raikou, M.; Kalsi, J. K.; Woolas, R.; Manchanda, R.; Arora, R.; Casey, L.; Dawnay, A.; Dobbs, S.; Leeson, S.; Mould, T.; Seif, M. W.; Sharma, A.; Williamson, K.; Liu, Y.; Fallowfield, L.; McGuire, A. J.; Campbell, S.; Skates, S. J.; Jacobs, I. J.; Parmar, M. Ovarian Cancer Population

Screening and Mortality after Long-Term Follow-up in the UK Collaborative Trial of Ovarian Cancer Screening (UKCTOCS): A Randomised Controlled Trial. *Lancet* **2021**, *397* (10290), 2182–2193. https://doi.org/10.1016/S0140-6736(21)00731-5.

(38) Van Nagell, J. R.; Hoff, J. T. Transvaginal Ultrasonography in Ovarian Cancer Screening: Current Perspectives. *Int. J. Womens. Health* **2014**, *6* (1), 25–33. https://doi.org/10.2147/IJWH.S38347.

(39) Akintomide, O. A.; Obasi, O. U. Intimate Patient Examinations: The Awareness, Acceptance and Practice Preference of Transvaginal Ultrasound Scan among Women in a South-Southern State of Nigeria. *J. Fam. Med. Prim. Care* **2019**, *8* (1), 109–114.

(40) Clement, S.; Candy, B.; Heath, V.; To, M.; Nicolaides, K. H. Transvaginal Ultrasound in Pregnancy: Its Acceptability to Women and Maternal Psychological Morbidity. *Ultrasound Obstet. Gynecol.* **2003**, *22* (5), 508–514. https://doi.org/10.1002/uog.893.

(41) Jordaens, S.; Zwaenepoel, K.; Tjalma, W.; Deben, C.; Beyers, K.; Vankerckhoven, V.; Pauwels, P.; Vorsters, A. Urine Biomarkers in Cancer Detection: A Systematic Review of Preanalytical Parameters and Applied Methods. *Int. J. Cancer* **2023**, *152* (10), 2186–2205. https://doi.org/10.1002/ijc.34434.

(42) Harpole, M.; Davis, J.; Espina, V. Current State of the Art for Enhancing Urine Biomarker Discovery. *Expert Rev. Proteomics* **2016**, *13* (6), 609–626. https://doi.org/10.1080/14789450.2016.1190651.

(43) Tan, W. S.; Teo, C. H.; Chan, D.; Heinrich, M.; Feber, A.; Sarpong, R.; Allan, J.; Williams, N.; Brew-Graves, C.; Ng, C. J.; Kelly, J. D, DETECT II trial collaborators. Mixed-Methods Approach to Exploring Patients' Perspectives on the Acceptability of a Urinary Biomarker Test in Replacing Cystoscopy for Bladder Cancer Surveillance. *BJU Int.* **2019**, *124* (3), 408–417. https://doi.org/10.1111/bju.14690.

(44) Shin, H. Y.; Lee, B.; Hwang, S. H.; Lee, D. O.; Sung, N. Y.; Park, J. Y.; Jun, J. K. Evaluation of Satisfaction with Three Different Cervical Cancer Screening Modalities: Clinician-Collected Pap Test vs. HPV Test by Self-Sampling vs. HPV Test by Urine Sampling. *J. Gynecol. Oncol.* **2019**, *30* (5), 1–10. https://doi.org/10.3802/jgo.2019.30.e76.

(45) Aspevall, O.; Hallander, H.; Gant, V.; Kouri, T. European Guidelines for Urinalysis: A Collaborative Document Produced by European Clinical Microbiologists and Clinical Chemists under ECLM in Collaboration with ESCMID. *Clin. Microbiol. Infect.* **2001**, *7* (4), 173–178. https://doi.org/10.1046/j.1198-743X.2001.00237.x.

(46) Hanžek, A.; Siatka, C.; Duc, A. C. E. Extracellular Urinary MicroRNAs as Non-

Invasive Biomarkers of Endometrial and Ovarian Cancer. *J. Cancer Res. Clin. Oncol.* **2023**, No. 0123456789. https://doi.org/10.1007/s00432-023-04675-5.

(47) Owens, G. L.; Barr, C. E.; White, H.; Njoku, K.; Crosbie, E. J. Urinary Biomarkers for the Detection of Ovarian Cancer: A Systematic Review. *Carcinogenesis* **2022**, *43* (4), 311–320. https://doi.org/10.1093/carcin/bgac016.

(48) Grayson, K.; Gregory, E.; Khan, G.; Guinn, B.-A. Urine Biomarkers for the Early Detection of Ovarian Cancer – Are We There Yet? *Biomark. Cancer* **2019**, *11*, 1179299X19830977. https://doi.org/10.1177/1179299x19830977.

(49) Jia, M.; Deng, J.; Cheng, X.; Yan, Z.; Li, Q. Diagnostic Accuracy of Urine HE4 in Patients with Ovarian Cancer : A Meta-Analysis. *Oncotarget* **2017**, *8* (6), 9660–9671.

(50) Sandow, J. J.; Rainczuk, A.; Infusini, G.; Makanji, M.; Bilandzic, M.; Wilson, A. L.; Fairweather, N.; Stanton, P. G.; Garama, D.; Gough, D.; Jobling, T. W.; Webb, A. i. Discovery and Validation of Novel Protein Biomarkers in Ovarian Cancer Patient Urine. *PROTEOMICS - Clin. Appl.* **2018**, *12* (3), 1700135. https://doi.org/https://doi.org/10.1002/prca.201700135.

(51) Badgwell, D.; Lu, Z.; Cole, L.; Fritsche, H.; Atkinson, E. N.; Somers, E.; Allard, J.; Moore, R. G.; Lu, K. H.; Bast, R. C. Urinary Mesothelin Provides Greater Sensitivity for Early Stage Ovarian Cancer than Serum Mesothelin, Urinary HCG Free Beta Subunit and Urinary HCG Beta Core Fragment. *Gynecol. Oncol.* **2007**, *106* (3), 490–497. https://doi.org/10.1016/j.ygyno.2007.04.022.

(52) Smith, C. R.; Batruch, I.; Bauça, J. M.; Kosanam, H.; Ridley, J.; Bernardini, M. Q.; Leung, F.; Diamandis, E. P.; Kulasingam, V. Deciphering the Peptidome of Urine from Ovarian Cancer Patients and Healthy Controls. *Clin. Proteomics* **2014**, *11* (1), 1–10. https://doi.org/10.1186/1559-0275-11-23.

(53) Ye, B.; Skates, S.; Mok, S. C.; Horick, N. K.; Rosenberg, H. F.; Vitonis, A.; Edwards, D.; Sluss, P.; Han, W. K.; Berkowitz, R. S.; Cramer, D. W. Proteomic-Based Discovery and Characterization of Glycosylated Eosinophil-Derived Neurotoxin and COOH-Terminal Osteopontin Fragments for Ovarian Cancer in Urine. *Clin. Cancer Res.* **2006**, *12* (2), 432–441. https://doi.org/10.1158/1078-0432.CCR-05-0461.

(54) Matsukawa, T.; Mizutani, S.; Matsumoto, K.; Kato, Y.; Yoshihara, M.; Kajiyama, H.; Shibata, K. Placental Leucine Aminopeptidase as a Potential Specific Urine Biomarker for Invasive Ovarian Cancer. *J. Clin. Med.* **2022**, *11* (1), 222. https://doi.org/10.3390/jcm11010222.

(55) Coticchia, C. M.; Curatolo, A. S.; Zurakowski, D.; Yang, J.; Daniels, K. E.; Matulonis,

U. A.; Moses, M. A. Urinary MMP-2 and MMP-9 Predict the Presence of Ovarian Cancer in Women with Normal CA125 Levels. *Gynecol. Oncol.* **2011**, *123* (2), 295–300. https://doi.org/10.1016/j.ygyno.2011.07.034.

(56) Nolen, B. M.; Orlichenko, L. S.; Marrangoni, A.; Velikokhatnaya, L.; Prosser, D.; Grizzle, W. E.; Ho, K.; Jenkins, F. J.; Bovbjerg, D. H.; Lokshin, A. E. An Extensive Targeted Proteomic Analysis of Disease-Related Protein Biomarkers in Urine from Healthy Donors. *PLoS One* **2013**, *8* (5), e63368. https://doi.org/10.1371/journal.pone.0063368.

(57) Moore, R. G.; Brown, A. K.; Miller, M. C.; Skates, S.; Allard, W. J.; Verch, T.; Steinhoff, M.; Messerlian, G.; DiSilvestro, P.; Granai, C. O.; Bast, R. C. The Use of Multiple Novel Tumor Biomarkers for the Detection of Ovarian Carcinoma in Patients with a Pelvic Mass. *Gynecol. Oncol.* **2008**, *108* (2), 402–408. https://doi.org/10.1016/j.ygyno.2007.10.017.

(58) Zhong, X.; Ran, R.; Gao, S.; Shi, M.; Shi, X.; Long, F.; Zhou, Y.; Yang, Y.; Tang, X.; Lin, A.; He, W.; Yu, T.; Han, T. L. Complex Metabolic Interactions between Ovary, Plasma, Urine, and Hair in Ovarian Cancer. *Front. Oncol.* **2022**, *12* (August), 1–16. https://doi.org/10.3389/fonc.2022.916375.

(59) Slupsky, C. M.; Steed, H.; Wells, T. H.; Dabbs, K.; Schepansky, A.; Capstick, V.; Faught, W.; Sawyer, M. B. Urine Metabolite Analysis Offers Potential Early Diagnosis of Ovarian and Breast Cancers. *Clin. Cancer Res.* **2010**, *16* (23), 5835–5841. https://doi.org/10.1158/1078-0432.CCR-10-1434.

(60) Niemi, R. J.; Roine, A. N.; Merja, R. Urinary Polyamines as Biomarkers for Ovarian Cancer Read the Full Text or Download the PDF : **2023**, 2023.

(61) Zhou, J.; Gong, G.; Tan, H.; Dai, F.; Zhu, X.; Chen, Y.; Wang, J.; Liu, Y.; Chen, P.; Wu, X.; Wen, J. Urinary MicroRNA-30a-5p Is a Potential Biomarker for Ovarian Serous Adenocarcinoma. *Oncol. Rep.* **2015**, *33* (6), 2915–2923. https://doi.org/10.3892/or.2015.3937.

(62) Záveský, L.; Jandáková, E.; Turyna, R.; Langmeierová, L.; Weinberger, V.; Záveská Drábková, L.; Hůlková, M.; Hořínek, A.; Dušková, D.; Feyereisl, J.; Minář, L.; Kohoutová, M. Evaluation of Cell-Free Urine MicroRNAs Expression for the Use in Diagnosis of Ovarian and Endometrial Cancers. A Pilot Study. *Pathol. Oncol. Res.* **2015**, *21* (4), 1027–1035. https://doi.org/10.1007/s12253-015-9914-y.

(63) Savolainen, K.; Scaravilli, M.; Ilvesmäki, A.; Staff, S.; Tolonen, T.; Mäenpää, J. U.; Visakorpi, T.; Auranen, A. Expression of the MiR - 200 Family in Tumor Tissue ,

Plasma and Urine of Epithelial Ovarian Cancer Patients in Comparison to Benign Counterparts. *BMC Res. Notes* **2020**, 1–7. https://doi.org/10.1186/s13104-020-05155-6.

(64) Hellstrom, I.; Heagerty, P. J.; Swisher, E. M.; Liu, P.; Jaffar, J.; Agnew, K.; Hellström, K. E. Detection of the HE4 Protein in Urine as a Biomarker for Ovarian Neoplasms. *Cancer Lett.* **2010**, *296* (1), 43–48.

(65) Liao, J. B.; Yip, Y. Y.; Swisher, E. M.; Agnew, K.; Hellstrom, K. E.; Hellstrom, I. Detection of the HE4 Protein in Urine as a Biomarker for Ovarian Neoplasms: Clinical Correlates. *Gynecol. Oncol.* **2015**, *137* (3), 430–435. https://doi.org/10.1016/j.ygyno.2015.03.044.

(66) Clauss, A.; Lilja, H.; Lundwall, Å. A Locus on Human Chromosome 20 Contains Several Genes Expressing Protease Inhibitor Domains with Homology to Whey Acidic Protein. *Biochem. J.* **2002**, *368* (1), 233–242. https://doi.org/10.1042/BJ20020869.

(67) Ramachandran, P.; Boontheung, P.; Xie, Y.; Sondej, M.; Wong, D. T.; Loo, J. A. Identification of N-Linked Glycoproteins in Human Saliva by Glycoprotein Capture and Mass Spectrometry. *J. Proteome Res.* **2006**, *5* (6), 1493–1503. https://doi.org/10.1021/pr050492k.

(68) Chhikara, N.; Saraswat, M.; Tomar, A. K.; Dey, S.; Singh, S.; Yadav, S. Human Epididymis Protein-4 (HE-4): A Novel Cross-Class Protease Inhibitor. *PLoS One* **2012**, *7* (11), e47672. https://doi.org/10.1371/journal.pone.0047672.

(69) Uniprot.org. *Human Epididymis Protein 4 (Q14508 · WFDC2_HUMAN)*.

(70) Kirchhoff, C.; Habben, I.; Iveli, R.; Krull, N. A Major Human Epididymis-Specific CDNA Encodes a Protein with Sequence Homology to Extracellular Proteinase Inhibitors. *Biol. Reprod.* **1991**, *45* (2), 350–357. https://doi.org/10.1095/biolreprod45.2.350.

(71) Kirchhoff, C. Molecular Characterization of Epididymal Proteins. *Rev. Reprod.* **1998**, *3* (2), 86–95. https://doi.org/10.1530/ror.0.0030086.

(72) Wang, K.; Gan, L.; Jeffery, E.; Gayle, M.; Gown, A. M.; Skelly, M.; Nelson, P. S.; Ng, W. V.; Schummer, M.; Hood, L.; Mulligan, J. Monitoring Gene Expression Profile Changes in Ovarian Carcinomas Using CDNA Microarray. *Gene* **1999**, *229* (1–2), 101–108. https://doi.org/10.1016/S0378-1119(99)00035-9.

(73) Bingle, L.; Singleton, V.; Bingle, C. D. The Putative Ovarian Tumour Marker Gene HE4 (WFDC2), Is Expressed in Normal Tissues and Undergoes Complex Alternative Splicing to Yield Multiple Protein Isoforms. *Oncogene* **2002**, *21* (17), 2768–2773.

https://doi.org/10.1038/sj.onc.1205363.

(74) Galgano, M. T.; Hampton, G. M.; Frierson, H. F. Comprehensive Analysis of HE4 Expression in Normal and Malignant Human Tissues. *Mod. Pathol.* **2006**, *19* (6), 847–853. https://doi.org/10.1038/modpathol.3800612.

(75) Schummer, M.; Ng, W. L. V.; Bumgarner, R. E.; Nelson, P. S.; Schummer, B.; Bednarski, D. W.; Hassell, L.; Baldwin, R. L.; Karlan, B. Y.; Hood, L. Comparative Hybridization of an Array of 21 500 Ovarian CDNAs for the Discovery of Genes Overexpressed in Ovarian Carcinomas. *Gene* **1999**, *238* (2), 375–385. https://doi.org/10.1016/S0378-1119(99)00342-X.

(76) Heliström, I.; Raycraft, J.; Hayden-Ledbetter, M.; Ledbetter, J. A.; Schummer, M.; McIntosh, M.; Drescher, C.; Urban, N.; Hellström, K. E. The HE4 (WFDC2) Protein Is a Biomarker for Ovarian Carcinoma. *Cancer Res.* **2003**, *63* (13), 3695–3700.

(77) Drapkin, R.; Von Horsten, H. H.; Lin, Y.; Mok, S. C.; Crum, C. P.; Welch, W. R.; Hecht, J. L. Human Epididymis Protein 4 (HE4) Is a Secreted Glycoprotein That Is Overexpressed by Serous and Endometrioid Ovarian Carcinomas. *Cancer Res.* **2005**, *65* (6), 2162–2169. https://doi.org/10.1158/0008-5472.CAN-04-3924.

(78) Wang, H.; Zhu, L.; Gao, J.; Hu, Z.; Lin, B. Promotive Role of Recombinant HE4 Protein in Proliferation and Carboplatin Resistance in Ovarian Cancer Cells. *Oncol. Rep.* **2015**, *33* (1), 403–412. https://doi.org/10.3892/or.2014.3549.

(79) James, N. E.; Chichester, C.; Ribeiro, J. R. Beyond the Biomarker: Understanding the Diverse Roles of Human Epididymis Protein 4 in the Pathogenesis of Epithelial Ovarian Cancer. *Front. Oncol.* **2018**, *24* (8), 124. https://doi.org/10.3389/fonc.2018.00124.

(80) Zhu, L.; Zhuang, H.; Wang, H.; Tan, M.; Schwab, C. L.; Deng, L.; Gao, J.; Hao, Y.; Li, X.; Gao, S.; Liu, J.; Lin, B. Overexpression of HE4 (Human Epididymis Protein 4) Enhances Proliferation, Invasion and Metastasis of Ovarian Cancer. *Oncotarget* **2016**, *7* (1), 729–744. https://doi.org/10.18632/ONCOTARGET.6327.

(81) Moore, R. G.; Hill, E. K.; Horan, T.; Yano, N.; Kim, K. K.; MacLaughlan, S.; Lambert-Messerlian, G.; Tseng, Y. T. D.; Padbury, J. F.; Craig Miller, M.; Lange, T. S.; Singh, R. K. HE4 (WFDC2) Gene Overexpression Promotes Ovarian Tumor Growth. *Sci. Rep.* **2014**, *4*, 3574. https://doi.org/10.1038/srep03574.

(82) Ribeiro, J. R.; Schorl, C.; Yano, N.; Romano, N.; Kim, K. K.; Singh, R. K.; Moore, R. G. HE4 Promotes Collateral Resistance to Cisplatin and Paclitaxel in Ovarian Cancer Cells. *J. Ovarian Res.* **2016**, *9* (1), 1–18. https://doi.org/10.1186/s13048-016-0240-0.

(83) Angioli, R.; Capriglione, S.; Aloisi, A.; Guzzo, F.; Luvero, D.; Miranda, A.; Damiani, P.; Montera, R.; Terranova, C.; Plotti, F. Can HE4 Predict Platinum Response during First-Line Chemotherapy in Ovarian Cancer? *Tumor Biol.* **2014**, *35* (7), 7009–7015. https://doi.org/10.1007/s13277-014-1836-x.

(84) Chen, W. T.; Gao, X.; Han, X. D.; Zheng, H.; Guo, L.; Lu, R. Q. HE4 as a Serum Biomarker for ROMA Prediction and Prognosis of Epithelial Ovarian Cancer. *Asian Pacific J. Cancer Prev.* **2014**, *15* (1), 101–105. https://doi.org/10.7314/APJCP.2014.15.1.101.

(85) Molina, R.; Escudero, J. M.; Augé, J. M.; Filella, X.; Foj, L.; Torné, A.; Lejarcegui, J.; Pahisa, J. HE4 a Novel Tumour Marker for Ovarian Cancer: Comparison with CA 125 and ROMA Algorithm in Patients with Gynaecological Diseases. *Tumour Biol.* **2011**, *32* (6), 1087–1095. https://doi.org/10.1007/s13277-011-0204-3.

(86) Zheng, H.; Gao, Y. Serum HE4 as a Useful Biomarker in Discriminating Ovarian Cancer From Benign Pelvic Disease. *Int. J. Gynecol. Cancer* **2012**, *22* (6), 1000 LP – 1005. https://doi.org/10.1097/IGC.0b013e318249bee7.

(87) Simmons, A. R.; Baggerly, K.; Bast, R. C. The Emerging Role of HE4 in the Evaluation of Epithelial Ovarian and Endometrial Carcinomas. *Oncol. (United States)* **2013**, *27* (6), 548–556.

(88) Nagy, B.; Krasznai, Z. T.; Balla, H.; Csobán, M.; Antal-Szalmás, P.; Hernádi, Z.; Kappelmayer, J. Elevated Human Epididymis Protein 4 Concentrations in Chronic Kidney Disease. *Ann. Clin. Biochem.* **2012**, *49* (4), 377–380. https://doi.org/10.1258/acb.2011.011258.

(89) Escudero, J. M.; Auge, J. M.; Filella, X.; Torne, A.; Pahisa, J.; Molina, R. Comparison of Serum Human Epididymis Protein 4 with Cancer Antigen 125 as a Tumor Marker in Patients with Malignant and Nonmalignant Diseases. *Clin. Chem.* **2011**, *57* (11), 1534–1544. https://doi.org/10.1373/clinchem.2010.157073.

(90) Blackman, A.; Mitchell, J.; Rowswell-Turner, R.; Singh, R.; Kim, K. K.; Eklund, E.; Skates, S.; Bast, R. C.; Messerlian, G.; Miller, M. C.; Moore, R. G. Analysis of Serum HE4 Levels in Various Histologic Subtypes of Epithelial Ovarian Cancer and Other Malignant Tumors. *Tumour Biol.* **2021**, *43* (1), 355–365. https://doi.org/10.3233/TUB-211546.

(91) Hallamaa, M.; Suvitie, P.; Huhtinen, K.; Matomäki, J.; Poutanen, M.; Perheentupa, A. Serum HE4 Concentration Is Not Dependent on Menstrual Cycle or Hormonal Treatment among Endometriosis Patients and Healthy Premenopausal Women.

Gynecol. Oncol. **2012**, *125* (3), 667–672. https://doi.org/10.1016/j.ygyno.2012.03.011.

(92) Moore, R. G.; Miller, M. C.; Eklund, E.; Lu, K. H.; Bast, R. C.; Lambert-Messerlian, G. Serum Levels of the Ovarian Cancer Biomarker HE4 Are Decreased in Pregnancy and Increase with Age. *Am. J. Obstet. Gynecol.* **2012**, *206* (4), 349.e1–349.e7. https://doi.org/10.1016/j.ajog.2011.12.028.Serum.

(93) Wu, L.; Dai, Z.-Y.; Qian, Y.-H.; Shi, Y.; Liu, F.-J.; Yang, C. Diagnostic Value of Serum Human Epididymis Protein 4 (HE4) in Ovarian Carcinoma: A Systematic Review and Meta-Analysis. *Int. J. Gynecol. cancer Off. J. Int. Gynecol. Cancer Soc.* **2012**, *22* (7), 1106–1112. https://doi.org/10.1097/IGC.0b013e318263efa2.

(94) Steffensen, K. D.; Waldstrøm, M.; Brandslund, I.; Petzold, M.; Jakobsen, A. The Prognostic and Predictive Value of Combined HE4 and CA-125 in Ovarian Cancer Patients. *Int. J. Gynecol. Cancer* **2012**, *22* (9), 1474 LP – 1482. https://doi.org/10.1097/IGC.0b013e3182681cfd.

(95) Fan, Q.; Luo, G.; Yi, T.; Wang, Q.; Wang, D.; Zhang, G.; Jiang, X.; Guo, X. Diagnostic Value of Urinary-to-Serum Human Epididymis Protein 4 Ratio in Ovarian Cancer. *Biomed. Reports* **2017**, *7* (1), 67–72. https://doi.org/10.3892/br.2017.913.

(96) Qu, W.; Gao, Q.; Chen, H.; Tang, Z.; Zhu, X. HE4-Test of Urine and Body Fluids for Diagnosis of Gynecologic Cancer. *Expert Rev. Mol. Diagn.* **2017**, *17* (3), 239–244. https://doi.org/10.1080/14737159.2017.1282824.

(97) Wang, S.; Zhao, X.; Khimji, I.; Akbas, R.; Qiu, W.; Edwards, D.; Cramer, D. W.; Ye, B.; Demirci, U. Integration of Cell Phone Imaging with Microchip ELISA to Detect Ovarian Cancer HE4 Biomarker in Urine at the Point-of-Care. *Lab Chip* **2011**, *11* (20), 3411–3418.

(98) Macuks, R.; Baidekalna, I.; Donina, S. Urinary Concentrations of Human Epidydimis Secretory Protein 4 (He4) in the Diagnosis of Ovarian Cancer: A Case-Control Study. *Asian Pacific J. Cancer Prev.* **2012**, *13* (9), 4695–4698. https://doi.org/10.7314/APJCP.2012.13.9.4695.

(99) Zhong-Qian, L.; Radwan, R.; Polkowski, J.; Raju, S.; Falcone, K.; Simamora, R.; Kettly, T.; Moore, R. G.; Barnes, G. Abstract LB-451: Detection of Urinary HE4 as a Biomarker for Epithelial Ovarian Cancer. *Cancer Res.* **2011**, *71* (8), LB-451. https://doi.org/https://doi.org/10.1158/1538-7445.AM2011-LB-451.

(100) Stiekema, A.; Stiekema, A.; Korse, C.; Linders, T.; van Baal, J.; den Broek, D. van; Kenter, G.; Lok, C. HE4 in Various Body Fluids: A Prospective Pilot Study. *Clin. Oncol. Res.* **2020**, *3* (10), 1–6. https://doi.org/10.31487/j.cor.2020.11.06.

(101) Njoku, K.; Barr, C. E.; Sutton, C. J. J.; Crosbie, E. J. Urine CA125 and HE4 for the Triage of Symptomatic Women with Suspected Endometrial Cancer. *Cancers (Basel).* **2022**, *14* (14), 1–16. https://doi.org/10.3390/cancers14143306.

(102) Komarova, N.; Kuznetsov, A. Inside the Black Box: What Makes Selex Better? *Molecules* **2019**, *24* (19), 3598. https://doi.org/10.3390/molecules24193598.

(103) Ellington, A. D.; Szostak, J. W. In Vitro Selection of RNA Molecules That Bind Specific Ligands. *Nature* **1990**, *346* (6287), 818–822. https://doi.org/10.1038/346818a0.

(104) Tuerk, C.; Gold, L. Systematic Evolution of Ligands by Exponential Enrichment: RNA Ligands to Bacteriophage T4 DNA Polymerase. *Science* **1990**, *249* (4968), 505–510. https://doi.org/10.1126/science.2200121.

(105) Robertson, D. L.; Joyce, G. F. Selection in Vitro of an RNA Enzyme That Specifically Cleaves Single-Stranded DNA. *Nature* **1990**, *344* (6265), 467–468. https://doi.org/10.1038/344467a0.

(106) Vorobyeva, M. A.; Davydova, A. S.; Vorobjev, P. E.; Pyshnyi, D. V.; Venyaminova, A. G. Key Aspects of Nucleic Acid Library Design for in Vitro Selection. *Int. J. Mol. Sci.* **2018**, *19* (2), 470. https://doi.org/10.3390/ijms19020470.

(107) Dunn, M. R.; Jimenez, R. M.; Chaput, J. C. Analysis of Aptamer Discovery and Technology. *Nat. Rev. Chem.* **2017**, *1* (10), 76. https://doi.org/10.1038/s41570-017-0076.

(108) Jeddi, I.; Saiz, L. Three-Dimensional Modeling of Single Stranded DNA Hairpins for Aptamer-Based Biosensors. *Sci. Rep.* **2017**, *7* (1), 1–13. https://doi.org/10.1038/s41598-017-01348-5.

(109) Song, K. M.; Lee, S.; Ban, C. Aptamers and Their Biological Applications. *Sensors* **2012**, *12* (1), 612–631. https://doi.org/10.3390/s120100612.

(110) Arshavsky-Graham, S.; Urmann, K.; Salama, R.; Massad-Ivanir, N.; Walter, J. G.; Scheper, T.; Segal, E. Aptamers: Vs. Antibodies as Capture Probes in Optical Porous Silicon Biosensors. *Analyst* **2020**, *145* (14), 4991–5003. https://doi.org/10.1039/d0an00178c.

(111) Han, J.; Gao, L.; Wang, J.; Wang, J. Application and Development of Aptamer in Cancer: From Clinical Diagnosis to Cancer Therapy. *J. Cancer* **2020**, *11* (23), 6902–6915. https://doi.org/10.7150/JCA.49532.

(112) Ciancio, D. R.; Vargas, M. R.; Thiel, W. H.; Bruno, M. A.; Giangrande, P. H.; Mestre, M. B. Aptamers as Diagnostic Tools in Cancer. *Pharmaceuticals* **2018**, *11* (3), 1–23.

https://doi.org/10.3390/ph11030086.

(113) Shigdar, S.; Schrand, B.; Giangrande, P. H.; de Franciscis, V. Aptamers: Cutting Edge of Cancer Therapies. *Mol. Ther.* **2021**, *29* (8), 2396–2411. https://doi.org/10.1016/j.ymthe.2021.06.010.

(114) Gao, F.; Yin, J.; Chen, Y.; Guo, C.; Hu, H.; Su, J. Recent Advances in Aptamer-Based Targeted Drug Delivery Systems for Cancer Therapy. *Front. Bioeng. Biotechnol.* **2022**, *10*, 972933. https://doi.org/10.3389/fbioe.2022.972933.

(115) Zhou, Z.; Liu, M.; Jiang, J. The Potential of Aptamers for Cancer Research. *Anal. Biochem.* **2018**, *549*, 91–95. https://doi.org/10.1016/j.ab.2018.03.008.

(116) Ng, E. W. M.; Shima, D. T.; Calias, P.; Cunningham, E. T. J.; Guyer, D. R.; Adamis, A. P. Pegaptanib, a Targeted Anti-VEGF Aptamer for Ocular Vascular Disease. *Nat. Rev. Drug Discov.* **2006**, *5* (2), 123–132. https://doi.org/10.1038/nrd1955.

(117) Yazdian-Robati, R.; Bayat, P.; Oroojalian, F.; Zargari, M.; Ramezani, M.; Taghdisi, S. M.; Abnous, K. Therapeutic Applications of AS1411 Aptamer, an Update Review. *Int. J. Biol. Macromol.* **2020**, *155*, 1420–1431. https://doi.org/10.1016/j.ijbiomac.2019.11.118.

(118) Hoellenriegel, J.; Zboralski, D.; Maasch, C.; Rosin, N. Y.; Wierda, W. G.; Keating, M. J.; Kruschinski, A.; Burger, J. A. The Spiegelmer NOX-A12, a Novel CXCL12 Inhibitor, Interferes with Chronic Lymphocytic Leukemia Cell Motility and Causes Chemosensitization. *Blood* **2014**, *123* (7), 1032–1039. https://doi.org/10.1182/blood-2013-03-493924.

(119) Hu, X.; Zhang, D.; Zeng, Z.; Huang, L.; Lin, X.; Hong, S. Aptamer-Based Probes for Cancer Diagnostics and Treatment. *Life (Basel, Switzerland)* **2022**, *12* (11), 1937. https://doi.org/10.3390/life12111937.

(120) Varty, K.; O'brien, C.; Ignaszak, A. Breast Cancer Aptamers: Current Sensing Targets, Available Aptamers, and Their Evaluation for Clinical Use in Diagnostics. *Cancers (Basel).* **2021**, *13* (16), 3984. https://doi.org/10.3390/cancers13163984.

(121) Shatunova, E. A.; Korolev, M. A.; Omelchenko, V. O.; Kurochkina, Y. D.; Davydova, A. S.; Venyaminova, A. G.; Vorobyeva, M. A. Aptamers for Proteins Associated with Rheumatic Diseases: Progress, Challenges, and Prospects of Diagnostic and Therapeutic Applications. *Biomedicines* **2020**, *8* (11), 1–44. https://doi.org/10.3390/biomedicines8110527.

(122) Wu, Y.; Zeng, X.; Gan, Q. A Compact Surface Plasmon Resonance Biosensor for Sensitive Detection of Exosomal Proteins for Cancer Diagnosis. *Methods Mol. Biol.*

2022, *2393*, 3–14. https://doi.org/10.1007/978-1-0716-1803-5_1.

(123) Loyez, M.; Lobry, M.; Hassan, E. M.; DeRosa, M. C.; Caucheteur, C.; Wattiez, R. HER2 Breast Cancer Biomarker Detection Using a Sandwich Optical Fiber Assay. *Talanta* **2021**, *221*, 121452. https://doi.org/10.1016/j.talanta.2020.121452.

(124) Wang, R. E.; Zhang, Y.; Cai, J.; Cai, W.; Gao, T. Aptamer-Based Fluorescent Biosensors. *Curr. Med. Chem.* **2011**, *18* (27), 4175–4184. https://doi.org/10.2174/092986711797189637.

(125) Zhang, K.; Pei, M.; Cheng, Y.; Zhang, Z.; Niu, C.; Liu, X.; Liu, J.; Guo, F.; Huang, H.; Lin, X. A Novel Electrochemical Aptamer Biosensor Based on Tetrahedral DNA Nanostructures and Catalytic Hairpin Assembly for CEA Detection. *J. Electroanal. Chem.* **2021**, *898*, 115635. https://doi.org/https://doi.org/10.1016/j.jelechem.2021.115635.

(126) Zhao, B.; Miao, P.; Hu, Z.; Zhang, X.; Geng, X.; Chen, Y.; Feng, L. Signal-on Electrochemical Aptasensors with Different Target-Induced Conformations for Prostate Specific Antigen Detection. *Anal. Chim. Acta* **2021**, *1152*, 338282. https://doi.org/10.1016/j.aca.2021.338282.

(127) Lam, S. Y.; Lau, H. L.; Kwok, C. K. Capture-SELEX: Selection Strategy, Aptamer Identification, and Biosensing Application. *Biosensors(Basel)* **2022**, *12* (12), 1142.

(128) Kaur, H. Recent Developments in Cell-SELEX Technology for Aptamer Selection. *Biochim. Biophys. Acta* **2018**, *1862* (10), 2323–2329. https://doi.org/10.1016/j.bbagen.2018.07.029.

(129) Darmostuk, M.; Rimpelova, S.; Gbelcova, H.; Ruml, T. Current Approaches in SELEX: An Update to Aptamer Selection Technology. *Biotechnol. Adv.* **2015**, *33* (6), 1141–1161. https://doi.org/10.1016/j.biotechadv.2015.02.008.

(130) Zhu, C.; Yang, G.; Ghulam, M.; Li, L.; Qu, F. Evolution of Multi-Functional Capillary Electrophoresis for High-Efficiency Selection of Aptamers. *Biotechnol. Adv.* **2019**, *37* (8), 107432,1-16. https://doi.org/10.1016/j.biotechadv.2019.107432.

(131) McKeague, M.; McConnell, E. M.; Cruz-Toledo, J.; Bernard, E. D.; Pach, A.; Mastronardi, E.; Zhang, X.; Beking, M.; Francis, T.; Giamberardino, A.; Cabecinha, A.; Ruscito, A.; Aranda-Rodriguez, R.; Dumontier, M.; DeRosa, M. C. Analysis of In Vitro Aptamer Selection Parameters. *J. Mol. Evol.* **2015**, *81* (5–6), 150–161. https://doi.org/10.1007/s00239-015-9708-6.

(132) Ni, X.; Castanares, M.; Mukherjee, A.; Lupold, S. E. Nucleic Acid Aptamers: Clinical Applications and Promising New Horizons. *Curr. Med. Chem.* **2011**, *18* (27), 4206–

4214. https://doi.org/10.2174/092986711797189600.

(133) Blank, M. Next-Generation Analysis of Deep Sequencing Data: Bringing Light into the Black Box of SELEX Experiments. *Methods Mol. Biol.* **2016**, *1380*, 85–95. https://doi.org/10.1007/978-1-4939-3197-2_7.

(134) Stoltenburg, R.; Strehlitz, B. Refining the Results of a Classical SELEX Experiment by Expanding the Sequence Data Set of an Aptamer Pool Selected for Protein A. *Int. J. Mol. Sci.* **2018**, *19* (2), 642. https://doi.org/10.3390/ijms19020642.

(135) Kaur, H.; Bhagwat, S. R.; Sharma, T. K.; Kumar, A. Analytical Techniques for Characterization of Biological Molecules - Proteins and Aptamers/Oligonucleotides. *Bioanalysis* **2019**, *11* (2), 103–117. https://doi.org/10.4155/bio-2018-0225.

(136) Pollard, T. D. A Guide to Simple and Informative Binding Assays. *Mol. Biol. Cell* **2010**, *21* (23), 4061–4067. https://doi.org/10.1091/mbc.E10-08-0683.

(137) Jing, M.; Bowser, M. T. Methods for Measuring Aptamer-Protein Equilibria: A Review. *Anal. Chim. Acta* **2011**, *686* (1–2), 9–18. https://doi.org/10.1016/j.aca.2010.10.032.

(138) Zhao, J.; Tan, W.; Zheng, J.; Su, Y.; Cui, M. Aptamer Nanomaterials for Ovarian Cancer Target Theranostics. *Front. Bioeng. Biotechnol.* **2022**, *10* (March), 1–21. https://doi.org/10.3389/fbioe.2022.884405.

(139) Hanžek, A.; Siatka, C.; Duc, A.-C. High-Specificity Nucleic Acid Aptamers for Detection of Ovarian Cancer Protein Biomarkers: Application in Diagnostics; *Aptamers* **2021**, *5*, 7–14.

(140) Lamberti, I.; Scarano, S.; Esposito, C. L.; Antoccia, A.; Antonini, G.; Tanzarella, C.; De Franciscis, V.; Minunni, M. In Vitro Selection of RNA Aptamers against CA125 Tumor Marker in Ovarian Cancer and Its Study by Optical Biosensing. *Methods* **2016**, *97*, 58–68. https://doi.org/10.1016/j.ymeth.2015.10.022.

(141) Scoville, D. J.; Uhm, T. K. B.; Shallcross, J. A.; Whelan, R. J. Selection of DNA Aptamers for Ovarian Cancer Biomarker CA125 Using One-Pot SELEX and High-Throughput Sequencing. *J. Nucleic Acids* **2017**, *2017*, 1–9. https://doi.org/10.1155/2017/9879135.

(142) Sadasivam, M.; Sakthivel, A.; Nagesh, N.; Hansda, S.; Veerapandian, M.; Alwarappan, S.; Manickam, P. Magnetic Bead-Amplified Voltammetric Detection for Carbohydrate Antigen 125 with Enzyme Labels Using Aptamer-Antigen-Antibody Sandwiched Assay. *Sensors Actuators, B Chem.* **2020**, *312*, 127985. https://doi.org/10.1016/j.snb.2020.127985.

(143) Gedi, V.; Song, C. K.; Kim, G. B.; Lee, J. O.; Oh, E.; Shin, B. S.; Jung, M.; Shim, J.; Lee, H.; Kim, Y. P. Sensitive On-Chip Detection of Cancer Antigen 125 Using a DNA Aptamer/Carbon Nanotube Network Platform. *Sensors Actuators, B Chem.* **2018**, *256*, 89–97. https://doi.org/10.1016/j.snb.2017.10.049.

(144) Chen, F.; Liu, Y.; Chen, C.; Gong, H.; Cai, C.; Chen, X. Respective and Simultaneous Detection Tumor Markers CA125 and STIP1 Using Aptamer-Based Fluorescent and RLS Sensors. *Sensors Actuators, B Chem.* **2017**, *245*, 470–476. https://doi.org/10.1016/j.snb.2017.01.155.

(145) Tripathi, P.; Sachan, M.; Nara, S. Novel SsDNA Ligand Against Ovarian Cancer Biomarker CA125 With Promising Diagnostic Potential. *Front. Chem.* **2020**, *8*, 400. https://doi.org/10.3389/fchem.2020.00400.

(146) Tripathi, P.; Kumar, A.; Sachan, M.; Gupta, S.; Nara, S. Aptamer-Gold Nanozyme Based Competitive Lateral Flow Assay for Rapid Detection of CA125 in Human Serum. *Biosens. Bioelectron.* **2020**, *165*, 112368. https://doi.org/10.1016/j.bios.2020.112368.

(147) Zhang, X.; Wang, Y.; Deng, H.; Xiong, X.; Zhang, H.; Liang, T.; Li, C. An Aptamer Biosensor for CA125 Quantification in Human Serum Based on Upconversion Luminescence Resonance Energy Transfer. *Microchem. J.* **2021**, *161*, 105761. https://doi.org/10.1016/j.microc.2020.105761.

(148) Eaton, R. M.; Shallcross, J. A.; Mael, L. E.; Mears, K. S.; Minkoff, L.; Scoville, D. J.; Whelan, R. J. Selection of DNA Aptamers for Ovarian Cancer Biomarker HE4 Using CE-SELEX and High-Throughput Sequencing. *Anal. Bioanal. Chem.* **2015**, *407* (23), 6965–6973. https://doi.org/10.1007/s00216-015-8665-7.

(149) Mansouri Majd, S.; Salimi, A. Ultrasensitive Flexible FET-Type Aptasensor for CA 125 Cancer Marker Detection Based on Carboxylated Multiwalled Carbon Nanotubes Immobilized onto Reduced Graphene Oxide Film. *Anal. Chim. Acta* **2018**, *1000*, 273–282. https://doi.org/10.1016/j.aca.2017.11.008.

(150) Farzin, L.; Sadjadi, S.; Shamsipur, M.; Sheibani, S.; Mousazadeh, M. hasan. Employing AgNPs Doped Amidoxime-Modified Polyacrylonitrile (PAN-Oxime) Nanofibers for Target Induced Strand Displacement-Based Electrochemical Aptasensing of CA125 in Ovarian Cancer Patients. *Mater. Sci. Eng. C* **2019**, *97*, 679–687. https://doi.org/10.1016/j.msec.2018.12.108.

(151) Ma, X.; Huang, G.; Ye, M.; Zhang, X.; Wang, Y.; Liang, T.; Deng, H.; Li, C. A Homogeneous Biosensor for Human Epididymis Protein 4 Based on Upconversion

Luminescence Resonance Energy Transfer. *Microchem. J.* **2021**, *164* (1), 106083. https://doi.org/10.1016/j.microc.2021.106083.

(152) Janssen, K. P. F.; Knez, K.; Pollet, J.; Roberts, S. J.; Schrooten, J.; Lammertyn, J. Assay Design Considerations for Use of Affinity Aptamer Amplification in Ultra-Sensitive Protein Assays Using Capillary Electrophoresis. *Anal. Methods* **2011**, *3* (9), 2156–2159. https://doi.org/10.1039/c1ay05124e.

(153) Ouellet, E.; Foley, J. H.; Conway, E. M.; Haynes, C. Hi-Fi SELEX: A High-Fidelity Digital-PCR Based Therapeutic Aptamer Discovery Platform. *Biotechnol. Bioeng.* **2015**, *112* (8), 1506–1522. https://doi.org/10.1002/bit.25581.

(154) Ang, A.; Ouellet, E.; Cheung, K. C.; Haynes, C. Highly Efficient and Reliable DNA Aptamer Selection Using the Partitioning Capabilities of Ddpcr: The Hi-Fi Selex Method. *Methods Mol. Biol.* **2018**, *1768*, 531–554. https://doi.org/10.1007/978-1-4939-7778-9_30.

(155) Sarigul, N.; Korkmaz, F.; Kurultak, İ. A New Artificial Urine Protocol to Better Imitate Human Urine. *Sci. Rep.* **2019**, *9* (1), 1–11. https://doi.org/10.1038/s41598-019-56693-4.

(156) Quang, N. N.; Bouvier, C.; Henriques, A.; Lelandais, B.; Ducongé, F. Time-Lapse Imaging of Molecular Evolution by High-Throughput Sequencing. *Nucleic Acids Res.* **2018**, *46* (15), 7480–7494. https://doi.org/10.1093/nar/gky583.

(157) Quang, N. N.; Perret, G.; Ducongé, F. Applications of High-Throughput Sequencing for in Vitro Selection and Characterization of Aptamers. *Pharmaceuticals* **2016**, *9* (4), 1–15. https://doi.org/10.3390/ph9040076.

(158) Bailey, T. L.; Williams, N.; Misleh, C.; Li, W. W. MEME: Discovering and Analyzing DNA and Protein Sequence Motifs. *Nucleic Acids Res.* **2006**, *34*, W369-73. https://doi.org/10.1093/nar/gkl198.

(159) Goujon, M.; McWilliam, H.; Li, W.; Valentin, F.; Squizzato, S.; Paern, J.; Lopez, R. A New Bioinformatics Analysis Tools Framework at EMBL-EBI. *Nucleic Acids Res.* **2010**, *38*, W695-9. https://doi.org/10.1093/nar/gkq313.

(160) Zuker, M. Mfold Web Server for Nucleic Acid Folding and Hybridization Prediction. *Nucleic Acids Res.* **2003**, *31* (13), 3406–3415. https://doi.org/10.1093/nar/gkg595.

(161) Damase, T. R.; Allen, P. B. Idiosyncrasies of Thermofluorimetric Aptamer Binding Assays. *Biotechniques* **2019**, *66* (3), 121–127.

(162) Hu, J.; Kim, J.; Easley, C. J. Quantifying Aptamer-Protein Binding via Thermofluorimetric Analysis. *Anal. Methods* **2015**, *7* (17), 7358–7362.

https://doi.org/doi:10.1039/c5ay00837a.

(163) Tasset, D. M.; Kubik, M. F.; Steiner, W. Oligonucleotide Inhibitors of Human Thrombin That Bind Distinct Epitopes. *J. Mol. Biol.* **1997**, *272* (5), 688–698. https://doi.org/10.1006/jmbi.1997.1275.

(164) Eaton, R. M.; Shallcross, J. A.; Mael, L. E.; Mears, K. S.; Minkoff, L.; Scoville, D. J.; Whelan, R. J. Selection of DNA Aptamers for Ovarian Cancer Biomarker HE4 Using CE-SELEX and High-Throughput Sequencing. *Anal. Bioanal. Chem.* **2015**, *407*, 6965–6973. https://doi.org/10.1007/s00216-015-8665-7.

(165) Wei, R.; Wong, J. P. C.; Kwok, H. F. Osteopontin - A Promising Biomarker for Cancer Therapy. *J. Cancer* **2017**, *8* (12), 2173–2183. https://doi.org/10.7150/jca.20480.

(166) Zhao, H.; Chen, Q.; Alam, A.; Cui, J.; Suen, K. C.; Soo, A. P.; Eguchi, S.; Gu, J.; Ma, D. The Role of Osteopontin in the Progression of Solid Organ Tumour. *Cell Death Dis.* **2018**, *9* (3), 356. https://doi.org/10.1038/s41419-018-0391-6.

(167) Hu, Z. De; Wei, T. T.; Yang, M.; Ma, N.; Tang, Q. Q.; Qin, B. D.; Fu, H. T.; Zhong, R. Q. Diagnostic Value of Osteopontin in Ovarian Cancer: Meta-Analysis and Systematic Review. *PLoS One* **2015**, *10* (5), 1–13. https://doi.org/10.1371/journal.pone.0126444.

(168) Cerne, K.; Hadzialjevic, B.; Skof, E.; Verdenik, I.; Kobal, B. Potential of Osteopontin in the Management of Epithelial Ovarian Cancer. *Radiol. Oncol.* **2019**, *53* (1), 105–115. https://doi.org/10.2478/raon-2019-0003.

(169) Kitagori, K.; Yoshifuji, H.; Oku, T.; Sasaki, C.; Miyata, H.; Mori, K. P.; Nakajima, T.; Ohmura, K.; Kawabata, D.; Yukawa, N.; Imura, Y.; Murakami, K.; Nakashima, R.; Usui, T.; Fujii, T.; Sakai, K.; Yanagita, M.; Hirayama, Y.; Mimori, T. Cleaved Form of Osteopontin in Urine as a Clinical Marker of Lupus Nephritis. *PLoS One* **2016**, *11* (12), 1–13. https://doi.org/10.1371/journal.pone.0167141.

(170) Beitland, S.; Nakstad, E. R.; Berg, J. P.; Trøseid, A.-M. S.; Brusletto, B. S.; Brunborg, C.; Lundqvist, C.; Sunde, K. Urine β-2-Microglobulin, Osteopontin, and Trefoil Factor 3 May Early Predict Acute Kidney Injury and Outcome after Cardiac Arrest. *Crit. Care Res. Pract.* **2019**, *2019*, 4384796. https://doi.org/10.1155/2019/4384796.

(171) Mansour, S. G.; Liu, C.; Jia, Y.; Reese, P. P.; Hall, I. E.; El-Achkar, T. M.; LaFavers, K. A.; Obeid, W.; Rosenberg, A. Z.; Daneshpajouhnejad, P.; Doshi, M. D.; Akalin, E.; Bromberg, J. S.; Harhay, M. N.; Mohan, S.; Muthukumar, T.; Schröppel, B.; Singh, P.; El-Khoury, J. M.; Weng, F. L.; Thiessen-Philbrook, H. R.; Parikh, C. R. Uromodulin

to Osteopontin Ratio in Deceased Donor Urine Is Associated With Kidney Graft Outcomes. *Transplantation* **2021**, *105* (4), 876–885. https://doi.org/10.1097/TP.0000000000003299.

(172) Tilli, T. M.; Franco, V. F.; Robbs, B. K.; Wanderley, J. L. M.; Da Silva, F. R. D. A.; De Mello, K. D.; Viola, J. P. B.; Weber, G. F.; Gimba, E. R. Osteopontin-c Splicing Isoform Contributes to Ovarian Cancer Progression. *Mol. Cancer Res.* **2011**, *9* (3), 280–293. https://doi.org/10.1158/1541-7786.MCR-10-0463.

(173) Marques, D. S.; Grativol, J.; Alves da Silva Peres, R.; da Rocha Matos, A.; Gimba, E. R. P. Osteopontin-c Isoform Levels Are Associated with SR and HnRNP Differential Expression in Ovarian Cancer Cell Lines. *Tumor Biol.* **2017**, *39* (9), 2017. https://doi.org/10.1177/1010428317725442.

(174) Brum, M. C. M.; Dos Santos Guimaraes, I.; Ferreira, L. B.; Rangel, L. B. A.; Maia, R. C.; de Moraes, G. N.; Gimba, E. R. P. Osteopontin-c Isoform Inhibition Modulates Ovarian Cancer Cell Cisplatin Resistance, Viability and Plasticity. *Oncol. Rep.* **2021**, *45* (2), 652–664. https://doi.org/10.3892/or.2020.7877.

(175) Sharma, S. Tumor Markers in Clinical Practice: General Principles and Guidelines. *Indian J. Med. Paediatr. Oncol. Off. J. Indian Soc. Med. Paediatr. Oncol.* **2009**, *30* (1), 1–8. https://doi.org/10.4103/0971-5851.56328.

(176) Thompson, C.; Kamran, W.; Dockrell, L.; Khalid, S.; Kumari, M.; Ibrahim, N.; O'Leary, J.; Norris, L.; Petzold, M.; O'Toole, S.; Gleeson, N. The Clearance of Serum Human Epididymis Protein 4 Following Primary Cytoreductive Surgery for Ovarian Carcinoma. *Int. J. Gynecol. cancer Off. J. Int. Gynecol. Cancer Soc.* **2018**, *28* (6), 1066–1072. https://doi.org/10.1097/IGC.0000000000001267.

(177) Thiel, W. H.; Bair, T.; Wyatt Thiel, K.; Dassie, J. P.; Rockey, W. M.; Howell, C. A.; Liu, X. Y.; Dupuy, A. J.; Huang, L.; Owczarzy, R.; Behlke, M. A.; McNamara, J. O.; Giangrande, P. H. Nucleotide Bias Observed with a Short SELEX RNA Aptamer Library. *Nucleic Acid Ther.* **2011**, *21* (4), 253–263. https://doi.org/10.1089/nat.2011.0288.

(178) Thiel, W. H.; Bair, T.; Peek, A. S.; Liu, X.; Dassie, J.; Stockdale, K. R.; Behlke, M. A.; Miller, F. J.; Giangrande, P. H. Rapid Identification of Cell-Specific, Internalizing RNA Aptamers with Bioinformatics Analyses of a Cell-Based Aptamer Selection. *PLoS One* **2012**, *7* (9), e43836. https://doi.org/10.1371/journal.pone.0043836.

(179) Takahashi, M.; Wu, X.; Ho, M.; Chomchan, P.; Rossi, J. J.; Burnett, J. C.; Zhou, J. High Throughput Sequencing Analysis of RNA Libraries Reveals the Influences of

Initial Library and PCR Methods on SELEX Efficiency. *Sci. Rep.* **2016**, *6*, 1–14. https://doi.org/10.1038/srep33697.

(180) Moreno, M.; García-Sacristán, A.; Martín, M. E.; González, V. M. Enzyme-Linked Oligonucleotide Assay (ELONA). *Methods Mol. Biol.* **2023**, *2570*, 235–242. https://doi.org/10.1007/978-1-0716-2695-5_18.

(181) Hanžek, A.; Ducongé, F.; Siatka, C.; Duc, A. C. E. Identification and Characterization of Aptamers Targeting Ovarian Cancer Biomarker Human Epididymis Protein 4 for the Application in Urine. *Cancers (Basel).* **2023**, *15* (2), 452. https://doi.org/10.3390/cancers15020452.

(182) Menon, U.; Karpinskyj, C.; Gentry-Maharaj, A. Ovarian Cancer Prevention and Screening. *Obstet. Gynecol.* **2018**, *31* (5), 909–927. https://doi.org/10.1097/AOG.0000000000002580.

(183) Oshi, M.; Murthy, V.; Takahashi, H.; Huyser, M.; Okano, M.; Tokumaru, Y.; Rashid, O. M.; Matsuyama, R.; Endo, I.; Takabe, K. Urine as a Source of Liquid Biopsy for Cancer. *Cancers (Basel).* **2021**, *13* (11), 1–15. https://doi.org/10.3390/cancers13112652.

(184) Wong, R.; Rosser, C. J. UroSEEK Gene Panel for Bladder Cancer Surveillance. *Translational andrology and urology*. China December 2019, pp S546–S549. https://doi.org/10.21037/tau.2019.12.41.

(185) Eich, M.-L.; Rodriguez Pena, M. D. C.; Springer, S. U.; Taheri, D.; Tregnago, A. C.; Salles, D. C.; Bezerra, S. M.; Cunha, I. W.; Fujita, K.; Ertoy, D.; Bivalacqua, T. J.; Tomasetti, C.; Papadopoulos, N.; Kinzler, K. W.; Vogelstein, B.; Netto, G. J. Incidence and Distribution of UroSEEK Gene Panel in a Multi-Institutional Cohort of Bladder Urothelial Carcinoma. *Mod. Pathol. an Off. J. United States Can. Acad. Pathol. Inc* **2019**, *32* (10), 1544–1550. https://doi.org/10.1038/s41379-019-0276-y.

(186) Jiang, Z.; Zhao, Y.; Tian, Y. Comparison of Diagnostic Efficacy by Two Urine PCA3 Scores in Prostate Cancer Patients Undergoing Repeat Biopsies. *Minerva Urol. Nefrol.* **2019**, *71* (4), 373–380. https://doi.org/10.23736/S0393-2249.18.03093-X.

(187) Kulabhusan, P. K.; Hussain, B.; Yüce, M. Current Perspectives on Aptamers as Diagnostic Tools and Therapeutic Agents. *Pharmaceutics* **2020**, *12* (7), 646,1-23. https://doi.org/10.3390/pharmaceutics12070646.

(188) Kammer, M. N.; Kussrow, A.; Gandhi, I.; Drabek, R.; Batchelor, R. H.; Jackson, G. W.; Bornhop, D. J. Quantification of Opioids in Urine Using an Aptamer-Based Free-Solution Assay. *Anal. Chem.* **2019**, *91* (16), 10582–10588.

https://doi.org/10.1021/acs.analchem.9b01638.

(189) Simmons, M. D.; Miller, L. M.; Sundström, M. O.; Johnson, S. Aptamer-Based Detection of Ampicillin in Urine Samples. *Antibiotics* **2020**, *9* (10), 1–16. https://doi.org/10.3390/antibiotics9100655.

(190) Gao, J.; Liu, N.; Zhang, X.; Yang, E.; Song, Y.; Zhang, J.; Han, Q. Utilizing the DNA Aptamer to Determine Lethal α-Amanitin in Mushroom Samples and Urine by Magnetic Bead-ELISA (MELISA). *Molecules* **2022**, *27* (2), 538. https://doi.org/10.3390/molecules27020538.

(191) Pla, L.; Sancenón, F.; Martínez-bisbal, M. C.; Bañuls, C.; Estañ, N.; Botello-marabotto, M.; Aznar, E.; Sáez, G.; Santiago-felipe, S.; Martínez-máñez, R. A New 8-Oxo-7,8-2'deoxyguanosine Nanoporous Anodic Alumina Aptasensor for Colorectal Cancer Diagnosis in Blood and Urine. *Nanoscale* **2021**, *13* (18), 8648–8657. https://doi.org/10.1039/d0nr07948k.

(192) Kim, E.; Kang, M.; Ban, C. Aptamer-Antibody Hybrid ELONA That Uses Hybridization Chain Reaction to Detect a Urinary Biomarker EN2 for Bladder and Prostate Cancer. *Sci. Rep.* **2022**, *12* (1), 1–8. https://doi.org/10.1038/s41598-022-15556-1.

(193) Musheev, M. U.; Krylov, S. N. Selection of Aptamers by Systematic Evolution of Ligands by Exponential Enrichment: Addressing the Polymerase Chain Reaction Issue. *Anal. Chim. Acta* **2006**, *564* (1), 91–96. https://doi.org/10.1016/j.aca.2005.09.069.

(194) Avci-Adali, M.; Paul, A.; Wilhelm, N.; Ziemer, G.; Wendel, H. P. Upgrading SELEX Technology by Using Lambda Exonuclease Digestion for Single-Stranded DNA Generation. *Molecules* **2010**, *15* (1), 1–11. https://doi.org/10.3390/molecules15010001.

(195) Roy, S.; Hennelly, S. P.; Lammert, H.; Onuchic, J. N.; Sanbonmatsu, K. Y. Magnesium Controls Aptamer-Expression Platform Switching in the SAM-I Riboswitch. *Nucleic Acids Res.* **2019**, *47* (6), 3158–3170. https://doi.org/10.1093/nar/gky1311.

(196) Owczarzy, R.; Moreira, B. G.; You, Y.; Behlke, M. A.; Wälder, J. A. Predicting Stability of DNA Duplexes in Solutions Containing Magnesium and Monovalent Cations. *Biochemistry* **2008**, *47* (19), 5336–5353. https://doi.org/10.1021/bi702363u.

(197) Mckeague, M.; Calzada, V.; Cerchia, L.; Derosa, M.; Heemstra, J. M.; Janjic, N.; Johnson, P. E.; Kraus, L.; Limson, J.; Mayer, G.; Nilsen-Hamilton, M.; Porciani, D.;

Sharma, T. K.; Suess, B.; Tanner, J. A.; Sarah Shigdar. The Minimum Aptamer Publication Standards (MAPS Guidelines) for de Novo Aptamer Selection. *Aptamers* **2022**, *6*, 10–18.

(198) Pruijm, M.; Ponte, B.; Ackermann, D.; Paccaud, F.; Guessous, I.; Ehret, G.; Pechère-Bertschi, A.; Vogt, B.; Mohaupt, M. G.; Martin, P.-Y.; Youhanna, S. C.; Nägele, N.; Vollenweider, P.; Waeber, G.; Burnier, M.; Devuyst, O.; Bochud, M. Associations of Urinary Uromodulin with Clinical Characteristics and Markers of Tubular Function in the General Population. *Clin. J. Am. Soc. Nephrol.* **2016**, *11* (1), 70–80. https://doi.org/10.2215/CJN.04230415.

(199) Julian, B. A.; Suzuki, H.; Suzuki, Y.; Tomino, Y.; Spasovski, G.; Novak, J. Sources of Urinary Proteins and Their Analysis by Urinary Proteomics for the Detection of Biomarkers of Disease. *Proteomics - Clin. Appl.* **2009**, *3* (9), 1029–1043. https://doi.org/10.1002/prca.200800243.

(200) Aitekenov, S.; Gaipov, A.; Bukasov, R. Review: Detection and Quantification of Proteins in Human Urine. *Talanta* **2020**, *223*, 121718.

(201) Mo, T.; Liu, X.; Luo, Y.; Zhong, L.; Zhang, Z.; Li, T.; Gan, L.; Liu, X.; Li, L.; Wang, H.; Sun, X.; Fan, D.; Qian, Z.; Wu, P.; Chen, X. Aptamer-Based Biosensors and Application in Tumor Theranostics. *Cancer Sci.* **2022**, *113* (1), 7–16. https://doi.org/10.1111/cas.15194.

(202) Reid, R.; Chatterjee, B.; Das, S. J.; Ghosh, S.; Sharma, T. K. Application of Aptamers as Molecular Recognition Elements in Lateral Flow Assays. *Anal. Biochem.* **2020**, *593*, 113574. https://doi.org/10.1016/j.ab.2020.113574.

(203) Chen, A.; Yang, S. Replacing Antibodies with Aptamers in Lateral Flow Immunoassay. *Biosens. Bioelectron.* **2015**, *71*, 230–242. https://doi.org/10.1016/j.bios.2015.04.041.

(204) Yu, Q.; Zhao, Q.; Wang, S.; Zhao, S.; Zhang, S.; Yin, Y.; Dong, Y. Development of a Lateral Flow Aptamer Assay Strip for Facile Identification of Theranostic Exosomes Isolated from Human Lung Carcinoma Cells. *Anal. Biochem.* **2020**, *594*, 2023. https://doi.org/10.1016/j.ab.2020.113591.

(205) Mandrekar, J. N. Simple Statistical Measures for Diagnostic Accuracy Assessment. *J. Thorac. Oncol.* **2010**, *5* (6), 763–764. https://doi.org/10.1097/JTO.0b013e3181dab122.